

ANTI-INFLAMMATORY COMPOUNDS IN HUMAN PERIPHERAL BLOOD MONONUCLEAR
CELLS FROM *DENDROBIUM* SPECIES



A Dissertation Submitted in Partial Fulfillment of the Requirements
for the Degree of Doctor of Philosophy in Pharmaceutical Sciences and Technology

FACULTY OF PHARMACEUTICAL SCIENCES

Chulalongkorn University

Academic Year 2022

Copyright of Chulalongkorn University

สารที่มีฤทธิ์ต้านอักเสบในเซลล์เม็ดเลือดขาวชนิดนิวเคลียสเดี่ยวของมนุษย์จากกล้วยไม้สกุลเดนโดร
เปียม



วิทยานิพนธ์นี้เป็นส่วนหนึ่งของการศึกษาตามหลักสูตรปริญญาวิทยาศาสตรดุษฎีบัณฑิต
สาขาวิชาเภสัชศาสตร์และเทคโนโลยี ไม่สังกัดภาควิชา/เทียบเท่า
คณะเภสัชศาสตร์ จุฬาลงกรณ์มหาวิทยาลัย
ปีการศึกษา 2565
ลิขสิทธิ์ของจุฬาลงกรณ์มหาวิทยาลัย

Thesis Title ANTI-INFLAMMATORY COMPOUNDS IN HUMAN
PERIPHERAL BLOOD MONONUCLEAR CELLS FROM
DENDROBIUM SPECIES

By Mr. Virunh Kongkatitham

Field of Study Pharmaceutical Sciences and Technology

Thesis Advisor Associate Professor BOONCHOO SRITULARAK, Ph.D.

Thesis Co Advisor Associate Professor CHATCHAI CHAOTHAM, Ph.D.
PD Dr. rer. nat. Chotima Böttcher

Accepted by the FACULTY OF PHARMACEUTICAL SCIENCES, Chulalongkorn
University in Partial Fulfillment of the Requirement for the Doctor of Philosophy

..... Dean of the FACULTY OF
PHARMACEUTICAL SCIENCES
(Professor PORNANONG ARAMWIT, Ph.D.)

DISSERTATION COMMITTEE

..... Chairman
(Professor Supachoke Mangmool, Ph.D.)

..... Thesis Advisor
(Associate Professor BOONCHOO SRITULARAK, Ph.D.)

..... Thesis Co-Advisor
(Associate Professor CHATCHAI CHAOTHAM, Ph.D.)

..... Thesis Co-Advisor
(PD Dr. rer. nat. Chotima Böttcher)

..... Examiner
(Assistant Professor CHAISAK CHANSRINIYOM, Ph.D.)

..... Examiner
(Assistant Professor PREEDAKORN CHUNHACHA, Ph.D.)

..... Examiner
(WORATOUCH THITIKORNPONG, Ph.D.)

วิรุฬห์ คงคดิธรรม : สารที่มีฤทธิ์ต้านอักเสบในเซลล์เม็ดเลือดขาวชนิดนิวเคลียสเดี่ยวของมนุษย์จาก
 กล้ามเนื้อสkeletalเดนโตรเบียม. (ANTI-INFLAMMATORY COMPOUNDS IN HUMAN PERIPHERAL
 BLOOD MONONUCLEAR CELLS FROM *DENDROBIUM* SPECIES) อ.ที่ปรึกษาหลัก : รศ. ภก.
 ดร.บุญชู ศรีตุลารักษ์, อ.ที่ปรึกษาร่วม : รศ. ภก. ดร.ฉัตรชัย เขาว์ธรรม, PD Dr. rer. nat. Chotima
 Böttcher

ในการศึกษานี้ สารใหม่ 4 ชนิด ได้แก่ dendrocumenols A, B และ D ซึ่งเป็นอนุพันธ์ของสารในกลุ่ม phenanthrene และ dendrocumenol C ซึ่งเป็นอนุพันธ์ของสารในกลุ่ม fluorenone และสารที่มีการ
 รายงานไว้แล้วอีก 4 ชนิด ได้แก่ gigantol, 3,7-dihydroxy-2,4,8-trimethoxyphenanthrene, densiflorol B
 และ cypripedin ถูกสกัดแยกจากสารสกัดหยาบเอทิลอะซิเตตจากหวายตะมอย โดยโครงสร้างของสารที่แยกได้
 จากหวายตะมอยได้รับการพิสูจน์โครงสร้างทางเคมีด้วยเทคนิคทางสเปกโตรสโคปี จากนั้นสารที่แยกได้จะถูก
 นำไปทดสอบฤทธิ์ต้านอักเสบในเซลล์เม็ดเลือดขาวชนิดนิวเคลียสเดี่ยวของมนุษย์ จากการทดสอบ พบว่า สาร
 dendrocumenol B และ D มีแนวโน้มฤทธิ์ต้านอักเสบที่ดีที่สุดจากการยับยั้งการแสดงออกของ tumor
 necrosis factor (TNF) และ interleukin-2 (IL-2) ในเซลล์โมโนไซด์และเม็ดเลือดขาวชนิดที และการศึกษาเชิง
 ลึกทางภูมิคุ้มกันโดยใช้ high-dimensional single-cell mass cytometry (CyTOF) สามารถยืนยันได้ว่า
 สาร dendrocumenol D มีฤทธิ์ต้านอักเสบจากผลของการปรับภูมิคุ้มกันผ่านการลดจำนวนประชากรของ
 เลือดขาวชนิดทีในเซลล์เม็ดเลือดขาวชนิดนิวเคลียสเดี่ยวของมนุษย์ที่ถูกกระตุ้นให้เกิดการอักเสบโดย phorbol-
 12-myristate-13-acetate และ ionomycin (PMA/Iono) อีกหนึ่งการศึกษา คือ สารในกลุ่ม bibenzyl 7 ชนิด
 ที่มีการรายงานการแยกสกัดได้จากกล้ามเนื้อสkeletalหวายชนิดต่าง ๆ ถูกนำมาทดสอบฤทธิ์ต้านอักเสบในเซลล์เม็ด
 เลือดขาวชนิดนิวเคลียสเดี่ยวของมนุษย์ที่ถูกกระตุ้นให้เกิดการอักเสบโดย lipopolysaccharide (LPS) จาก
 ผลทดสอบพบว่า สาร moscatilin และ crepidatin มีฤทธิ์ยับยั้งการแสดงออกของ TNF ในเซลล์โมโนไซด์ได้ดี
 ที่สุด และการศึกษาเชิงลึกทางภูมิคุ้มกันโดยใช้ CyTOF สามารถยืนยันได้ว่า สาร crepidatin มีฤทธิ์ต้านอักเสบ
 จากผลของการปรับภูมิคุ้มกันผ่านการลดจำนวน เนทเชอรัล คิลเลอร์ เซลล์ (NK) เซลล์โมโนไซด์ที่เกี่ยวข้อง
 กับโปรตีนการอักเสบ pSTAT5⁺ และเซลล์โมโนไซด์ที่มีการแสดงออกของโมเลกุล co-stimulatory ชนิด CD86

สาขาวิชา เภสัชศาสตร์และเทคโนโลยี

ปีการศึกษา 2565

ลายมือชื่อนิสิต

ลายมือชื่อ อ.ที่ปรึกษาหลัก

ลายมือชื่อ อ.ที่ปรึกษาร่วม

ลายมือชื่อ อ.ที่ปรึกษาร่วม

6271006033 : MAJOR PHARMACEUTICAL SCIENCES AND TECHNOLOGY

KEYWORD: Dendrobium crumenatum, immunomodulatory effect, PBMCs, Dendrobium genus, bibenzyls, Anti-inflammatory effect

Virunh Kongkatitham : ANTI-INFLAMMATORY COMPOUNDS IN HUMAN PERIPHERAL BLOOD MONONUCLEAR CELLS FROM *DENDROBIUM* SPECIES. Advisor: Assoc. Prof. BOONCHOO SRITULARAK, Ph.D. Co-advisor: Assoc. Prof. CHATCHAI CHAOTHAM, Ph.D., PD Dr. rer. nat. Chotima Böttcher

In these studies, four new compounds including three phenanthrene derivatives (dendrocruenols A, B and D) and one fluorenone (dendrocruenol C) and four known compounds including gigantol, 3,7-dihydroxy-2,4,8-trimethoxyphenanthrene, densiflorol B and cypripedin were isolated from *Dendrobium crumenatum* Sw. Each structure of isolated compounds from *D. crumenatum* was elucidated by spectroscopic data. These isolated compounds were then evaluated for anti-inflammatory effects in human peripheral blood mononuclear cells (PBMCs). Among the tested compounds, dendrocruenols B and D showed the most promising anti-inflammatory effects through inhibition of tumor necrosis factor tumor (TNF) and interleukin-2 (IL-2) in monocytes and T cells. The deep immune profiling using high-dimensional single-cell mass cytometry (CyTOF) could confirm the anti-inflammatory effects based on immunomodulation of dendrocruenol D through the decreasing of activated T cell population in phorbol-12-myristate-13-acetate and ionomycin (PMA/Iono) stimulation in human PBMCs. Next, the seven known bibenzyls isolated from *Dendrobium* plants were investigated the immunomodulatory effects in lipopolysaccharide (LPS)-induced human PBMCs. Two bibenzyls, moscatilin and crepidatin, exhibited the strongest inhibitory effect of TNF-expressed monocytes. The deep immune profiling using CyTOF could confirm the anti-inflammatory activity based on immunomodulation effect of crepidatin through reduction of NK cells, pSTAT5⁺ non-classical monocytes and monocytes expressing co-stimulatory molecule CD86.

Field of Study: Pharmaceutical Sciences and Technology Student's Signature

Academic Year: 2022 Advisor's Signature
Co-advisor's Signature
Co-advisor's Signature

ACKNOWLEDGEMENTS

I wish to appreciate my advisor, Associate Professor Boonchoo Sritularak, Ph.D., my co-advisors, Associate Professor Chatchai Chaotham, Ph.D. and PD. Dr. rer. nat. Chotima Böttcher, and Professor Kittisak Likhitwitayawuid, Ph.D., for their endless support, many helps and valuable guidance for this dissertation. I would not have succeeded my dissertation and research articles without their beneficial advice and kindness that I have received from them.

I am grateful for all assistance from the members of my thesis committee, my friends and all staff of the Department of Pharmacognosy and Pharmaceutical Botany, Faculty of Pharmaceutical Sciences, Chulalongkorn University.

I would like to thank my friends from Experimental and Clinical Research Center, a cooperation between the Max Delbrück Center for Molecular Medicine in the Helmholtz Association and Charité–Universitätsmedizin Berlin, especially Adeline Dehlinger and Meng Wang for their helps and support when I did the research in Berlin, Germany.

In addition, I would like to thankfully acknowledge Second Century Fund (C2F), Chulalongkorn University for supporting my research.

Finally, I want to express my special gratitude to my family, my friends and especially to my love, Nutchka Kongsin, for their love, encouragement and many supports.

Virunh Kongkatitham

TABLE OF CONTENTS

	Page
.....	iii
ABSTRACT (THAI).....	iii
.....	iv
ABSTRACT (ENGLISH).....	iv
ACKNOWLEDGEMENTS.....	v
TABLE OF CONTENTS.....	vi
LIST OF TABLES.....	1
LIST OF FIGURES.....	2
ABBREVIATIONS and SYMBOLS.....	5
CHAPTER I INTRODUCTION.....	9
Rationale.....	9
Objectives.....	12
Hypothesis.....	12
Scope.....	12
Benefits.....	13
CHAPTER II LITERATURE REVIEWS.....	14
2.1 Pathways of inflammation.....	14
2.2 Store-operated calcium entry (SOCE) pathway.....	17
2.3 Natural products for anti-inflammation based on immune modulatory effects.....	17
2.4 <i>Dendrobium</i> genus: Phytochemical and biological activities.....	19
CHAPTER III Research articles.....	134

3.1 Immunomodulatory Effects of New Phenanthrene Derivatives from <i>Dendrobium crumenatum</i>	134
3.2 Diverse modulatory effects of bibenzyls from <i>Dendrobium</i> species on human immune cell responses under inflammatory conditions	167
CHAPTER IV DISCUSSION	189
CHAPTER V CONCLUSION	192
APPENDIX	193
REFERENCES	215
VITA	240



LIST OF TABLES

Table 1 Bibenzyls and derivatives in the <i>Dendrobium</i> species.....	28
Table 2 Phenanthrenes and derivatives in the <i>Dendrobium</i> species.....	53
Table 3 Flavonoids in the genus <i>Dendrobium</i>	77
Table 4 Terpenoids and alkaloids in the genus <i>Dendrobium</i>	84
Table 5 Fluorenones and fluorenes in the genus <i>Dendrobium</i>	103
Table 6 Coumarins in the genus <i>Dendrobium</i>	106
Table 7 Lignans and neolignans in the genus <i>Dendrobium</i>	108
Table 8 Miscellaneous compounds in the genus <i>Dendrobium</i>	115
Table 9 ¹ H and ¹³ C-NMR Spectral Data of 1 and 2 in Acetone- <i>d</i> ₆ (δ in ppm, <i>J</i> in Hz)	138
Table 10 ¹ H and ¹³ C-NMR Spectral Data of 3 in Acetone- <i>d</i> ₆ (δ in ppm, <i>J</i> in Hz).....	140
Table 11 ¹ H (300 MHz) and ¹³ C-NMR (75 MHz) Spectral Data of 4 in CDCl ₃ (δ in ppm, <i>J</i> in Hz).....	142
Table 12 The CyTOF antibody list.....	160
Table 13 The CyTOF antibody list.....	178

LIST OF FIGURES

Figure 1 Structures of bibenzyls and derivatives from <i>Dendrobium</i> species.....	42
Figure 2 Structures of phenanthrenes and derivatives from <i>Dendrobium</i> species....	65
Figure 3 Structures of flavonoids from <i>Dendrobium</i> species.....	81
Figure 4 Structures of terpenoids and alkaloids from <i>Dendrobium</i> species.....	92
Figure 5 Structures of fluorenones and fluorenes from <i>Dendrobium</i> species.....	105
Figure 6 Structures of coumarins from <i>Dendrobium</i> species.....	107
Figure 7 Structures of lignans and neolignans from <i>Dendrobium</i> species.....	111
Figure 8 Structures of miscellaneous compounds from <i>Dendrobium</i> species.....	124
Figure 9 <i>Dendrobium crumenatum</i> Sw.....	133
Figure 10 Experimental CD and calculated ECD spectra of compound 4	143
Figure 11 Structure of isolated compounds from <i>D. crumenatum</i>	144
Figure 12 HMBC (arrow), NOESY (double headed dashed arrow) and ¹ H- ¹ H COSY (bold line) correlations of compounds 1-4	144
Figure 13 Analysis using flow cytometry.....	146
Figure 14 Determination of immune modulatory effects.....	147
Figure 15 Cytotoxicity of compounds 2 and 4	149
Figure 16 Bar graphs show the percent of frequency of inflammatory cytokines (TNF- α , IL-2, and IFN- γ) expression in the immune cells of MS PBMCs after 4 h treatment with DMSO and the two new active compounds 2 and 4 from <i>D. crumenatum</i> with or without PMA/ionomycin stimulation.....	149
Figure 17 Determination of Ca ²⁺ influx.....	150
Figure 18 Evaluation of immune modulatory effects using deep immune profiling by CyTOF.....	152
Figure 19 Chemical structures of seven known bibenzyls from <i>Dendrobium</i> plants	173
Figure 20 Flow cytometry analysis.....	179

Figure 21 Bar graphs show the mean frequency (%) of inflammatory cytokines (TNF- α , IL-2 and IFN- γ) expression in T cells, monocytes and B cells after 4 h incubation with 1, 5, 10 or 20 μ M seven known bibenzyls with or without LPS stimulation.....	180
Figure 22 (A) Dot plots demonstrate gating strategy from flow cytometry in cytotoxicity staining with Annexin V and 7-AAD in human PBMCs used to obtain CD45 cells (G4) and determine the apoptosis state including live cells (G5), early (G6) and late apoptosis (G7). (B) Bar graphs show the mean frequency (%) changes of live cells and apoptosis state in human PBMCs treated with bibenzyl compounds 3 , 4 and DMSO, compared with only cells with medium.....	183
Figure 23 Deep immune profiling using CyTOF.....	186
Figure 24 Ethical number for studying in human cells.....	194
Figure 25 Permission for reusing the research article in this dissertation.....	195
Figure 26 The Flow chart of the extraction steps from <i>D. crumenatum</i>	196
Figure 27 ^1H NMR spectrum of dendrocruenenol A (1) (500 MHz) in acetone- d_6	197
Figure 28 ^{13}C NMR spectrum of dendrocruenenol A (1) (125 MHz) in acetone- d_6	197
Figure 29 HSQC spectrum of dendrocruenenol A (1) in acetone- d_6	198
Figure 30 COSY spectrum of dendrocruenenol A (1) in acetone- d_6	198
Figure 31 HMBC spectrum of dendrocruenenol A (1) in acetone- d_6	199
Figure 32 NOESY spectrum of dendrocruenenol A (1) in acetone- d_6	199
Figure 33 HR-ESI-MS spectrum of dendrocruenenol A (1).....	200
Figure 34 IR spectrum of dendrocruenenol A (1).....	200
Figure 35 ^1H NMR spectrum of dendrocruenenol B (2) (300 MHz) in acetone- d_6	201
Figure 36 ^{13}C NMR spectrum of dendrocruenenol B (2) (75 MHz) in acetone- d_6	201
Figure 37 HSQC spectrum of dendrocruenenol B (2) in acetone- d_6	202
Figure 38 NOESY spectrum of compound DPR-6 (in acetone- d_6).....	202
Figure 39 HMBC spectrum of compound DPR-6 (in acetone- d_6).....	203
Figure 40 HR-ESI-MS spectrum of dendrocruenenol B (2).....	203
Figure 41 IR spectrum of dendrocruenenol B (2).....	204
Figure 42 ^1H NMR spectrum of dendrocruenenol C (3) (500 MHz) in acetone- d_6	204

Figure 43 ^{13}C NMR spectrum of dendrocumenol C (3) (125 MHz) in acetone- d_6	205
Figure 44 HSQC spectrum of dendrocumenol C (3) in acetone- d_6	205
Figure 45 COSY spectrum of dendrocumenol C (3) in acetone- d_6	206
Figure 46 HMBC spectrum of dendrocumenol C (3) in acetone- d_6	206
Figure 47 NOESY spectrum of dendrocumenol C (3) in acetone- d_6	207
Figure 48 HR-ESI-MS spectrum of dendrocumenol C (3).....	207
Figure 49 IR spectrum of dendrocumenol C (3).....	208
Figure 50 ^1H NMR spectrum of dendrocumenol D (4) (300 MHz) in CDCl_3	208
Figure 51 ^{13}C NMR spectrum of dendrocumenol D (4) (75 MHz) in CDCl_3	209
Figure 52 HSQC spectrum of dendrocumenol D (4) in CDCl_3	209
Figure 53 COSY spectrum of dendrocumenol D (4) in CDCl_3	210
Figure 54 HMBC spectrum of dendrocumenol D (4) in CDCl_3	210
Figure 55 NOESY spectrum of dendrocumenol D (4) in CDCl_3	211
Figure 56 ^1H NMR spectrum of dendrocumenol D (4) (500 MHz) in acetone- d_6	211
Figure 57 ^{13}C NMR spectrum of dendrocumenol D (4) (125 MHz) in acetone- d_6	212
Figure 58 HSQC spectrum of dendrocumenol D (4) in acetone- d_6	212
Figure 59 HMBC spectrum of dendrocumenol D (4) in acetone- d_6	213
Figure 60 NOESY spectrum of dendrocumenol D (4) in acetone- d_6	213
Figure 61 HR-ESI-MS spectrum of dendrocumenol D (4).....	214
Figure 62 IR spectrum of dendrocumenol D (4).....	214

ABBREVIATIONS and SYMBOLS

AP-1	=	Activator protein 1
AMPK	=	Adenosine monophosphate-activated protein kinase
α	=	Alpha
β	=	Beta
BuOH	=	Butanol
Ca^{2+}	=	Calcium
^{13}C	=	Carbon
$^{\circ}\text{C}$	=	Celsius
δ	=	Chemical shift
CKD	=	Chronic kidney disease
CLRs	=	C-type lectin receptors
CNS	=	Central nervous system
COPD	=	Chronic obstructive pulmonary disease
COSY	=	Homonuclear correlation spectroscopy
CRAC	=	Ca^{2+} -release activated Ca^{2+}
J	=	Coupling constant
CC	=	Column chromatography
CyTOF	=	High-dimensional single-cell mass cytometry
DAMPs	=	Danger-associated molecular patterns
DSS	=	Dextran sulfate sodium
CH_2Cl_2	=	Dichloromethane
DMSO	=	Dimethylsulfoxide
d	=	Doublet
dd	=	Double doublets
ECD	=	Electronic circular dichroism
EDTA	=	Ethylenediaminetetraacetic acid

EGCG	=	Epigallocatechin gallate
ER	=	Endoplasmic reticulum
ERK	=	Extracellular signal-regulated kinase
EtOAc	=	Ethyl acetate
FA	=	Formaldehyde
FBS	=	Fetal bovine serum
γ	=	Gamma
g	=	Gram
Hz	=	Hertz
HMBC	=	Heteronuclear multiple bond correlation
HSQC	=	Heteronuclear single quantum coherence
HR-ESI-MS	=	High-resolution electrospray ionization mass spectrometry
OH	=	Hydroxyl
IBD	=	Inflammatory bowel diseases
IFN	=	Interferon
I κ B	=	Inhibitory κ B
IKK	=	Inhibitory κ B kinase
IL	=	Interleukin
Iono	=	Ionomycin
IP ₃	=	Inositol-1,4,5-trisphosphate
IR	=	Infrared
IRAK	=	IL-1 receptor-associated kinase
IRF	=	Interferon regulatory factor
JAK	=	Janus kinase
JNK	=	c-Jun N-terminal kinase
λ	=	Lambda
L	=	Liter
LPS	=	Lipopolysaccharide

MAPK	=	Mitogen-activated protein kinase
MDA	=	Malondialdehyde
MeO	=	Methoxy
μ	=	Micro
mg	=	Milligram
mL	=	Milliliter
min	=	Minutes
ϵ	=	Molar absorptivity
$\Delta\epsilon$	=	Molar circular-dichroic absorption
MS	=	Multiple sclerosis
MyD88	=	Myeloid differentiation primary response protein 88
<i>m/z</i>	=	Mass per charge ratio
NFAT	=	Nuclear factor of activated T cells
NF- κ B	=	Nuclear factor kappa B
NLRs	=	NOD-like receptors
NMR	=	Nuclear magnetic resonance
NOESY	=	Nuclear Overhauser effect spectroscopy
NO	=	Nitric oxide
ORAI	=	Calcium release-activated calcium modulator
PAMPs	=	Pathogen-associated molecular patterns
PBS	=	Phosphate buffered saline
PBMCs	=	Peripheral blood mononuclear cells
PMA	=	Phorbol-12-myristate-13-acetate
PRRs	=	Pattern-recognition receptors
^1H	=	Proton
ppm	=	Parts per million
RIG	=	Retinoic acid-inducible gene
RIP	=	Receptor-interacting protein
RLRs	=	Retinoic acid-inducible gene-I-like receptors

RPMI	=	Roswell Park Memorial Institute
SOCE	=	Store-operated Ca ²⁺ entry
STAT	=	Signal transducer and activator of transcription
STIM	=	Stromal interaction molecule
TAB	=	TAK1-binding protein
TAK	=	Transforming growth factor- β -activated kinase
TBK	=	TANK-binding kinase
TCM	=	Traditional Chinese medicine
TCR	=	T cells receptor
Th	=	T helper
TICAM-1	=	TIR domain-containing adaptor molecule 1
TICAM-2	=	TIR domain-containing adaptor molecule 2
TIR	=	Toll/interleukin-1 receptor/resistance protein
TLC	=	Thin-layer chromatography
TLRs	=	Toll-like receptors
TNF	=	Tumor necrosis factor
TRAF	=	Tumor necrosis factor receptor-associated factor
TRIF	=	TIR-domain containing adapter-inducing IFN- β
TRAM	=	TIR domain-containing adaptor molecule 2
UBC	=	ubiquitin-conjugating enzyme
UV	=	Ultraviolet
VLC	=	Vacuum-liquid chromatography
H ₂ O	=	Water

CHAPTER I

INTRODUCTION

Rationale

Inflammation is the biological process which responds to the harmful conditions and stimuli such as tissue damage, infections and toxic substances and maintains the tissue homeostasis steadily (Medzhitov, 2008; Serhan, 2017). The inflammatory response is also associated with innate immune cells including neutrophils, dendritic cells, macrophages and monocytes (Muszynski et al., 2016). These immune cells also regulate the inflammation through interaction with endogenous and exogenous molecules (Nowarski et al., 2013). In addition, the dysregulated inflammatory response can induce acute and chronic inflammation resulting to cause several diseases, for instance, cardiovascular diseases, immune disorders, pancreatitis, hepatitis, chronic kidney disease (CKD), asthma and chronic obstructive pulmonary disease (COPD), inflammatory bowel diseases (IBD) and central nervous system diseases (Parkinson's disease and Alzheimer's disease) (Chen et al., 2018; Roe, 2021; Shukla et al., 2021; Sorriento & Iaccarino, 2019). Innate immune cells express the receptors which recognize pathogens such as lipopolysaccharide (LPS), known as pathogen-associated molecular patterns (PAMPs) or danger-associated molecular patterns (DAMPs) from tissue damages (Amarante-Mendes et al., 2018; Tang et al., 2012). The interaction between the pathogens or PAMPs with the immune receptors also activates several intracellular signals, for example, intracellular phosphorylated molecules and store-operated Ca^{2+} entry (SOCE) pathway resulting in the increasing of inflammatory cytokines production such

as interleukin-2 (IL-2) and interferon-gamma (IFN- γ) and tumor necrosis factor (TNF) (Machura et al., 2007; Phongpreecha et al., 2020; Shaw & Feske, 2012).

Human peripheral blood mononuclear cells (PBMCs), isolated from the whole blood using density gradient centrifugation, are common widely used in toxicology and inflammatory studies (Klinder et al., 2018; Obasanmi et al., 2023; Puleo et al., 2017). To stimulate the inflammatory condition in PBMCs, LPS and phorbol-12-myristate-13-acetate/ionomycin (PMA/Iono) are usually used for inducing the inflammatory response resulting to increase the expression of inflammatory cytokines (Ngkelo et al., 2012; Ye et al., 2011). Therefore, the inhibition of the inflammatory mediators in human PBMCs is considered as a model for anti-inflammatory activity (Leelawat & Leelawat, 2018; Ramírez-Pérez et al., 2020).

To regulate the inflammatory cytokines expression in the immune cells is the target of anti-inflammation. Nowadays, there are several natural products or active compounds showed the potential anti-inflammation based on immune modulatory effects. The phytochemical constituents act through many pathways such as enhancing the immune response, decreasing inflammatory cytokines secretion and inhibition of inflammation-associated genes expression (Haddad et al., 2005; Moudgil & Venkatesha, 2022; Zhong et al., 2022). These active compounds which showed immune modulatory effects in *in vitro*, *in vivo* and clinical trials were isolated from various plants such as *Vitis vinifera*, *Curcuma longa*, *Camellia sinensis* and so on (Chugtai et al., 2018; Moudgil & Venkatesha, 2022; Zhong et al., 2022).

Dendrobium genus is one of the largest genera in the Orchidaceae family and discovered more than 1,500 species around Asia and Australia (Pridgeon et al., 2014; Wang et al., 2020). The phytochemical investigations of *Dendrobium* species have been reported and divided to several phytochemical groups such as bibenzyls,

phenanthrenes, terpenoids, alkaloids, phenolics and polysaccharide (He et al., 2020; Lam et al., 2015). Furthermore, the secondary metabolites from this genus have been showed the various pharmacological activities such as anticancer, antidiabetic, antibacterial, hepatoprotective and neuroprotective, antioxidant, anti-inflammatory and immune modulatory activity (Lam et al., 2015; Teixeira da Silva & Ng, 2017).

A number of immune modulatory compounds from *Dendrobium* plants have been showed in many studies. For instance, polysaccharides from *Dendrobium officinale* Kimura et Migo and water extracts from *Dendrobium thysiflorum* B.S.Williams showed immune modulatory effects in THP-1 and RAW264.7 macrophage cells, respectively (Qiang et al., 2018; M. Zhang et al., 2018). Moreover, the potent immunomodulatory constituents such as polysaccharides from *Dendrobium devonianum* and *D. officinale* have been reported in the mice models (Sun et al., 2022; Wei et al., 2022; Xie et al., 2022). Particularly, a bibenzyl derivative, 4,5-dihydroxy-3,3',4'-trimethoxybibenzyl, from *Dendrobium lindleyi* Steud. exhibited the downmodulation of the TNF expression in monocytes in human PBMCs (Khoonrit et al., 2020). Based on the immunomodulatory activity from *Dendrobium* species, the bibenzyl and isolated compounds from *Dendrobium* plants showed potent anti-inflammation and immunomodulatory effects. Therefore, in this dissertation, the isolated compounds from *Dendrobium crumenatum* and bibenzyl compounds from *Dendrobium* species were selected for investigating of anti-inflammatory activities based on immune modulatory effects in human PBMCs. The research article “**Immunomodulatory effects of new phenanthrene derivatives from *Dendrobium crumenatum***” published in *Journal of Natural Products* and the manuscript “**Diverse modulatory effects of bibenzyls from *Dendrobium* species**

on human immune cell responses under inflammatory conditions” submitted into the journal were included in this dissertation.

Objectives

1. To isolate the chemical constituents from *Dendrobium crumenatum* and determine the chemical structure of each isolated compound.
2. To investigate the anti-inflammation based on immunomodulatory effect of *D. crumenatum*'s compounds in PMA/Iono-treated human PBMCs and mechanism of action.
3. To determine the immune modulatory activity of known bibenzyl compounds from *Dendrobium* plants in LPS-treated human PBMCs and mechanism of action.

Hypothesis

1. The chemical constituents of *D. crumenatum* might be isolated and elucidated the structure of each compound.
2. The active compounds from *D. crumenatum* could be shown the anti-inflammation based on immunomodulatory effect in PMA/Iono-treated human PBMCs through decreasing of activated T cells.
3. The bibenzyl compounds from *Dendrobium* species could exhibit immune modulatory activity in LPS-treated human PBMCs through reduction of inflammatory immune cells.

Scope

The chemical constituents were isolated from *Dendrobium crumenatum* and elucidated the structures using spectroscopic data. These isolated compounds were tested in anti-inflammation and immunomodulatory effects in PMA/Iono-treated

human PBMCs. In addition, the known bibenzyls from *Dendrobium* plants were determined the immune modulatory activity in LPS-treated human PBMCs and investigated the related inflammatory immune cells.

Benefits

This study can be the information of *Dendrobium*'s phytochemical studies and for developing to herbal medicine for treatment of inflammatory diseases.



CHAPTER II

LITERATURE REVIEWS

2.1 Pathways of inflammation

Inflammation is the defense mechanism associated with immune cells including neutrophils, dendritic cells, macrophages and monocytes and immune response against irritant such as pathogens, toxic substances or damaged cells (Medzhitov, 2010; Muszynski et al., 2016). It responds to cellular changing and results to recovery the damaged tissues. If the cause of inflammation is still remained or the abnormality of control mechanisms is occurred, it can be developed to various chronic diseases such as cardiovascular diseases, immune disorders, pancreatitis, hepatitis, chronic kidney disease (CKD), asthma and chronic obstructive pulmonary disease (COPD), inflammatory bowel diseases (IBD) and central nervous system diseases (Parkinson's disease and Alzheimer's disease) (Chen et al., 2018; Roe, 2021; Shukla et al., 2021; Sorriento & Iaccharino, 2019). The inflammation that is occurred by the immune response can react to microbes with conserved motifs called pathogen associated molecular patterns (PAMPs) (Geremia et al., 2014). The microbial antigens such as lipopolysaccharide (LPS) are recognized by the receptors, known as pattern-recognition receptors (PRRs) which classified to four different classes including C-type lectin receptors (CLRs) and Toll-like receptors (TLRs) which found in transmembrane, and Retinoic acid-inducible gene (RIG)-I-like receptors (RLRs) and NOD-like receptors (NLRs) which found in cytoplasm (Takeuchi & Akira, 2010). TLRs are mainly found in immune cells such as monocytes, macrophages and dendritic cells and represent ten groups in mammals, especially TLR4 (Hari et al., 2010). LPS, the endotoxins from gram-negative bacteria, is recognized by TLR4 on the cell surface and promotes various signaling cascades resulting to increase the production of the pro-inflammatory cytokines (Mazgaen & Gurung, 2020). Several functional proteins have been reported for interaction with TLRs such as myeloid

differentiation primary response protein 88 (MyD88), Toll/interleukin-1 receptor/resistance protein (TIR) domain-containing adaptor protein including MyD88 adaptor-like protein, known as Mal, TIR domain-containing adaptor molecule 1 or TIR-domain containing adapter-inducing IFN- β (TICAM-1 or TRIF) and TIR domain-containing adaptor molecule 2 (TICAM-2 or TRAM) is important for cell signaling (O'Neill et al., 2003). The MyD88 is mainly interacted with most of TLRs. TLR signaling cascade is mainly divided into two pathways including the MyD88-dependent and MyD88-independent pathways (Joosten et al., 2016).

MyD88 is the main protein for all TLRs downstream signaling except TLR3 (Akira et al., 2006). After the recognition from TLR4, MyD88 is linked to TLR by bridging of Mal and binds with IL-1 receptor-associated kinase (IRAK)-4 and IRAK1/2 to form Myddosome which is necessary for immune response against inflammation (Lin et al., 2010). Further downstream, the IRAK complex from Myddosome formation interacts with tumor necrosis factor receptor-associated factor 6 (TRAF6). Then, TRAF6 interacts with transforming growth factor- β -activated kinase 1 (TAK1) and forms complex with TAK1-binding protein 1 (TAB1), TAB2, and TAB3 by the ubiquitin-conjugating enzyme 13 (UBC13) and ubiquitin-conjugating enzyme variant 1A (UEV1A) (Chen, 2012). After that, TAK1 activates two different cascades including inhibitory κ B (I κ B) kinase (IKK) in nuclear factor kappa B (NF- κ B) and mitogen-activated protein kinases (MAPK) pathways (Wang et al., 2001). TAK1 binds to IKK complex including IKK α , IKK β and IKK γ and activates NF- κ B inhibitory protein I κ B phosphorylation resulting in degradation of proteasome and releasing the transcription factor NF- κ B. Then, the free NF- κ B translocates into the nucleus and regulates the expression of proinflammatory cytokine genes (O'Neill & Bowie, 2007). Moreover, TAK1 also activates the MAPK members including extracellular signal-regulated kinase (ERK), c-Jun N-terminal kinase (JNK) and p38 resulting to activates the activator protein 1 (AP-1) (Vallejo, 2011). The activation of AP-1 and NF- κ B via MyD88 can regulate the expression of proinflammatory cytokines such as TNF- α , interleukin 1 and 6 (IL-1 and IL-6) (Terrell et al., 2006).

The second main pathway of TLR signaling is the MyD88-independent pathway or TRIF-dependent pathway. TLR is initiated linked with TRIF and connected to TRAM (Fitzgerald et al., 2003). Then, TRIF associated with TRAM reacts with TRAF3 to activate TANK-binding kinase 1 (TBK1) and IKK ϵ resulting to phosphorylate the interferon regulatory factor 3 (IRF3) and activate IRAK1 and IKK ϵ resulting to phosphorylate the interferon regulatory factor 7 (IRF7) (Tatematsu et al., 2010). Activated IRFs dimers translocate to nucleus and increase the expression of IFN genes (Tenover et al., 2007). Furthermore, TRIF can promote the NF- κ B in MyD88-independent pathway through the same pathway of MyD88-dependent via the activation of TRAF6 and TAK1 (Sato et al., 2003). Moreover, TRIF can bind the adapter receptor-interacting protein 1 (RIP1) resulting to activate the NF- κ B and translocate into nucleus to promote several proinflammatory cytokine genes (Gay et al., 2014).

Moreover, LPS can induce the inflammatory response in the immune cells through the phosphorylated molecules such as phosphorylated signal transducer and activator of transcription 3 and 5 (pSTAT3 and pSTAT5) in the Janus kinase/signal transducer and activator of transcription (JAK/STAT) pathway (Cacciapaglia et al., 2020; Phongpreecha et al., 2020).

Otherwise, phorbol 12-myristate 13-acetate (PMA), a potent inflammatory agent, is used to stimulate the inflammatory condition in PBMCs (Chang et al., 2020). PMA/Iono stimulation is related to the complex signaling of T cells receptor (TCR). PMA stimulates the inflammatory proteins such as IKK and MAPK, while ionomycin activates the calcineurin and the level of intracellular Ca²⁺ (Macián et al., 2002). These two stimulations also activate the intracellular molecules including NF- κ B, AP-1 and nuclear factor of activated T cells (NFAT) resulting to induce the expression of inflammatory cytokines such as IL-2 and IFN- γ (Brignall et al., 2017; Macián et al., 2002).

2.2 Store-operated calcium entry (SOCE) pathway

PMA/Iono not only activates the inflammatory pathway through NF- κ B and MAPK but also stimulates the expression of inflammatory cytokines through the activation of intracellular Ca^{2+} level via SOCE pathway (Haverstick et al., 1997). The activation of TCR in T cells transfers the second signaling molecules, inositol-1,4,5-trisphosphate (IP_3) (Prakriya & Lewis, 2015). Subsequently, IP_3 bind to IP_3 receptors (IPRs) at the endoplasmic reticulum (ER) which are the permeable Ca^{2+} channels (Feske et al., 2015). IPRs are then opening resulting in the decreasing of the Ca^{2+} level in ER (Prakriya & Lewis, 2015). After that, the stromal interaction molecule 1 and 2 (STIM1 and STIM2) in ER which changing the conformation bind to and open the Ca^{2+} -release activated Ca^{2+} (CRAC) channel including calcium release-activated calcium modulator 1, 2 and 3 (ORAI1, ORAI2 and ORAI3) in plasma membrane resulting in the Ca^{2+} influx, called store-operated Ca^{2+} entry (SOCE) (Avila-Medina et al., 2018). The Ca^{2+} influx also activates calcineurin to dephosphorylate NFAT which translocate to nucleus and then activates the several intracellular molecules resulting to promote the cytokines expression (Hann et al., 2020).

2.3 Natural products for anti-inflammation based on immune modulatory effects

Nowadays, there are several natural products or active compounds showed the potential anti-inflammation based on immune modulatory effects via many pathways such as promoting the immune response and reduction of inflammatory gene expression and cytokines secretion (Haddad et al., 2005; Moudgil & Venkatesha, 2022; Zhong et al., 2022). For example, parthenolide, a sesquiterpene lactone, from *Tanacetum parthenium* L. (feverfew) exhibited significant reduction of the inflammatory cytokines secretion including interleukin-1 (IL-1), IL-6, TNF- α and prostaglandin E2 (PGE2) in LPS-induced human PBMCs (Shah et al., 2010). A stilbene named resveratrol from *Vitis vinifera* or *Polygonum cuspidatum* can activate adenosine monophosphate-activated protein kinase (AMPK) and sirtuin-1 resulting to

inhibit NF- κ B function in T cells and also inhibit TLR expression NF- κ B activity in dendritic cells (Malaguarnera, 2019). In dextran sulfate sodium (DSS)-induced colitis model, resveratrol deduced the infiltration of T cells and neutrophils in lamina propria and lymph nodes and inhibited p53 and NF- κ B pathway (Singh et al., 2010). Furthermore, resveratrol demonstrated strong inhibition of IL-1, IL-6, TNF- α and malondialdehyde (MDA) level and increasing of glutathione level in monocytes isolated from PBMCs of myocardial infarction patients (Chugtai et al., 2018). In addition, curcumin from *Curcuma longa* diminished the production of IL-6 and IL-23 in dendritic cells, reduced IL-17 production in T cells and inhibited IFN- γ production through modulating the STAT4 function (Fahey et al., 2007; Zhao et al., 2017). Moreover, curcumin showed the reduction of IL-12 through inhibition of STAT3, STAT4 and JAK2 in JAK-STAT pathway in multiple sclerosis mice model and decreased the inflammatory cytokines including IL-7, IL-15 and IL-21 via blocking JAK1 and STAT5 (Natarajan & Bright, 2002; Zhong et al., 2021). Boswellic acids, pentacyclic triterpenes, isolated from the gum resin of the *Boswellia* genus exhibited the inhibition of IFN- γ and IL-2 production in T cells (Chevrier et al., 2005). Epigallocatechin gallate (EGCG), a polyphenol catechin from tea, suppressing the TNF- α and IFN- γ expressed levels in the joints of mice and inhibited the IL-17 and IFN- γ production from T cells in multiple sclerosis mouse model (Byun et al., 2014; Sun et al., 2013). In DSS-induced colitis model, EGCG showed anti-inflammatory and immunomodulatory activities through many pathways including deduction of TNF- α , decreasing of IL-6 and IL-17 through the blocking of STAT3 expression and inhibition of inflammatory cytokines via mediation of TLR4/MyD88 and NF- κ B pathway (Bing et al., 2017; Oz et al., 2013; Xu et al., 2015). A diterpene triperoxide, triptolide, from Chinese herb *Tripterygium wilfordii* Hook f. exhibited the inhibition of IL-2 and IFN- γ production in human T cells (Chan et al., 1999). Triptolide also decreased IL-6, IL-1b and TNF- α though inhibition of JAK2 and STAT3 in arthritic rats and inhibited the p-I κ B α level of NF- κ B pathway in multiple sclerosis mice model (Fan et al., 2016; Wang et al., 2008). In SOCE model,

ellagic acid showed significant suppressing of IL-2 and IFN- γ expression levels through inhibition of SOCE-mediated Ca²⁺ influx in T cells (Murphy et al., 2020).

2.4 *Dendrobium* genus: Phytochemical and biological activities

Dendrobium is one of the largest genera in Orchidaceae family distributed around Asia and Australia with more than 1,500 species (Pridgeon et al., 2014; Wang et al., 2020). *Dendrobium* plants such as *Dendrobium nobile*, *Dendrobium chrysotoxum* Lindl. And *Dendrobium officinale* Kimura et Migo and their various parts have been used as folk medicine in many Asian countries for a long time (Mou et al., 2021). For instance, *Dendrobium* plants are known as “Shi hu” in China and have been used as traditional Chinese medicine (TCM) for treatment various symptoms such as reducing fever, nourishing Yin, promoting the production of body fluids and enhancing the immunity (Lin et al., 2018; Yang, Wang, et al., 2006b). In Thailand, they found *Dendrobium draconis* Rchb.f. used as a blood tonic in traditional medicine (Ng et al., 2012). Moreover, *D. officinale* was approved by China FDA to use as medicinal materials and other three plants including *Dendrobium fimbriatum* Hook., *D. chrysotoxum* and *D. nobile* are available for clinical usage (Y. Wang et al., 2019).

In Thailand, *Dendrobium* plants have been discovered and reported more than 100 species as follows (Herbarium, 2014; Phueakhlai et al., 2018; Rujichaiyimon et al., 2019).

<i>Dendrobium acerosum</i> Lindl.	กล้วยไม้มีอนาง Kluai mai mue nang
<i>D. aciculare</i> Lindl.	เอื้องใบเข็ม
<i>D. acinaciforme</i> Roxb.	เอื้องยอดสร้อย Ueang yot soi
<i>D. aduncum</i> Lindl.	N/A
<i>D. albosanguineum</i> Lindl.	เอื้องตางัว Ueang ta ngua
<i>D. aloifolium</i> (Blume) Rchb.f.	เอื้องมณี Ueang mani
<i>D. anceps</i> Sw.	N/A

<i>D. angulatum</i> Lindl.	N/A
<i>D. anosmum</i> Lindl.	เอื้องสาย Ueang sai
<i>D. aphyllum</i> (Roxb.) C.E.C. Fisch.	เอื้องวงช้าง Ueang nguang chang
<i>D. bellatulum</i> Rolfe	เอื้องแซะภู Ueng sae phu
<i>D. bensoniae</i> Rchb.f.	เอื้องสายดอกขาว
<i>D. bicameratum</i> Lindl.	เอื้องเข็ม Ueang khem
<i>D. bifarium</i> Lindl.	N/A
<i>D. bilobulatum</i> Seidenf.	กล้วยไม้ก้างปลา Klui mai kang pla
<i>D. blumei</i> Lindl.	N/A
<i>D. brevimentum</i> Seidenf.	N/A
<i>D. brymerianum</i> Rchb.f.	เอื้องคำฝอย Ueang kham foi
<i>D. calicopsis</i> Ridl.	N/A
<i>D. capillipes</i> Rchb.f.	เอื้องคำกิว Ueang kham kio
<i>D. cariniferum</i> Rchb.f.	เอื้องกาจก Ueang kachok
<i>D. chittimae</i> Seidenf.	เอื้องจิตติมา Ueang chittima
<i>D. christyanum</i> Rchb.f.	เอื้องแซะภูกระดิ่ง Ueang sae phu kradueng
<i>D. chrysanthum</i> Lindl.	เอื้องสายมรกต Ueang sai morakot
<i>D. chrysocrepis</i> C.S.P.Parish & Rchb.f. ex Hook.f.	เอื้องถุงทอง Ueang thung thong
<i>D. chrysotoxum</i> Lindl.	เอื้องคำ Ueang kham
<i>D. ciliatilabellum</i> Seidenf.	หวายเขาเขี้ยว Wai khao khiao
<i>D. clavator</i> Ridl.	N/A
<i>D. compactum</i> Rolfe ex Hackett	เอื้องข้าวตอก Ueang khao tok

<i>D. compressum</i> Lindl.	หวายแบนตะนาวศรี Wai baen tanao si
<i>D. concinnum</i> Miq.	หางเปีย Hang pia
<i>D. confinale</i> Kerr	N/A
<i>D. cowenii</i> P. O'Byrne & J.J. Verm.	N/A
<i>D. crepidatum</i> Lindl. & Paxton	เอื้องสายน้ำเขียว Ueang sai nam khiao
<i>D. cretaceum</i> Lindl.	N/A
<i>D. crocatum</i> Hook.f.	เอื้องนางนวล Ueang nang nuan
<i>D. cruentum</i> Rchb.f.	เอื้องนกแก้ว Ueang nok kaeo
<i>D. crumenatum</i> Sw.	หวายตะมอย Wai tamoi
<i>D. crystallinum</i> Rchb.f.	เอื้องนางพ่อน Ueang nang fon
<i>D. cumulatum</i> Lindl.	เอื้องสายสีดอก Ueang sai si dok
<i>D. curviflorum</i> Rolfe	N/A
<i>D. cuspidatum</i> Lindl.	เอื้องข้าวตอกปากแหลม
<i>D. dantaniense</i> Guillaumin	เอื้องเข็ม Ueang khem
<i>D. delacourii</i> Guillaumin	เอื้องดอกมะขาม Ueang dok ma kham
<i>D. deltatum</i> Seidenf.	N/A
<i>D. denneanum</i> Kerr	N/A
<i>D. densiflorum</i> Lindl.	เอื้องมอนไข่ Ueang mon khai
<i>D. denudans</i> D. Don	เอื้องสายจำปา Ueang sai champa
<i>D. devonianum</i> Paxton	เอื้องเมียง Ueang miang
<i>D. dickasonii</i> L. O. Williams	เอื้องเคี้ยว Ueang khia
<i>D. dixanthum</i> Rchb.f.	เอื้องเทียน Ueang thian

<i>D. dixonianum</i> Rolfe ex Downie	เอื้องข้าวตอกเหลือง
<i>D. draconis</i> Rchb.f.	เอื้องเงิน Ueang ngoen
<i>D. elliotianum</i> P. O'Byrne	หวายเจดีย์ Wai chedi
<i>D. ellipsophyllum</i> Tang & Wang	เอื้องทอง Ueang thong
<i>D. erostelle</i> Seidenf.	N/A
<i>D. erosum</i> (Blume) Lindl.	N/A
<i>D. eserre</i> Seidenf.	N/A
<i>D. exile</i> Schltr.	เอื้องเสียน Ueang sian
<i>D. falconeri</i> Hook.	เอื้องสายวิสูตร Ueang sai wisut
<i>D. farmeri</i> Paxton	เอื้องมัจฉาญ Ueang matchanu
<i>D. fimbriatum</i> Hook.	เอื้องค้ำน้อย Ueang kham noi
<i>D. findlayanum</i> C.S.P. Parish & Rchb.f.	พวงหยก Phuang yok
<i>D. flexile</i> Ridl.	N/A
<i>D. formosum</i> Roxb. ex Lindl.	เอื้องเงินหลวง Ueang ngoen luang
<i>D. friedericksianum</i> Rchb.f.	เอื้องเหลืองจันทบูร Ueang lueang chantabun
<i>D. fuerstenbergianum</i> Schltr.	เอื้องแซะภูกระดึง Ueang sae phukradueng
<i>D. fyychianum</i> Bateman ex Rchb.f.	หวายพม่า Wai phama
<i>D. garrettii</i> Seidenf.	หวายการ์เรต Wai karet
<i>D. gibsonii</i> Paxton	เอื้องค้ำสาย Ueang kham sai
<i>D. grande</i> Hook.f.	เอื้องแพงใบใหญ่ Ueang pheang bai yai
<i>D. gratiotissimum</i> Rchb.f.	เอื้องกิงดำ Ueang king dam
<i>D. gregulus</i> Seidenf.	เอื้องมะต้อม Ueang ma tom

<i>D. griffithianum</i> Lindl.	เอื้องมัจฉาณู Ueang matchanu
<i>D. harveyanum</i> Rchb.f.	เอื้องคำฝอย Ueang kham foi
<i>D. hendersonii</i> Hawkes & Heller	หวายตะมอยน้อย Wai tamoi noi
<i>D. henryi</i> Schltr.	เอื้องสุริยัน Ueang suriyan
<i>D. hercoglossum</i> Rchb.f.	เอื้องดอกมะเขือ Ueang dok ma kuea
<i>D. heterocarpum</i> Lindl.	เอื้องสีตาล Ueang si tan
<i>D. hymenanthum</i> Rchb.f.	เอื้องน้อยกลีบบาง Ueang noi klip bang
<i>D. hymenopterum</i> Hook.f.	N/A
<i>D. incurvum</i> Lindl.	N/A
<i>D. indivisum</i> (Blume) Miq. var. <i>indivisum</i>	ตานเสี้ยนไม้ Tan sian mai
<i>D. indivisum</i> (Blume) Miq. var. <i>lampangense</i> Rolfe	N/A
<i>D. indivisum</i> (Blume) Miq. var. <i>pallidum</i> Seidenf.	ก้างปลา Kang pla
<i>D. indragiriense</i> Schltr.	N/A
<i>D. infundibulum</i> Lindl.	เอื้องตาเหิน Ueang ta hoen
<i>D. intricatum</i> Gagnep.	เอื้องชมพู Ueang chomphu
<i>D. jenkinsii</i> Wall. ex Lindl.	เอื้องผึ้งน้อย Ueang phueng noi
<i>D. kanburiense</i> Seidenf.	หวายเมืองกาญจน์ Wai muang kan
<i>D. keithii</i> Ridl.	หางเปีย Hang pia
<i>D. kentrophyllum</i> Hook.f.	ก้างปลาใหญ่
<i>D. kontumense</i> Gagnep.	เอื้องเงินวิลาศ Ueang ngoen wilat

<i>D. kratense</i> Kerr	N/A
<i>D. lagarum</i> Seidenf.	N/A
<i>D. lanpongense</i> J.J.Sm.	N/A
<i>D. lamyaiiae</i> Seidenf.	N/A
<i>D. leonis</i> (Lindl.) Rchb.f.	เอื้องตะขาบใหญ่ Ueang ta khap yai
<i>D. lindleyi</i> Steud.	เอื้องผึ้ง Ueang phueng
<i>D. linguella</i> Rchb.f.	N/A
<i>D. lituiflorum</i> Lindl.	เอื้องสายม่วง Ueang sai muang
<i>D. lueckelianum</i> Fessel & Wolff	N/A
<i>D. mannii</i> Ridl.	เอื้องหางปลา Ueang hang pla
<i>D. metachilinum</i> Rchb.f.	N/A
<i>D. monticola</i> Hunt & Summerh	N/A
<i>D. moschatum</i> (Buch.-Ham.) Sw.	เอื้องจำปา Ueang champa
<i>D. mucronatum</i> Seidenf.	N/A
<i>D. nanocompactum</i> Seidenf.	N/A
<i>D. nathanielis</i> Rchb.f.	เกล็ดน้มนิม Klet nim
<i>D. ochreatum</i> Lindl.	เอื้องตะขาบ Ueang ta khap
<i>D. oligophyllum</i> Gagnep.	ข้าวตอกปราจีน Khao tok prachin
<i>D. pachyglossum</i> Parish & Rchb.f	เอื้องขนหมู Ueang khon mu
<i>D. pachyphyllum</i> (Kuntze) Bakh.f.	เอื้องน้อย Ueang noi
<i>D. palpebrae</i> Lindl.	เอื้องมัจฉา Ueang matcha
<i>D. pandaneti</i> Ridl.	N/A

<i>D. panduriferum</i> Hook.f.	N/A
<i>D. parciflorum</i> Rchb.f. ex Lindl.	เอื้องดอกขาวใบแบน Ueang dok khao bai baen
<i>D. parcum</i> Rchb.f.	เอื้องก้านก๊ว Ueang kan kio
<i>D. parishii</i> Rchb.f.	เอื้องครั่ง Ueang khrang
<i>D. parvum</i> Seidenf.	N/A
<i>D. peguanum</i> Lindl.	หวายเปกู Wai peku
<i>D. pendulum</i> Roxb.	เอื้องไม้เท้าฤๅษี Ueang mai thao ruesi
<i>D. perpaulum</i> Seidenf.	เอื้องข้าวตอกอินทนนท์ Ueang khao tok inthanon
<i>D. planibulbe</i> Lindl.	N/A
<i>D. polyanthum</i> Wall. ex Lindl.	เอื้องสายประสาธ Ueang sai prasat
<i>D. porphyrochilum</i> Lindl.	เอื้องเฉวียน Ueang chawian
<i>D. praecinctum</i> Rchb.f.	หวายภูหลวง Wai phu luang
<i>D. proteranthum</i> Seidenf.	หวายน้อยภูหลวง Wai noi phu luang
<i>D. pulchellum</i> Roxb. ex Lindl.	เอื้องคำตาควาย Ueang kham ta khwai
<i>D. pychnostachyum</i> Lindl.	เศวตสอดสี Sawet sot si
<i>D. rhodostele</i> Ridl.	N/A
<i>D. ruckeri</i> Lindl.	N/A
<i>D. salaccense</i> (Blume) Lindl.	เอื้องใบไผ่ Ueang bai phai
<i>D. sanguinolentum</i> Lindl.	N/A
<i>D. scabrilingue</i> Lindl.	เอื้องแซะ Ueang sae
<i>D. schilhaueri</i> Ormerod & Pedersen	N/A
<i>D. secundum</i> (Blume) Lindl.	เอื้องแปรงสีฟัน Ueang preang si fan

<i>D. senile</i> Parish & Rchb.f.	เอื้องชะนี Ueang chani
<i>D. setifolium</i> Ridl.	N/A
<i>D. signatum</i> Rchb.f.	เอื้องเค้งกีว Ueang khao kio
<i>D. singaporense</i> Hawkes & Heller	N/A
<i>D. sinuatum</i> (Lindl.) Lindl. ex Rchb.f.	N/A
<i>D. sociale</i> J.J.Sm.	N/A
<i>D. strongylanthum</i> Rchb.f.	เอื้องเข้าลม Ueang yao lom
<i>D. stuposum</i> Lindl.	เอื้องสาย Ueang sai
<i>D. subulatum</i> (Blume) Lindl.	N/A
<i>D. sukhakulii</i> hort.	หวายสุขะกุล Wai sukhakun
<i>D. sulcatum</i> Lindl.	เอื้องจำปาน่าน Ueang champa nan
<i>D. superbiens</i> Rchb.f.	หวายคิง Wai khing
<i>D. sutepense</i> Rolfe ex Downie	เอื้องมะลิ Ueang mali
<i>D. terminale</i> Parish & Rchb.f.	เอื้องแพ่งโสภา Ueang phaeng sopha
<i>D. thysiflorum</i> Rchb.f.	เอื้องมอนไขใบมอน Ueang mon khai bai mon
<i>D. tortile</i> Lindl.	เอื้องไม้ตึง Ueang mai tueng
<i>D. trigonopus</i> Rchb.f.	เอื้องคำเหลี่ยม Ueang kham liam
<i>D. trinervium</i> Ridl.	เทียนลิง Thian ling
<i>D. truncatum</i> Lindl.	N/A
<i>D. umbonatum</i> Seidenf.	N/A
<i>D. unicum</i> Seidenf.	เอื้องครั่งแสด Ueang krang saet
<i>D. uniflorum</i> Griff.	เอื้องทอง Ueang thong
<i>D. venustum</i> Teijsm. & Binn	ข้าวเหนียวลิง Khao niao ling

<i>D. villosulum</i> Lindl.	กล้วยห้วยนา Kluai ya na
<i>D. viridulum</i> Ridl.	N/A
<i>D. wardianum</i> R. Warner	เอื้องมณีไตรรงค์ Ueang mani traorong
<i>D. wattii</i> (Hook.f.) Rchb.f.	เอื้องแซะ Ueang sae (
<i>D. williamsonii</i> Day & Rchb.f.	N/A
<i>D. xanthophlebium</i> Lindl.	เอื้องแซะภูลังกา
<i>D. ypsilon</i> Seidenf.	เอื้องแบนปากตัด Ueang baen pak tat (General)

The phytochemical studies of *Dendrobium* plants have been reported and categorized based on the structure of their secondary metabolites such as bibenzyls, phenanthrenes, terpenoids, fluorenones, coumarins and lignans (He et al., 2020; Lam et al., 2015) [Figure 1-8 and Table 1-8].

Table 1 Bibenzyls and derivatives in the *Dendrobium* species.

Compounds	Plant name	Plant part	References
Aloifol I [1]	<i>D. longicornu</i>	Stem	(Hu et al., 2008a)
	<i>D. williamsonii</i>	Whole plant	(M. Yang et al., 2018)
	<i>D. infundibulum</i>	Whole plant	(Na Ranong et al., 2019)
	<i>D. scabrilingue</i>	Whole plant	(Sarakulwattana et al., 2020)
	<i>D. gibsonii</i>	Whole plant	(Thant et al., 2020)
	<i>D. senile</i>	Whole plant	(Pann Phyu et al., 2022)
Amoenylin [2]	<i>D. amoenum</i>	Whole plant	(Majumder et al., 1999)
	<i>D. williamsonii</i>	Whole plant	(M. Yang et al., 2018)
Batatasin [3]	<i>D. longicornu</i>	Stem	(Hu et al., 2008a)
	<i>D. plicatile</i>	Stem	(Yamaki & Honda, 1996)
Batatasin III [4]	<i>D. aphyllum</i>	Whole plant	(Chen, Li, et al., 2008)
		Stem	(Yang et al., 2015)
	<i>D. cariniferum</i>	Stem	(Chen, Liu, et al., 2008)
	<i>D. chrysotoxum</i>	Whole plant	(Y.-P. Li et al., 2009)

Table 1 Bibenzyls and derivatives in the *Dendrobium* species (Continued).

Compounds	Plant name	Plant part	References
Batatasin III [4]	<i>D. draconis</i>	Stem	(Sritularak, Anuwat, et al., 2011)
	<i>D. formosum</i>	Whole plant	(Inthongkaew et al., 2017)
	<i>D. gratiosissimum</i>	Stem	(Zhang et al., 2008)
	<i>D. loddigesii</i>	Stem	(Ito et al., 2010)
	<i>D. venustum</i>	Whole plant	(Sukphan et al., 2014)
	<i>D. infundibulum</i>	Whole plant	(Na Ranong et al., 2019)
	<i>D. scabrilingue</i>	Whole plant	(Sarakulwattana et al., 2020)
	<i>D. plicatile</i>	Stem	(Chen et al., 2020)
Brittonin A [5]	<i>D. secundum</i>	Stem	(Sritularak, Duangrak, et al., 2011)
Chrysotobibenzyl [6]	<i>D. aurantiacum</i> var. <i>denneanum</i>	Stem	(Yang, Wang, et al., 2006a)
	<i>D. capillipes</i>	Stem	(Phechrmeekha et al., 2012)
	<i>D. chrysanthum</i>	Stem	(Yang, Qin, et al., 2006)
	<i>D. chryseum</i>	Stem	(Ma, Wang, Yin, et al., 1998)

Table 1 Bibenzyls and derivatives in the *Dendrobium* species (Continued).

Compounds	Plant name	Plant part	References
Chrysotobibenzyl [6]	<i>D. chrysotoxum</i>	Stem	(Hu et al., 2012)
	<i>D. nobile</i>	Stem	(Zhang et al., 2007)
	<i>D. pulchellum</i>	Stem	(Chanvorachote et al., 2013)
Chrysotoxine [7]	<i>D. aurantiacum</i> var. <i>denneanum</i>	Stem	(Yang, Wang, et al., 2006a)
	<i>D. chrysanthum</i>	Stem	(Yang, Qin, et al., 2006)
	<i>D. chryseum</i>	Stem	(Ma, Wang, Yin, et al., 1998)
	<i>D. nobile</i>	Stem	(Zhang et al., 2007)
	<i>D. pulchellum</i>	Stem	(Chanvorachote et al., 2013)
	<i>D. lindleyi</i>	Whole plant	(Khoonrit et al., 2020)
Crepidatin [8]	<i>D. aurantiacum</i> var. <i>denneanum</i>	Whole plant	(Liu et al., 2009)
	<i>D. capillipes</i>	Stem	(Phechrmeekha et al., 2012)
	<i>D. chrysanthum</i>	Stem	(Yang, Qin, et al., 2006)

Table 1 Bibenzyls and derivatives in the *Dendrobium* species (Continued).

Compounds	Plant name	Plant part	References
Crepidatin [8]	<i>D. crepidatum</i>	Whole plant	(Majumder & Chatterjee, 1989)
	<i>D. crepidatum</i>	Root	(Ding et al., 2021)
	<i>D. nobile</i>	Stem	(Zhang et al., 2007)
	<i>D. pulchellum</i>	Stem	(Chanvorachote et al., 2013)
Cumulatin [9]	<i>D. cumulatum</i>	Whole plant	(Majumder & Pal, 1993)
Dendrobin A [10]	<i>D. nobile</i>	Stem	(Wang et al., 1985)
3,3'-Dihydroxy-4,5-dimethoxybibenzyl [11]	<i>D. williamsonii</i>	Whole plant	(Rungwichaniwat et al., 2014)
	<i>D. infundibulum</i>	Whole plant	(Na Ranong et al., 2019)
3,4'-Dihydroxy-5-methoxybibenzyl [12]	<i>D. amoenum</i>	Whole plant	(Majumder et al., 1999)
	<i>D. catenatum</i>	Stem	(Zhu et al., 2021)
3,4'-Dihydroxy-5,5'-dimethoxydihydrostilbene [13]	<i>D. nobile</i>	Stem	(Hwang et al., 2010)
4,5-Dihydroxy-3,3'-dimethoxybibenzyl [14]	<i>D. nobile</i>	Stem	(Ye & Zhao, 2002)
Erianin [15]	<i>D. chrysotoxum</i>	Stem	(Hu et al., 2012)
	<i>D. terminale</i>	Whole plant	(Cheng et al., 2022)

Table 1 Bibenzyls and derivatives in the *Dendrobium* species (Continued).

Compounds	Plant name	Plant part	References
Gigantol [16]	<i>D. aphyllum</i>	Whole plant	(Chen, Li, et al., 2008)
	<i>D. aurantiacum</i> var. <i>denneanum</i>	Whole plant	(Liu et al., 2009)
	<i>D. brymerianum</i>	Whole plant	(Klongkumnuankarn et al., 2015)
	<i>D. densiflorum</i>	Stem	(Fan et al., 2001)
	<i>D. devonianum</i>	Whole plant	(Sun et al., 2014)
	<i>D. draconis</i>	Stem	(Sritularak, Anuwat, et al., 2011)
	<i>D. formosum</i>	Whole plant	(Inthongkaew et al., 2017)
	<i>D. gratiosissimum</i>	Stem	(Zhang et al., 2008)
	<i>D. loddigesii</i>	Whole plant	(Ito et al., 2010)
	<i>D. longicornu</i>	Stem	(Hu et al., 2008a)
	<i>D. nobile</i>	Stem	(Zhang et al., 2007)
	<i>D. officinale</i>	Stem	(Zhao et al., 2018)
	<i>D. polyanthum</i>	Stem	(Hu et al., 2009)
	<i>D. trigonopus</i>	Stem	(Hu et al., 2008b)
	<i>D. venustum</i>	Whole plant	(Sukphan et al., 2014)
	<i>D. palpebrae</i>	Whole plant	(Kyokong et al., 2019)

Table 1 Bibenzyls and derivatives in the *Dendrobium* species (Continued).

Compounds	Plant name	Plant part	References
Gigantol [16]	<i>D. lindleyi</i>	Whole plant	(Khoonrit et al., 2020)
	<i>D. scabrilingue</i>	Whole plant	(Sarakulwattana et al., 2020)
	<i>D. pachyglossum</i>	Whole plant	(Warinhomhoun et al., 2021)
4-Hydroxy-3,5,3'-trimethoxybibenzyl [17]	<i>D. nobile</i>	Stem	(Ye & Zhao, 2002)
5-Hydroxy-3,4,3',4',5'-pentamethoxybibenzyl [18]	<i>D. secundum</i>	Stem	(Phechrmeekha et al., 2012)
Isoamoenylin [19]	<i>D. amoenum</i>	Whole plant	(Majumder et al., 1999)
Moniliformine [20]	<i>D. williamsonii</i>	Whole plant	(M. Yang et al., 2018)
Moscatilin [21]	<i>D. amoenum</i>	Whole plant	(Majumder et al., 1999)
	<i>D. aurantiacum</i> var. <i>denneanum</i>	Stem	(Yang, Wang, et al., 2006a)
	<i>D. brymerianum</i>	Whole plant	(Klongkumnuankarn et al., 2015)
	<i>D. chrysanthum</i>	Stem	(Yang, Qin, et al., 2006)

Table 1 Bibenzyls and derivatives in the *Dendrobium* species (Continued).

Compounds	Plant name	Plant part	References
Moscatilin [21]	<i>D. densiflorum</i>	Stem	(Fan et al., 2001)
	<i>D. ellipsophyllum</i>	Whole plant	(Tanagornmeatar et al., 2014)
	<i>D. formosum</i>	Whole plant	(Inthongkaew et al., 2017)
	<i>D. gratiosissimum</i>	Stem	(Zhang et al., 2008)
	<i>D. loddigesii</i>	Whole plant	(Chen et al., 1994)
	<i>D. longicornu</i>	Stem	(Hu et al., 2008a)
	<i>D. moscatum</i>	Whole plant	(Majumder & Sen, 1987)
	<i>D. nobile</i>	Stem	(Miyazawa et al., 1999)
	<i>D. polyanthum</i>	Stem	(Hu et al., 2009)
	<i>D. pulchellum</i>	Stem	(Chanvorachote et al., 2013)
	<i>D. secundum</i>	Stem	(Sritularak, Duangrak, et al., 2011)
	<i>D. williamsonii</i>	Whole plant	(M. Yang et al., 2018)
	<i>D. parishii</i>	Whole plant	(Kongkatitham et al., 2018)
<i>D. palpebrae</i>	Whole plant	(Kyokong et al., 2019)	

Table 1 Bibenzyls and derivatives in the *Dendrobium* species (Continued).

Compounds	Plant name	Plant part	References
Moscatilin [21]	<i>D. infundibulum</i>	Whole plant	(Na Ranong et al., 2019)
	<i>D. lindleyi</i>	Whole plant	(Khooonrit et al., 2020)
	<i>D. plicatile</i>	Stem	(Chen et al., 2020)
	<i>D. pachyglossum</i>	Whole plant	(Warinhomhoun et al., 2021)
	<i>D. crepidatum</i>	Root	(Ding et al., 2021)
	<i>D. terminale</i>	Whole plant	(Cheng et al., 2022)
	<i>D. senile</i>	Whole plant	(Pann Phyu et al., 2022)
3,3',4-Trihydroxy bibenzyl [22]	<i>D. longicornu</i>	Stem	(Hu et al., 2008a)
3,3',5-Trihydroxy bibenzyl [23]	<i>D. cariniferum</i>	Whole plant	(Chen, Liu, et al., 2008)
3,5,4'-Trihydroxy bibenzyl [24]	<i>D. gratiosissimum</i>	Stem	(Zhang et al., 2008)
4,5,4'-Trihydroxy-3,3'-dimethoxybibenzyl [25]	<i>D. secundum</i>	Stem	(Sritularak, Duangrak, et al., 2011)
	<i>D. ellipsophyllum</i>	Whole plant	(Tanagornmeatar et al., 2014)

Table 1 Bibenzyls and derivatives in the *Dendrobium* species (Continued).

Compounds	Plant name	Plant part	References
4,5,4'-Trihydroxy-3,3'-dimethoxybibenzyl [25]	<i>D. parishii</i>	Whole plant	(Kongkatitham et al., 2018)
	<i>D. palpebrae</i>	Whole plant	(Kyokong et al., 2019)
	<i>D. parishii</i>	Whole plant	(Kongkatitham et al., 2018)
Tristin [26]	<i>D. palpebrae</i>	Whole plant	(Kyokong et al., 2019)
	<i>D. chrysotoxum</i>	Stem	(Hu et al., 2012)
	<i>D. densiflorum</i>	Stem	(Fan et al., 2001)
	<i>D. gratiosissimum</i>	Stem	(Zhang et al., 2008)
	<i>D. longicornu</i>	Stem	(Hu et al., 2008a)
	<i>D. officinale</i>	Stem	(Zhao et al., 2018)
	<i>D. trigonopus</i>	Stem	(Hu et al., 2008b)
Dendromoniliside E [27]	<i>D. nobile</i>	Stem	(Miyazawa et al., 1999)
4,3',4'-Trihydroxy-3,5-dimethoxybibenzyl [28]	<i>D. parishii</i>	Whole plant	(Kongkatitham et al., 2018)
5,4'-Dihydroxy-3,4,3'-trimethoxybibenzyl [29]	<i>D. infundibulum</i>	Whole plant	(Na Ranong et al., 2019)
4,5-Dihydroxy-3,3',4'-trimethoxybibenzyl [30]	<i>D. lindleyi</i>	Whole plant	(Khoonrit et al., 2020)
2-Chloro-3,4'-dihydroxy-3',5-dimethoxybibenzyl [31]	<i>D. plicatile</i>	Stem	(Chen et al., 2020)

Table 1 Bibenzyls and derivatives in the *Dendrobium* species (Continued).

Compounds	Plant name	Plant part	References
Dendrophenol [32]	<i>D. candidum</i>	Stem	(Li et al., 2008)
	<i>D. crepidatum</i>	Root	(Ding et al., 2021)
3,4-Dihydroxy-5,4'-dimethoxybibenzyl [33]	<i>D. candidum</i>	Stem	(Li et al., 2008)
	<i>D. signatum</i>	Whole plant	(Mittraphab et al., 2016)
	<i>D. signatum</i>	Aerial part	(Khumploy et al., 2021)
	<i>D. tortile</i>	Whole plant	(Limpanit et al., 2016)
	<i>D. infundibulum</i>	Whole plant	(Na Ranong et al., 2019)
	<i>D. harveyanum</i>	Whole plant	(Maitreesophon et al., 2022)
4,4'-Dihydroxy-3,5-dimethoxybibenzyl [34]	<i>D. candidum</i>	Stem	(Li et al., 2008)
	<i>D. ellipsophyllum</i>	Whole plant	(Tanagornmeatar et al., 2014)
	<i>D. williamsonii</i>	Whole plant	(M. Yang et al., 2018)
	<i>D. signatum</i>	Aerial part	(Khumploy et al., 2021)
Loddigesiinol C [35]	<i>D. loddigesii</i>	Whole plant	(Ito et al., 2010)
3-O-Methylgigantol [36]	<i>D. candidum</i>	Stem	(Li et al., 2008)
	<i>D. plicatile</i>	Stem	(Yamaki & Honda, 1996)

Table 1 Bibenzyls and derivatives in the *Dendrobium* species (Continued).

Compounds	Plant name	Plant part	References
Dendrocandin A [37]	<i>D. candidum</i>	Stem	(Li et al., 2008)
Dendrocandin B [38]	<i>D. candidum</i>	Stem	(Li et al., 2008)
	<i>D. signatum</i>	Whole plant	(Mittraphab et al., 2016)
	<i>D. signatum</i>	Aerial part	(Khumploy et al., 2021)
	<i>D. harveyanum</i>	Whole plant	(Maitreesophon et al., 2022)
Dendrocandin C [39]	<i>D. candidum</i>	Stem	(Li et al., 2008)
Dendrocandin D [40]	<i>D. candidum</i>	Stem	(Li et al., 2008)
Dendrocandin E [41]	<i>D. candidum</i>	Stem	(Li et al., 2008)
	<i>D. parishii</i>	Whole plant	(Kongkatitham et al., 2018)
Dendrocandin F [42]	<i>D. candidum</i>	Stem	(Li et al., 2008)
Dendrocandin G [43]	<i>D. candidum</i>	Stem	(Li et al., 2008)
Dendrocandin H [44]	<i>D. candidum</i>	Stem	(Li et al., 2008)
Dendrosinen A [45]	<i>D. sinense</i>	Whole plant	(Chen et al., 2014)
Dendrosinen B [46]	<i>D. sinense</i>	Whole plant	(Chen et al., 2014)
	<i>D. infundibulum</i>	Whole plant	(Na Ranong et al., 2019)
Dendrosinen C [47]	<i>D. sinense</i>	Whole plant	(Chen et al., 2014)
Dendrosinen D [48]	<i>D. sinense</i>	Whole plant	(Chen et al., 2014)

Table 1 Bibenzyls and derivatives in the *Dendrobium* species (Continued).

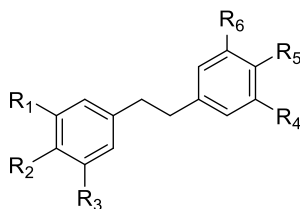
Compounds	Plant name	Plant part	References
Dendrocandin I [49]	<i>D. candidum</i>	Stem	(Li et al., 2008)
	<i>D. signatum</i>	Whole plant	(Mittraphab et al., 2016)
	<i>D. signatum</i>	Aerial part	(Khumploy et al., 2021)
Dendrocandin V [50]	<i>D. catenatum</i>	Stem	(Zhu et al., 2021)
Dendrocandin W [51]	<i>D. catenatum</i>	Stem	(Zhu et al., 2021)
Densiflorol A [52]	<i>D. densiflorum</i>	Stem	(Fan et al., 2001)
Longicornuol A [53]	<i>D. longicornu</i>	Stem	(Hu et al., 2008a)
Trigonopol A [54]	<i>D. trigonopus</i>	Stem	(Hu et al., 2008b)
Trigonopol B [55]	<i>D. chrysotoxum</i>	Stem	(Hu et al., 2012)
	<i>D. trigonopus</i>	Stem	(Hu et al., 2008b)
Crepidatuol A [56]	<i>D. crepidatum</i>	Stem	(Li et al., 2013)
Crepidatuol B [57]	<i>D. crepidatum</i>	Stem	(Li et al., 2013)
Loddigesiinol D [58]	<i>D. loddigesii</i>	Whole plant	(Ito et al., 2010)
Dencryol A [59]	<i>D. crystallinum</i>	Stem	(Wang et al., 2009)
Dencryol B [60]	<i>D. crystallinum</i>	Stem	(Wang et al., 2009)
Dengraol A [61]	<i>D. gratiosissimum</i>	Stem	(Zhang et al., 2008)
Dengraol B [62]	<i>D. gratiosissimum</i>	Stem	(Zhang et al., 2008)
4-[2-(3-Hydroxyphenol)-1-methoxyethyl]-2,6-dimethoxy phenol [63]	<i>D. longicornu</i>	Stem	(Hu et al., 2008a)
Nobilin A [64]	<i>D. nobile</i>	Stem	(Zhang et al., 2006)

Table 1 Bibenzyls and derivatives in the *Dendrobium* species (Continued).

Compounds	Plant name	Plant part	References
Nobilin B [65]	<i>D. nobile</i>	Stem	(Zhang et al., 2006)
	<i>D. crepidatum</i>	Root	(Ding et al., 2021)
Nobilin C [66]	<i>D. nobile</i>	Stem	(Zhang et al., 2006)
Nobilin D [67]	<i>D. nobile</i>	Stem	(Zhang et al., 2007)
Nobilin E [68]	<i>D. nobile</i>	Stem	(Zhang et al., 2007)
Dendrofalconerol A [69]	<i>D. falconeri</i>	Stem	(Sritularak & Likhitwitayawuid, 2009)
	<i>D. signatum</i>	Whole plant	(Mittraphab et al., 2016)
	<i>D. tortile</i>	Whole plant	(Limpanit et al., 2016)
	<i>D. harveyanum</i>	Whole plant	(Maitreesophone et al., 2022)
Dendrofalconerol B [70]	<i>D. falconeri</i>	Stem	(Sritularak & Likhitwitayawuid, 2009)
	<i>D. harveyanum</i>	Whole plant	(Maitreesophone et al., 2022)
Dendrosignatol [71]	<i>D. signatum</i>	Whole plant	(Mittraphab et al., 2016)
(-)-Dendroparishiol [72]	<i>D. parishii</i>	Whole plant	(Kongkatitham et al., 2018)

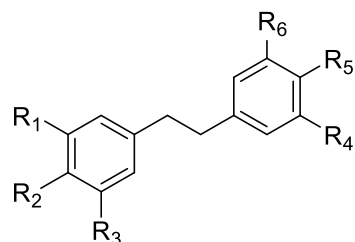
Table 1 Bibenzyls and derivatives in the *Dendrobium* species (Continued).

Compounds	Plant name	Plant part	References
6"-de-O-methyldendrofindlaphenol A [73]	<i>D. findlayanum</i>	Stem	(D. Yang et al., 2018)
	<i>D. signatum</i>	Aerial part	(Khumploy et al., 2021)
Dendrofindlaphenol A [74]	<i>D. findlayanum</i>	Stem	(D. Yang et al., 2018)
Dendrofindlaphenol B [75]	<i>D. findlayanum</i>	Stem	(D. Yang et al., 2018)
	<i>D. catenatum</i>	Stem	(Zhu et al., 2021)
Dendrofindlaphenol C [76]	<i>D. findlayanum</i>	Stem	(D. Yang et al., 2018)
Dendronbibisline C [77]	<i>D. nobile</i>	Stem	(Cheng et al., 2020)
Dendronbibisline D [78]	<i>D. nobile</i>	Stem	(Cheng et al., 2020)
Dendroscabrols B [79]	<i>D. scabrilingue</i>	Whole plant	(Sarakulwattana et al., 2020)
Dendropachol [80]	<i>D. pachyglossum</i>	Whole plant	(Warinhomhoun et al., 2021)
Dengratiol A [81]	<i>D. gratiosissimum</i>	Stem	(Sun et al., 2021)
Dengratiol B [82]	<i>D. gratiosissimum</i>	Stem	(Sun et al., 2021)
Dengratiol C [83]	<i>D. gratiosissimum</i>	Stem	(Sun et al., 2021)
Dengratiol D [84]	<i>D. gratiosissimum</i>	Stem	(Sun et al., 2021)
Dendrosonside B [85]	<i>D. 'Sonia'</i>	Stem	(Qiu et al., 2023)



	R ₁	R ₂	R ₃	R ₄	R ₅	R ₆
[1] Aloifol I	OMe	OH	OMe	OH	H	H
[2] Amoenylin	OMe	OH	OMe	H	OMe	H
[3] Batatasin	OMe	H	H	OH	H	OH
[4] Batatasin III	OH	H	OMe	H	H	OH
[5] Brittonin A	OMe	OMe	OMe	OMe	OMe	OMe
[6] Chrysotobibenzyl	OMe	OMe	OMe	OMe	OMe	H
[7] Chrysotoxine	OMe	OH	OMe	OMe	OMe	H
[8] Crepidatin	OMe	OMe	OMe	OMe	OH	H
[9] Cumulatin	OMe	OMe	OH	OH	OMe	OMe
[10] Dendrobin A	OH	OH	OMe	H	H	OMe
[11] 3,3'-Dihydroxy-4,5-dimethoxybibenzyl	OMe	OMe	OH	H	H	OH
[12] 3,4'-Dihydroxy-5-methoxybibenzyl	OH	H	OMe	H	OH	H
[13] 3,4'-Dihydroxy-5,5'-dimethoxydihydrostilbene	OH	H	OMe	OMe	OH	H
[14] 4,5-Dihydroxy-3,3'-dimethoxybibenzyl	OMe	OH	OH	H	H	OMe

Figure 1 Structures of bibenzyls and derivatives from *Dendrobium* species.



	R ₁	R ₂	R ₃	R ₄	R ₅	R ₆
[15] Erianin	OMe	OMe	OMe	H	OMe	OH
[16] Gigantol	OMe	H	H	H	OH	OMe
[17] 4-Hydroxy-3,5,3' trimethoxybibenzyl	OMe	OH	OMe	H	H	OMe
[18] 5-Hydroxy-3,4,3',4',5' pentamethoxybibenzyl	OMe	OMe	OH	OMe	OMe	OMe
[19] Isoamoenylin	OMe	OMe	OMe	H	H	OH
[20] Moniliformine	OH	OH	OMe	H	OMe	H
[21] Moscatilin	OMe	OH	OMe	H	OH	OMe
[22] 3,3',4-Trihydroxybibenzyl	OH	OH	H	H	H	OH
[23] 3,3',5-Trihydroxybibenzyl	OH	H	OH	H	H	OH
[24] 3,5,4'-Trihydroxybibenzyl	OH	H	OH	H	OH	H

Figure 1 Structures of bibenzyls and derivatives from *Dendrobium* species (Continued).

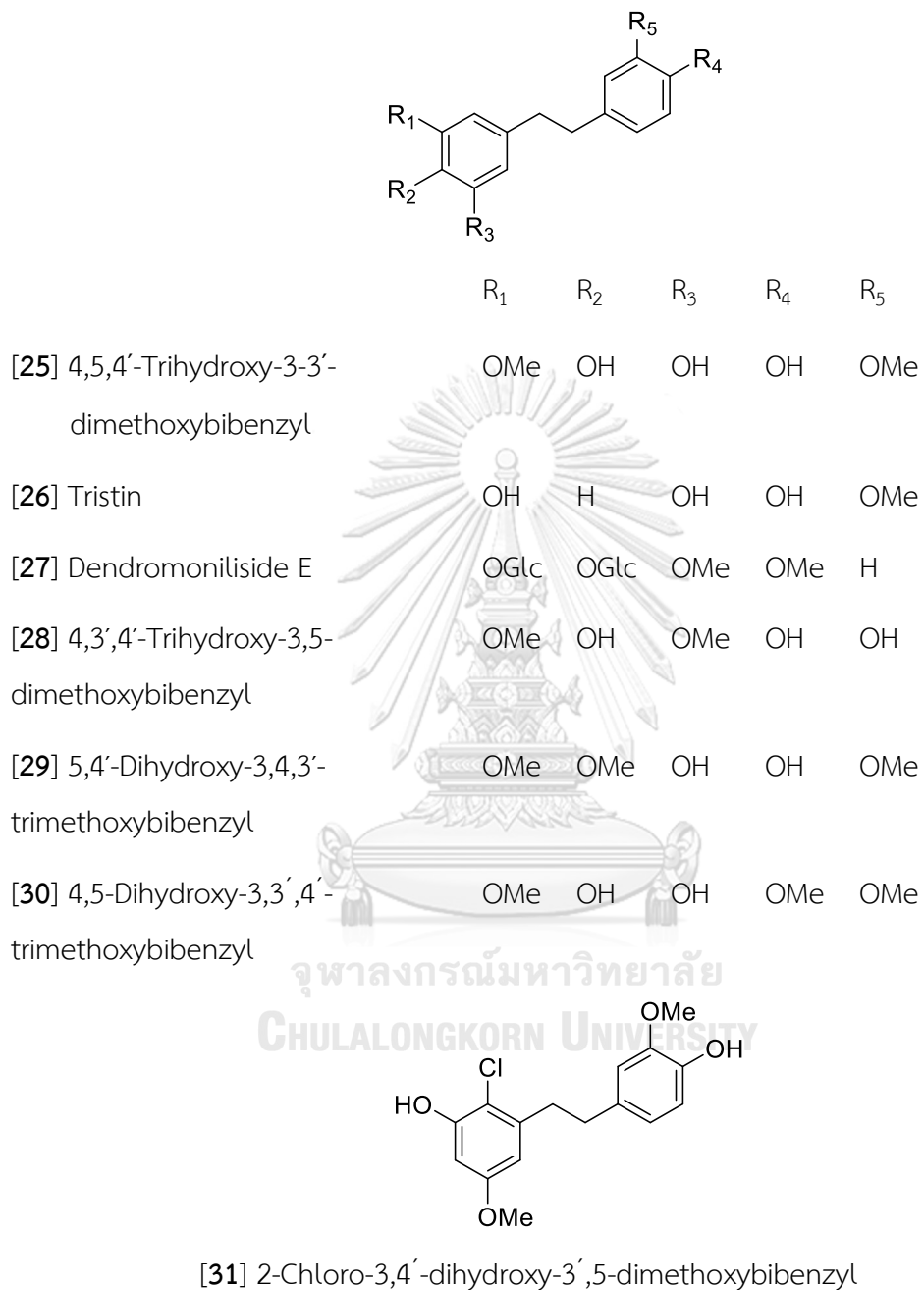
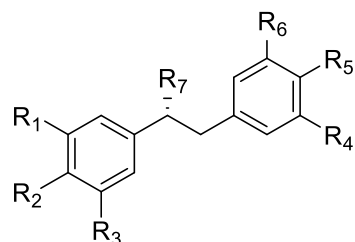
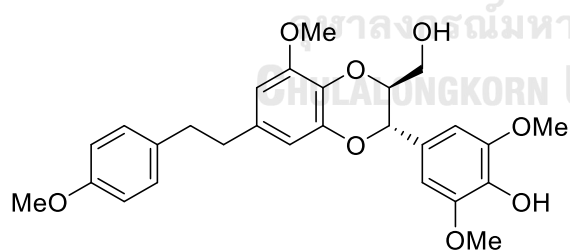


Figure 1 Structures of bibenzyls and derivatives from *Dendrobium* species (Continued).



	R ₁	R ₂	R ₃	R ₄	R ₅	R ₆	R ₇
[32] Dendrophenol	OMe	OH	OMe	OH	OH	H	H
[33] 3,4-Dihydroxy-5,4'- dimethoxybibenzyl	OH	OH	OMe	H	OMe	H	H
[34] 4,4'-Dihydroxy-3,5- dimethoxybibenzyl	OMe	OH	OMe	H	OH	H	H
[35] Loddigesiinol C	OMe	OH	OMe	H	OH	OMe	OMe
[36] 3-O-Methylgigantol	OMe	H	OH	OMe	OMe	H	H
[37] Dendrocandin A	OMe	OH	OH	H	OMe	H	OMe



Dendrocandin B [38]

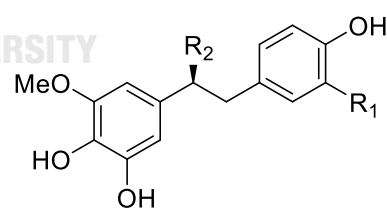
[39] Dendrocandin C: R₁ = H, R₂ = OMe[40] Dendrocandin D: R₁ = H, R₂ = OEt[41] Dendrocandin E: R₁ = OH, R₂ = H

Figure 1 Structures of bibenzyls and derivatives from *Dendrobium* species
(Continued).

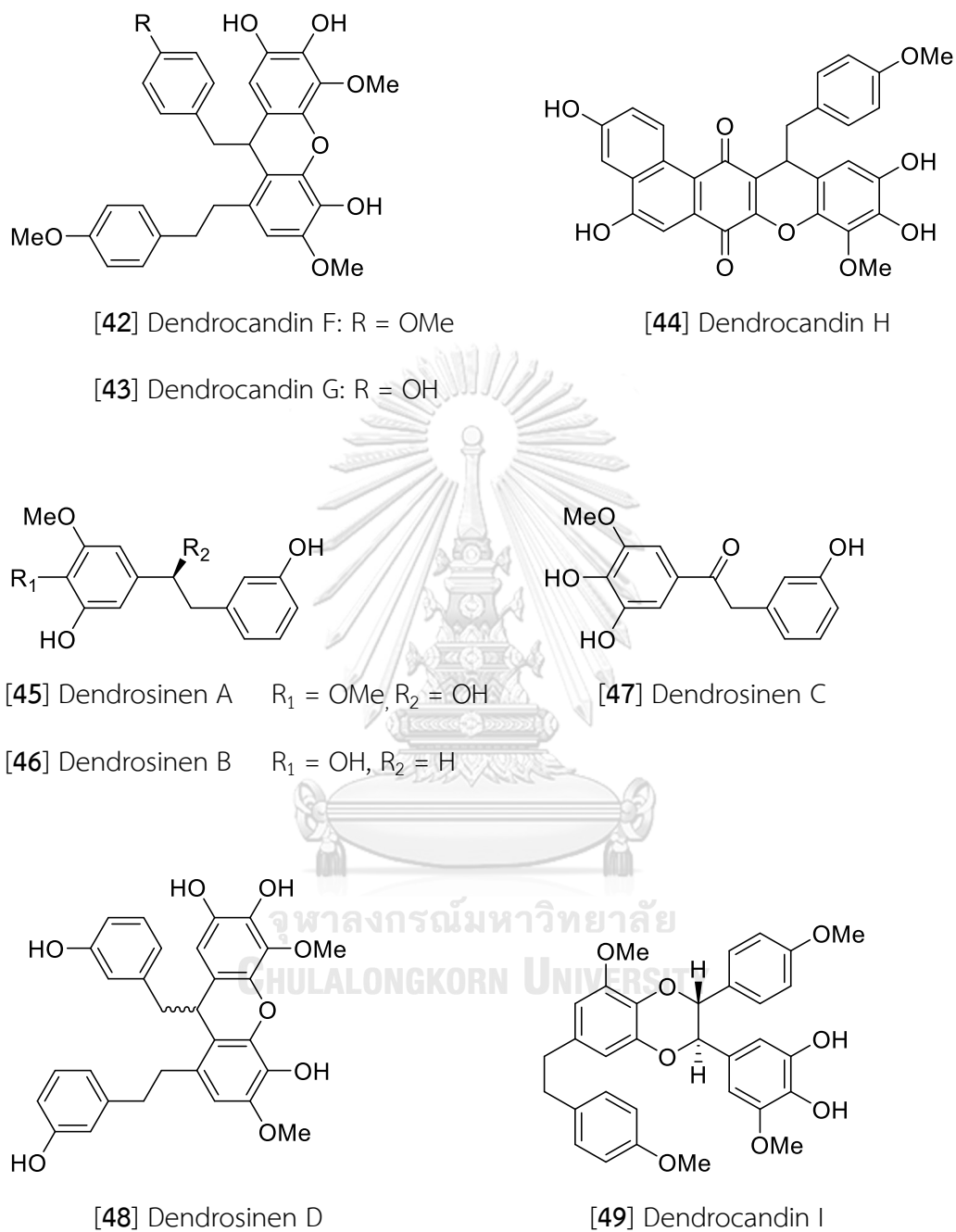


Figure 1 Structures of bibenzyls and derivatives from *Dendrobium* species (Continued).

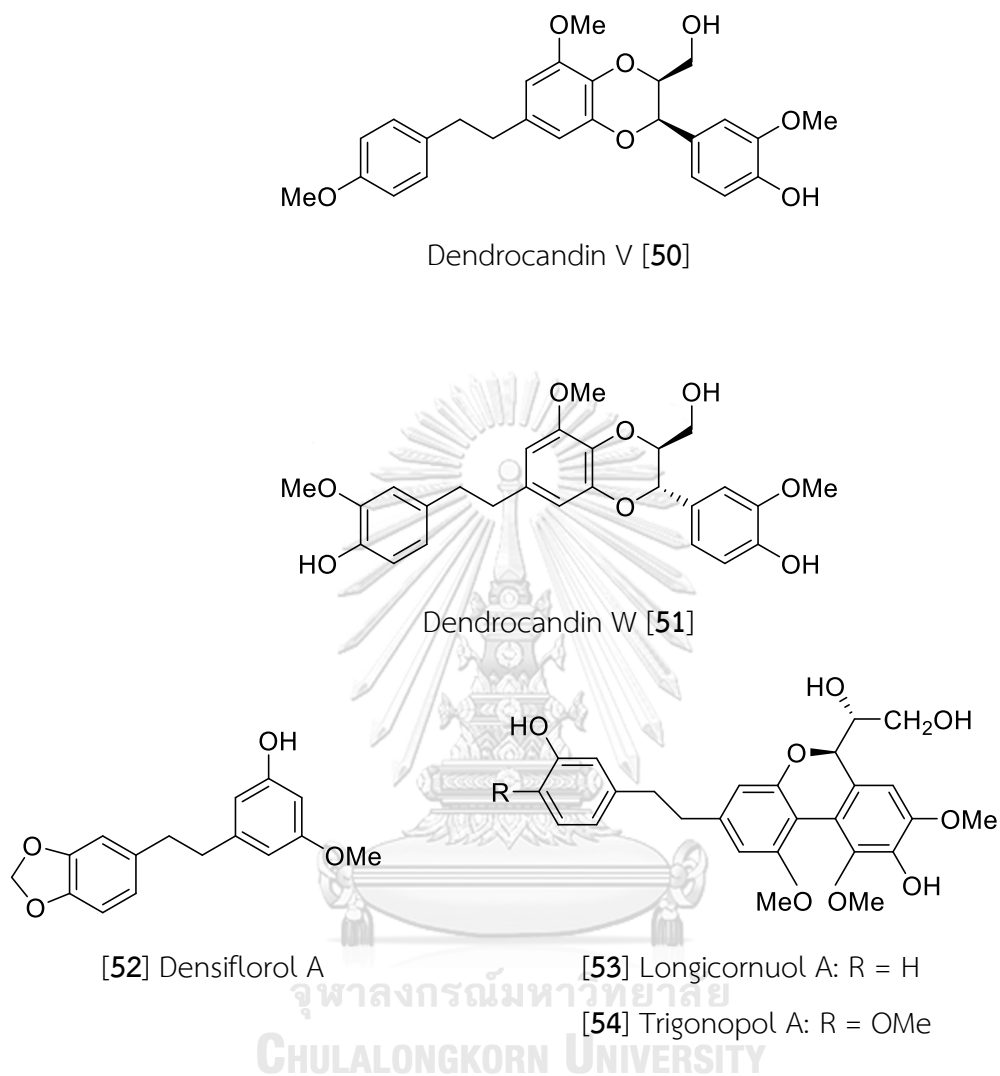


Figure 1 Structures of bibenzyls and derivatives from *Dendrobium* species (Continued).

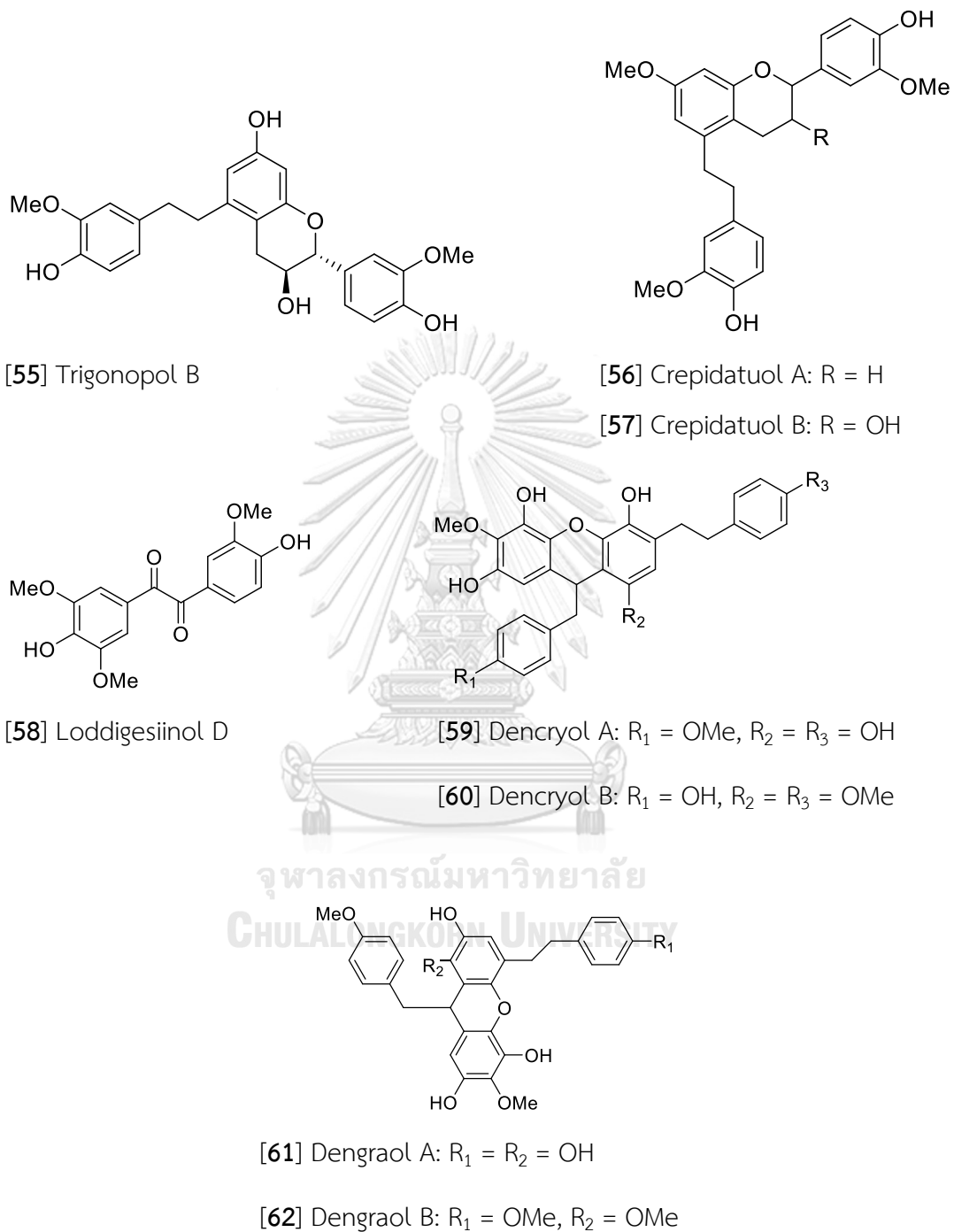


Figure 1 Structures of bibenzyls and derivatives from *Dendrobium* species (Continued).

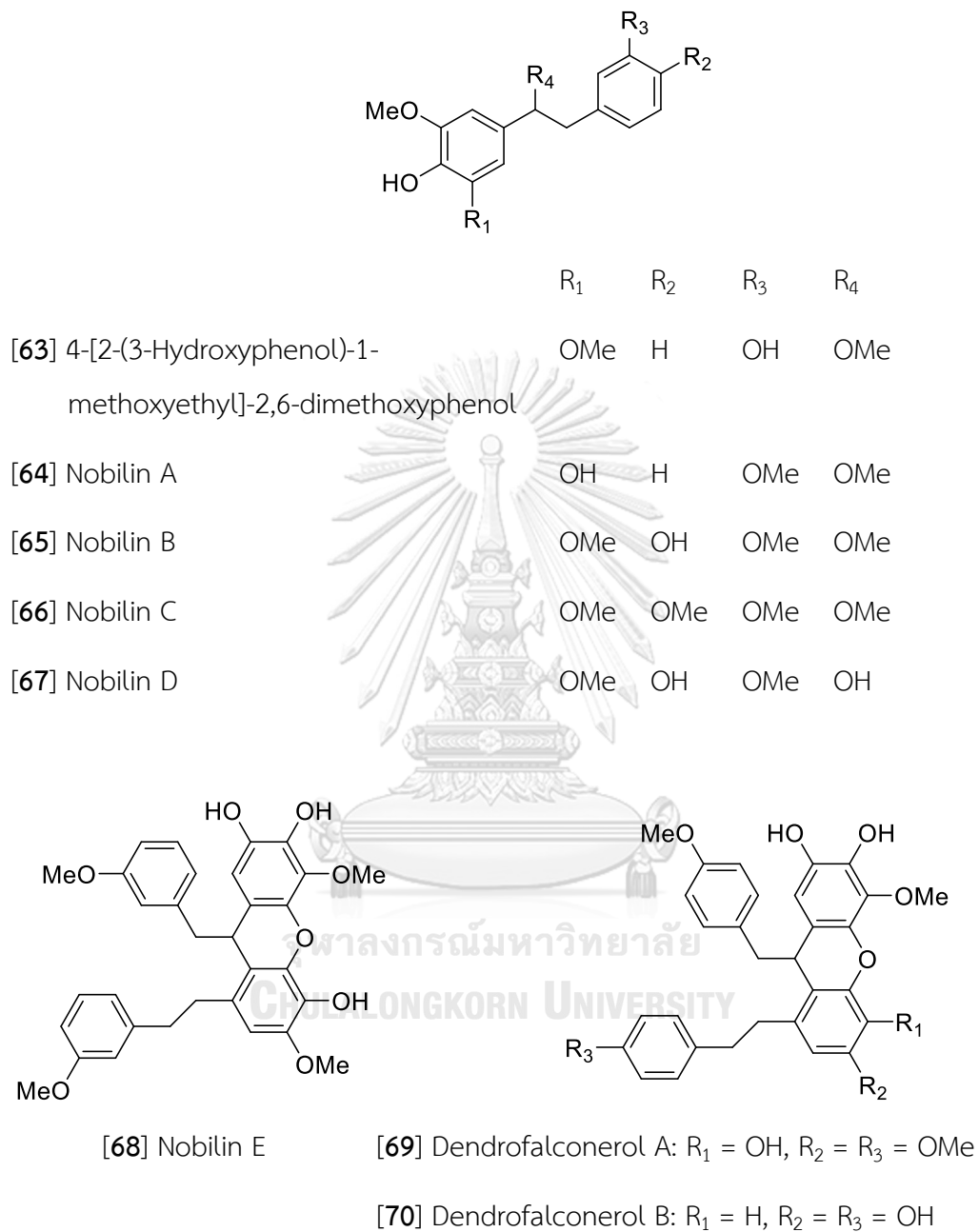
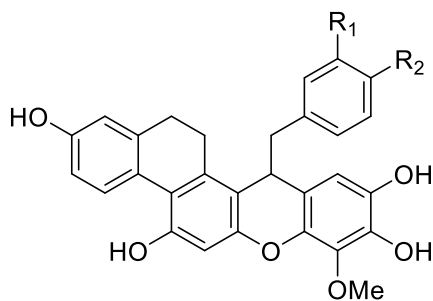
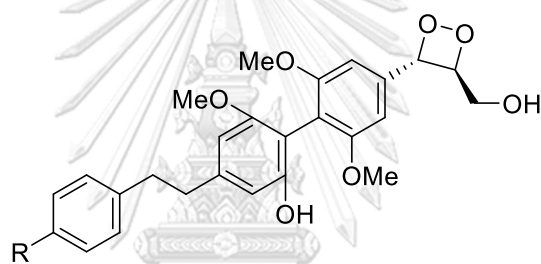


Figure 1 Structures of bibenzyls and derivatives from *Dendrobium* species (Continued).



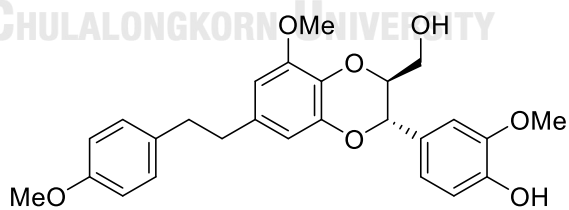
[71] Dendrosignatol: $R_1 = \text{H}$, $R_2 = \text{OMe}$

[72] (-)-Dendroparishiol: $R_1 = \text{OMe}$, $R_2 = \text{OH}$



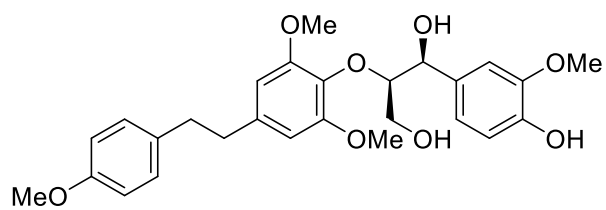
[73] 6''-de-O-methyldendrofindlaphenol A: $R = \text{OH}$

[74] Dendrofindlaphenol A: $R = \text{OMe}$

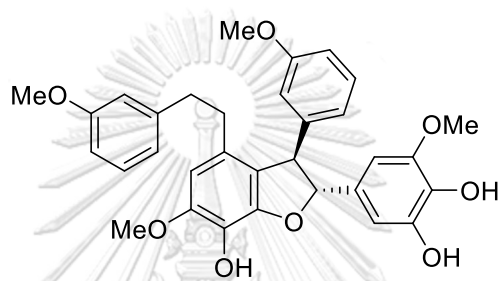


[75] Dendrofindlaphenol B

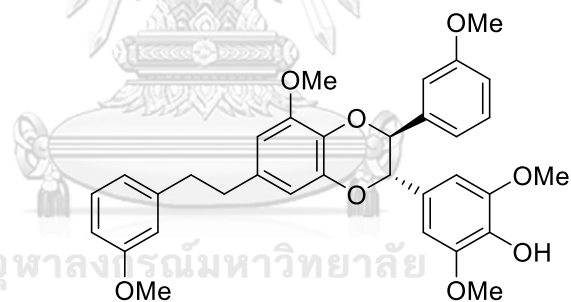
Figure 1 Structures of bibenzyls and derivatives from *Dendrobium* species
(Continued).



[76] Dendrofindlaphenol C



[77] Dendronbibisline C



[78] Dendronbibisline D

Figure 1 Structures of bibenzyls and derivatives from *Dendrobium* species
(Continued).

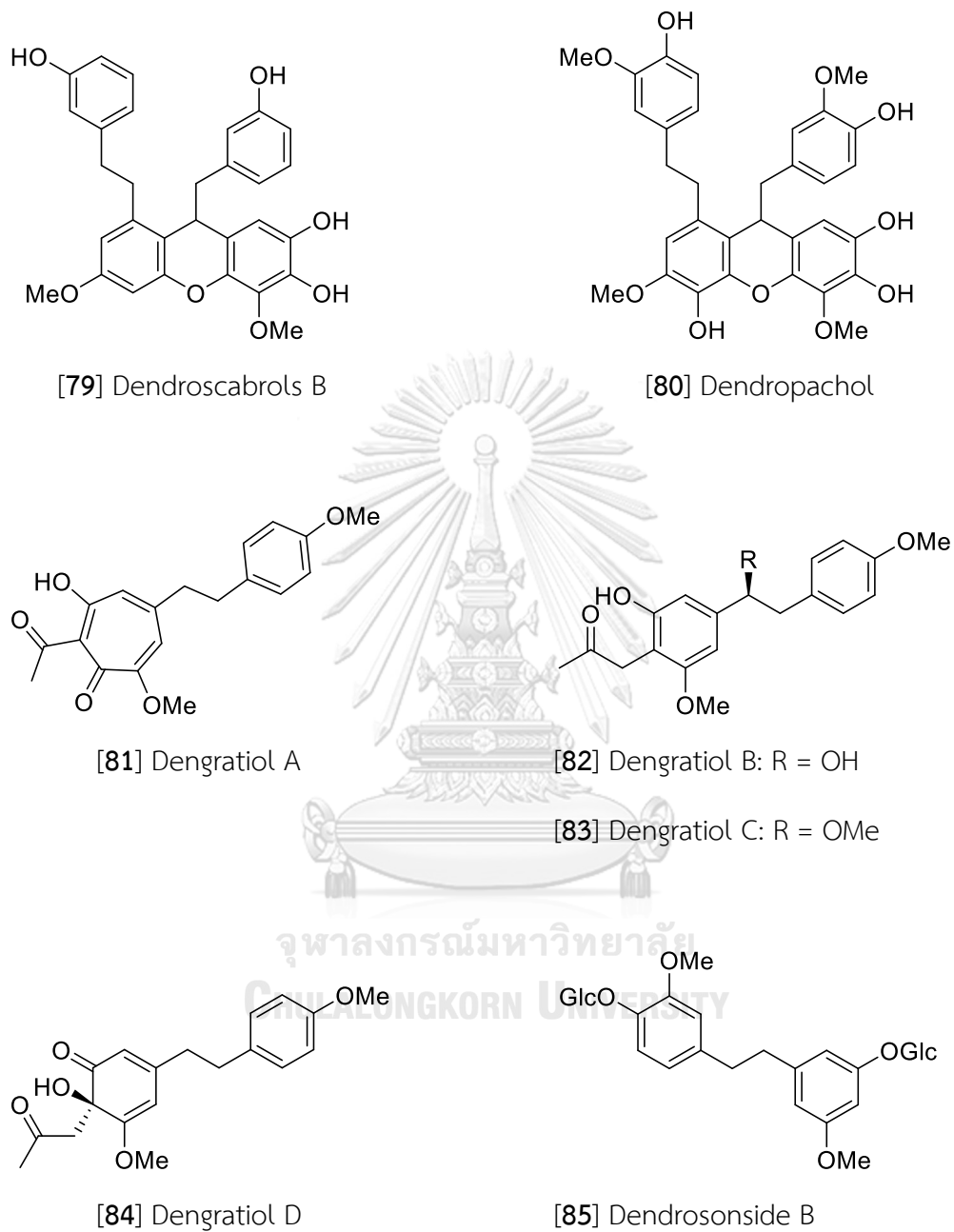


Figure 1 Structures of bibenzyls and derivatives from *Dendrobium* species (Continued).

Table 2 Phenanthrenes and derivatives in the *Dendrobium* species.

Compounds	Plant name	Plant part	References
4,4',8,8'-tetramethoxy[1,1'-biphenanthrene]-2,2',7,7'-tetrol [86]	<i>D. senile</i>	Whole plant	(Pann Phyu et al., 2022)
2,2',7,7'-tetrahydroxy-4,4'-dimethoxy-1,1'-biphenanthrene [87]	<i>D. senile</i>	Whole plant	(Pann Phyu et al., 2022)
2,2'-Dihydroxy-3,3',4,4',7,7'-hexamethoxy-9,9',10,10'-tetrahydro-1,1'-biphenanthrene [88]	<i>D. nobile</i>	Stem	(Yang et al., 2007)
2,2'-Dimethoxy-4,4',7,7'-tetrahydroxy-9,9',10,10'-tetrahydro-1,1'-biphenanthrene [89]	<i>D. plicatile</i>	Stem	(Yamaki & Honda, 1996)
Flavanthrin [90]	<i>D. aphyllum</i>	Whole plant	(Chen, Li, et al., 2008)
Phoyunnanin C [91]	<i>D. venustum</i>	Whole plant	(Sukphan et al., 2014)
Phoyunnanin E [92]	<i>D. venustum</i>	Whole plant	(Sukphan et al., 2014)
Amoenumin [93]	<i>D. amoenum</i>	Whole plant	(Veerraju et al., 1989)
Crystalltone [94]	<i>D. chrysotoxum</i>	Stem	(Hu et al., 2012)
	<i>D. crystallinum</i>	Stem	(Wang et al., 2009)

Table 2 Phenanthrenes and derivatives in the *Dendrobium* species (Continued).

Compounds	Plant name	Plant part	References
Chrysotoxol A [95]	<i>D. chrysotoxum</i>	Stem	(Hu et al., 2012)
Chrysotoxol B [96]	<i>D. chrysotoxum</i>	Stem	(Hu et al., 2012)
Confusarin [97]	<i>D. chryseum</i>	Stem	(Ma, Wang, Yin, et al., 1998)
	<i>D. chrysotoxum</i>	Stem	(Hu et al., 2012)
	<i>D. formosum</i>	Whole plant	(Inthongkaew et al., 2017)
	<i>D. nobile</i>	Stem	(Zhang et al., 2008)
	<i>D. officinale</i>	Stem	(Zhao et al., 2018)
2,6-Dihydroxy-1,5,7-trimethoxy-phenanthrene [98]	<i>D. densiflorum</i>	Stem	(Fan et al., 2001)
	<i>D. palpebrae</i>	Whole plant	(Kyokong et al., 2019)
Dendrochrysanene [99]	<i>D. chrysanthum</i>	Stem	(Yang, Qin, et al., 2006)
Bulbophyllanthrin [100]	<i>D. nobile</i>	Stem	(Hwang et al., 2010)
Denthyrsinin [101]	<i>D. thyrsoforum</i>	Stem	(Zhang et al., 2005)
	<i>D. plicatile</i>	Stem	(Chen et al., 2020)
5-Hydroxy-2,4-dimethoxy-phenanthrene [102]	<i>D. loddigesii</i>	Whole plant	(Ito et al., 2010)
3-Hydroxy-2,4,7-trimethoxy-phenanthrene [103]	<i>D. nobile</i>	Stem	(Yang et al., 2007)

Table 2 Phenanthrenes and derivatives in the *Dendrobium* species (Continued).

Compounds	Plant name	Plant part	References
Cypripedin [104]	<i>D. densiflorum</i>	Stem	(Fan et al., 2001)
	<i>D. lindleyi</i>	Whole plant	(Khoonrit et al., 2020)
Densiflorol B [105]	<i>D. densiflorum</i>	Stem	(Fan et al., 2001)
	<i>D. venustum</i>	Whole plant	(Sukphan et al., 2014)
Denbinobin [106]	<i>D. moniliforme</i>	Stem	(Lin et al., 2001)
	<i>D. nobile</i>	Stem	(Yang et al., 2007)
Fimbriatone [107]	<i>D. nobile</i>	Stem	(Zhang et al., 2008)
	<i>D. pulchellum</i>	Stem	(Chanvorachote et al., 2013)
Loddigesiinol B [108]	<i>D. loddigesii</i>	Whole plant	(Ito et al., 2010)
Dendronone [109]	<i>D. chrysanthum</i>	Stem	(Yang, Qin, et al., 2006)
	<i>D. longicornu</i>	Stem	(Hu et al., 2008a)
Ephemeranthoquinone [110]	<i>D. plicatile</i>	Stem	(Yamaki & Honda, 1996),
5-Methoxy-7-hydroxy-9,10-dihydro-1,4-phenanthrenequinone [111]	<i>D. draconis</i>	Stem	(Sritularak, Anuwat, et al., 2011)
	<i>D. formosum</i>	Whole plant	(Inthongkaew et al., 2017)
Moniliformin [112]	<i>D. moniliforme</i>	Stem	(Lin et al., 2001)

Table 2 Phenanthrenes and derivatives in the *Dendrobium* species (Continued).

Compounds	Plant name	Plant part	References
Moscatin [113]	<i>D. aphyllum</i>	Whole plant	(Chen, Li, et al., 2008)
	<i>D. chrysanthum</i>	Stem	(Yang, Qin, et al., 2006)
	<i>D. chrysotoxum</i>	Whole plant	(Y.-P. Li et al., 2009)
	<i>D. densiflorum</i>	Stem	(Fan et al., 2001)
	<i>D. polyanthum</i>	Stem	(Hu et al., 2009)
	<i>D. senile</i>	Whole plant	(Pann Phyu et al., 2022)
Dendroscabrols A [114]	<i>D. scabrilinque</i>	Whole plant	(Sarakulwattana et al., 2020)
2,5,7-trihydroxy-4-methoxyphenanthrene [115]	<i>D. senile</i>	Whole plant	(Pann Phyu et al., 2022)
Bleformin G [116]	<i>D. senile</i>	Whole plant	(Pann Phyu et al., 2022)
Coelonin [117]	<i>D. aphyllum</i>	Whole plant	(Chen, Li, et al., 2008)
	<i>D. formosum</i>	Whole plant	(Inthongkaew et al., 2017)
	<i>D. nobile</i>	Stem	(Yang et al., 2007)
	<i>D. devonianum</i>	Stem	(Wu et al., 2019)
	<i>D. scabrilinque</i>	Whole plant	(Sarakulwattana et al., 2020)
	<i>D. plicatile</i>	Stem	(Chen et al., 2020)

Table 2 Phenanthrenes and derivatives in the *Dendrobium* species (Continued).

Compounds	Plant name	Plant part	References
9,10-Dihydromoscatin [118]	<i>D. polyanthum</i>	Stem	(Hu et al., 2009)
9,10-Dihydrophenanthrene-2,4,7-triol [119]	<i>D. polyanthum</i>	Stem	(Hu et al., 2009)
4,5-Dihydroxy-2,3-dimethoxy-9,10-dihydrophenanthrene [120]	<i>D. ellipsophyllum</i>	Whole plant	(Tanagornmeatar et al., 2014)
	<i>D. sinense</i>	Whole plant	(Chen et al., 2014)
	<i>D. pachyglossum</i>	Whole plant	(Warinhomhoun et al., 2021)
4,5-Dihydroxy-2,6-dimethoxy-9,10-dihydrophenanthrene [121]	<i>D. chrysotoxum</i>	Stem	(Hu et al., 2012)
	<i>D. devonianum</i>	Stem	(Wu et al., 2019)
4,5-Dihydroxy-3,7-dimethoxy-9,10-dihydrophenanthrene [122]	<i>D. nobile</i>	Stem	(Ye & Zhao, 2002)
4,5-Dihydroxy-2-methoxy-9,10-dihydrophenanthrene [123]	<i>D. nobile</i>	Stem	(Zhang et al., 2007)

Table 2 Phenanthrenes and derivatives in the *Dendrobium* species (Continued).

Compounds	Plant name	Plant part	References
Lusianthridin [124]	<i>D. brymerianum</i>	Whole plant	(Klongkumnuankarn et al., 2015)
	<i>D. formosum</i>	Whole plant	(Inthongkaew et al., 2017)
	<i>D. venustum</i>	Whole plant	(Sukphan et al., 2014)
	<i>D. palpebrae</i>	Whole plant	(Kyokong et al., 2019)
	<i>D. scabrilinque</i>	Whole plant	(Sarakulwattana et al., 2020)
	<i>D. gibsonii</i>	Whole plant	(Thant et al., 2020)
	<i>D. plicatile</i>	Stem	(Chen et al., 2020; Yamaki & Honda, 1996)
2,7-Dihydroxy-3,4,6-trimethoxy-9,10-dihydrophenanthrene [125]	<i>D. densiflorum</i>	Stem	(Fan et al., 2001)
2,8-Dihydroxy-3,4,7-trimethoxy-9,10-dihydrophenanthrene [126]	<i>D. nobile</i>	Stem	(Yang et al., 2007)

Table 2 Phenanthrenes and derivatives in the *Dendrobium* species (Continued).

Compounds	Plant name	Plant part	References
4,7-Dihydroxy-2,3,6-trimethoxy-9,10-dihydrophenanthrene [127]	<i>D. rotundatum</i>	Whole plant	(Majumder & Pal, 1992)
Ephemeralanthol A [128]	<i>D. nobile</i>	Stem	(Hwang et al., 2010; Yang et al., 2007)
	<i>D. officinale</i>	Stem	(Zhao et al., 2018)
	<i>D. infundibulum</i>	Whole plant	(Na Ranong et al., 2019)
	<i>D. gibsonii</i>	Whole plant	(Thant et al., 2020)
Ephemeralanthol C [129]	<i>D. nobile</i>	Stem	(Hwang et al., 2010; Yang et al., 2007)
Erianthridin [130]	<i>D. formosum</i>	Whole plant	(Inthongkaew et al., 2017)
	<i>D. nobile</i>	Stem	(Hwang et al., 2010)
	<i>D. plicatile</i>	Stem	(Chen et al., 2020; Yamaki & Honda, 1996)
Flavanthridin [131]	<i>D. nobile</i>	Stem	(Hwang et al., 2010)
Hircinol [132]	<i>D. aphyllum</i>	Stem	(Yang et al., 2015)
	<i>D. draconis</i>	Stem	(Sritularak, Anuwat, et al., 2011)
	<i>D. formosum</i>	Whole plant	(Inthongkaew et al., 2017)

Table 2 Phenanthrenes and derivatives in the *Dendrobium* species (Continued).

Compounds	Plant name	Plant part	References
3-Hydroxy-2,4,7-trimethoxy-9,10-dihydrophenanthrene [133]	<i>D. nobile</i>	Stem	(Yang et al., 2007)
	<i>D. hainanense</i>	Aerial part	(Zhang et al., 2019)
3,4-dimethoxy-1-(methoxymethyl)-9,10-dihydrophenanthrene-2,7-diol [134]	<i>D. hainanense</i>	Aerial part	(Zhang et al., 2019)
2,4,7-trihydroxy-3-methoxy-9,10-dihydrophenanthrene [135]	<i>D. terminale</i>	Whole plant	(Cheng et al., 2022)
Dendroinfundin A [136]	<i>D. infundibulum</i>	Whole plant	(Na Ranong et al., 2019)
4,7-dihydroxy-2,3,8-trimethoxy-9,10-dihydrophenanthrene [137]	<i>D. terminale</i>	Whole plant	(Cheng et al., 2022)
Dendroinfundin B [138]	<i>D. infundibulum</i>	Whole plant	(Na Ranong et al., 2019)
2-Hydroxy-4,7-dimethoxy-9,10-dihydrophenanthrene [139]	<i>D. nobile</i>	Stem	(Yang et al., 2007)

Table 2 Phenanthrenes and derivatives in the *Dendrobium* species (Continued).

Compounds	Plant name	Plant part	References
7-Methoxy-9,10-dihydrophenanthrene-2,4,5-triol [140]	<i>D. draconis</i>	Stem	(Sritularak, Anuwat, et al., 2011)
2,5,7-Trihydroxy-4-methoxy-9,10-dihydrophenanthrene [141]	<i>D. formosum</i>	Whole plant	(Inthongkaew et al., 2017)
	<i>D. longicornu</i>	Stem	(Hu et al., 2008a)
Plicatol C [142]	<i>D. plicatile</i>	Stem	(Honda & Yamaki, 2000)
Rotundatin [143]	<i>D. rotundatum</i>	Whole plant	(Majumder & Pal, 1992)
2,5-Dihydroxy-3,4-dimethoxyphenanthrene [144]	<i>D. nobile</i>	Stem	(Yang et al., 2007)
2,5-Dihydroxy-4,9-dimethoxyphenanthrene [145]	<i>D. nobile</i>	Stem	(Zhang et al., 2008)
	<i>D. senile</i>	Whole plant	(Pann Phyu et al., 2022)
	<i>D. palpebrae</i>	Whole plant	(Kyokong et al., 2019)
2,8-Dihydroxy-3,4,7-trimethoxyphenanthrene [146]	<i>D. nobile</i>	Stem	(Yang et al., 2007)

Table 2 Phenanthrenes and derivatives in the *Dendrobium* species (Continued).

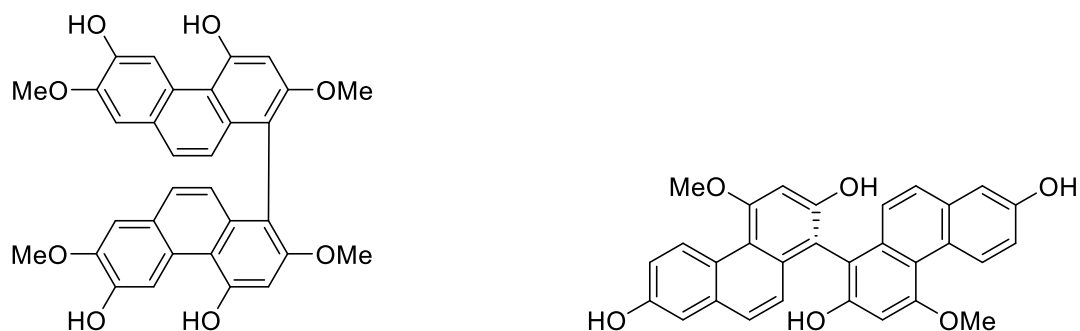
Compounds	Plant name	Plant part	References
Epheranthol B [147]	<i>D. chrysotoxum</i>	Stem	(Hu et al., 2012)
	<i>D. plicatile</i>	Stem	(Yamaki & Honda, 1996)
Fimbriol B [148]	<i>D. nobile</i>	Stem	(Hwang et al., 2010; Yang et al., 2007)
Flavanthrinin [149]	<i>D. brymerianum</i>	Whole plant	(Klongkumnuankarn et al., 2015)
	<i>D. nobile</i>	Stem	(Zhang et al., 2008)
	<i>D. venustum</i>	Whole plant	(Sukphan et al., 2014)
	<i>D. parishii</i>	Whole plant	(Kongkatitham et al., 2018)
Loddigesiinol A [150]	<i>D. loddigesii</i>	Whole plant	(Ito et al., 2010)
Nudol [151]	<i>D. formosum</i>	Whole plant	(Inthongkaew et al., 2017)
	<i>D. nobile</i>	Stem	(Yang et al., 2007)
	<i>D. rotundatum</i>	Whole plant	(Majumder & Pal, 1992)
	<i>D. plicatile</i>	Stem	(Chen et al., 2020)
Plicatol A [152]	<i>D. nobile</i>	Stem	(Yang et al., 2007)
	<i>D. plicatile</i>	Stem	(Honda & Yamaki, 2000)
Plicatol B [153]	<i>D. plicatile</i>	Stem	(Honda & Yamaki, 2000)

Table 2 Phenanthrenes and derivatives in the *Dendrobium* species (Continued).

Compounds	Plant name	Plant part	References
2,3,5-Trihydroxy-4,9-dimethoxyphenanthrene [154]	<i>D. nobile</i>	Stem	(Yang et al., 2007)
3,4,8-Trimethoxy phenanthrene-2,5-diol [155]	<i>D. nobile</i>	Stem	(Hwang et al., 2010)
Aphyllone [156]	<i>D. nobile</i>	Stem	(Hwang et al., 2010)
(S)-2,4,5,9-Tetrahydroxy-9,10-dihydro phenanthrene [157]	<i>D. fimbriatum</i>	Stem	(Xu et al., 2014)
1,5,7-Trimethoxy phenanthren-2-ol [158]	<i>D. nobile</i>	Stem	(Kim et al., 2015)
1,5-Dihydroxy-3,4,7-trimethoxy-9,10-dihydrophenanthrene [159]	<i>D. moniliforme</i>	Whole plant	(Lin et al., 2001)
2,5,9S-Trihydroxy-9,10-dihydro phenanthrene-4-O- β -D-glucopyranoside [160]	<i>D. primulinum</i>	Whole plant	(Ye et al., 2016)
Loddigesiinol G [161]	<i>D. loddigesii</i>	Stem	(Lu et al., 2014)
Loddigesiinol H [162]	<i>D. loddigesii</i>	Stem	(Lu et al., 2014)
Loddigesiinol I [163]	<i>D. loddigesii</i>	Stem	(Lu et al., 2014)
Loddigesiinol J [164]	<i>D. loddigesii</i>	Stem	(Lu et al., 2014)

Table 2 Phenanthrenes and derivatives in the *Dendrobium* species (Continued).

Compounds	Plant name	Plant part	References
Dendrocandin P1 [165]	<i>D. officinale</i>	Stem	(Zhao et al., 2018)
Dendrocandin P2 [166]	<i>D. officinale</i>	Stem	(Zhao et al., 2018)
Orchinol [167]	<i>D. officinale</i>	Stem	(Zhao et al., 2018)
2,4,7-Trihydroxy-9,10-dihydro-phenanthrene [168]	<i>D. officinale</i>	Stem	(Zhao et al., 2018)
4-Methoxy-5,9R-dihydroxy-9,10-dihydrophenanthrene 2-O-β-D-glucopyranoside [169]	<i>D. nobile</i>	Stem	(Zhou et al., 2017)
Dendropalpebrone [170]	<i>D. palpebrae</i>	Whole plant	(Kyokong et al., 2019)
Dendrodevonin A [171]	<i>D. devonianum</i>	Stem	(Wu et al., 2019)
Dendrodevonin B [172]	<i>D. devonianum</i>	Stem	(Wu et al., 2019)
Dendronbibisline A [173]	<i>D. nobile</i>	Stem	(Cheng et al., 2020)
Dendronbibisline B [174]	<i>D. nobile</i>	Stem	(Cheng et al., 2020)
Dendrososide A [175]	<i>D. 'Sonia'</i>	Stem	(Qiu et al., 2023)

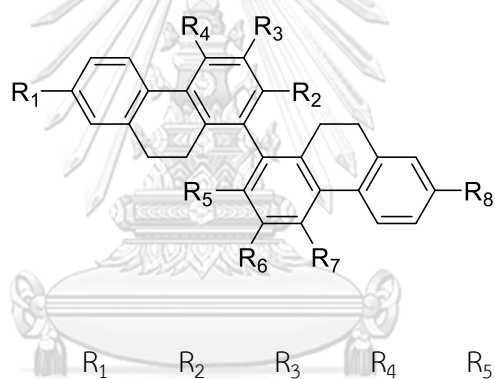


[86] 4,4',8,8'-tetramethoxy

[1,1'-biphenanthrene]-2,2',7,7'-tetrol

[87] 2,2',7,7'-tetrahydroxy-4,4'-

dimethoxy-1,1' biphenanthrene



[88] 2,2'-Dihydroxy-

3,3',4,4',7,7'-hexamethoxy-9,9',10,10'-

tetrahydro-1,1'-biphenanthrene

[89] 2,2'-Dimethoxy-

4,4',7,7'-tetrahydroxy-9,9',10,10'-tetrahydro-

1,1'-biphenanthrene

[90] Flavanthrin

	R ₁	R ₂	R ₃	R ₄	R ₅	R ₆	R ₇	R ₈
[88]	OMe	OH	OMe	OMe	OH	OMe	OMe	OMe
[89]	OH	OMe	H	OH	OMe	H	OH	OH
[90]	OH	OH	H	OMe	OH	H	OMe	OH

Figure 2 Structures of phenanthrenes and derivatives from *Dendrobium* species.

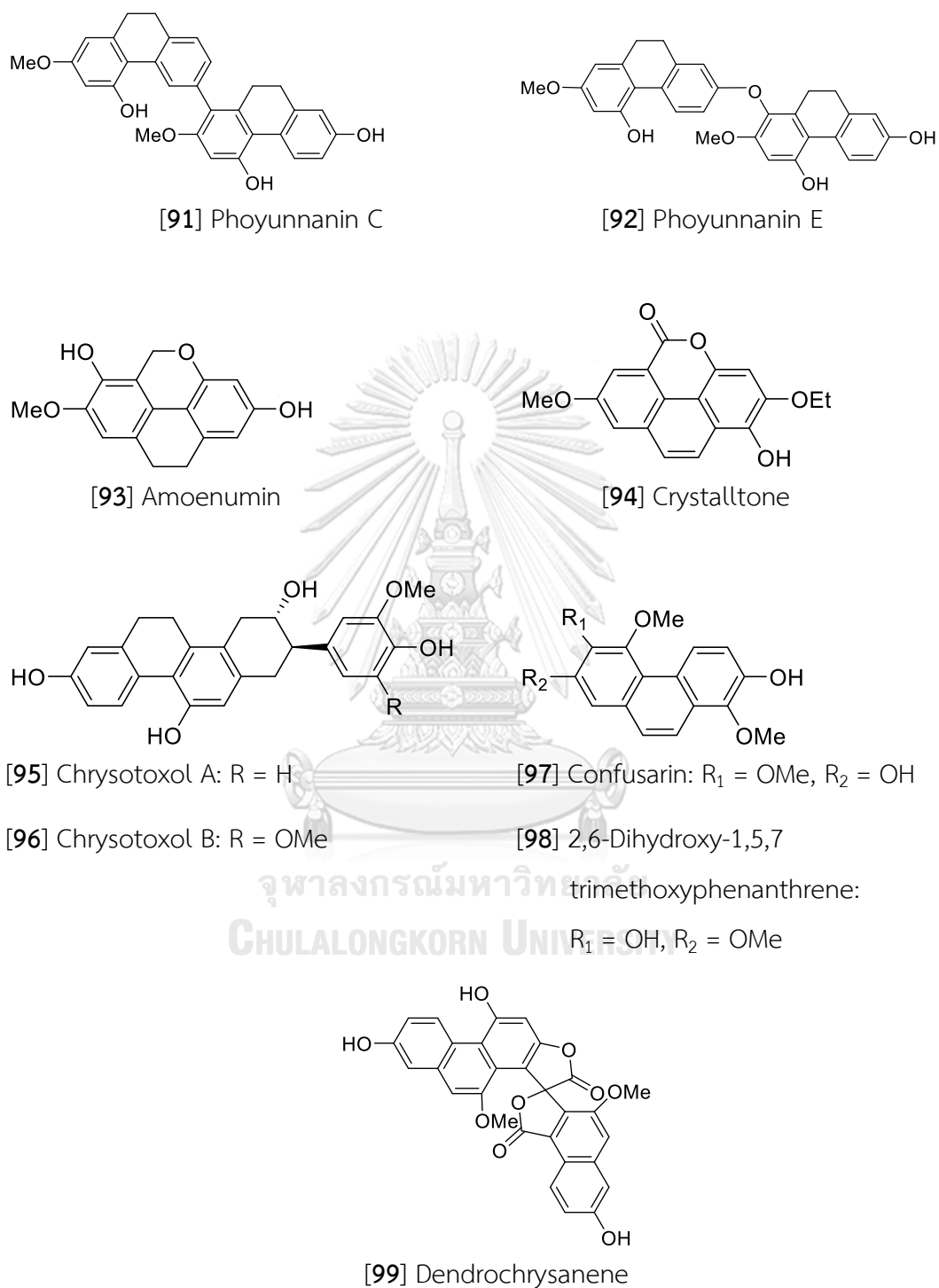
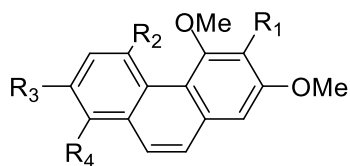
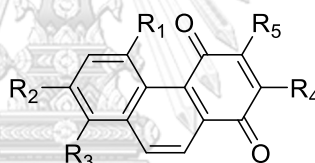


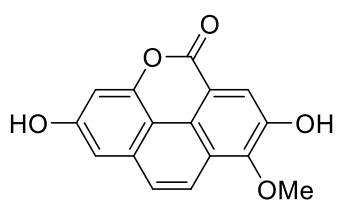
Figure 2 Structures of phenanthrenes and derivatives from *Dendrobium* species (Continued).



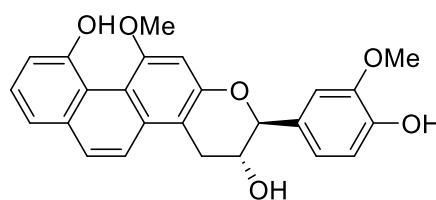
	R ₁	R ₂	R ₃	R ₄
[100] Bulbophyllanthrin	OH	OH	H	H
[101] Denthysin	OH	H	OH	OMe
[102] 5-Hydroxy-2,4-dimethoxy-phenanthrene	H	OH	H	H
[103] 3-Hydroxy-2,4,7-trimethoxy-phenanthrene	OH	H	OMe	H



	R ₁	R ₂	R ₃	R ₄	R ₅
[104] Cypripedin	H	OH	OMe	OMe	H
[105] Densiflorol B	H	OH	H	OMe	H
[106] Denbinobin	OH	OMe	H	H	OMe

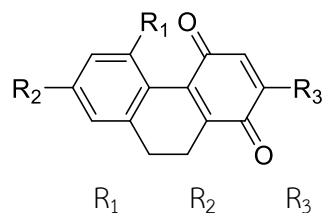


Fimbriatone [107]

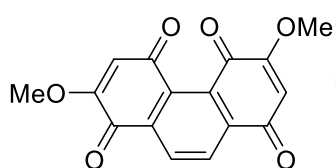


[108] Loddigesinol B

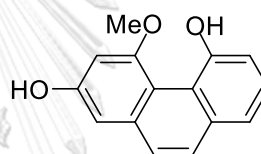
Figure 2 Structures of phenanthrenes and derivatives from *Dendrobium* species (Continued).



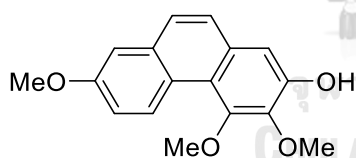
[109] Dendronone	OH	OMe	H
[110] Ephemeranthoquinone	H	OH	OMe
[111] 5-Methoxy-7-hydroxy- 9,10-dihydro-1,4-phenanthrenequinone	OMe	OH	H



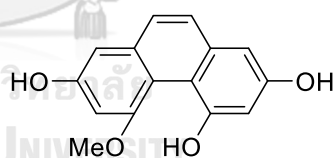
[112] Moniliformin



[113] Moscatin

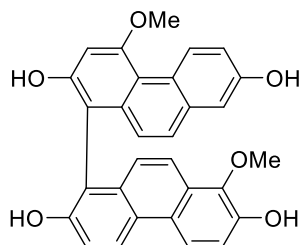


[114] Dendroscabrols A



[115] 2,5,7-trihydroxy-4-methoxyphenanthrene

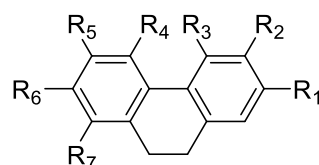
Figure 2 Structures of phenanthrenes and derivatives from *Dendrobium* species (Continued).



[116] Bleformin G

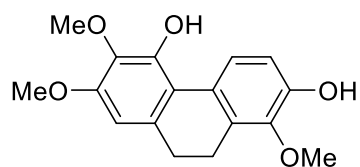
	R ₁	R ₂	R ₃	R ₄	R ₅	R ₆
[117] Coelonin	OH	H	OMe	H	H	OH
[118] 9,10-Dihydromoscatin	H	H	OH	OMe	H	OH
[119] 9,10-Dihydrophenanthrene-2,4,7-triol	OH	H	OH	H	H	OH
[120] 4,5-Dihydroxy-2,3-dimethoxy-9,10-dihydrophenanthrene	OMe	OMe	OH	OH	H	H
[121] 4,5-Dihydroxy-2,6-dimethoxy-9,10-dihydrophenanthrene	OMe	H	OH	OH	OMe	H
[122] 4,5-Dihydroxy-3,7-dimethoxy-9,10-dihydrophenanthrene	H	OMe	OH	OH	H	OMe
[123] 4,5-Dihydroxy-2-methoxy-9,10-dihydrophenanthrene		OMe	H	OH	OH	H
[124] Lusianthridin	OMe	H	OH	H	H	OH

Figure 2 Structures of phenanthrenes and derivatives from *Dendrobium* species (Continued).

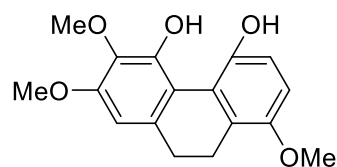


	R ₁	R ₂	R ₃	R ₄	R ₅	R ₆	R ₇
[125] 2,7-Dihydroxy-3,4,6-trimethoxy-9,10-dihydrophenanthrene	OH	OMe	OMe	H	OMe	OH	H
[126] 2,8-Dihydroxy-3,4,7-trimethoxy-9,10-dihydrophenanthrene	OH	OMe	OMe	H	H	OMe	OH
[127] 4,7-Dihydroxy-2,3,6-trimethoxy-9,10-dihydrophenanthrene	OMe	OMe	OH	H	OMe	OH	H
[128] Ephemeranthol A	OH	H	H	OH	OMe	OMe	H
[129] Ephemeranthol C	OH	OH	OMe	OH	H	H	H
[130] Erianthridin	OH	OMe	OMe	H	H	OH	H
[131] Flavanthridin	OH	H	H	OMe	OH	OMe	H
[132] Hircinol	OH	H	OMe	OH	H	H	H
[133] 3-Hydroxy-2,4,7-trimethoxy-9,10-dihydrophenanthrene	OMe	OH	OMe	H	H	OMe	H
[134] 3,4-dimethoxy-1-(methoxymethyl)-9,10-dihydrophenanthrene-2,7-diol	OH	H	H	OMe	OMe	OH	CH ₂ -OMe
[135] 2,4,7-trihydroxy-3-methoxy-9,10-dihydrophenanthrene	OH	H	H	OH	OMe	OH	H
[136] Dendroinfundin A	OMe	H	H	OH	OMe	OMe	H

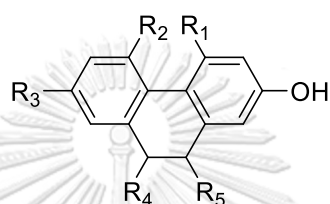
Figure 2 Structures of phenanthrenes and derivatives from *Dendrobium* species (Continued).



[137] 4,7-dihydroxy-2,3,8-trimethoxy-9,10-dihydrophenanthrene



[138] Dendroinfundin B



[139] 2-Hydroxy-4,7-dimethoxy-9,10-dihydrophenanthrene

	R ₁	R ₂	R ₃	R ₄	R ₅
[139]	OMe	H	OMe	H	H
[140]	OH	OH	OMe	H	H
[141]	OMe	OH	OH	H	H
[142]	H	OMe	OH	H	OMe
[143]	H	OMe	OH	H	OH

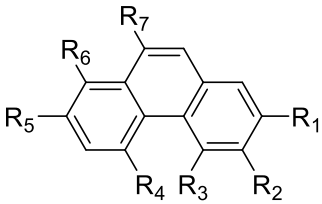
[140] 7-Methoxy-9,10-dihydrophenanthrene-2,4,5-triol

[141] 2,5,7-Trihydroxy-4-methoxy-9,10-dihydrophenanthrene

[142] Plicatol C

[143] Rotundatin

Figure 2 Structures of phenanthrenes and derivatives from *Dendrobium* species (Continued).



	R ₁	R ₂	R ₃	R ₄	R ₅	R ₆	R ₇
[144] 2,5-Dihydroxy-3,4-dimethoxyphenanthrene	OH	OMe	OMe	OH	H	H	H
[145] 2,5-Dihydroxy-4,9-dimethoxyphenanthrene	OH	H	OMe	OH	H	H	OMe
[146] 2,8-Dihydroxy-3,4,7-trimethoxyphenanthrene	OH	OMe	OMe	H	OMe	OH	H
[147] Epheranthol B	H	H	OMe	OH	OMe	H	H
[148] Fimbriol B	OH	OMe	OH	H	H	H	H
[149] Flavanthrinin	H	H	OMe	H	OH	H	H

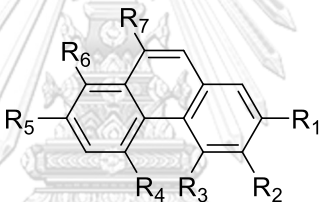


Figure 2 Structures of phenanthrenes and derivatives from *Dendrobium* species (Continued).

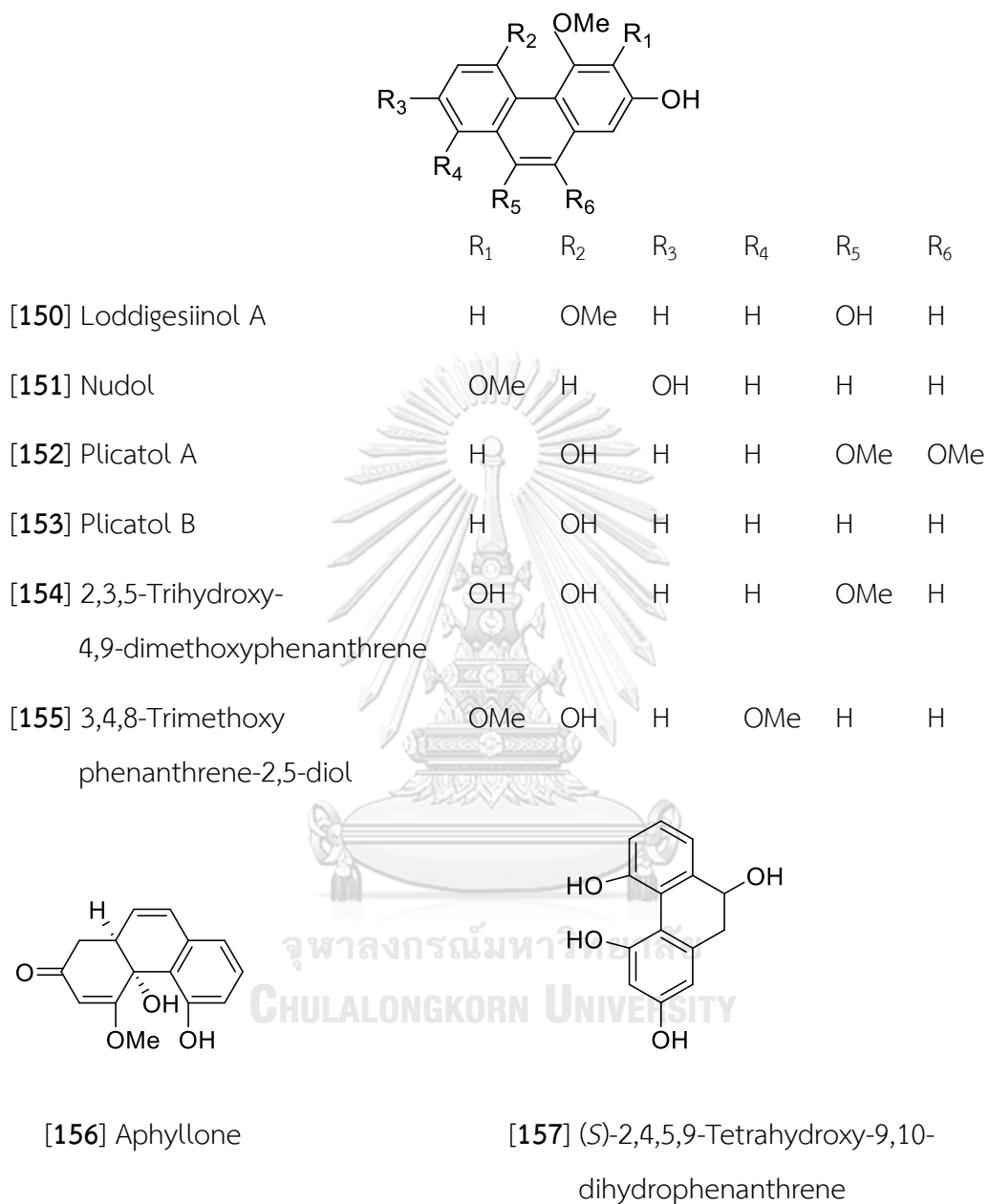
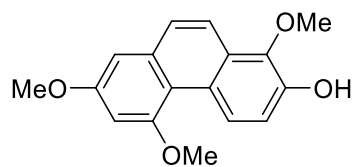
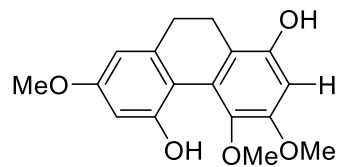


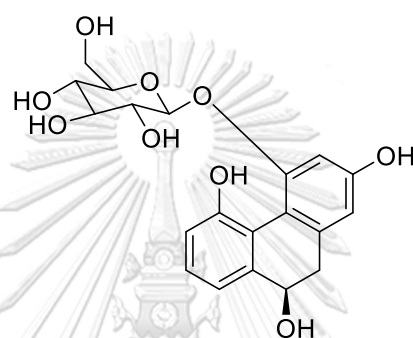
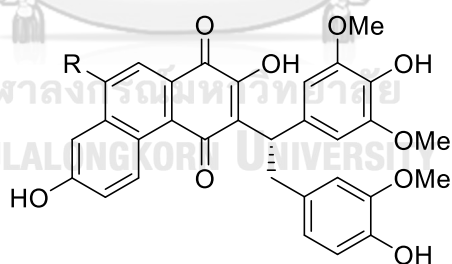
Figure 2 Structures of phenanthrenes and derivatives from *Dendrobium* species (Continued).



[158] 1,5,7-Trimethoxyphenanthren-2-ol



[159] 1,5-Dihydroxy-3,4,7-trimethoxy-9,10-dihydrophenanthrene

[160] 2,5,9S-Trihydroxy-9,10-dihydrophenanthrene-4-O- β -D-glucopyranoside

[161] Loddigesiinol G: R = H

[162] Loddigesiinol H: R = OH

Figure 2 Structures of phenanthrenes and derivatives from *Dendrobium* species (Continued).

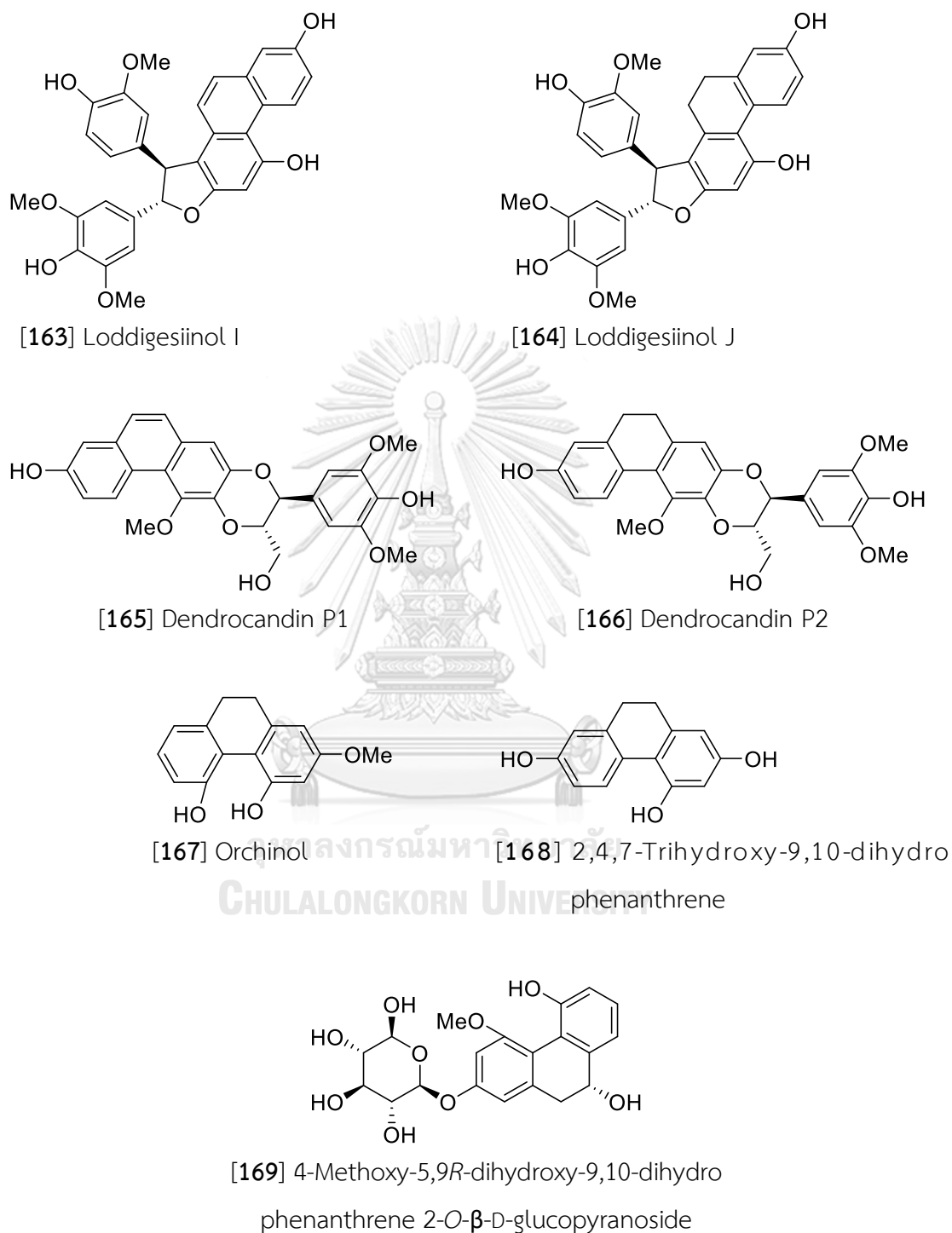


Figure 2 Structures of phenanthrenes and derivatives from *Dendrobium* species (Continued).

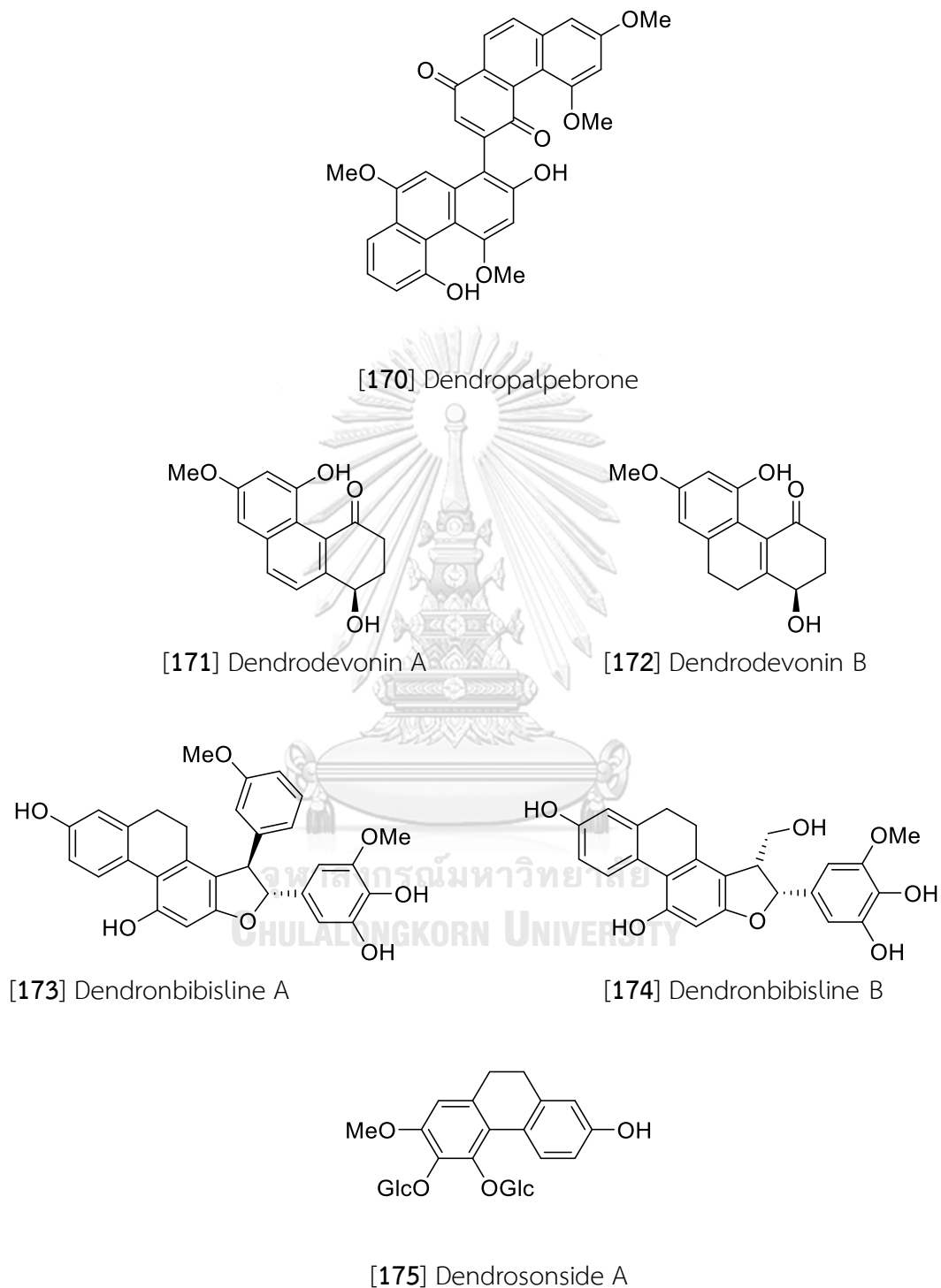


Figure 2 Structures of phenanthrenes and derivatives from *Dendrobium* species (Continued).

Table 3 Flavonoids in the genus *Dendrobium*.

Compounds	Plant	Plant part	Reference
(2S)-Homoeriodictyol [176]	<i>D. densiflorum</i>	Stem	(Fan et al., 2001)
	<i>D. ellipsophyllum</i>	Whole plant	(Tanagornmeatar et al., 2014)
Naringenin [177]	<i>D. aurantiacum</i> var. <i>denneanum</i>	Stem	(Yang, Wang, et al., 2006a)
	<i>D. densiflorum</i>	Stem	(Fan et al., 2001)
	<i>D. longicornu</i>	Stem	(Hu et al., 2008a)
(2S)-Eriodictyol [178]	<i>D. trigonopus</i>	Stem	(Hu et al., 2008b)
	<i>D. ellipsophyllum</i>	Whole plant	(Tanagornmeatar et al., 2014)
	<i>D. tortile</i>	Whole plant	(Limpanit et al., 2016)
Vicenin-2 [179]	<i>D. aurantiacum</i> var. <i>denneanum</i>	Stem	(Xiong et al., 2013)
Apigenin [180]	<i>D. crystallinum</i>	Stem	(Wang et al., 2009)
	<i>D. williamsonii</i>	Whole plant	(Rungwichaniwat et al., 2014)
5,6-Dihydroxy-4'-methoxyflavone [181]	<i>D. chrysotoxum</i>	Stem	(Hu et al., 2012)

Table 3 Flavonoids in the genus *Dendrobium* (Continued).

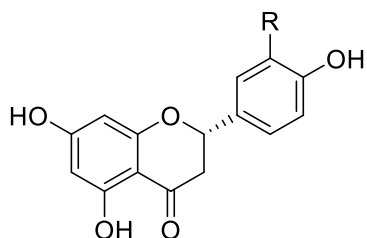
Compounds	Plant	Plant part	Reference
Chrysoeriol [182]	<i>D. ellipsophyllum</i>	Whole plant	(Tanagornmeatar et al., 2014)
Luteolin [183]	<i>D. aurantiacum</i> var. <i>denneanum</i>	Whole plant	(Liu et al., 2009)
	<i>D. ellipsophyllum</i>	Whole plant	(Tanagornmeatar et al., 2014)
6-C-(α -Arabinopyranosyl)-8-C-[(2-O- α -rhamnopyranosyl)- β -galactopyranosyl] apigenin [184]	<i>D. huoshanense</i>	Aerial part	(Chang et al., 2010)
6-C-(α -Arabinopyranosyl)-8-C-[(2-O- α -rhamnopyranosyl)- β -glucopyranosyl] apigenin [185]	<i>D. huoshanense</i>	Aerial part	(Chang et al., 2010)
6'''-Glucosyl-vitexin [186]	<i>D. crystallinum</i>	Stem	(Wang et al., 2009)
Isoschaftoside [187]	<i>D. huoshanense</i>	Aerial part	(Chang et al., 2010)
Isoviolanthin [188]	<i>D. crystallinum</i>	Stem	(Wang et al., 2009)

Table 3 Flavonoids in the genus *Dendrobium* (Continued).

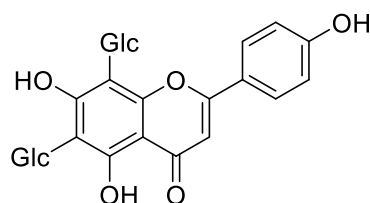
Compounds	Plant	Plant part	Reference
6-C-[(2-O- α -Rhamno pyranosyl)- β -gluco pyranosyl]-8-C-(α -arabinopyranosyl) apigenin [189]	<i>D. huoshanense</i>	Aerial part	(Chang et al., 2010)
6-C-(β -Xylopyranosyl)-8-C-[(2-O- α -rhamno pyranosyl)- β -gluco pyranosyl]apigenin [190]	<i>D. huoshanense</i>	Aerial part	(Chang et al., 2010)
Kaempferol [191]	<i>D. aurantiacum</i> var. <i>denneanum</i>	Stem	(Yang, Wang, et al., 2006a)
Kaempferol-3-O- α -L rhamnopyranoside [192]	<i>D. secundum</i>	Stem	(Phechrmeekha et al., 2012)
Kaempferol-3,7-O-di- α -L-rhamnopyranoside [193]	<i>D. secundum</i>	Stem	(Phechrmeekha et al., 2012)
Kaempferol-3-O- α -L-rhamnopyranosyl-(1 \rightarrow 2)- β -D-gluco pyranoside [194]	<i>D. capillipes</i>	Stem	(Phechrmeekha et al., 2012)

Table 3 Flavonoids in the genus *Dendrobium* (Continued).

Compounds	Plant	Plant part	Reference
Kaempferol-3-O- α -L-rhamnopyranosyl-(1 \rightarrow 2)- β -D-xylopyranoside [195]	<i>D. capillipes</i>	Stem	(Phechrmeekha et al., 2012)
Quercetin-3-O-L-rhamnopyranoside [196]	<i>D. secundum</i>	Stem	(Phechrmeekha et al., 2012)
Quercetin-3-O- α -L-rhamnopyranosyl-(1 \rightarrow 2)- β -D-xylopyranoside [197]	<i>D. capillipes</i>	Stem	(Phechrmeekha et al., 2012)
5-Hydroxy-3-methoxyflavone-7-O-[β -D-apiosyl-(1 \rightarrow 6)]- β -D-glucoside [198]	<i>D. devonianum</i>	Stem	(Sun et al., 2014)
Isorhamnetin-3-O- β -D-rutinoside [199]	<i>D. nobile</i>	Stem	(Zhou et al., 2017)



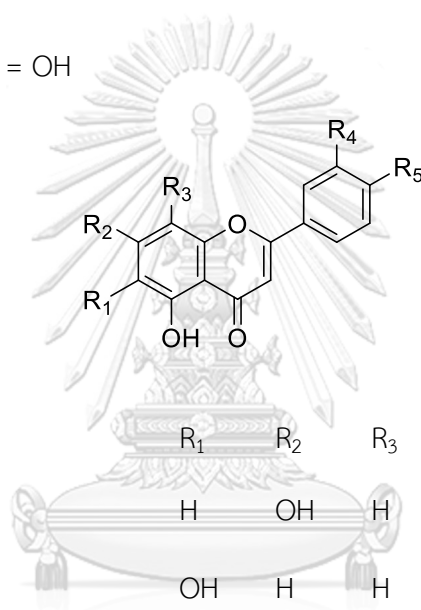
[176] (2S)-Homoeriodictyol: R = OMe



[179] Vicenin-2

[177] Naringenin: R = H

[178] (2S)-Eriodictyol: R = OH



[180] Apigenin

R ₁	R ₂	R ₃	R ₄	R ₅
H	OH	H	H	OH

[181] 5,6-Dihydroxy-4'-methoxyflavone

OH	H	H	H	OMe
----	---	---	---	-----

[182] Chrysoeriol

H	OH	H	OMe	OH
---	----	---	-----	----

[183] Luteolin

H	OH	H	OH	OH
---	----	---	----	----

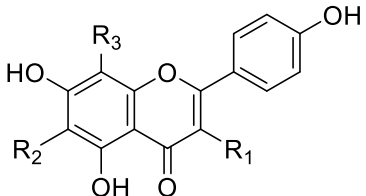
[184] 6-C-(α -Arabinopyranosyl)-8-C-[(2-O- α -rhamnopyranosyl)- β -galactopyranosyl]apigenin

-Ara	OH	-Gal-Rha	H	OH
------	----	----------	---	----

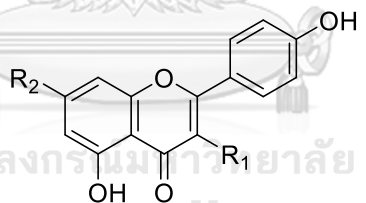
[185] 6-C-(α -Arabinopyranosyl)-8-C-[(2-O- α -rhamnopyranosyl)- β -glucopyranosyl]apigenin

-Ara	OH	-Glc-Rha	H	OH
------	----	----------	---	----

Figure 3 Structures of flavonoids from *Dendrobium* species.

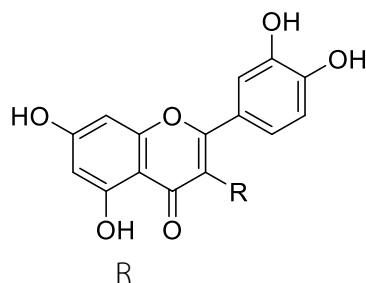


	R ₁	R ₂	R ₃
[186] 6'''-Glucosyl-vitexin	H	H	-Glc
[187] Isoschaftoside	H	-Ara	-Glc
[188] Isoviolanthin	H	-Rha	-Glc
[189] 6-C-[(2-O- α -Rhamnopyranosyl)- β -glucopyranosyl]-8-C-(α -arabinopyranosyl)apigenin	H	-Glc-Rha	-Ara
[190] 6-C-(β -Xylopyranosyl)-8-C-[(2-O- α -rhamnopyranosyl)- β -glucopyranosyl]apigenin	H	-Xyl	-Glc-Rha
[191] Kaempferol	OH	H	H



	R ₁	R ₂
[192] Kaempferol-3-O- α -L-rhamnopyranoside	O-Rha	OH
[193] Kaempferol-3,7-O-di- α -L-rhamnopyranoside	O-Rha	O-Rha
[194] Kaempferol-3-O- α -L-rhamnopyranosyl-(1 \rightarrow 2)- β -D-glucopyranoside	O-Glc-Rha	OH
[195] Kaempferol-3-O- α -L-rhamnopyranosyl-(1 \rightarrow 2)- β -D-xylopyranoside	O-Xyl-Rha	OH

Figure 3 Structures of flavonoids from *Dendrobium* species (Continued).

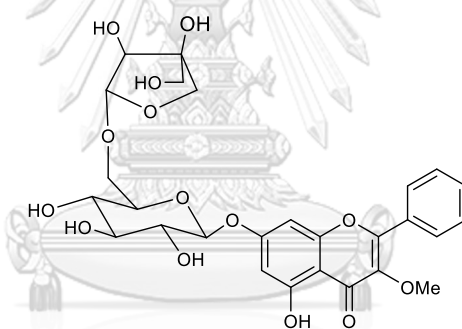


[196] Quercetin-3-O- α -L-rhamnopyranoside

O-Rha

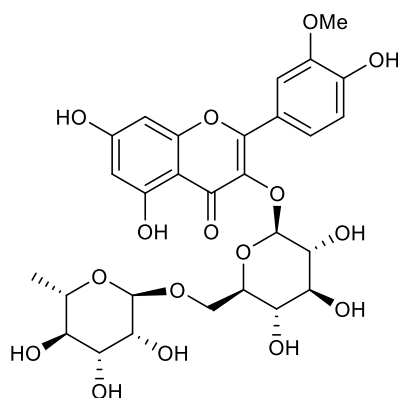
[197] Quercetin-3-O- α -L-rhamnopyranosyl-(1 \rightarrow 2)- β -D-xylopyranoside

O-Xyl-Rha



[198] 5-Hydroxy-3-methoxy-flavone-7-O-[\mathbf{\beta}-D-apiosyl-(1 \rightarrow 6)]-\mathbf{\beta}-D-glucoside

CHULALONGKORN UNIVERSITY



[199] Isorhamnetin-3-O-\mathbf{\beta}-D-rutinoside

Figure 3 Structures of flavonoids from *Dendrobium* species (Continued).

Table 4 Terpenoids and alkaloids in the genus *Dendrobium*.

Compounds	Plant	Plant part	Reference
Aduncin [200]	<i>D. longicornu</i>	Stem	(Hu et al., 2008a)
Amoenin [201]	<i>D. aduncum</i>	Whole plant	(Dahmén & Leander, 1978)
	<i>D. williamsonii</i>	Whole plant	(M. Yang et al., 2018)
Amotin [202]	<i>D. amoenum</i>	Whole plant	(Majumder et al., 1999)
α -Dihydropicrotoxinin [203]	<i>D. amoenum</i>	Whole plant	(Majumder et al., 1999)
Dendrobane A [204]	<i>D. moniliforme</i>	Stem	(Bi et al., 2004)
Dendronobilin A [205]	<i>D. nobile</i>	Stem	(Zhang et al., 2007)
Dendronobilin B [206]	<i>D. wardianum</i>	Stem	(Fan et al., 2013)
	<i>D. williamsonii</i>	Whole plant	(Yang et al., 2019)
Dendronobilin C [207]	<i>D. crystallinum</i>	Stem	(Wang et al., 2009)
Dendronobilin D [208]	<i>D. nobile</i>	Stem	(Zhang et al., 2007)

Table 4 Terpenoids and alkaloids in the genus *Dendrobium* (Continued).

Compounds	Plant	Plant part	Reference
Dendronobilin E [209]	<i>D. nobile</i>	Stem	(Zhang et al., 2007)
Dendronobilin F [210]	<i>D. nobile</i>	Stem	(Zhang et al., 2007)
Dendronobilin F [210]	<i>D. signatum</i>	Aerial part	(Khumploy et al., 2021)
Dendronobilin G [211]	<i>D. nobile</i>	Stem	(Zhang et al., 2007)
Dendronobilin H [212]	<i>D. nobile</i>	Stem	(Zhang et al., 2007)
Dendronobilin I [213]	<i>D. nobile</i>	Stem	(Zhang et al., 2007)
	<i>D. findlayanum</i>	Stem	(Dan et al., 2019)
Dendronobilin J [214]	<i>D. nobile</i>	Stem	(Zhang et al., 2007)
Dendronobilin K [215]	<i>D. wardianum</i>	Stem	(Fan et al., 2013)
Dendronobilin L [216]	<i>D. nobile</i>	Stem	(Zhang et al., 2007)
Dendronobilin M [217]	<i>D. nobile</i>	Stem	(Zhang et al., 2008)

Table 4 Terpenoids and alkaloids in the genus *Dendrobium* (Continued).

Compounds	Plant	Plant part	Reference
Dendronobilin N [218]	<i>D. nobile</i>	Stem	(Zhang et al., 2008)
	<i>D. findlayanum</i>	Stem	(Dan et al., 2019)
Dendrowardol A [219]	<i>D. nobile</i>	Stem	(Zhang et al., 2008)
Dendrowardol B [220]	<i>D. nobile</i>	Stem	(Zhang et al., 2008)
Dendrowardol C [221]	<i>D. wardianum</i>	Stem	(Fan et al., 2013)
Corchoionoside C [222]	<i>D. wardianum</i>	Stem	(Fan et al., 2013)
Crystallinin [223]	<i>D. wardianum</i>	Stem	(Fan et al., 2013)
Findlayanin [224]	<i>D. polyanthum</i>	Stem	(Hu et al., 2009)
3-Hydroxy-2-oxodendrobine [225]	<i>D. findlayanum</i>	Whole plant	(Qin et al., 2011)
Dendrobine [226]	<i>D. nobile</i>	Stem	(Wang et al., 1985)
	<i>D. findlayanum</i>	Stem	(D. Yang et al., 2018)
Dendromonilaside A [227]	<i>D. nobile</i>	Stem	(Zhang et al., 2007)
Dendromonilaside B [228]	<i>D. moniliforme</i>	Stem	(Zhao et al., 2003)

Table 4 Terpenoids and alkaloids in the genus *Dendrobium* (Continued).

Compounds	Plant	Plant part	Reference
Dendromonilaside C [229]	<i>D. moniliforme</i>	Stem	(Zhao et al., 2003)
Dendromonilaside D [230]	<i>D. moniliforme</i>	Stem	(Zhao et al., 2003)
Dendronobiloside A [231]	<i>D. moniliforme</i>	Stem	(Zhao et al., 2003)
	<i>D. nobile</i>	Stem	(Zhang et al., 2007)
Dendronobiloside B [232]	<i>D. nobile</i>	Stem	(Ye & Zhao, 2002; Zhao et al., 2001)
Dendronobiloside C [233]	<i>D. nobile</i>	Stem	(Ye & Zhao, 2002; Zhao et al., 2001)
Dendronobiloside D [234]	<i>D. nobile</i>	Stem	(Ye & Zhao, 2002; Zhao et al., 2001)
Dendronobiloside E [235]	<i>D. nobile</i>	Stem	(Ye & Zhao, 2002; Zhao et al., 2001)

Table 4 Terpenoids and alkaloids in the genus *Dendrobium* (Continued).

Compounds	Plant	Plant part	Reference
Dendroside A [236]	<i>D. moniliforme</i>	Stem	(Zhao et al., 2003)
	<i>D. nobile</i>	Stem	(Ye & Zhao, 2002; Zhao et al., 2001)
	<i>D. findlayanum</i>	Stem	(Dan et al., 2019)
Dendroside B [237]	<i>D. nobile</i>	Stem	(Ye & Zhao, 2002)
Dendroside C [238]	<i>D. moniliforme</i>	Stem	(Zhao et al., 2003)
	<i>D. nobile</i>	Stem	(Ye & Zhao, 2002)
Dendroside D [239]	<i>D. nobile</i>	Stem	(Ye & Zhao, 2002)
Dendroside E [240]	<i>D. nobile</i>	Stem	(Ye & Zhao, 2002)
Dendroside F [241]	<i>D. moniliforme</i>	Stem	(Zhao et al., 2003)
Dendroside G [242]	<i>D. nobile</i>	Stem	(Ye & Zhao, 2002)
Dendrowillin A [243]	<i>D. williamsonii</i>	Whole plant	(M. Yang et al., 2018)

Table 4 Terpenoids and alkaloids in the genus *Dendrobium* (Continued).

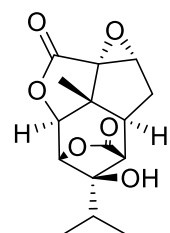
Compounds	Plant	Plant part	Reference
Dendrowillin B [244]	<i>D. williamsonii</i>	Whole plant	(M. Yang et al., 2018)
(-)-Picrotin [245]	<i>D. williamsonii</i>	Whole plant	(M. Yang et al., 2018)
Asiatic acid [246]	<i>D. parishii</i>	Whole plant	(Kongkatitham et al., 2018)
Dendroterpene A [247]	<i>D. nobile</i>	Stem	(P. Wang et al., 2019)
Dendroterpene B [248]	<i>D. nobile</i>	Stem	(P. Wang et al., 2019)
Dendroterpene C [249]	<i>D. nobile</i>	Stem	(P. Wang et al., 2019)
Dendroterpene D [250]	<i>D. nobile</i>	Stem	(P. Wang et al., 2019)
Dendroterpene E [251]	<i>D. nobile</i>	Stem	(Wang et al., 2022)
Dendrofindlayanoside A [252]	<i>D. findlayanum</i>	Stem	(Dan et al., 2019)
Dendrofindlayanoside B [253]	<i>D. findlayanum</i>	Stem	(Dan et al., 2019)
Dendrofindlayanoside C [254]	<i>D. findlayanum</i>	Stem	(Dan et al., 2019)

Table 4 Terpenoids and alkaloids in the genus *Dendrobium* (Continued).

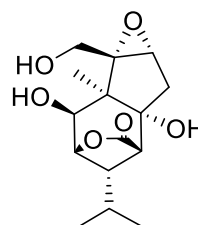
Compounds	Plant	Plant part	Reference
Dendrofindlayanobilin A [255]	<i>D. findlayanum</i>	Stem	(Dan et al., 2019)
Dendroxine [256]	<i>D. signatum</i>	Aerial part	(Khumploy et al., 2021)
7-hydroxy dendroterpene B [257]	<i>D. signatum</i>	Aerial part	(Khumploy et al., 2021)
N-methoxycarbonyl dendrobine [258]	<i>D. nobile</i>	Stem	(Zhang et al., 2022)
Dendronboic acid [259]	<i>D. nobile</i>	Stem	(Zhang et al., 2022)
2-hydroxydendrobine [260]	<i>D. findlayanum</i>	Stem	(D. Yang et al., 2018)
Findlayine A [261]	<i>D. findlayanum</i>	Stem	(D. Yang et al., 2018)
Findlayine B [262]	<i>D. findlayanum</i>	Stem	(D. Yang et al., 2018)
Findlayine C [263]	<i>D. findlayanum</i>	Stem	(D. Yang et al., 2018)
Findlayine D [264]	<i>D. findlayanum</i>	Stem	(D. Yang et al., 2018)

Table 4 Terpenoids and alkaloids in the genus *Dendrobium* (Continued).

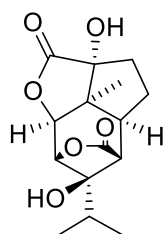
Compounds	Plant	Plant part	Reference
Crepidine [265]	<i>D. crepidatum</i>	Stem	(Xu et al., 2019)
Isocrepidamine [266]	<i>D. crepidatum</i>	Stem	(Xu et al., 2019)
Crepidamine [267]	<i>D. crepidatum</i>	Stem	(Xu et al., 2019)
Dendrocrepine [268]	<i>D. crepidatum</i>	Stem	(Xu et al., 2020)
Dendrocrepidine B [269]	<i>D. crepidatum</i>	Stem	(Xu et al., 2020)
Crepidatumines A [270]	<i>D. crepidatum</i>	Stem	(Xu et al., 2020)
Crepidatumines B [271]	<i>D. crepidatum</i>	Stem	(Xu et al., 2020)
Crepidatumines C [272]	<i>D. crepidatum</i>	Stem	(Xu et al., 2019)
Crepidatumines D [273]	<i>D. crepidatum</i>	Stem	(Xu et al., 2019)
Dendrocrepidamine [274]	<i>D. crepidatum</i>	Root	(Ding et al., 2021)
Dendroxine B [275]	<i>D. nobile</i>	Stem	(Zhang et al., 2023)
Denrine B [276]	<i>D. nobile</i>	Stem	(Zhang et al., 2023)
Anosmine [277]	<i>D. parishii</i>	Whole plant	(Kongkatitham et al., 2018)



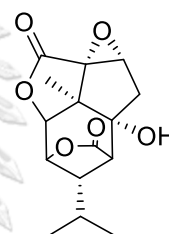
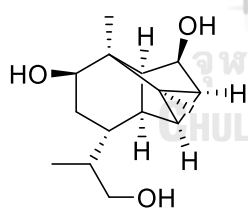
[200] Aduncin



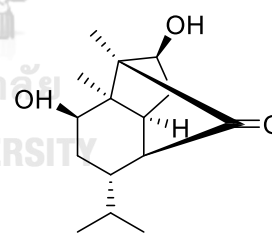
[201] Amoenin



[202] Amotin

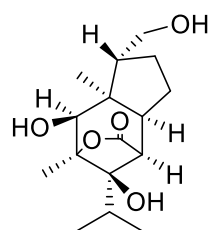
[203] α -Dihydropicrotoxinin

[204] Dendrobane A

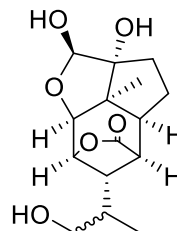


[205] Dendronobilin A

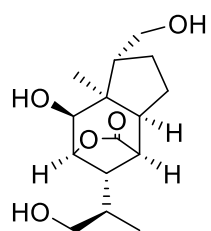
Figure 4 Structures of terpenoids and alkaloids from *Dendrobium* species.



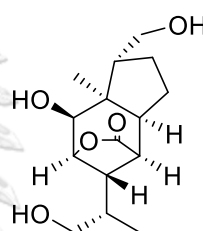
[206] Dendronobilin B



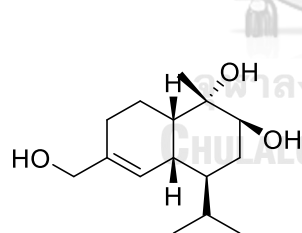
[207] Dendronobilin C



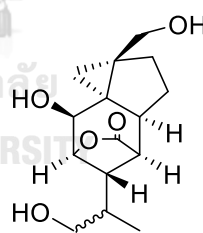
[208] Dendronobilin D



[209] Dendronobilin E

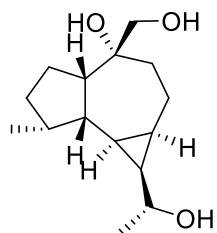


[210] Dendronobilin F

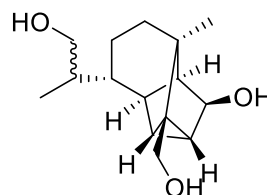


[211] Dendronobilin G

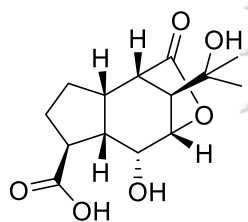
Figure 4 Structures of terpenoids and alkaloids from *Dendrobium* species (Continued).



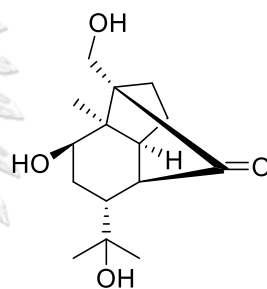
[212] Dendronobilin H



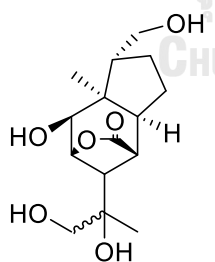
[213] Dendronobilin I



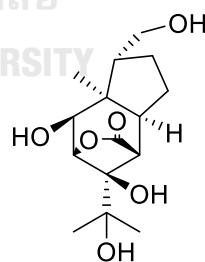
[214] Dendronobilin J



[215] Dendronobilin K

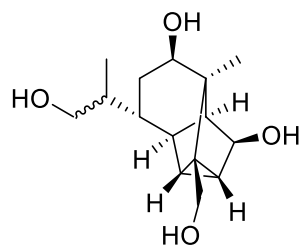


[216] Dendronobilin L

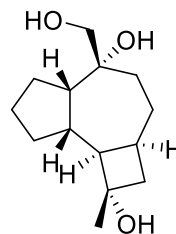


[217] Dendronobilin M

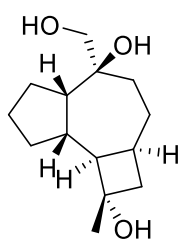
Figure 4 Structures of terpenoids and alkaloids from *Dendrobium* species (Continued).



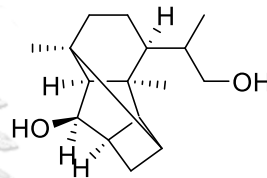
[218] Dendronobilin N



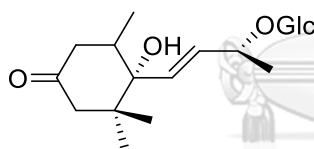
[219] Dendrowardol A



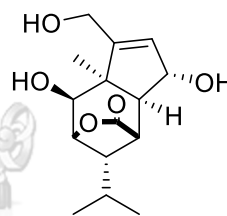
[220] Dendrowardol B



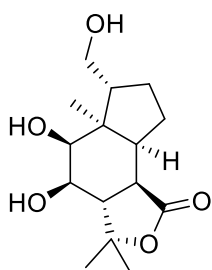
[221] Dendrowardol C



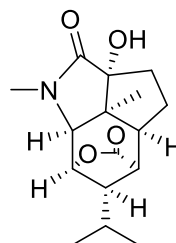
[222] Corchoionoside C



[223] Crystallinin

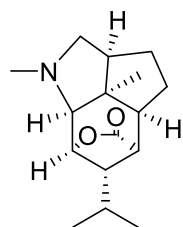


[224] Findlayanin

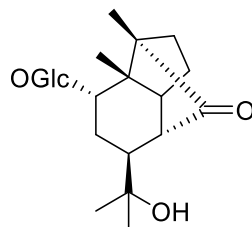


[225] 3-Hydroxy-2-oxodendrobine

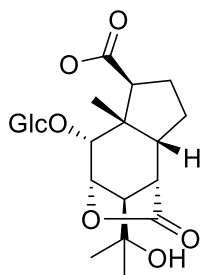
Figure 4 Structures of terpenoids and alkaloids from *Dendrobium* species
(Continued).



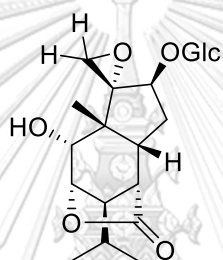
[226] Dendrobine



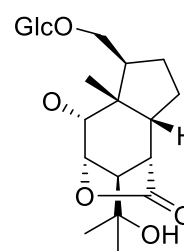
[227] Dendromonilide A



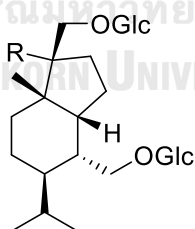
[228] Dendromonilide B



[229] Dendromonilide C



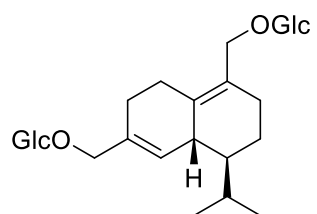
[230] Dendromonilide D



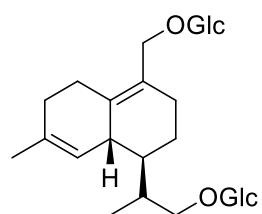
[231] Dendronobiloside A: R = H

[232] Dendronobiloside B: R = OH

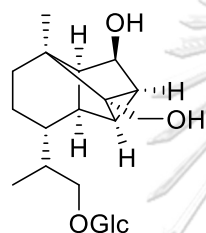
Figure 4 Structures of terpenoids and alkaloids from *Dendrobium* species
(Continued).



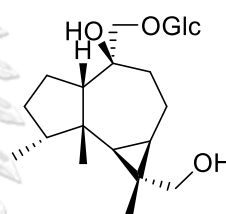
[233] Dendronobiloside C



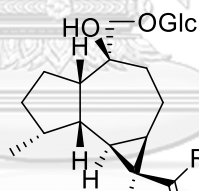
[234] Dendronobiloside D



[235] Dendronobiloside E

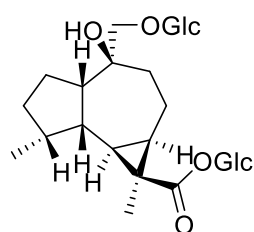


[236] Dendroside A

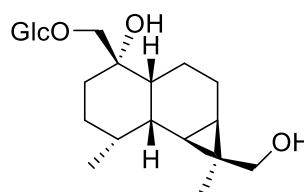


[237] Dendroside B: R = OGlc

[238] Dendroside C: R = OH

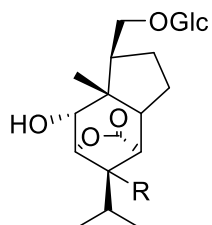


[239] Dendroside D



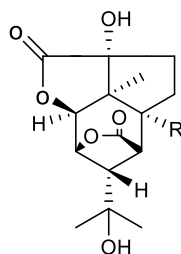
[240] Dendroside E

Figure 4 Structures of terpenoids and alkaloids from *Dendrobium* species
(Continued).

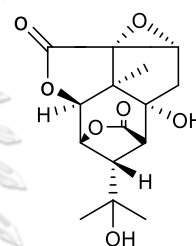


[241] Dendroside F: R = H

[242] Dendroside G: R = OH

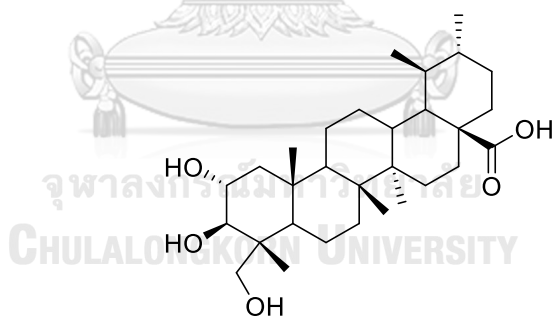


[243] Dendrowillin A: R = OH

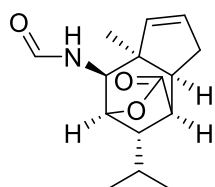


[245] (-)-Picrotin

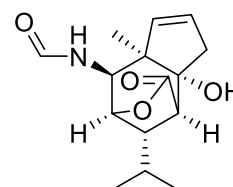
[244] Dendrowillin B: R = H



[246] Asiatic acid

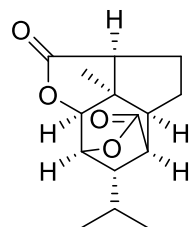


[247] Dendroterpene A

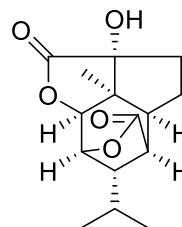


[248] Dendroterpene B

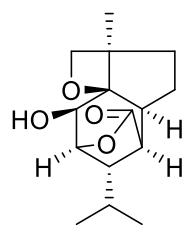
Figure 4 Structures of terpenoids and alkaloids from *Dendrobium* species (Continued).



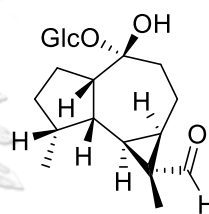
[249] Dendroterpene C



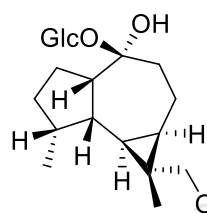
[250] Dendroterpene D



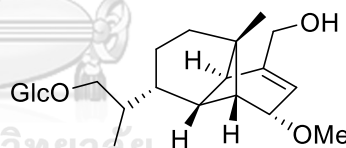
[251] Dendroterpene E



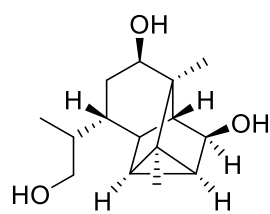
[252] Dendrofindlayanoside A



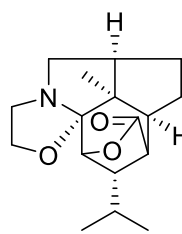
[253] Dendrofindlayanoside B



[254] Dendrofindlayanoside C



[255] Dendrofindlayanobilin A



[256] Dendroxine

Figure 4 Structures of terpenoids and alkaloids from *Dendrobium* species (Continued).

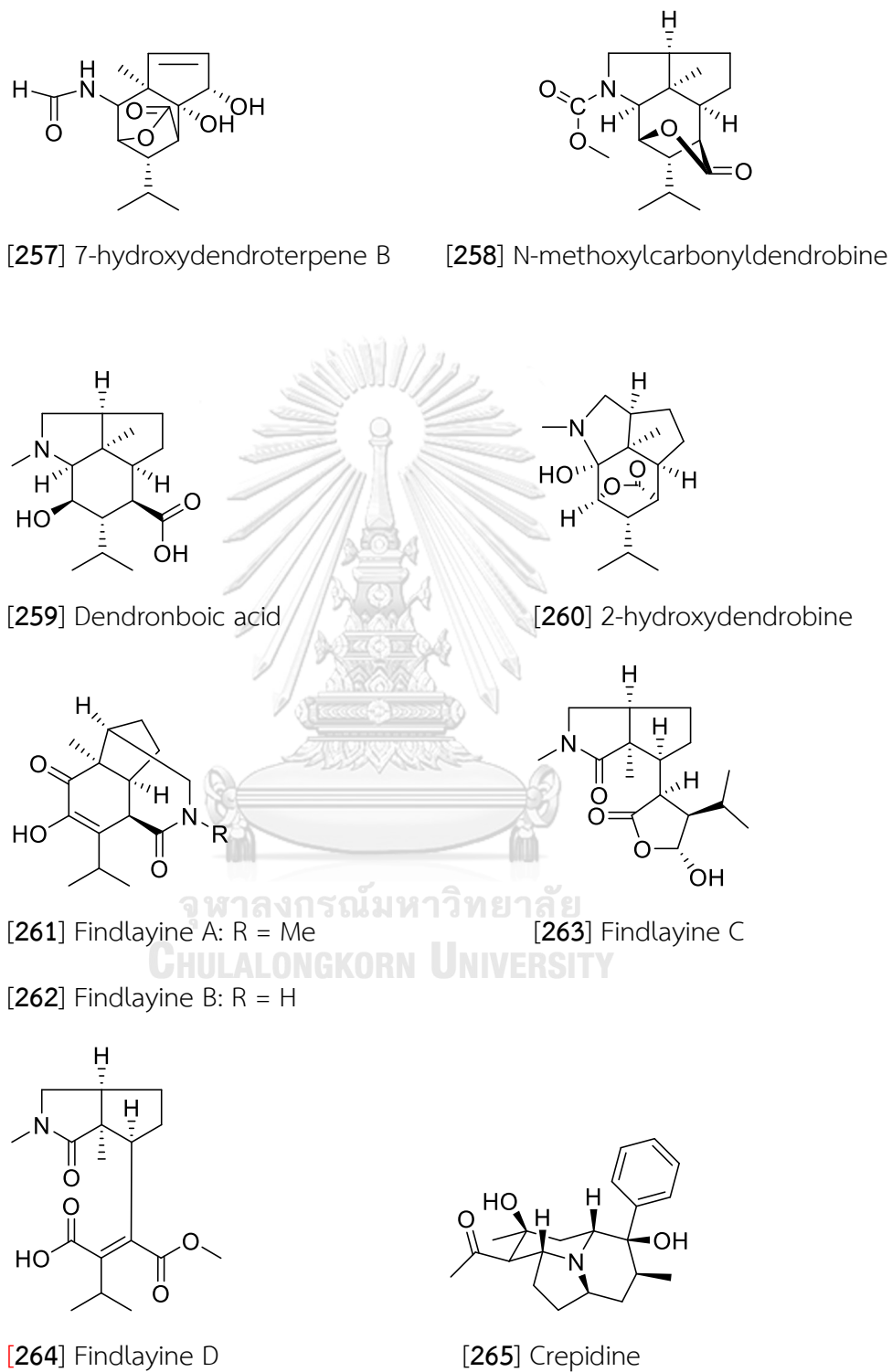


Figure 4 Structures of terpenoids and alkaloids from *Dendrobium* species (Continued).

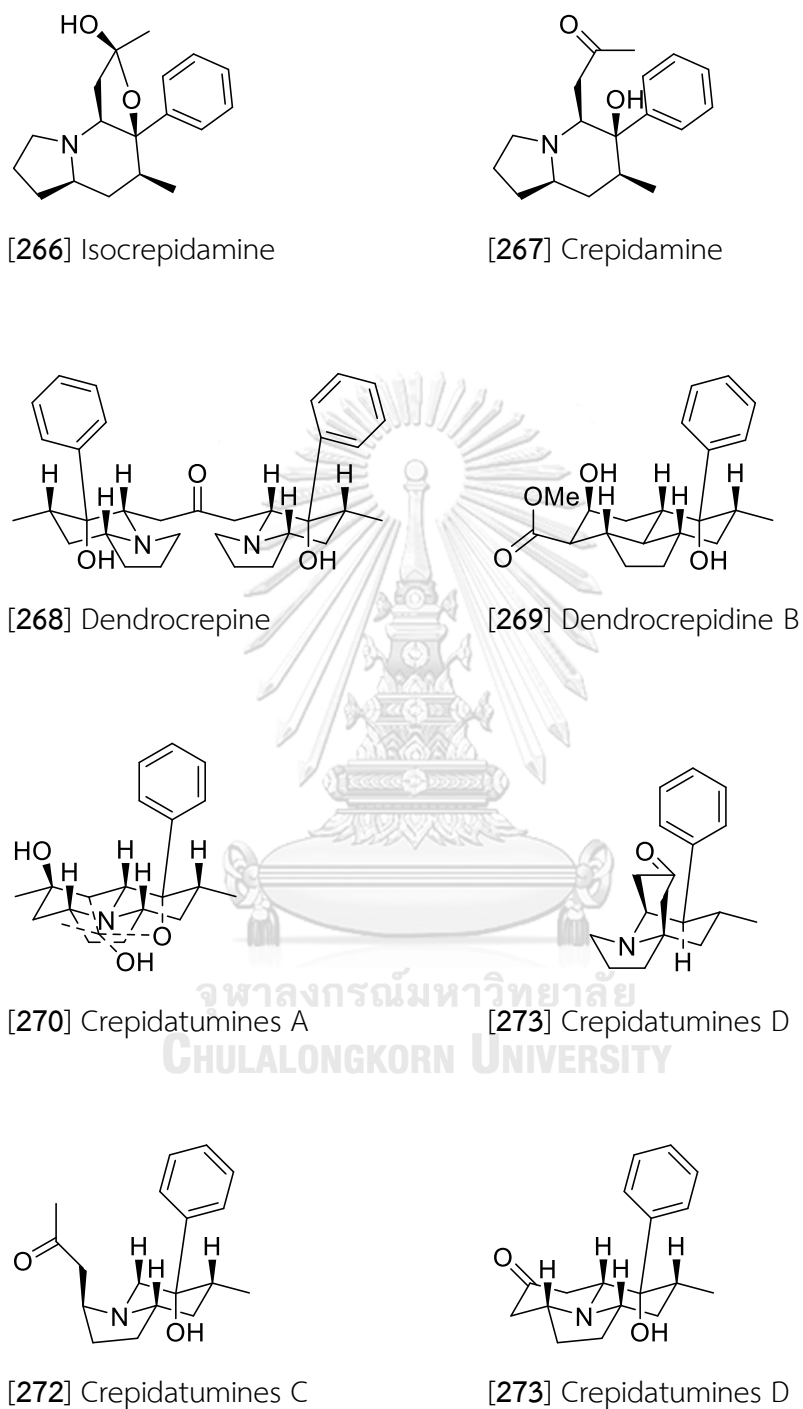
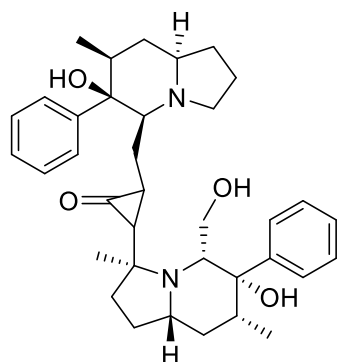
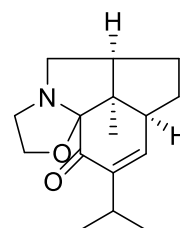


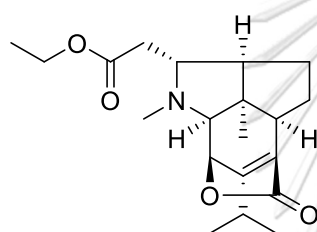
Figure 4 Structures of terpenoids and alkaloids from *Dendrobium* species (Continued).



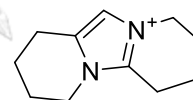
[274] Dendrocrepidamine



[275] Dendroxine B



[276] Denrine B



[277] Anosmine

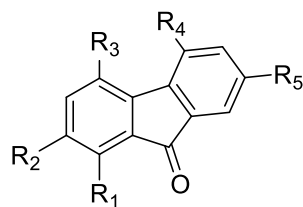
Figure 4 Structures of terpenoids and alkaloids from *Dendrobium* species
(Continued).

Table 5 Fluorenones and fluorenes in the genus *Dendrobium*.

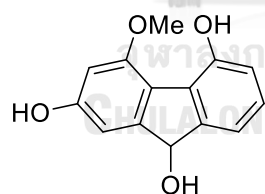
Compounds	Plant	Plant part	Reference
Denchrysan A [278]	<i>D. chrysotoxum</i>	Whole plant	(Y.-P. Li et al., 2009)
	<i>D. gibsonii</i>	Whole plant	(Thant et al., 2020)
Denchrysan B [279]	<i>D. brymerianum</i>	Whole plant	(Klongkumnuankarn et al., 2015)
	<i>D. chrysotoxum</i>	Whole plant	(Y.-P. Li et al., 2009)
Dendroflorin [280]	<i>D. aurantiacum</i> var. <i>denneanum</i>	Stem	(Yang, Wang, et al., 2006a)
	<i>D. brymerianum</i>	Whole plant	(Klongkumnuankarn et al., 2015)
	<i>D. palpebrae</i>	Whole plant	(Kyokong et al., 2019)
Dengibsin [281]	<i>D. aurantiacum</i> var. <i>denneanum</i>	Stem	(Yang, Wang, et al., 2006a)
	<i>D. chrysanthum</i>	Stem	(Yang, Qin, et al., 2006)
	<i>D. chrysotoxum</i>	Whole plant	(Y.-P. Li et al., 2009)

Table 5 Fluorenones and fluorenes in the genus *Dendrobium* (Continued).

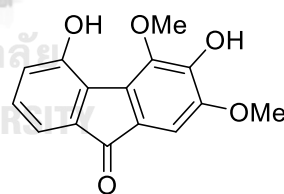
Nobilone [282]	<i>D. brymerianum</i>	Whole plant	(Klongkumnuankarn et al., 2015)
	<i>D. nobile</i>	Stem	(Zhang et al., 2007)
	<i>D. palpebrae</i>	Whole plant	(Kyokong et al., 2019)
	<i>D. gibsonii</i>	Whole plant	(Thant et al., 2020)
	<i>D. terminale</i>	Whole plant	(Cheng et al., 2022)
1,4,5-Trihydroxy-7-methoxy-9H-fluoren-9-one [283]	<i>D. chrysotoxum</i>	Whole plant	(Y.-P. Li et al., 2009)
2,4,7-Trihydroxy-1,5-dimethoxy-9-fluorenone [284]	<i>D. chrysotoxum</i>	Stem	(Yang et al., 2004)
Dengibsinin [285]	<i>D. gibsonii</i>	Whole plant	(Thant et al., 2020)
Fluorene			
4-Methoxy-9H-fluorene-2,5,9-triol [286]	<i>D. gibsonii</i>	Whole plant	(Thant et al., 2020)
Dihydrodengibsinin [287]	<i>D. gibsonii</i>	Whole plant	(Thant et al., 2020)



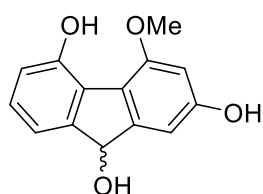
	R ₁	R ₂	R ₃	R ₄	R ₅
[278] Denchrysan A	H	OH	OH	OMe	OH
[280] Dendroflorin	OH	H	OH	OMe	OH
[281] Dengibsin	H	OH	OMe	OH	H
[282] Nobilone	H	OH	H	OMe	OH
[283] 1,4,5-Trihydroxy-7-methoxy- 9H-fluoren-9-one	OH	H	OH	OH	OMe
[284] 2,4,7-trihydroxy-1,5-dimethoxy- 9-fluorenone	OMe	OH	OH	OMe	OH



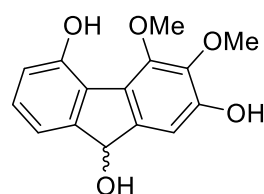
[279] Denchrysan B



[285] Dengibsinin



[286] 4-Methoxy-9H-fluorene-2,5,9-triol

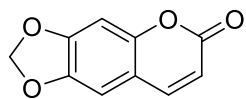


[287] Dihydrodengibsinin

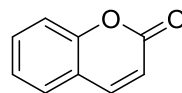
Figure 5 Structures of fluorenones and fluorenes from *Dendrobium* species.

Table 6 Coumarins in the genus *Dendrobium*.

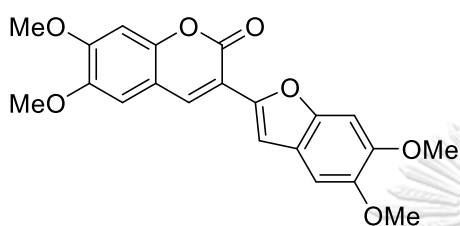
Compounds	Plant	Plant part	Reference
Ayapin [288]	<i>D. densiflorum</i>	Stem	(Fan et al., 2001)
Coumarin [289]	<i>D. aurantiacum</i> var. <i>denneanum</i>	Stem	(Yang, Wang, et al., 2006a)
	<i>D. clavatum</i> var. <i>aurantiacum</i>	Stem	(Chang et al., 2001)
Denthyrsin [290]	<i>D. thyriflorum</i>	Stem	(Zhang et al., 2005)
Scoparone [291]	<i>D. densiflorum</i>	Stem	(Fan et al., 2001)
	<i>D. thyriflorum</i>	Stem	(Zhang et al., 2005)
	<i>D. williamsonii</i>	Whole plant	(M. Yang et al., 2018)
	<i>D. palpebrae</i>	Whole plant	(Kyokong et al., 2019)
Scopoletin [292]	<i>D. densiflorum</i>	Stem	(Fan et al., 2001)
Dendrocoumarin [293]	<i>D. nobile</i>	Stem	(Zhou et al., 2017)
Itolide A [294]	<i>D. nobile</i>	Stem	(Zhou et al., 2017)



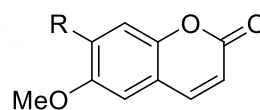
[288] Ayapin



[289] Coumarin



[290] Denthyrsin



[291] Scoparone: R = OMe

[292] Scopoletin: R = OH

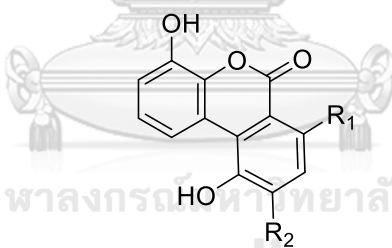
[293] Dendrocoumarin: R₁ = H, R₂ = OH[294] Itolide A: R₁ = OH, R₂ = H

Figure 6 Structures of coumarins from *Dendrobium* species.

Table 7 Lignans and neolignans in the genus *Dendrobium*.

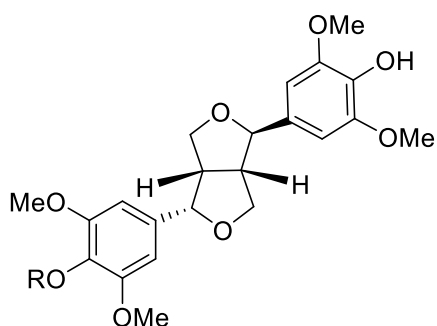
Compounds	Plant	Plant part	Reference
Episingaresinol [295]	<i>D. chrysotoxum</i>	Stem	(Hu et al., 2012)
	<i>D. longicornu</i>	Stem	(Hu et al., 2008a)
	<i>D. nobile</i>	Stem	(Zhang et al., 2008)
Episingaresinol 4''-O- β -D-glucopyranoside [296]	<i>D. moniliforme</i>	Stem	(Zhao et al., 2003)
(-)-(7 <i>S</i> ,8 <i>R</i> ,7' <i>E</i>)-4-Hydroxy-3,3',5,5'-tetramethoxy-8,4'-oxyneolign-7'-ene-7,9'-bis-O- β -D-glucopyranoside [297]	<i>D. aurantiacum</i> var. <i>denneanum</i>	Stem	(Xiong et al., 2013)
Lyoniresinol [298]	<i>D. chrysanthum</i>	Stem	(Yang, Qin, et al., 2006)
(-)-Syringaresinol-4,4'-bis-O- β -D-glucopyranoside [299]	<i>D. aurantiacum</i> var. <i>denneanum</i>	Stem	(Xiong et al., 2013)
Syringaresinol-4-O-D-monoglucopyranoside [300]	<i>D. aurantiacum</i> var. <i>denneanum</i>	Stem	(Xiong et al., 2013)
(-)-Medioresinol [301]	<i>D. loddigesii</i>	Whole plant	(Ito et al., 2010)

Table 7 Lignans and neolignans in the genus *Dendrobium* (Continued).

Compounds	Plant	Plant part	Reference
(-)-Pinoresinol [302]	<i>D. loddigesii</i>	Whole plant	(Ito et al., 2010)
	<i>D. devonianum</i>	Stem	(Wu et al., 2019)
	<i>D. nobile</i>	Stem	(Cheng et al., 2020)
Syringaresinol [303]	<i>D. secundum</i>	Stem	(Sritularak, Duangrak, et al., 2011)
	<i>D. williamsonii</i>	Whole plant	(M. Yang et al., 2018)
	<i>D. nobile</i>	Stem	(Cheng et al., 2020)
Erythro-1-(4-O- β -D-glucopyranosyl-3-methoxyphenyl)-2-[4-(3-hydroxypropyl)-2,6-dimethoxyphenoxy]-1,3-propanediol [304]	<i>D. longicornu</i>	Stem	(Hu et al., 2008a)
Acanthoside B [305]	<i>D. chrysanthum</i>	Stem	(Yang, Qin, et al., 2006)
Liriodendrin [306]	<i>D. brymerianum</i>	Whole plant	(Klongkumnuankarn et al., 2015)
	<i>D. pulchellum</i>	Stem	(Chanvorachote et al., 2013)

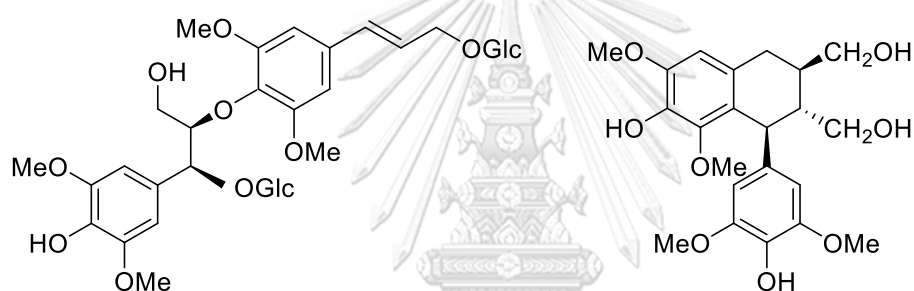
Table 7 Lignans and neolignans in the genus *Dendrobium* (Continued).

Compounds	Plant	Plant part	Reference
(-)-(8 <i>R</i> ,7' <i>E</i>)-4-Hydroxy-3,3',5,5'-tetramethoxy-8,4'-oxyneolign-7'-ene-9,9'-diol 4,9-bis- <i>O</i> - β -D-glucopyranoside [307]	<i>D. aurantiacum</i> var. <i>denneanum</i>	Stem	(Li et al., 2014)
(-)-(8 <i>S</i> ,7' <i>E</i>)-4-Hydroxy-3,3',5,5'-tetramethoxy-8,4'-oxyneolign-7'-ene-9,9'-diol 4,9-bis- <i>O</i> - β -D-glucopyranoside [308]	<i>D. aurantiacum</i> var. <i>denneanum</i>	Stem	(Li et al., 2014)
(-)-(8 <i>R</i> ,7' <i>E</i>)-4-Hydroxy-3,3',5,5',9'-penta-methoxy-8,4'-oxyneolign-7'-ene-9-ol 4,9-bis- <i>O</i> - β -D-glucopyranoside [309]	<i>D. aurantiacum</i> var. <i>denneanum</i>	Stem	(Li et al., 2014)
(7 <i>S</i> ,8 <i>R</i>)-Dehydrodiconiferyl alcohol 9'- β -D-glucopyranoside [310]	<i>D. nobile</i>	Stem	(Zhou et al., 2017)
Dehydrodiconiferylalcohol-4- β -D-glucoside [311]	<i>D. nobile</i>	Stem	(Zhou et al., 2017)
Balanophonin [312]	<i>D. williamsonii</i>	Whole plant	(M. Yang et al., 2018)

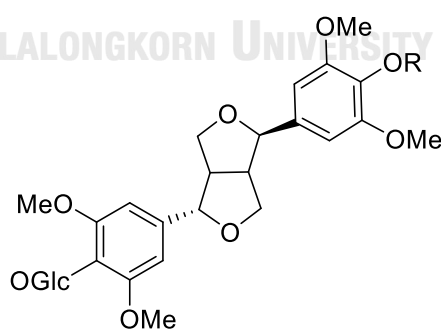


[295] Episyringaresinol: R = H

[296] Episyringaresinol 4''-O-β-D-glucopyranoside: R = Glc

[297] (-)-(7*S*,8*R*,7'*E*)-4-Hydroxy-
3,3',5,5'-tetramethoxy-8,4'-oxyneolign-
7'-ene-7,9'-bis-O-β-D-glucopyranoside

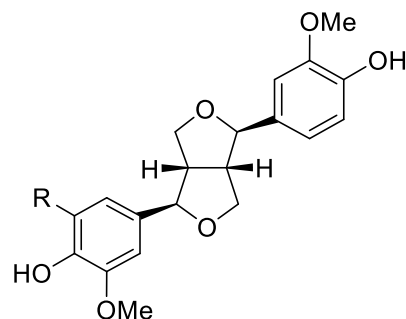
[298] Lyoniresinol



[299] (-)-Syringaresinol-4,4'-bis-O-β-D-glucopyranoside: R = Glc

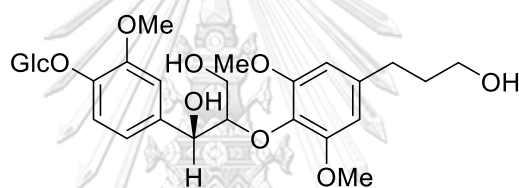
[300] Syringaresinol-4-O-D-monoglucopyranoside: R = H

Figure 7 Structures of lignans and neolignans from *Dendrobium* species.

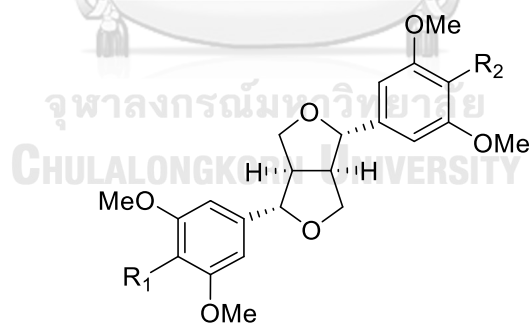


[301] (-)-Medioresinol: R = OMe

[302] (-)-Pinoresinol: R = H

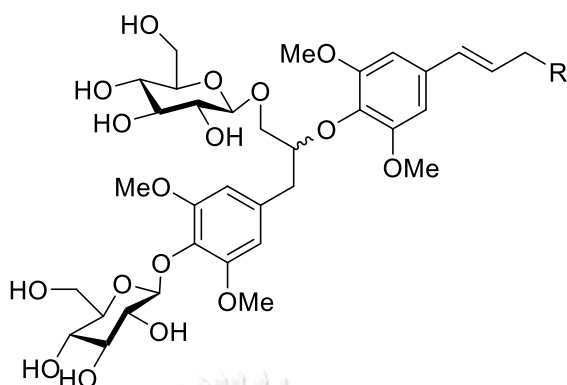


[303] Erythro-1-(4-O- β -D-glucopyranosyl-3-methoxyphenyl)-2-[4-(3-hydroxypropyl)-2,6-dimethoxyphenoxy]-1,3-propanediol



	R ₁	R ₂
[304] Syringaresinol	OH	OH
[305] Acanthoside B	OGlc	OH
[306] Liriodendrin	OGlc	OGlc

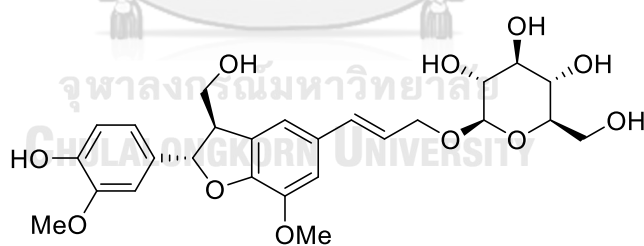
Figure 7 Structures of lignans and neolignans from *Dendrobium* species (Continued).



[307] (-)-(8*R*,7'*E*)-4-Hydroxy-3,3',5,5'-tetramethoxy-8,4'-oxyneolign-
7'-ene-9,9'-diol 4,9-bis-O- β -D-glucopyranoside: R = OH; 8*R*

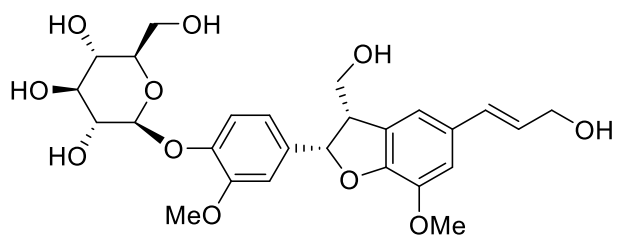
[308] (-)-(8*S*,7'*E*)-4-Hydroxy-3,3',5,5'-tetramethoxy-8,4'-oxyneolign-
7'-ene-9,9'-diol 4,9-bis-O- β -D-glucopyranoside: R = OH; 8*S*

[309] (-)-(8*R*,7'*E*)-4-Hydroxy-3,3',5,5',9'-pentamethoxy-8,4'-oxyneolign-
7'-ene-9-ol 4,9-bis-O- β -D-glucopyranoside: R = OMe; 8*R*

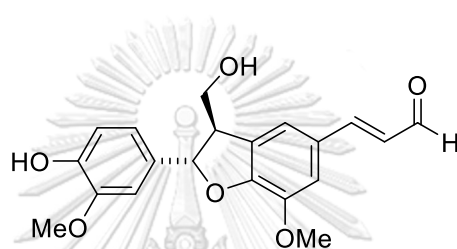


[310] (7*S*,8*R*)-Dehydrodiconiferyl alcohol 9'- β -D-glucopyranoside

Figure 7 Structures of lignans and neolignans from *Dendrobium* species (Continued).



[311] Dehydrodiconiferyl alcohol-4- β -D-glucoside



[312] Balanophonin

Figure 7 Structures of lignans and neolignans from *Dendrobium* species (Continued).

Table 8 Miscellaneous compounds in the genus *Dendrobium*.

Compounds	Plant	Plant part	Reference
Aliphatic acid derivatives			
Aliphatic acids [313]	<i>D. clavatum</i> var. <i>aurantiacum</i>	Stem	(Chang et al., 2001)
Aliphatic alcohols [314]	<i>D. clavatum</i> var. <i>aurantiacum</i>	Stem	(Chang et al., 2001)
Dendrodevonic acid A [315]	<i>D. devonianum</i>	Stem	(Wu et al., 2019)
Dendrodevonic acid B [316]	<i>D. devonianum</i>	Stem	(Wu et al., 2019)
Malic acid [317]	<i>D. huoshanense</i>	Aerial part	(Chang et al., 2010)
Dimethyl malate [318]	<i>D. huoshanense</i>	Aerial part	(Chang et al., 2010)
(-)-Shikimic acid [319]	<i>D. fuscescens</i>	Whole plant	(Talapatra et al., 1989)
	<i>D. huoshanense</i>	Aerial part	(Chang et al., 2010)
	<i>D. longicornu</i>	Stem	(Hu et al., 2008a)
	<i>D. pulchellum</i>	Stem	(Chanvorachote et al., 2013)
Isopentyl butyrate [320]	<i>D. huoshanense</i>	Aerial part	(Chang et al., 2010)

Table 8 Miscellaneous compounds in the genus *Dendrobium* (Continued).

Compounds	Plant	Plant part	Reference
Benzoic acid derivatives and phenolic compounds			
3-Hydroxy-2-methoxy-5,6-dimethylbenzoic acid [321]	<i>D. crystallinum</i>	Stem	(Wang et al., 2009)
Salicylic acid [322]	<i>D. huoshanense</i>	Aerial part	(Chang et al., 2010)
	<i>D. williamsonii</i>	Whole plant	(M. Yang et al., 2018)
Vanilloside [323]	<i>D. denneanum</i>	Stem	(Pan et al., 2012)
Gallic acid [324]	<i>D. longicornu</i>	Whole plant	(J.-T. Li et al., 2009)
Syringic acid [325]	<i>D. crystallinum</i>	Stem	(Wang et al., 2009)
Vanillic acid [326]	<i>D. crystallinum</i>	Stem	(Wang et al., 2009)
	<i>D. williamsonii</i>	Whole plant	(Rungwichaniwat et al., 2014)
Antiarol [327]	<i>D. chrysotoxum</i>	Stem	(Hu et al., 2012)
Ethylhaematommate [328]	<i>D. longicornu</i>	Whole plant	(J.-T. Li et al., 2009)

Table 8 Miscellaneous compounds in the genus *Dendrobium* (Continued).

Compounds	Plant	Plant part	Reference
<i>p</i> -Hydroxy-benzaldehyde [329]	<i>D. devonianum</i>	Whole plant	(Sun et al., 2014)
	<i>D. falconeri</i>	Stem	(Sritularak & Likhitwitayawuid, 2009)
	<i>D. tortile</i>	Whole plant	(Limpanit et al., 2016)
	<i>D. williamsonii</i>	Whole plant	(M. Yang et al., 2018)
Methyl β -orsellinate [330]	<i>D. longicornu</i>	Stem	(Hu et al., 2008a)
Protocatechuic acid [331]	<i>D. nobile</i>	Stem	(Ye & Zhao, 2002)
Tachioside [332]	<i>D. denneanum</i>	Stem	(Pan et al., 2012)
Alkyl 4'-hydroxy- <i>trans</i> -cinnamates [333]	<i>D. clavatum</i> var. <i>aurantiacum</i>	Stem	(Chang et al., 2001)
Alkyl <i>trans</i> -ferulate [334]	<i>D. clavatum</i> var. <i>aurantiacum</i>	Stem	(Chang et al., 2001)
Defuscin [335]	<i>D. aurantiacum</i> var. <i>denneanum</i>	Stem	(Yang, Wang, et al., 2006a)
	<i>D. moniliforme</i>	Stem	(Bi et al., 2004)

Table 8 Miscellaneous compounds in the genus *Dendrobium* (Continued).

Compounds	Plant	Plant part	Reference
<i>n</i> -Octacosyl ferulate [336]	<i>D. aurantiacum</i> <i>var.</i> <i>denneanum</i>	Stem	(Yang, Wang, et al., 2006a)
	<i>D. moniliforme</i>	Stem	(Bi et al., 2004)
<i>n</i> -Triacosyl <i>p</i> -hydroxy- <i>cis</i> -cinnamate [337]	<i>D. moniliforme</i>	Stem	(Bi et al., 2004)
Tetratriacontanyl- <i>trans</i> - <i>p</i> -coumarate [338]	<i>D. williamsonii</i>	Whole plant	(Rungwichaniwat et al., 2014)
<i>n</i> -Docosyl <i>trans</i> -ferulate [339]	<i>D. longicornu</i>	Whole plant	(J.-T. Li et al., 2009)
	<i>D. williamsonii</i>	Whole plant	(Rungwichaniwat et al., 2014)
<i>trans</i> -Tetracosyl ferulate [340]	<i>D. tortile</i>	Whole plant	(Limpanit et al., 2016)
<i>cis</i> -Hexacosanoyl ferulate [341]	<i>D. tortile</i>	Whole plant	(Limpanit et al., 2016)
Ferulaldehyde [342]	<i>D. longicornu</i>	Whole plant	(J.-T. Li et al., 2009)

Table 8 Miscellaneous compounds in the genus *Dendrobium* (Continued).

Compounds	Plant	Plant part	Reference
Ferulic acid [343]	<i>D. secundum</i>	Stem	(Sritularak, Duangrak, et al., 2011)
2-(<i>p</i> -Hydroxyphenyl) ethyl <i>p</i> -coumarate [344]	<i>D. falconeri</i>	Stem	(Sritularak & Likhitwitayawuid, 2009)
Dihydroconiferyl dihydro- <i>p</i> -coumarate [345]	<i>D. formosum</i>	Whole plant	(Inthongkaew et al., 2017)
	<i>D. nobile</i>	Stem	(Cheng et al., 2020)
	<i>D. hainanense</i>	Aerial part	(Zhang et al., 2019)
	<i>D. devonianum</i>	Stem	(Wu et al., 2019)
1-[4-(β -D-Glucopyranosyloxy)-3,5-dimethoxyphenyl]-1-propanone [346]	<i>D. aurantiacum</i> var. <i>denneanum</i>	Stem	(Xiong et al., 2013)
3-Hydroxy-1-(4-hydroxy-3,5-dimethoxyphenyl)-1-propanone [347]	<i>D. williamsonii</i>	Whole plant	(M. Yang et al., 2018)
Coniferyl alcohol [348]	<i>D. trigonopus</i>	Stem	(Hu et al., 2008b)

Table 8 Miscellaneous compounds in the genus *Dendrobium* (Continued).

Compounds	Plant	Plant part	Reference
Decumbic acid A [349]	<i>D. nobile</i>	Stem	(Zhou et al., 2016)
Decumbic acid B [350]	<i>D. nobile</i>	Stem	(Zhou et al., 2016)
(-)-Decumbic acid [351]	<i>D. nobile</i>	Stem	(Zhou et al., 2016)
(+)-Dendrolactone [352]	<i>D. nobile</i>	Stem	(Zhou et al., 2016)
4-(3-Hydroxyphenyl)-2-butanone [353]	<i>D. nobile</i>	Stem	(Zhou et al., 2016)
3-Hydroxy-1(3-methoxy-4-hydroxyphenyl)-propan-1-one [354]	<i>D. nobile</i>	Stem	(Zhou et al., 2016)
3',4',5'-Trimethoxy cinnamyl acetate [355]	<i>D. nobile</i>	Stem	(Zhou et al., 2016)
<i>p</i> -Hydroxyphenyl propionic methyl ester [356]	<i>D. aphyllum</i>	Whole plant	(Chen, Li, et al., 2008)
Phloretic acid [357]	<i>D. ellipsophyllum</i>	Whole plant	(Tanagornmeatar et al., 2014)

Table 8 Miscellaneous compounds in the genus *Dendrobium* (Continued).

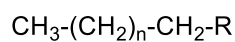
Compounds	Plant	Plant part	Reference
Dihydroconiferyl alcohol [358]	<i>D. longicornu</i>	Stem	(Hu et al., 2008a)
Salidrosol [359]	<i>D. chrysotoxum</i>	Stem	(Hu et al., 2012)
Shashenoside I [360]	<i>D. aurantiacum</i> var. <i>denneanum</i>	Stem	(Xiong et al., 2013)
Syringin [361]	<i>D. aurantiacum</i> var. <i>denneanum</i>	Stem	(Xiong et al., 2013)
Tetracosyl(<i>Z</i>)- <i>p</i> -coumarate [362]	<i>D. falconeri</i>	Whole plant	(Sritularak & Likhitwitayawuid, 2009)
Koaburaside [363]	<i>D. nobile</i>	Stem	(Zhou et al., 2017)
Juniperoside [364]	<i>D. nobile</i>	Stem	(Zhou et al., 2017)
(3 <i>R</i> ,3' <i>S</i> ,4 <i>R</i> ,4' <i>S</i>)-3,3',4,4'-Tetrahydro-6,6'-dimethoxy[3,3'-bi-2 <i>H</i> -benzopyran]-4,4'-diol [365]	<i>D. williamsonii</i>	Whole plant	(M. Yang et al., 2018)

Table 8 Miscellaneous compounds in the genus *Dendrobium* (Continued).

Compounds	Plant	Plant part	Reference
2-hydroxy-3-(4-hydroxy-3-methoxyphenyl)-3-methoxypropyl 3-(4-hydroxyphenyl)propanoate [366]	<i>D. hainanense</i>	Aerial part	(Zhang et al., 2019)
Others			
3,6,9-Trihydroxy-3,4-dihydroanthracen-1-(2H)-one [367]	<i>D. chrysotoxum</i>	Stem	(Hu et al., 2012)
Palmarumycin JC2 [368]	<i>D. crystallinum</i>	Stem	(Wang et al., 2009)
Dehydrovomifoliol [369]	<i>D. loddigesii</i>	Whole plant	(Ito et al., 2010)
2,6-Dimethoxy Benzoquinone [370]	<i>D. chryseum</i>	Stem	(Ma et al., 1998)
4-(2-Hydroxypropyl)- 2(5H)-furanone [371]	<i>D. tortile</i>	Whole plant	(Limpanit et al., 2016)
5,7-Dihydroxy-chromen- 4-one [372]	<i>D. ellipsophyllum</i>	Whole plant	(Tanagornmeatar et al., 2014)
Ergosta-8(9),22-diene-3,5,6,7-tetraol [373]	<i>D. williamsonii</i>	Whole plant	(M. Yang et al., 2018)

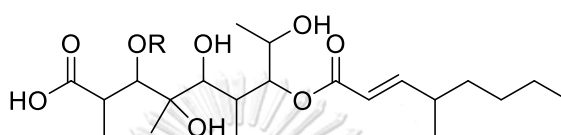
Table 8 Miscellaneous compounds in the genus *Dendrobium* (Continued).

Compounds	Plant	Plant part	Reference
Stigmast-4-en-3 α , 6 β -diol [374]	<i>D. williamsonii</i>	Whole plant	(M. Yang et al., 2018)
3 β -Hydroxy-5 α ,8 α -epidioxyergosta-6,9,22-triene [375]	<i>D. williamsonii</i>	Whole plant	(M. Yang et al., 2018)
Betulin [376]	<i>D. williamsonii</i>	Whole plant	(M. Yang et al., 2018)
β -Sitosterol [377]	<i>D. williamsonii</i>	Whole plant	(M. Yang et al., 2018)
Daucosterol [378]	<i>D. williamsonii</i>	Whole plant	(M. Yang et al., 2018)
	<i>D. harveyanum</i>	Whole plant	(Maitreesophone et al., 2022)
(-)-6R-sigmatone [379]	<i>D. signatum</i>	Aerial part	(Khumploy et al., 2021)



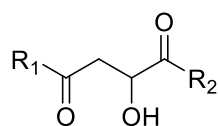
[313] Aliphatic acids: R = COOH, n = 19-31

[314] Aliphatic alcohol: R = OH, n = 22-32



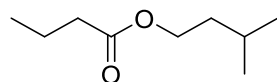
[315] Dendrodevonic acid A: R = H

[316] Dendrodevonic acid B: R = Acetyl

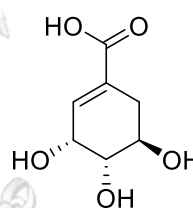


[317] Malic acid: R₁ = R₂ = OH

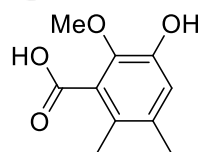
[318] Dimethyl malate: R₁ = R₂ = OMe



[320] Isopentyl butyrate

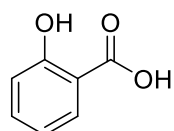


[319] (-)-Shikimic acid

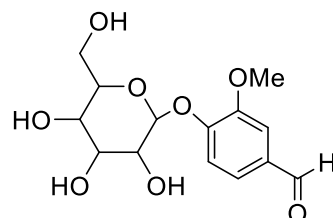


[321] 3-Hydroxy-2-methoxy-5,6-dimethylbenzoic acid

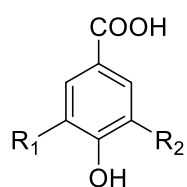
Figure 8 Structures of miscellaneous compounds from *Dendrobium* species.



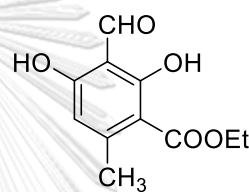
[322] Salicylic acid



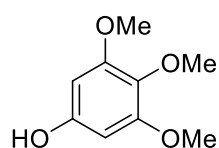
[323] Vanilloside

[324] Gallic acid: $R_1 = \text{OH}$, $R_2 = \text{OH}$ [325] Syringic acid: $R_1 = \text{OMe}$, $R_2 = \text{OMe}$ [326] Vanillic acid: $R_1 = \text{H}$, $R_2 = \text{OMe}$ [331] Protocatechuic acid: $R_1 = \text{H}$, $R_2 = \text{OH}$

CHULALONGKORN UNIVERSITY



[327] Antiarol



[328] Ethylhaematommate

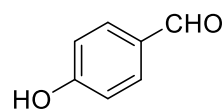
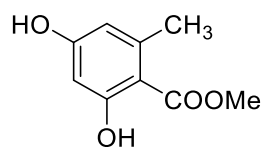
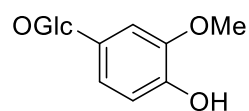
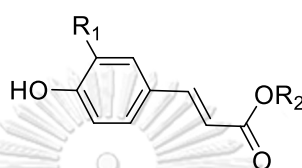
[329] *p*-Hydroxybenzaldehyde

Figure 8 Structures of miscellaneous compounds from *Dendrobium* species (Continued).

[330] Methyl β -orsellinate

[332] Tachioside



[333] Alkyl 4'-hydroxy-*trans*-cinnamates: $R_1 = \text{H}$, $R_2 = \text{C}_n\text{H}_{2n+1}$, $n = 22-32$

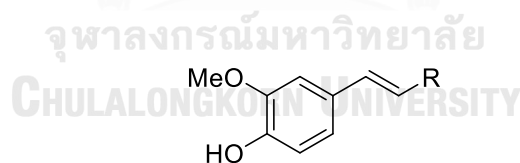
[334] Alkyl *trans*-ferulate: $R_1 = \text{OMe}$, $R_2 = \text{C}_n\text{H}_{2n+1}$, $n = 18-28, 30$

[335] Defuscin: $R_1 = \text{OMe}$, $R_2 = (\text{CH}_2)_{27}\text{CH}_3$

[336] *n*-Octacosyl ferulate: $R_1 = \text{OMe}$, $R_2 = (\text{CH}_2)_{28}\text{CH}_3$

[337] *n*-Triacontyl *p*-hydroxy-*cis*-cinnamate: $R_1 = \text{H}$, $R_2 = \text{C}_{30}\text{H}_{61}$

[338] Tetratriacontanyl-*trans-p*-coumarate: $R_1 = \text{H}$, $R_2 = (\text{CH}_2)_{33}\text{CH}_3$



[339] *n*-Docosyl *trans*-ferulate: $R = \text{COOCH}_2(\text{CH}_2)_{20}\text{CH}_3$

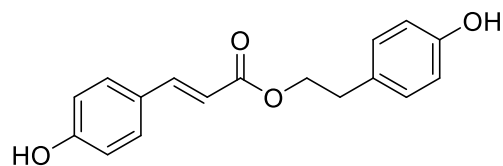
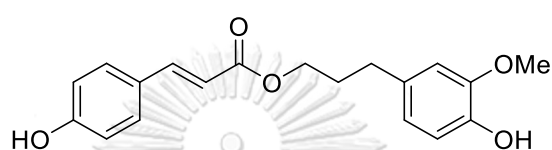
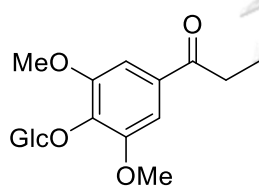
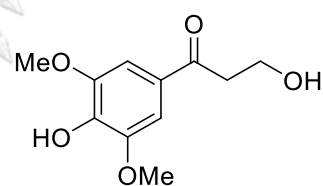
[340] *trans*-Tetracosyl ferulate: $R = \text{COOCH}_2(\text{CH}_2)_{22}\text{CH}_3$

[341] *cis*-Hexacosanoyl ferulate: $R = \text{COOCH}_2(\text{CH}_2)_{24}\text{CH}_3$

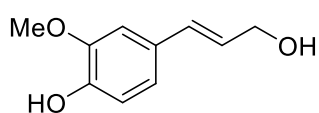
[342] Ferulaldehyde: $R = \text{CHO}$

[343] Ferulic acid: $R = \text{COOH}$

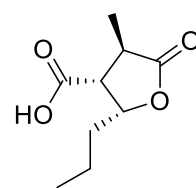
Figure 8 Structures of miscellaneous compounds from *Dendrobium* species (Continued).

[344] 2-(*p*-Hydroxyphenyl) ethyl *p*-coumarate[345] Dihydroconiferyl dihydro-*p*-coumarate[346] 1-[4-(β -D-Glucopyranosyloxy)-3,5-dimethoxyphenyl]-1-propanone

[347] 3-Hydroxy-1-(4-hydroxy-3,5-dimethoxyphenyl)-1-propanone

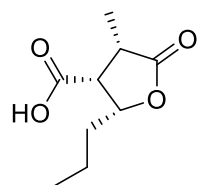


[348] Coniferyl alcohol

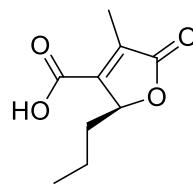


[349] Decumbic acid A

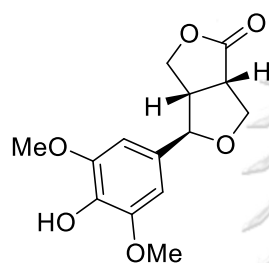
Figure 8 Structures of miscellaneous compounds from *Dendrobium* species (Continued).



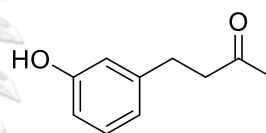
[350] Decumbic acid B



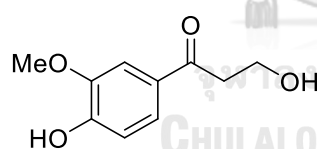
[351] (-)-Decumbic acid



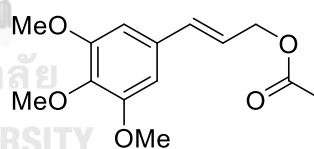
[352] (+)-Dendrolactone



[353] 4-(3-Hydroxyphenyl)-2-butanone

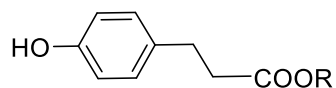


[354] 3-Hydroxy-1-(3-methoxy-4-hydroxyphenyl)-propan-1-one

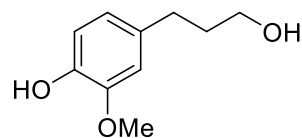


[355] 3',4',5'-Trimethoxy cinnamyl acetate

Figure 8 Structures of miscellaneous compounds from *Dendrobium* species (Continued).

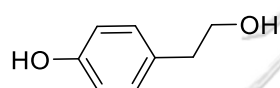


[356] *p*-Hydroxyphenyl propionic
methyl ester: R = CH₃

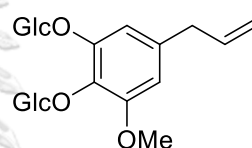


[358] Dihydroconiferyl alcohol

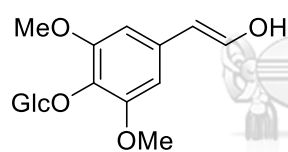
[357] Phloretic acid: R = OH



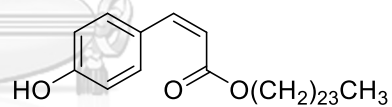
[359] Salidroside



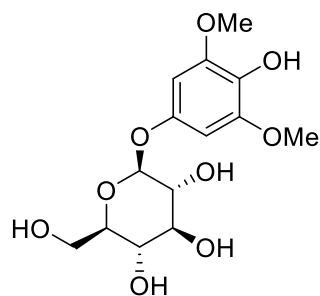
[360] Shashenoside I



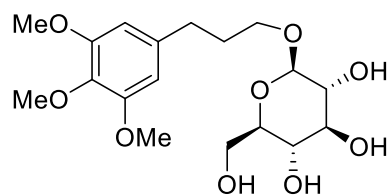
[361] Syringin



[362] Tetracosyl (*Z*)-*p*-coumarate

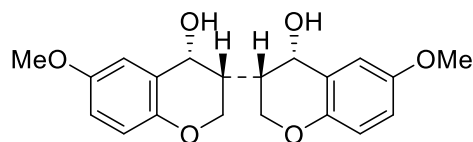


[363] Koaburaside

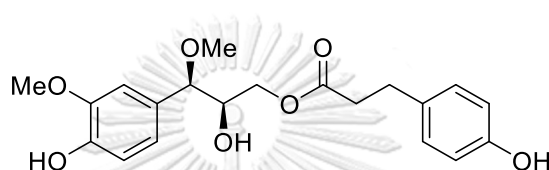


[364] Juniperoside

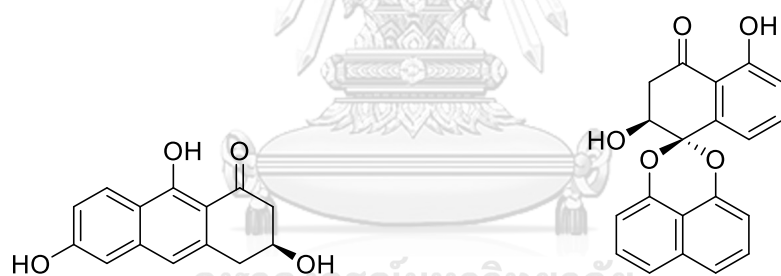
Figure 8 Structures of miscellaneous compounds from *Dendrobium* species
(Continued).



[365] (3*R*,3'*S*,4*R*,4'*S*)-3,3',4,4'-Tetrahydro-6,6'-
dimethoxy[3,3'-bi-2*H*-benzopyran]-4,4'-diol

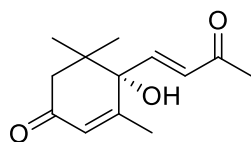


[366] 2-hydroxy-3-(4-hydroxy-3-methoxyphenyl)-3-
methoxypropyl 3-(4-hydroxyphenyl) propanoate

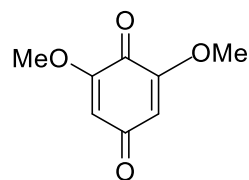


[367] 3,6,9-Trihydroxy-3,4-
dihydroanthracen-1-(2*H*)-one

[368] Palmarumycin JC2

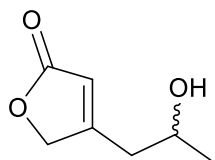


[369] Dehydrovomifoliol

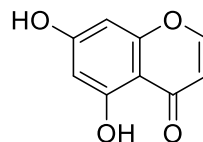


[370] 2,6-Dimethoxybenzoquinone

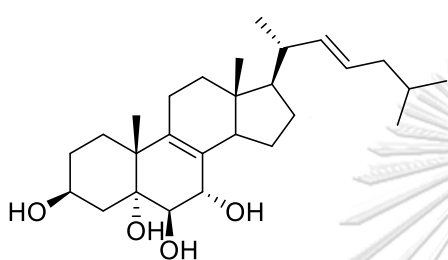
Figure 8 Structures of miscellaneous compounds from *Dendrobium* species
(Continued).



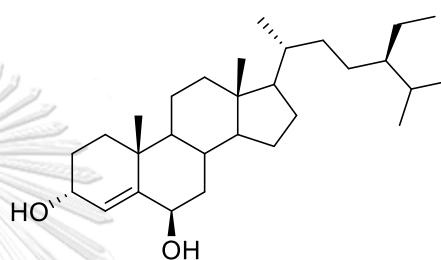
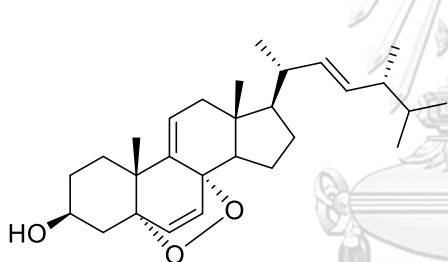
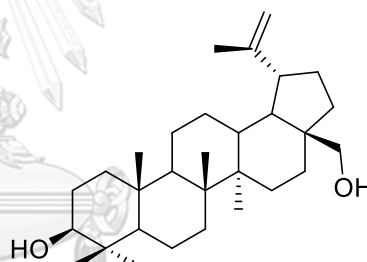
[371] 4-(2-Hydroxypropyl)-2(5H)-furanone



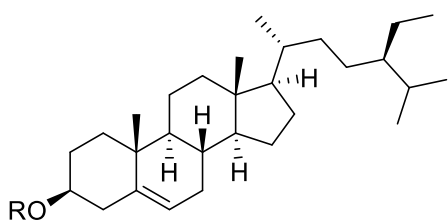
[372] 5,7-Dihydroxy-chromen-4-one



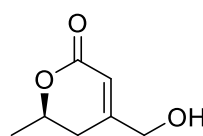
[373] Ergosta-8(9),22-diene-3,5,6,7-tetraol

[374] Stigmast-4-en-3 α , 6 β -diol[375] 3 β -Hydroxy-5 α ,8 α -epidioxyergosta-6,9,22-triene

[376] Betulin

[377] β -Sitosterol: R = H

[378] Daucosterol: R = Glc



[379] (-)-6R-sigmatone

Figure 8 Structures of miscellaneous compounds from *Dendrobium* species
(Continued).

The pharmacological studies of this plants also have been revealed to several activities such as anticancer, antidiabetic, antimicrobial, hepatoprotective and neuroprotective, antiplatelet aggregation, immunomodulating, antioxidant, and especially anti-inflammatory activity (Teixeira da Silva & Ng, 2017). For the anti-inflammatory activity based on immunomodulatory effects, the extracts and active compounds from *Dendrobium* genus have been reported in several studies. For instance, the water extracts of *D. chrysotoxum* and *D. thyrsiflorum* inhibited nitric oxide (NO) in LPS-induced RAW264.7 macrophage cells (Qiang et al., 2018). Moreover, the water extracts of *D. thyrsiflorum* showed the suppressing of IL-6 and TNF- α through inhibition of ERK and JNK phosphorylation in MAPK pathway (Qiang et al., 2018). The polysaccharides isolated from *D. officinale* demonstrated the anti-inflammatory activity. For example, polysaccharides isolated from *D. officinale* leaves significantly inhibited the expression of TLR-4, MyD88 and TRAF-6 in LPS-stimulated THP-1 cells (M. Zhang et al., 2018). Furthermore, polysaccharides from *D. officinale* leaves showed the suppressing of pro-inflammatory cytokines including TNF- α , IL-6, and IL-1 β in cyclophosphamide-treated mice (Xie et al., 2022). In addition, 4,5-dihydroxy-3,3',4'-trimethoxybibenzyl [30], a bibenzyl derivative, isolated from *D. lindleyi* exhibited the downmodulation of the TNF expression in a dose-dependent manner in LPS-induced human peripheral blood mononuclear cells (Khoonrit et al., 2020).

***Dendrobium crumenatum* Sw.**

The pigeon orchid named "*Dendrobium crumenatum*" was first published in *Journal fur die Botanik* by Swedish botanist in 1799 (Wiert, 2012). It is distributed in China, India and southeast Asia including in Thailand called "Wai Tamoi" (Meesawat & Kanchanapoom, 2007). Using this orchid in traditional medicine has been reported including treatment of earache using juices from *D. crumenatum* in Malaysia and applying as poultice for curing boils and pimples (Wiert, 2012). This plant is an epiphytic orchid (size 40-100 cm) with pseudobulbs. The flower is 3-4 cm, white, having white three sepals and two petals with yellow disc on the lip (Meesawat &

Kanchanapoom, 2007; Ram et al., 2015). However, the phytochemical studies and biological activities of this plant have not been reported.



Figure 9 *Dendrobium crumenatum* Sw.



CHAPTER III

Research articles

3.1 Immunomodulatory Effects of New Phenanthrene Derivatives from *Dendrobium crumenatum*

Virunh Kongkatitham, Adeline Dehlinger, Meng Wang, Preeyaporn Poldorn, Carl Weidinger, Marilena Letizia, Chatchai Chaotham, Carolin Otto, Klemens Ruprecht, Friedemann Paul, Thanyada Rungrotmongkol, Kittisak Likhitwitayawuid, Chotima Böttcher,* and Boonchoo Sritularak*

ABSTRACT: Three new phenanthrene derivatives (**1**, **2**, **4**), one new fluorenone (**3**), and four known compounds (**5–8**) were isolated from the ethyl acetate extract of *Dendrobium crumenatum* Sw. stems using column chromatography. The chemical structures were elucidated by analysis of spectroscopic data. The absolute configuration of **4** was determined by electronic circular dichroism calculation. We also evaluated the immunomodulatory effects of compounds isolated from *D. crumenatum* in human peripheral blood mononuclear cells from healthy individuals and those from patients with multiple sclerosis in vitro. Dendrocruenol B (**2**) and dendrocruenol D (**4**) showed strong immunomodulatory effects on both CD3⁺ T cells and CD14⁺ monocytes. Compounds **2** and **4** could reduce IL-2 and TNF production in T cells and monocytes that were treated with phorbol-12-myristate-13-acetate and ionomycin (PMA/Iono). Deep immune profiling using high-dimensional single-cell mass cytometry could confirm immunomodulatory effects of **4**, quantified by the reduction of activated T cell population under PMA/Iono stimulation, in comparison to the stimulated T cells without treatment.

Dendrobium is one of the largest genera in the flowering family Orchidaceae, with more than 1500 species, mostly found in Asia and Australia (Zhang et al., 2007). Several species of *Dendrobium* plants have been used as traditional medicines in

China, India, and Southeast Asia for treatment of skin disorders, reducing fever, headache and stomachache, and promoting body fluids (Wang, 2021a, 2021b). *Dendrobium crumenatum* Sw. (Thai name Wai Tamoi) is an epiphytic plant that is distributed around Southeast Asia (Thailand, Philippines, Indonesia), India, and Hawaii (Meesawat et al., 2008; Ram et al., 2015; Vaddhanaphuti, 2005). *D. crumenatum* has been used in traditional medicine as juices for treatment of earache and a poultice for curing boils and pimples (Wiat, 2012). Extracts from *D. crumenatum* exhibited potential antimicrobial activity (Sandrasagaran et al., 2014). Since this invasive orchid is easy to grow (Clifford & Kobayashi, 2012; Foster et al., 2019), it is of interest to evaluate its potential use in phytomedicine. Therefore, we aimed to screen the active immunomodulatory effects of isolated compounds from *D. crumenatum* in human peripheral blood mononuclear cells (PBMCs). The phytochemical study of this orchid has not yet been reported. *Dendrobium* species are important sources of bibenzyls, phenanthrenes, alkaloids, flavonoids, and sesquiterpenoids (Lam et al., 2015), very often reported with biological activities (Cakova et al., 2017; Khoonrit et al., 2020; Teixeira da Silva & Ng, 2017). The inflammatory response is a body defending process to regulate injury or infection involving diverse immune cell types (e.g., monocytes, dendritic cells, neutrophil T and B cells) and multiple cell signaling pathways (Muszynski et al., 2016). In the present investigation, the immunomodulatory effects of compounds from *D. crumenatum* were evaluated using experimental ex vivo model of stimulated human PBMCs. Two new phenanthrenes, dendrocrumenols B and D, showed anti-inflammatory effects, characterized by a reduced production of inflammatory cytokines. These effects were detected in both myeloid and lymphoid compartments of the immune system and could be explained by the reduction of activated T cells and inflammatory monocytes, quantified by using high-dimensional single-cell mass cytometry (CyTOF). Our findings suggested promising therapeutic potential of compounds purified from *D. crumenatum* in regulating immune responses to inflammatory conditions, a

common feature in diverse diseases including neuroinflammation such as in multiple sclerosis.

RESULTS AND DISCUSSION

Compound **1**, a brown amorphous solid, gave a $[M - H]^-$ at m/z 285.0811 (calcd for 285.0763 $C_{16}H_{13}O_5$) by HR-ESI-MS analysis, suggesting the molecular formula $C_{16}H_{14}O_5$. The IR spectrum showed absorption bands for a hydroxyl (3273 cm^{-1}) and an aromatic ring ($2962, 1618\text{ cm}^{-1}$). The UV absorption peaks at λ_{max} ($\log \epsilon$) 224 (2.51), 280 (1.20), and 295 (1.07) nm and two *ortho*-coupled doublets of H-9 (δ_{H} 8.03, d, $J = 9.5$ Hz) and H-10 (δ_{H} 7.89, d, $J = 9.5$ Hz) in the ^1H NMR spectrum supported a phenanthrene skeleton of **1** (Sarakulwattana et al., 2020). The ^1H NMR spectrum also exhibited two doublet aromatic protons at δ_{H} 8.89 (1H, d, $J = 9.0$ Hz, H-5) and δ_{H} 7.42 (1H, d, $J = 9.0$ Hz, H-6), one singlet aromatic proton at δ_{H} 7.39 (1H, s, H-1), two methoxy groups at δ_{H} 4.11 (3H, s, MeO-2) and 3.97 (3H, s, MeO-8), and one hydroxyl proton at δ_{H} 8.48 (1H, s, HO-7) (**Table 9**). On ring A, a doublet proton of H-5 was assigned by HMBC correlations of H-5 and H-10 with C-8a (δ_{C} 127.5). The assignment of H-6 was based on the HMBC correlations of H-6 and H-9 with C-4b (δ_{C} 123.0) and ^1H - ^1H COSY correlations of H-5 and H-6 (**Figure 12**). The hydroxyl group (δ_{H} 8.48) was placed at C-7 according to its NOESY cross-peak with H-6 (**Figure 12**). The first methoxy group was located at C-8, as shown by its NOESY interactions with H-9 and HO-7. It was confirmed by three-bond correlations of H-6, H-9, HO-7, and MeO-8 with C-8 (δ_{C} 142.5) in the HMBC spectrum. On ring B, the singlet proton at δ_{H} 7.39 was assigned as H-1 on the basis of the HMBC correlation between H-10 and C-1 (δ_{C} 105.3) and its NOESY correlation with H-10. A NOESY cross-peak between MeO-2 and H-1 placed the second methoxy group at C-2. Based on the above spectral evidence, **1** was characterized as 3,4,7-trihydroxy-2,8-dimethoxyphenanthrene and named dendrocumenol A.

Compound **2** was obtained as a brown amorphous solid. The molecular formula $C_{16}H_{16}O_5$ was determined from its HR-ESI-MS $[M + H]^+$ at m/z 289.1072 (calcd for $C_{16}H_{17}O_5$, 289.1076). The IR spectrum showed the absorption bands at 3390

(hydroxyl), 2961, 1615 (aromatic ring), and 1490 (methylene) cm^{-1} and the UV at λ_{max} (log ϵ) 224 (2.51), 280 (1.20), and 295 (1.07) nm, suggestive of a dihydrophenanthrene nucleus (Na Ranong et al., 2019). It was confirmed by the presence of two methylene proton signals at δ_{H} 2.73 (2H, dd, $J = 7.8, 6.0$ Hz, H2-9) and δ_{H} 2.60 (2H, dd, $J = 7.8, 6.0$ Hz, H2-10), which exhibited one-bond correlation to the carbon atom at δ_{C} 21.7 (C-9) and 29.3 (C-10) in the HSQC spectrum. For ring A of **2**, the ^1H NMR disclosed the presence of two *ortho*-coupled aromatic protons at δ_{H} 7.69 (1H, d, $J = 8.4$ Hz, H-5) and δ_{H} 6.73 (1H, d, $J = 8.4$ Hz, H-6) (**Table 9**). The assignment of H-5 was confirmed by the three-bond correlations of H-5 and H2-10 with C-8a (δ_{C} 124.9). For ring B, the ^1H NMR spectrum showed one aromatic singlet proton at δ_{H} 6.65, which was assigned as H-1 based on its HMBC correlation with C-10 (δ_{C} 29.3) (**Figure 12**). The location of the methoxy groups at C-2 (δ_{C} 146.4) and C-4 (δ_{C} 145.6) was determined according to their NOESY cross-peak with H-1 and H-5, respectively (**Figure 12**). Therefore, compound **2** was identified as 3,7,8-trihydroxy-2,4-dimethoxydihydrophenanthrene and has been named dendrocruenenol B.

Compound **3** was isolated as a red powder. The negative HR-ESI-MS displayed a $[\text{M} - \text{H}]^-$ at m/z 287.0557 (calcd for $\text{C}_{15}\text{H}_{11}\text{O}_6$, 287.0556), indicating the molecular formula $\text{C}_{15}\text{H}_{12}\text{O}_6$. The IR spectrum showed absorptions for hydroxyl (3336 cm^{-1}), carbonyl (1727 cm^{-1}), and aromatic ring ($2925, 1671 \text{ cm}^{-1}$) groups. The presence of a fluorenone skeleton was based on the UV at λ_{max} (log ϵ) 219 (3.70), and 249 (1.44) nm (Zhang et al., 2007). This was supported by 12 aromatic carbons and one carbonyl carbon (δ_{C} 193.9) in the ^{13}C NMR spectrum (**Table 10**). The ^1H NMR spectrum revealed signals for three aromatic protons at δ_{H} 6.60–6.86, two methoxy groups at δ_{H} 4.08 (3H, s, MeO-1) and 3.96 (3H, s, MeO-4), and one hydroxyl proton at δ_{H} 8.64 (1H, s, HO-8). On ring A, three substituents were attached to the aromatic ring, as suggested by the presence of a signal for one singlet proton at δ_{H} 6.86, which was assigned as H-2 based on its HMBC correlations with C-4 (δ_{C} 142.8) and C-8b (δ_{C} 121.7). The first methoxy group (δ_{H} 4.08) was attached at C-1 as evidenced by its NOESY cross-peak with H-2 (**Figure 12**).

Table 9 ^1H and ^{13}C -NMR Spectral Data of **1** and **2** in Acetone- d_6 (δ in ppm, J in Hz).

Position	1 ^a		2 ^b	
	δ_{C} , type	δ_{H}	δ_{C} , type	δ_{H}
1	105.3, CH	7.39, s	107.3, CH	6.65, s
2	150.7, C		146.4, C	
3	132.2, C		138.6, C	
4	149.2, C		145.6, C	
4a	113.0, C		120.7, C	
4b	123.0, C		125.4, C	
5	123.3, CH	8.89, d (9.0)	118.7, CH	7.69, d (8.4)
6	119.2, CH	7.42, d (9.0)	112.3, CH	6.73, d (8.4)
7	147.8, C		143.3, C	
8	142.5, C		141.3, C	
8a	127.5, C		124.9, C	
9	120.6, CH	8.03, d (9.5)	21.7, CH ₂	2.73, dd (7.8, 6.0)
10	127.8, CH	7.89, d (9.5)	29.3, CH ₂	2.60, dd (7.8, 6.0)
10a	130.7, C		128.7, C	
MeO-2	56.4, CH ₃	4.11, s	55.5, CH ₃	3.83, s
MeO-4			58.9, CH ₃	3.62, s
MeO-8	61.5, CH ₃	3.97, s		
HO-7		8.48, s		

^aRecorded at 500 MHz for ^1H and 125 MHz for ^{13}C -NMR data.

^bRecorded at 300 MHz for ^1H and 75 MHz for ^{13}C -NMR data.

The HMBC correlations of H-2 and MeO-4 (δ_{H} 3.96) with C-4 (δ_{C} 142.8) indicated the substitution of the second methoxy group at C-4. For ring B, the ^1H NMR spectrum displayed two *ortho*-coupled aromatic proton signals at δ_{H} 6.60 (1H, d, J = 9.0 Hz, H-6) and δ_{H} 6.85 (1H, d, J = 9.0 Hz, H-7) and one singlet proton signal of a hydroxyl

group at δ_{H} 8.64 (1H, s, HO-8). The hydroxyl group was placed at C-8 (δ_{C} 145.3), in agreement with NOESY correlations observed between MeO-1 and HO-8 (**Figure 12**). The assignment of H-6 was deduced from its ^1H - ^1H COSY correlation with H-7 and three-bond couplings of H-6 with C-8 (δ_{C} 145.3) and C-9a (δ_{C} 117.7) in the HMBC spectrum (**Figure 12**). The HMBC correlation between H-7 and C-8a (δ_{C} 123.8) was also observed. This compound almost had the same structure as that of chrysotoxone, a fluorenone previously isolated from *Dendrobium chrysotoxum* (Ma, Wang, Xu, et al., 1998), except for the hydroxyl group on ring A of compound **3** was located at C-3. Based on the above spectral evidence, compound **3** was concluded as 3,5,8-trihydroxy-1,4-dimethoxy-9-fluorenone and given the trivial name dendrocruenol C.

Compound **4** was isolated as a dark green powder. The molecular formula $\text{C}_{31}\text{H}_{20}\text{O}_8$ was obtained from its $[\text{M} + \text{Na}]^+$ ion at m/z 543.1067 (calcd for $\text{C}_{31}\text{H}_{20}\text{O}_8\text{Na}$ 543.1056) in the HR-ESI-MS. The IR spectrum displayed absorption bands for hydroxyl (3394 cm^{-1}), carbonyl (1647 cm^{-1}), aromatic ($2924, 1621\text{ cm}^{-1}$), and ether (1228 cm^{-1}) functionalities. The UV spectrum showed absorptions at λ_{max} ($\log \epsilon$) 219 (4.99), 274 (2.24), 320 (1.46), and 396 (0.41) nm. The chemical structure of **4** was proposed as a dimer of a phenanthrene derivative based on the analysis of its HR-ESI-MS and NMR data (Kyokong et al., 2019). First, we determined ^1H NMR in acetone- d_6 , but H-9 and H-10 of the phenanthrene skeleton displayed as a sharp singlet signal at δ_{H} 8.06 (2H). Therefore, we changed the solvent to CDCl_3 , and the phenanthrene structure was confirmed by the presence of two pairs of *ortho*-coupled doublet protons at δ_{H} 7.40 (1H, d, $J = 9.0\text{ Hz}$, H-10'), δ_{H} 7.90 (1H, d, $J = 8.7\text{ Hz}$, H-9), δ_{H} 8.15 (1H, d, $J = 8.7\text{ Hz}$, H-10), and δ_{H} 8.18 (1H, d, $J = 9.0\text{ Hz}$, H-9') in the ^1H NMR spectrum (**Table 11**). The analysis of the ^1H - ^1H COSY spectrum supported an *ortho*-coupled correlation of H-9 with H-10 and H-9' with H-10' (**Figure 12**).

Table 10 ^1H and ^{13}C -NMR Spectral Data of **3** in Acetone- d_6 (δ in ppm, J in Hz).

3^a		
Position	δ_{C} , type	δ_{H}
1	149.3, C	
2	107.2, CH	6.86, s
3	153.3, C	
4	142.8, C	
4a	126.1, C	
5	153.0, C	
6	119.6, CH	6.60, d (9.0)
7	128.5, CH	6.85, d (9.0)
8	145.3, C	
8a	123.8, C	
8b	121.7, C	
9	193.9, C	
9a	117.7, C	
MeO-1	57.9, CH ₃	4.08, s
MeO-4	62.4, CH ₃	3.96, s
HO-8		8.64, s

^aRecorded at 500 MHz for ^1H and 125 MHz for ^{13}C -NMR data.

The ^1H NMR of **4** also displayed additional four aromatic proton signals at δ_{H} 6.81–9.56, two olefinic proton signals at δ_{H} 5.84 (1H, s, H-3') and δ_{H} 5.97 (1H, s, H-3), and resonances for three methoxyl groups at δ_{H} 3.65 (3H, s, MeO-2'), δ_{H} 3.93 (3H, s, MeO-8'), and δ_{H} 4.00 (MeO-7). For the first phenanthrene nucleus, an *ortho*-quinone structure of ring A was supported by signals of two carbonyl carbons at δ_{C} 177.6 (C-1) and δ_{C} 180.0 (C-2) in the ^{13}C NMR spectrum. The HMBC correlations of H-3 and H-10 with C-1 established the position of the carbonyl group at C-1. For ring B, the ^1H NMR

exhibited two broad singlet proton signals at δ_{H} 6.81 (1H, br s, H-6) and δ_{H} 6.94 (1H, br s, H-8). The assignment of H-8 was deduced from its three-bond correlation with C-9 (δ_{C} 129.3) observed in the HMBC spectrum. The first methoxyl group (δ_{H} 4.00) should be attached at C-7 (δ_{C} 162.7), according to NOESY interactions between H-6 and H-8 (**Figure 12**). Regarding the second phenanthrene derivative, the ^1H NMR spectrum of ring A' showed signals for two doublets at δ_{H} 7.46 (1H, d, $J = 9.6$ Hz, H-6') and δ_{H} 9.56 (1H, d, $J = 9.6$ Hz, H-5'). The proton signal of H-5' was assigned by the HMBC correlations of H-5' and H-10' with C-8a' (δ_{C} 129.3). The NOESY correlations between MeO-8' (δ_{C} 3.93) and H-9' placed the second methoxyl at C-8' (δ_{C} 139.2). For ring B', the singlet olefinic proton signal at δ_{H} 5.84 was assigned as H-3' based on its HMBC correlation with C-4a' (δ_{C} 124.9). The third methoxyl group (δ_{C} 3.65) was located at C-2', as evidenced by its NOESY cross-peak with H-3' (**Figure 12**). The two monomers were connected through a C-C linkage between C-4 (δ_{C} 149.9) and C-1' (δ_{C} 78.0) and an ether bond between C-1' and the oxygen atom at C-5 (δ_{C} 152.7), forming a spiro skeleton. This was supported by the HMBC correlations of H-3, H-3', and H-10' with C-1'. The absolute configuration of C-1' was determined by comparison of the experimental electronic circular dichroism (ECD) spectrum with the calculated ECD curves. The ECD spectrum of **4** showed the positive and negative Cotton effects at 217 and 229 nm, respectively, which matched the **4** (*R*) curve in the calculated ECD (**Figure 10**). The assignment of the configuration of C-1' was proposed as *R*. On the basis of the above spectral evidence, the structure of **4** was established as shown, and the trivial name dendrocumenol D was given to the compound.

Table 11 ^1H (300 MHz) and ^{13}C -NMR (75 MHz) Spectral Data of **4** in CDCl_3
(δ in ppm, J in Hz).

4 ^a		
Position	δ_{C} , type	δ_{H}
1	177.6, C	
2	180.0, C	
3	126.0, CH	5.97, s
4	149.9, C	
4a	125.7, C	
4b	113.0, C	
5	152.7, C	
6	104.4, CH	6.81, br s
7	162.7, C	
8	100.6, CH	6.94, br s
8a	138.2, C	
9	129.3, CH	7.90, d (8.7)
10	125.8, CH	8.15, d (8.7)
10a	123.9, C	
1'	78.0, C	
2'	169.5, C	
3'	103.4, CH	5.84, s
4'	186.9, C	
4a'	124.9, C	
4b'	125.7, C	
5'	125.5, CH	9.56, d (9.6)
6'	120.8, CH	7.46, d (9.6)
7'	146.7, C	
8'	139.2, C	
8a'	129.3, C	
9'	127.1, CH	8.18, d (9.0)
10'	124.7, CH	7.40, d (9.0)
10a'	125.8, C	
MeO-7	55.8, CH ₃	4.00, s
MeO-2'	56.7, CH ₃	3.65, s
MeO-8'	62.1, CH ₃	3.93, s

^aRecorded at 300 MHz for ^1H and 75 MHz for ^{13}C -NMR data.

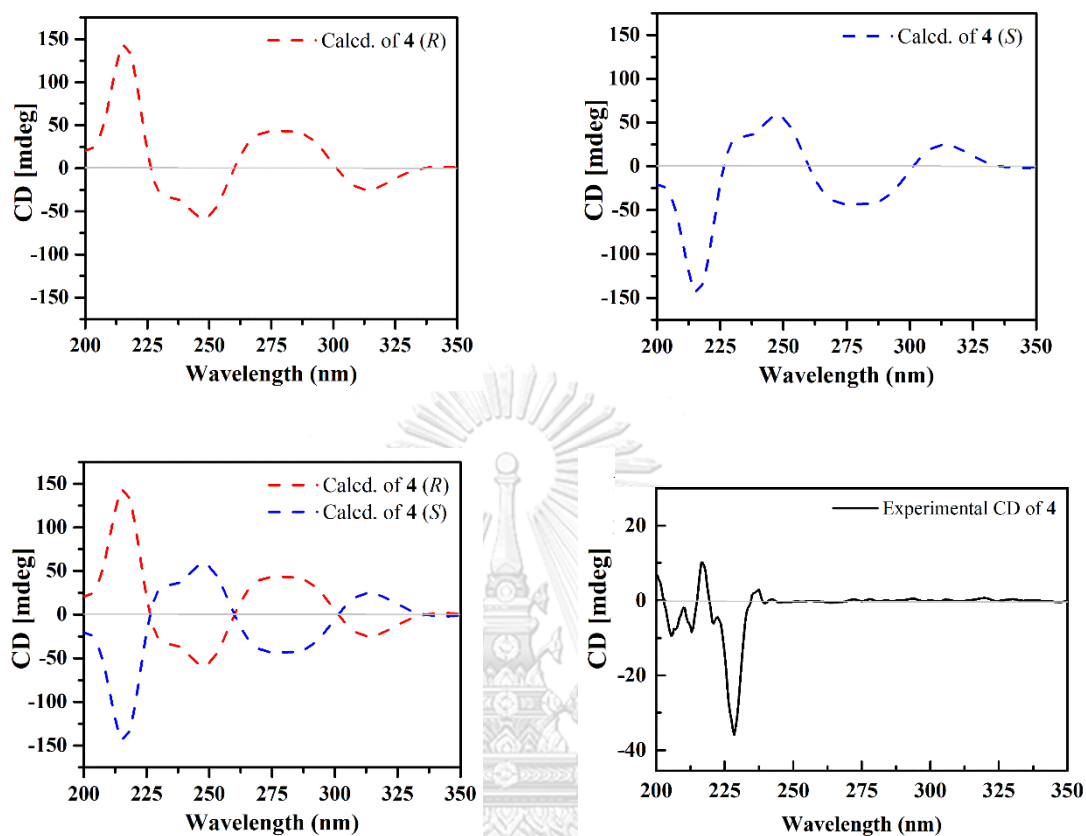


Figure 10 Experimental CD and calculated ECD spectra of compound 4.

Known compounds including gigantol (**5**) (Sritularak, Anuwat, et al., 2011), 3,7-dihydroxy-2,4,8-trimethoxyphenanthrene (**6**) (Majumder et al., 1998), densiflorol B (**7**) (Sukphan et al., 2014), and cypripedin (**8**) (Wattanathamsan et al., 2018) were isolated, and the structures were identified by comparison of their NMR and MS spectra with literature data [Figure 11].

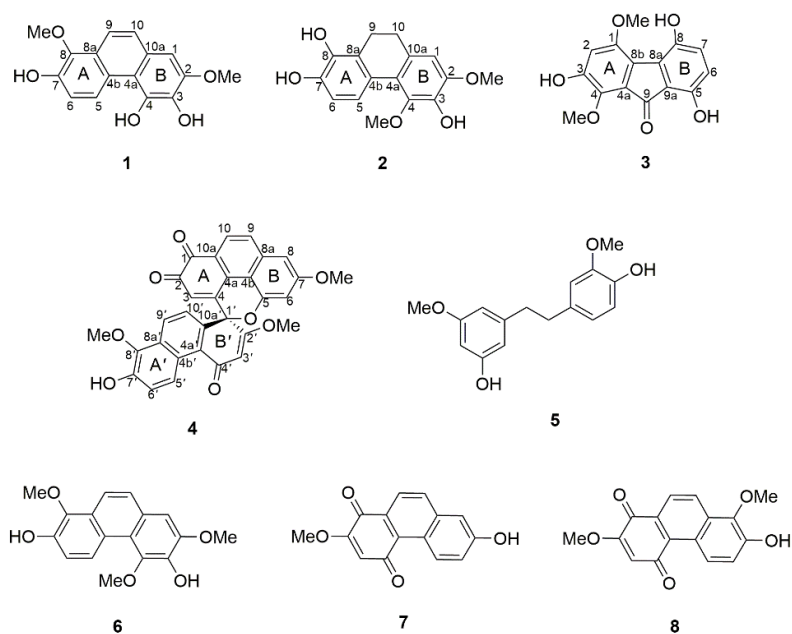


Figure 11 Structure of isolated compounds from *D. crumenatum*.

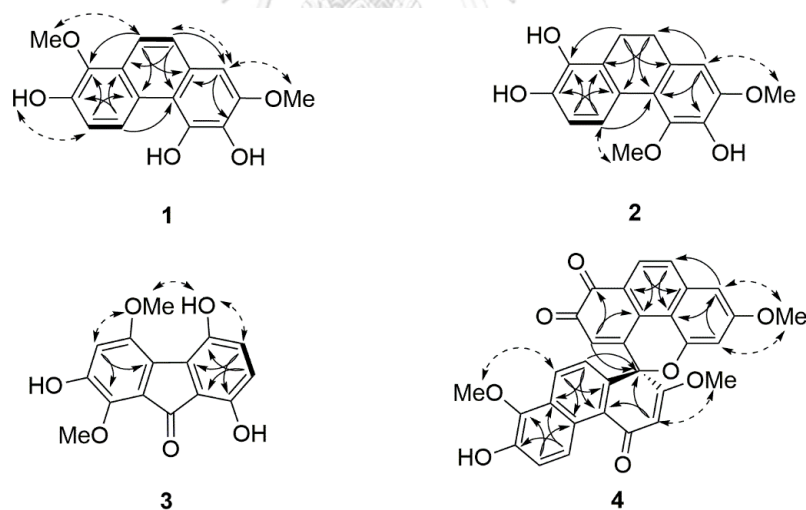


Figure 12 HMBC (arrow), NOESY (double headed dashed arrow) and ^1H - ^1H COSY (bold line) correlations of compounds 1–4.

To investigate the immune modulatory effects from *D. crumenatum*'s compounds on human immune cells, we induced the inflammatory conditions in human PBMCs using PMA/ionomycin ex vivo stimulation in the presence of six purified compounds from *D. crumenatum*, including dendrocrumenol B (2),

dendrocruenenol D (**4**), gigantol (**5**), 3,7-dihydroxy-2,4,8- trimethoxyphenanthrene (**6**), densiflorol B (**7**), and cypripedin (**8**). The isolation yield of dendrocruenenol A (**1**) and dendrocruenenol C (**3**) was not enough for biological testing. All compounds were diluted in DMSO, and therefore DMSO-treated PBMCs were also used as a control condition. Briefly, after 4 h of PMA/ionomycin stimulation, PBMCs were characterized, and the immune modulatory effects of the compounds were evaluated using flow cytometry. Under PMA/ionomycin stimulation, we detected an increased frequency of TNF-expressing CD3⁻CD14⁺ cells, as well as the increased frequencies of IL-2- and IFN- γ -expressing CD3⁺ T cells (**Figure 13**), compared to the untreated PBMCs. In comparison to the PMA/ionomycin-treated condition, we quantified significantly diminished frequencies of PMA/ ionomycin-induced IL-2-expressing CD3⁺ T cells after the treatment with *D. crumenatum* compounds, more significantly with compounds **2**, **4**, **6**, and **8**. Only compound **4** could reduce the abundance of IFN- γ -expressing CD3⁺ activated T cells as well as the frequency of TNF-expressing CD14⁺ inflammatory monocytes (**Figure 14**). We also detected decreased frequencies of IL-2- and IFN- γ -expressing CD3⁺ activated T cells in control PBMCs treated with high-dose DMSO (an equal amount used for 20 μ M compound solutions), compared to the nonstimulated PBMCs (**Figure 14**).

Taken together, we found immune modulatory effects on the CD3⁺ T cell population of all *D. crumenatum* compounds, including two new compounds, dendrocruenenols B and D. Only dendrocruenenol D provided strong immune modulatory effects on both CD3⁺ T cell and CD3⁻ monocyte populations. To exclude the causes of cell death from active compounds from *D. crumenatum* which may interfere with the results showing decreased frequency of activated immune cells that were obtained from flow cytometry, we determined the state of apoptosis in human PMBCs in the presence of *D. crumenatum* compounds. Both dendrocruenenols B (**2**) and D (**4**) did not present any significant increased cell death in both early and late apoptotic states (**Figure 15**). Hence, dendrocruenenols B and D were selected for further investigation.

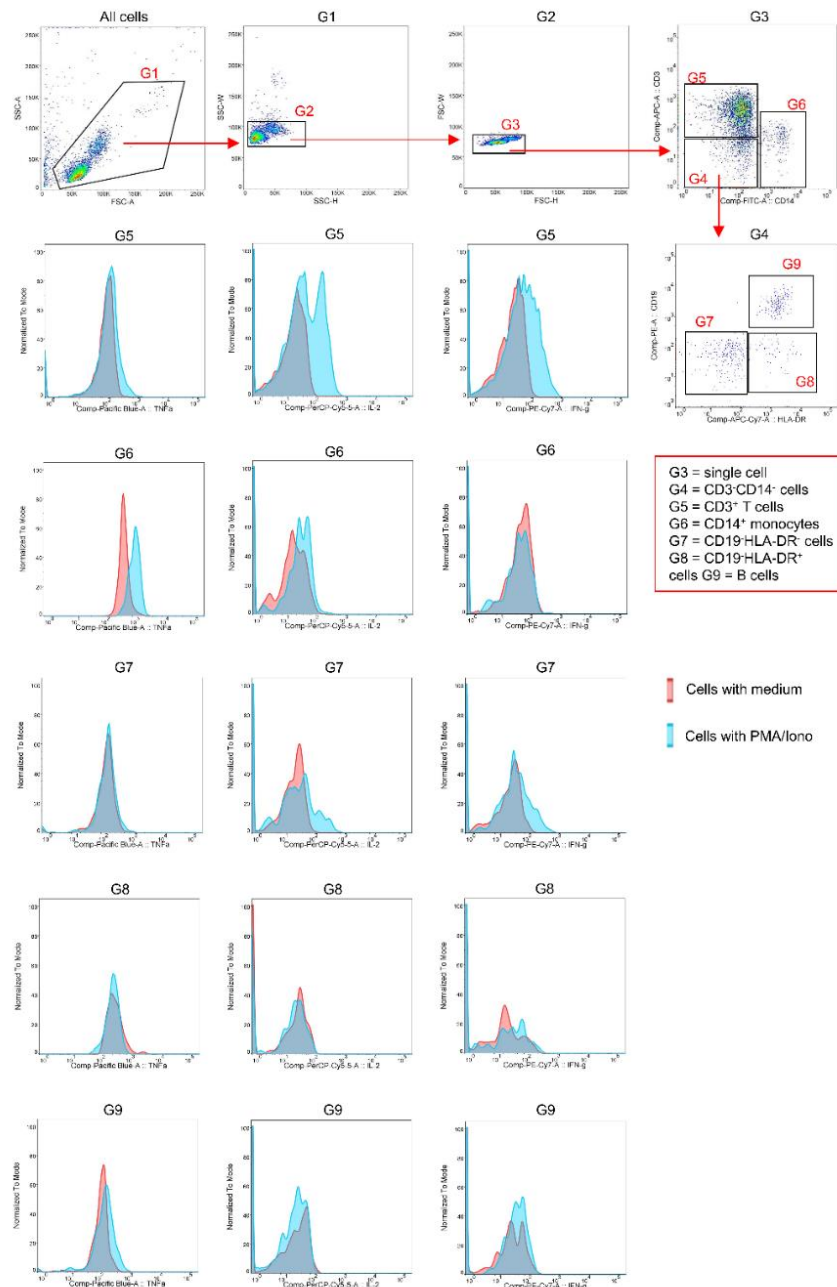


Figure 13 Analysis using flow cytometry. Dot plots and histograms exhibit a flow cytometric gating strategy in PMA/Iono-induced inflammatory cytokine (TNF- α , IL-2, and IFN- γ) expression in human PBMCs obtaining the CD3⁺ T cells (G5), CD14⁺ monocytes (G6), and B cells (G9). CD19⁻HLA-DR⁺ (G8) and B cells (G9) did not express TNF- α , IL-2, and IFN- γ .

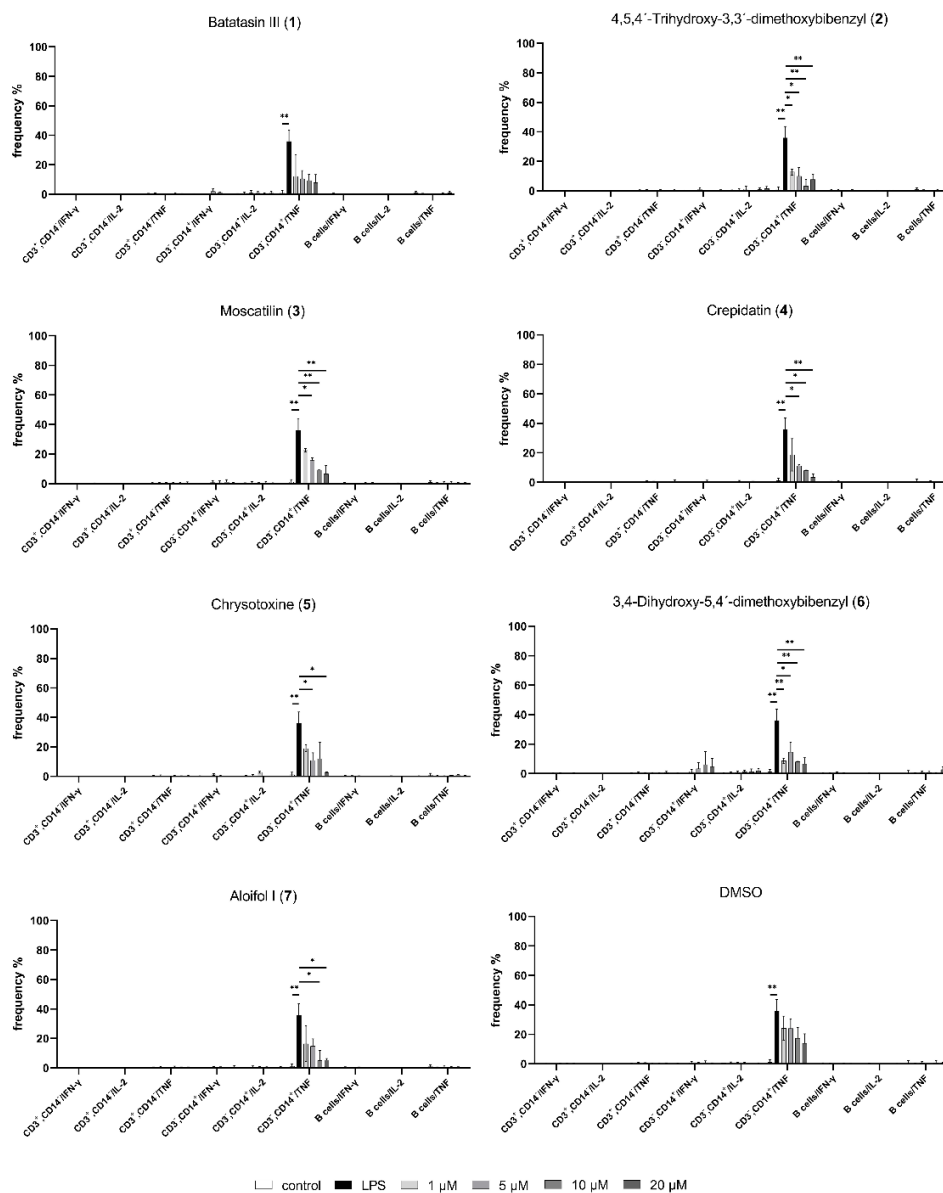


Figure 14 Determination of immune modulatory effects. Bar graphs show the percent of frequency of inflammatory cytokine (TNF- α , IL-2, and IFN- γ) expression in the immune cells of healthy PBMCs (three biological replicates) after 4 h of treatment with 1–20 μ M DMSO and six isolated compounds from *D. crumenatum* with or without PMA/ionomycin stimulation. Two repeated experiments were performed. One-way ANOVA followed the correction of multiple comparisons (Tukey test), *** P < 0.001, ** P < 0.01, * P < 0.05.

We tested whether immune modulatory effects of dendrocruenols B and D, which were observed in PMA-treated PBMCs from healthy individuals, could also be found in PBMCs from patients with inflammatory conditions. We performed the same *ex vivo* stimulation experiment of PBMCs from patients with multiple sclerosis (MS) using PMA/ ionomycin conditions. The immunopathogenesis of MS occurs throughout the disease course involving multiple cell types including T and B cells as well as myeloid and nature killer cells. Immunopathogenesis results in chronic inflammatory responses across different body compartments including the central nervous system (CNS) (Bar-Or & Li, 2021). Inhibition or diminishing imbalanced interactions between activated/inflammatory and regulatory subpopulations will more likely lead to an improvement of disease severity. In line with the results obtained from PBMCs from healthy individuals, both dendrocruenols B (**2**) and D (**4**) showed strong immune modulatory effects, resulting in strong reduction of IL-2-, IFN- γ -, and TNF-expressing CD3⁺ T cells (**Figure 16**). However, the effects appeared to be restricted to T cells, and no significant differences were found in CD14⁺ monocytes.

Next, we investigated whether immune modulatory effects on T cells provided by dendrocruenols B and D may be controlled by store-operated calcium entry (SOCE), as has been shown previously in inflammatory bowel disease (Letizia et al., 2022). Similar to our previous study (Letizia et al., 2022), the reduction of SOCE dependent Ca²⁺ influx by active compounds dendrocruenols B and D was determined by flow cytometry in comparison to the calcium release-activated channel inhibitor (CM4620).

After incubation with 1 μ M CM4620, 10 μ M DMSO, and dendrocruenol B or D for 4 h, we observed that DMSO treated PBMCs showed no different changing of Ca²⁺ influx rate compared to untreated control cells (**Figure 17**). The treatment of CM4620 in PBMCs strongly decreased the Ca²⁺ influx rate in CD4⁺ and CD8⁺ T cells compared to untreated control and DMSO-treated cells (**Figure 17**). However, the treatment of dendrocruenols B and D in PBMCs showed no significant differences in the rate of Ca²⁺ influx in CD4⁺ and CD8⁺ T cells, compared to the control groups. In

conclusion, dendrocrumenols B and D exhibited an inhibition of inflammatory cytokine production in T cells independently of SOCE pathway.

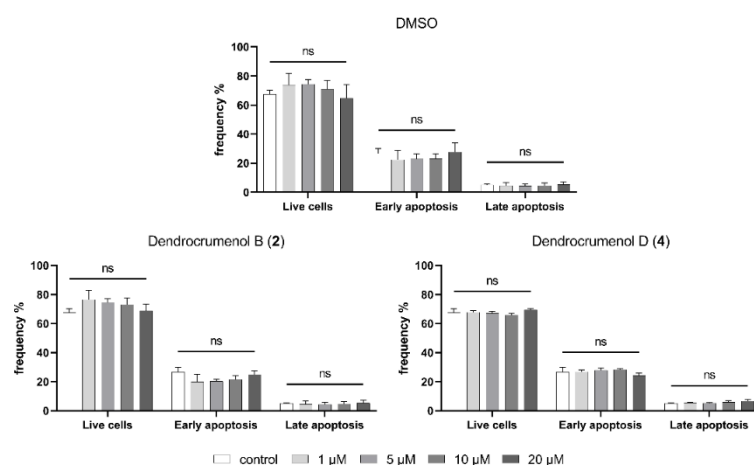


Figure 15 Cytotoxicity of compounds **2** and **4**. Bar graphs show the percent of frequency of changing number of live cells and state of apoptosis in human PBMCs treated with DMSO and the two new compounds **2** and **4** from *D. crumenatus*, compared to cells with medium. Three biological replicates were used in this study.

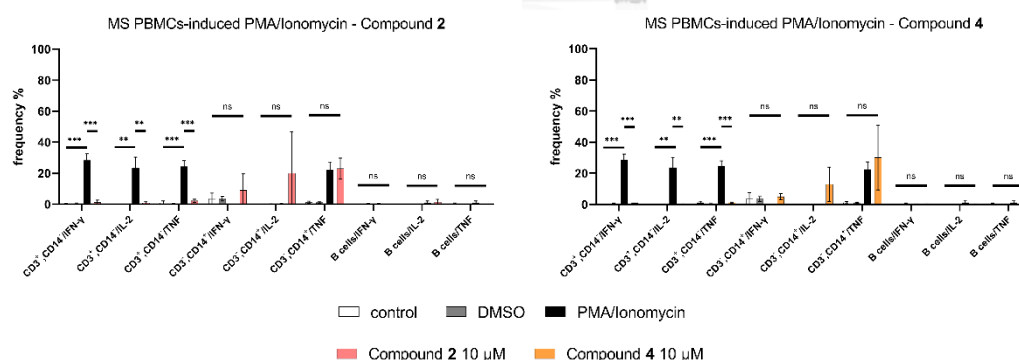


Figure 16 Bar graphs show the percent of frequency of inflammatory cytokines (TNF- α , IL-2, and IFN- γ) expression in the immune cells of MS PBMCs after 4 h treatment with DMSO and the two new active compounds **2** and **4** from *D. crumenatus* with or without PMA/ionomycin stimulation. Two repeated experiments were performed. One-way ANOVA followed the correction of multiple comparisons (Tukey test), *** $P < 0.001$, ** $P < 0.01$.

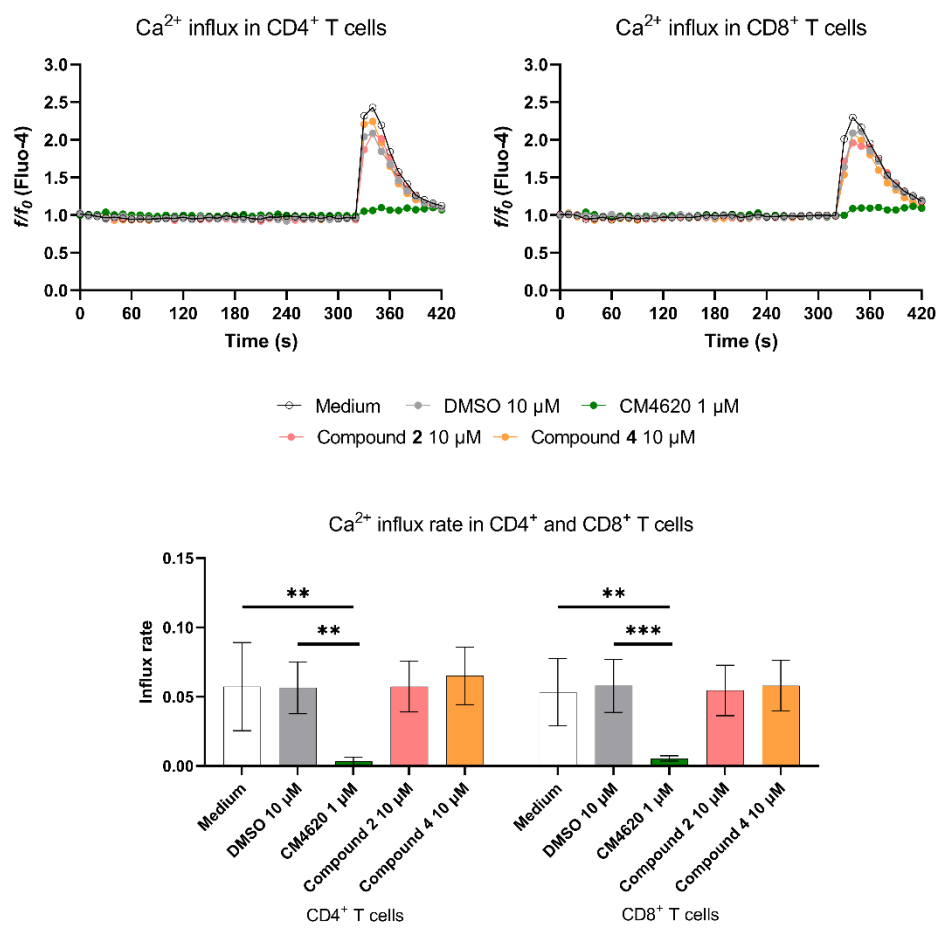


Figure 17 Determination of Ca²⁺ influx. Dot plots and bar graphs demonstrate the reduction of Ca²⁺ influx in CD4⁺ and CD8⁺ T cells treated with CM4620, DMSO, and the two new active compounds **2** and **4** from *D. crumenatum* compared with untreated PBMCs (three biological replicates). Two repeated experiments were performed. One-way ANOVA followed the correction of multiple comparisons (Tukey test), *** $P < 0.001$, ** $P < 0.01$, * $P < 0.05$.

Due to the limitation of cell numbers of PBMCs from MS patients, we decided to further investigate only dendrocruenenol D (**4**). Although dendrocruenenols B and D provided similar immune modulatory effects and showed low/no cytotoxicity, dendrocruenenol D seemed to provide higher effects and less cytotoxicity (**Figures**

15, 16 and 17). To deeply characterize the immune modulatory effects of dendrocrumenol D (**4**) on PMA-treated PBMCs, we simultaneously immune profiled PBMCs with all conditions using our previously validated CyTOF workflow with some optimization (see **Experimental Section** for more details) (Böttcher, Fernández-Zapata, et al., 2019). Briefly, the antibodies, which was designed to encompass the major circulating immune cell subsets [T & B cells, myeloid cells (monocytes, macrophages, and dendritic cells), natural killer (NK) cells], activity-related markers, chemokine receptors, and cell subset markers. After CyTOF acquisition, the data were preprocessed as previously described, including the steps of debarcoding, compensation, and quality control (**Figure 18A**) (Böttcher, Fernández-Zapata, et al., 2019; Böttcher, Schlickeiser, et al., 2019; Fernández Zapata et al., 2022). To further evaluate the phenotypic differences of immune cells between the analyzed groups, we performed the clustering analysis using our previous data analysis workflow (Fernández Zapata et al., 2022). A total of 20 clusters were identified (**Figure 18B**). We detected three differential abundant clusters between the experimental groups, clusters 11, 15, and 17 (**Figure 18C**).

Among three different treatment groups of PBMCs from healthy individuals, we detected one differentially abundant cluster, cluster 11: CD161⁺ CD3⁺Tbet⁺CD4⁻CD8⁻CD14⁻ double negative T cells. This subpopulation of T cells was found to increase after PMA treatment in all three control PBMCs analyzed (**Figure 18D**).

The frequency of this subpopulation was decreased after dendrocrumenol D (Comp-**4**) treatment in all individuals. However, this subpopulation was not significantly different between the analyzed conditions of PBMCs from MS patients. Instead, we detected an increased frequency of CTLA4⁺CRTH2⁺ CD8⁺ T cells in both PMA-stimulated and **4**-treated, PMA-stimulated (Comp-**4**+PMA) groups (**Figure 18E**). Interestingly, similar subsets of CD8⁺ T cells were suggested to play a regulatory role in different conditions of immune challenge (Chan et al., 2014; Tsuda et al., 2001). Strikingly, we also detected a reduction of the frequency of reactive ICOS⁺ CD4⁺ T cells in all PMA-stimulated, Comp-**4**-treated PBMCs from MS patients (**Figure 18F**).

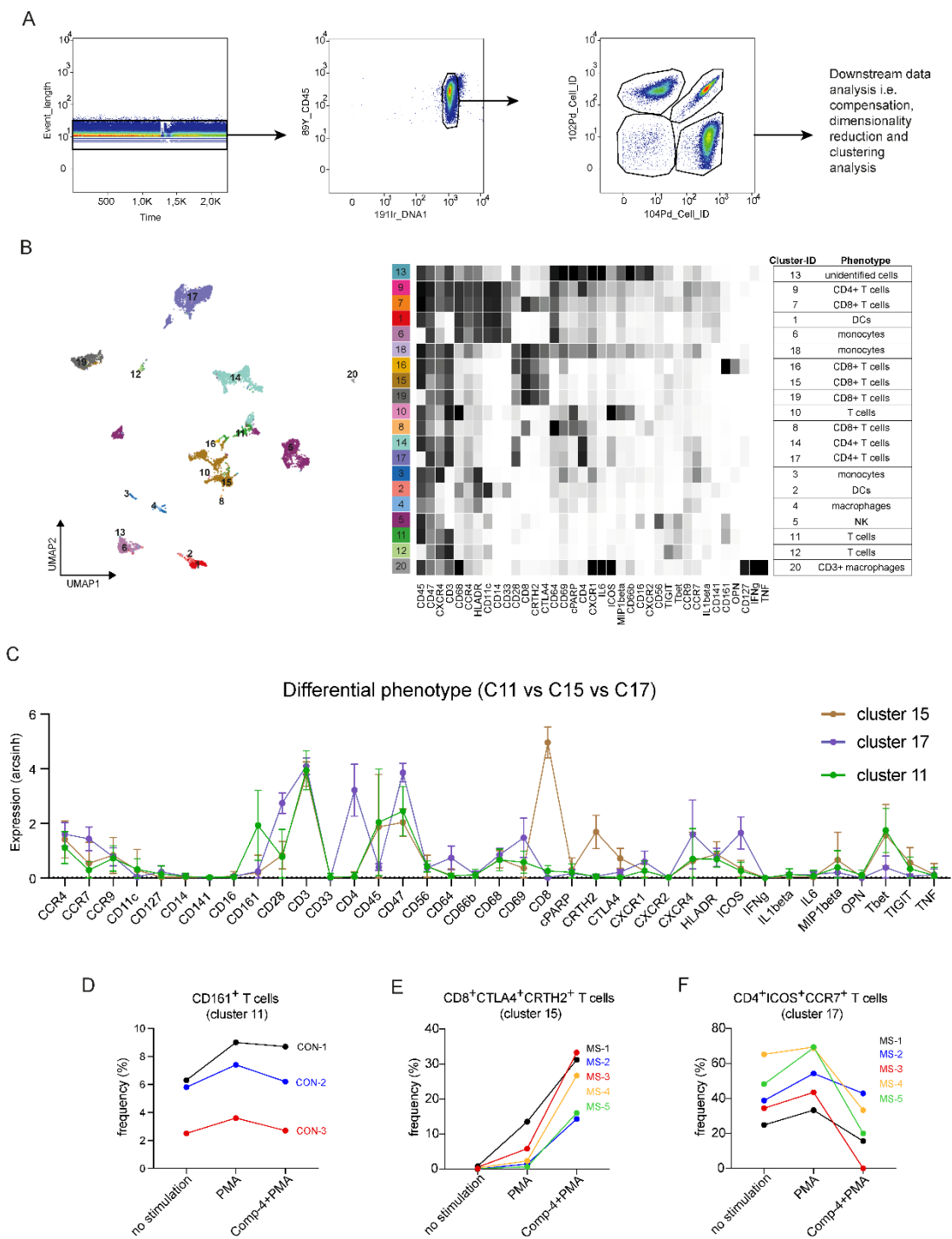


Figure 18 Evaluation of immune modulatory effects using deep immune profiling by CyTOF. (A) Gating strategy for CyTOF data prior to downstream analysis, selection of

single CD45⁺ cells, and de-barcoding based on Boolean gating of palladium barcodes. (B) UMAP projection (left image) from all samples; coloring indicates 1–20 clusters representing diverse immune cell phenotypes, defined by the FlowSOM algorithm, and the heatmap cluster (right image) depicting the median expression levels of all markers analyzed. Heat colors of expression levels have been scaled for each marker individually (to the 1st and 5th quintiles) (black, high expression; white, no expression). (C) Line graph of the arcsinh marker expression (mean \pm SD) between differentially abundant clusters (C11, C15, and C17). (D) The frequency plot of differentially abundant cluster CD161⁺ T cells between different treatment conditions of PBMCs from all three control individuals. (E and F) The frequency plots of differentially abundant clusters CD8⁺CTLA4⁺CRTH2⁺CD8⁺ (E) and ICOS⁺CCR7⁺CD4⁺ (F) T cells between different treatment conditions of PBMCs from all five MS patients.

Taken together, we demonstrated herein immune modulatory effects of active compounds from *D. crumenatum* in both healthy PBMCs and those from MS patients. Interestingly, these positive effects appeared to be different between healthy and disease PBMCs. These compounds, especially dendrocruenol D, appear as promising compounds for further development in preclinical settings for the treatment of (neuro)inflammatory diseases/conditions. In summary, we demonstrated herein immune modulatory effects of the new compounds dendrocruenols B and D on both healthy T cells and monocytes in vitro, resulting in the reduction of T cells and monocytes expressing inflammatory mediators. Reduced proportion of these inflammatory subpopulations of T cells and monocytes was independent of SOCE pathway and Ca²⁺ influx. In MS-PBMCs, immune modulatory effects were detected only in T cell populations. Results obtained from both flow cytometry and CyTOF confirmed immune modulatory effects of dendrocruenol D in MS-PBMCs, possibly via the improvement of the balance between regulatory and reactive (inflammatory mediator expressing) T cell subpopulations. Our results suggest that dendrocruenol D may potentially be of

interest as an in vivo immune modulatory lead compound in a broad spectrum of inflammation-driven diseases. Although *Dendrobium* species used as medicinal herbs in the pharmaceutical industry are harvested from the wild, causing the decrease of wild populations, *D. crumenatum* is useless and invasive, and thus can ideally be harvested and used for future investigations.

EXPERIMENTAL SECTION

General Experimental Procedures. The optical rotation was recorded using an ATAGO POLAX-2L polarimeter (Minato-ku, Tokyo, Japan). CD spectra were measured by a Jasco J-815 CD spectrophotometer (Hachioji, Tokyo, Japan). Ultraviolet–visible (UV–vis) spectra were recorded with a Milton Roy Spectronic 3000 Array spectrophotometer (Rochester, Monroe, NY, USA). Infrared (IR) spectra were recorded using a PerkinElmer FT-IR 1760X spectrophotometer (Boston, MA, USA). Nuclear magnetic resonance (NMR) spectra were recorded on a Bruker Avance DPX-300FT NMR spectrometer or a Bruker Avance III HD 500 NMR spectrometer (Billerica, MA, USA). High-resolution mass (HR-ESI-MS) spectra were obtained from a Bruker MicroTOF mass spectrometer ESI-MS (Billerica). Vacuum-liquid chromatography (VLC) and column chromatography (CC) were carried out on silica gel (Merck, NJ, USA) at a particle size of 63–200 μm and 40–63 μm , respectively. Sephadex LH-20 (Merck, NJ, USA) was used for fractionation and purification. Thin-layer chromatography (TLC) was performed on silica gel 60 F254 plates (Merck, NJ, USA) under UV light. Phorbol-12-myristate-13-acetate (PMA), ionomycin, brefeldin A, dimethyl sulfoxide (DMSO), and CRAC channel inhibitor (CM4620) were purchased from Sigma-Aldrich (St. Louis, MO, USA). Roswell Park Memorial Institute (RPMI) 1640, fetal bovine serum (FBS), phosphate buffered saline (PBS), 16% w/v formaldehyde (FA), and SMART TUBE INC Proteomic Stabilizer were purchased from Thermo Fisher Scientific Inc. (Rockford, IL, USA). Cell staining buffer was purchased from Fluidigm (South San Francisco, CA, USA).

Plant Material. Samples of *Dendrobium crumenatum* were purchased from Chatuchak market in August 2018. Plant identification was performed by one of the authors (B.S.). A voucher specimen (BS-Dcrum-082561) has been deposited at the Department of Pharmacognosy and Pharmaceutical Botany, Faculty of Pharmaceutical Sciences, Chulalongkorn University.

Extraction and Isolation. Dried and powdered stems of *D. crumenatum* (4.3 kg) were extracted with MeOH (3 × 20 L) at room temperature, giving a MeOH extract (220 g). The MeOH extract was diluted in 1000 mL of H₂O–MeOH (1:1) and partitioned with EtOAc (3 × 1000 mL) to obtain an EtOAc extract (126 g). The aqueous phase was then partitioned with *n*-BuOH (3 × 1000 mL) to give a butanol extract (50 g) and an aqueous extract (35 g). The EtOAc fraction was subjected to VLC on silica gel with EtOAc–hexane gradient mixtures (0:100 → 8:2) to obtain 11 fractions (A–K). These obtained fractions were checked by TLC analysis. Fraction G (5.2 g) was fractionated by chromatography on Sephadex LH-20 (MeOH) to give six fractions (GI–GVI). Fraction GII (1.9 g) was further purified by CC over silica gel using a gradient elution of EtOAc–hexane (3:7 → 1:1) to give gigantol (**5**) (41.6 mg) and **1** (1.8 mg). Fraction GIII (1.2 g) was separated by CC on silica gel with a gradient of EtOAc–hexane (2:8 → 7:3) to yield six fractions (GIII1–GIII6). Fraction GIII2 (269.4 mg) was separated by chromatography on Sephadex LH-20 (MeOH) and then purified by CC on silica gel using elution of EtOAc–toluene (1:9) to furnish 3,7-dihydroxy-2,4,8-trimethoxyphenanthrene (**6**) (54.4 mg). Fraction GIII4 (210.4 mg) was fractionated by chromatography on Sephadex LH-20 (acetone) to give two fractions (GIII4a and GIII4b). Densiflorol B (**7**) (37.5 mg) and cypripedin (**8**) (56.0 mg) were obtained from fractions GIII4a and GIII4b, respectively, after purification by CC on silica gel, eluted with MeOH–toluene (5:95) from GIII4a and EtOAc–toluene (2:8) from GIII4b. Fraction GIII6 (70.2 mg) was separated by chromatography on Sephadex LH-20 (MeOH) and then by CC on silica gel with EtOAc–toluene mixture (3:7) to give **2** (10.7 mg). Compound **3** (10.7 mg) was obtained from fraction GIV (368.1 mg) after isolation by

CC over silica gel using gradient elution of EtOAc–hexane (0:100 → 1:1) and chromatography on Sephadex LH-20 (MeOH). Fraction H (10.5 g) was separated by CC on silica gel with an acetone–hexane gradient (1:9 → 6:4) and further subjected to repeated CC on silica gel with a MeOH–CH₂Cl₂ gradient (0:100 → 5:95) to give four fractions (HV1–HV4). Separation of fraction HV2 (1.0 g) by CC over silica gel using gradient elution of acetone–CH₂Cl₂ (5:95 → 3:7) and then purification by CC on silica gel with an EtOAc–toluene mixture (1:1) yielded **4** (28.9 mg).

Dendrocruenol A (1): brown amorphous solid, UV (MeOH) λ_{\max} (log ϵ) 224 (2.51), 280 (1.20), 295 (1.07) nm; IR ν_{\max} 3273, 2962, 1618, 1594, 1484, 1289 cm⁻¹; HR-ESI-MS [M – H]⁻ m/z 285.0811 (calcd for C₁₆H₁₃O₅ 285.0763); ¹H and ¹³C NMR data, see **Table 9**.

Dendrocruenol B (2): brown amorphous solid, UV (MeOH) λ_{\max} (log ϵ) 224 (2.51), 280 (1.20), 295 (1.07) nm; IR ν_{\max} 3390, 2961, 1615, 1490, 1281 cm⁻¹; HR-ESI-MS [M + H]⁺ m/z 289.1072 (calcd for C₁₆H₁₇O₅ 289.1076); ¹H and ¹³C NMR data, see **Table 9**.

Dendrocruenol C (3): red powder, UV (MeOH) λ_{\max} (log ϵ) 219 (3.70), 249 (1.44) nm; IR ν_{\max} 3336, 2956, 2925, 1727, 1671, 1493, 1286 cm⁻¹; HR-ESI-MS [M – H]⁻ m/z 287.0557 (calcd for C₁₅H₁₁O₆ 287.0556); ¹H and ¹³C NMR data, see **Table 10**.

Dendrocruenol D (4): dark green powder, $[\alpha]_D^{20}$ –6.18 (c 0.05, MeOH); UV (MeOH) λ_{\max} (log ϵ) 219 (4.99), 274 (2.24), 320 (1.46), 396 (0.41) nm; ECD (MeOH) λ_{\max} ($\Delta\epsilon$) 217 (+0.01), 229 (–0.03) nm; IR ν_{\max} 3394, 2924, 2853, 1647, 1621, 1471, 1424, 1282, 1228 cm⁻¹; HR-ESI-MS [M + Na]⁺ m/z 543.1067 (calcd for C₃₁H₂₀O₈Na 543.1056); ¹H and ¹³C NMR data, see **Table 11**.

ECD Calculation. The possible configurations of compound **4** were optimized using DFT calculation at the B3LYP/6-31g(d,p) level. The computed ECD spectra were calculated using time-dependent density functional theory (TD-DFT) at the B3LYP/6-311++g(d,p) level. The geometry optimization and TD-DFT calculations were both performed with the continuum model (PCM) solvation model with MeOH. All

calculations were performed using the Gaussian16 program package (Frisch et al., 2016). The ECD spectra were simulated with overlapping Gaussian functions with a $\sigma = 0.25$ eV fitting parameter using the SpecDis1.64 program (Bruhn et al., 2013). The more reliable length gauge representation was used for ECD spectra.

Ethics and Cells. This study was approved by the Ethics Committee of Charité–Universitätsmedizin Berlin (EA1/187/17). Buffy coats used in this research were obtained from three healthy donors and five patients with multiple sclerosis. Human PBMCs were isolated and aliquoted at 20×10^6 cells/mL, as described in the previous study (Khoonrit et al., 2020), and were then cryopreserved in a liquid nitrogen tank.

PMA/Ionomycin Stimulation in PBMCs. Frozen PBMCs were resuspended in RPMI 1640 medium with 10% FBS, and then the concentration was adjusted to 10×10^6 cells/mL. Cells were seeded at a density of 5×10^5 cells per well in an ultralow-attachment 96-well plate (Corning, New York, USA). Different concentrations of DMSO and compounds were added in the corresponding well. Subsequently, PMA (20 ng/mL) and ionomycin (100 μ g/mL) were added into the well plate for stimulation of the cultured cells and incubated 37 °C for 2 h. After incubation, brefeldin A (10 μ g/mL) was added into the wells and further incubated for 2 h. Cells were then harvested and washed with PBS. Finally, cells were incubated with 10% bovine serum albumin (BSA) and SMART TUBE INC Proteomic Stabilizer at RT for 12 min and were then stored at –80 °C before staining.

Measurement of Cytokines in PMA/Ionomycin-Treated PBMCs Using Flow Cytometry. PMA/ionomycin-treated PBMCs were thawed and washed twice with staining buffer. For blocking unspecific antibodies, cells were incubated with FcR-blocking buffer (1:100; Miltenyi Biotec, Bergisch Gladbach, Germany) at 4 °C for 10 min. Cells were then stained at 4 °C for 20 min with immunofluorescent-conjugated antibodies for extracellular proteins including CD14 (FITC, RMO52, Beckman Coulter), CD3 (APC, HIT3a, Biolegend), HLA-DR (APC/Cy7, L243, Biolegend), and CD19 (PE, HIB19, Biolegend) diluted in staining buffer (0.5% BSA in PBS containing 2 mM EDTA). After

that, cells were washed with staining buffer and were then fixed with 2% MeOH-free FA at 4 °C for 30 min. Cells were washed with staining buffer and were then stained at 4 °C for 30 min with immunofluorescent-conjugated intracellular antibodies including IFN- γ (PE/Cy7, 4S.B3, Biolegend), IL-2 (PerCP/Cy5.5, MQ1-17H12, Biolegend), and TNF (brilliant violet, MAb11, Biolegend) diluted in permeabilization buffer (eBioscience, CA, USA). After incubation with intracellular antibodies, cells were washed and then fixed with 4% MeOH-free FA at 4 °C for 10 min. Fixed cells were washed with staining buffer and centrifugated at 600 g at 12 °C for 5 min. The supernatants were discarded and collected only as pellets. Finally, pellets were resuspended in staining buffer and were measured by a BD CANTO II flow cytometer (BD Biosciences, NJ, USA) with BD DIVA version 8.1 software. Data analysis was performed using FlowJo software version 10.1 (Ashland, OR, USA).

PMA/Ionomycin-Treated Healthy PBMCs Analyzed by CyTOF.

PMA/ionomycin-treated PBMCs were stained and analyzed using our previous standard protocol (Böttcher, Fernández-Zapata, et al., 2019). Briefly, after fixation and storage at -80 °C, cells were thawed and subsequently stained with premade combinations of the palladium isotopes ^{102}Pd , ^{104}Pd , ^{105}Pd , ^{106}Pd , ^{108}Pd , and ^{110}Pd (Cell-ID 20-plex Pd barcoding kit, Fluidigm). There is a unique combination of three different palladium isotopes, which allows having up to 20 different unique barcodes. Cells were stained for 30 min at RT and then washed twice with cell staining buffer (0.5% bovine serum albumin in PBS, containing 2 mM EDTA). The samples were pooled together, washed, and further stained with antibodies, purchased pre-conjugated to metal isotopes (Fluidigm) or conjugated in house by using the MaxPar X8 kit (Fluidigm) following the manufacturer's protocol (**Table 12**). The pooled samples were resuspended in 50 μL of antibody cocktail against surface markers and incubated for 30 min at 4 °C. After incubation, cells were washed twice with staining buffer and subsequently fixed overnight with 2% MeOH-free formaldehyde solution. Fixed cells were washed with staining buffer, then resuspended with 100 μL of intracellular antibody cocktail in permeabilization buffer.

After 30 min of incubation at RT, the samples were washed twice with staining buffer and resuspended in 1 mL of iridium mix (1:1000 iridium in PBS containing 2% FA) for 30 min at RT. Cells were washed twice with staining buffer and kept at 4 °C until CyTOF measurement.

Mass cytometry data processing and analysis were performed as previously described (Böttcher, Fernández-Zapata, et al., 2019). Briefly, initial manual gating of CD45⁺DNA⁺ and gating out of CD3⁺CD19⁺ cells and de-barcoding according to the barcode combination were performed on FlowJo. De-barcoded samples were exported as individual FCS files for further analysis. Using the R package CATALYST, each file was compensated for signal spillover. For further analysis we used previously described scripts and workflows. We created multidimensional scaling (MDS) plots on median marker expression from all markers for first evaluation of the overall similarities between samples and conditions. In order to perform unsupervised clustering, we used the FlowSOM/ConsensusClusterPlus algorithms of the CATALYST package. We opted for a total number of 20 meta-clusters based on the phenotypic heatmaps and the delta area plot. We generated UMAP representations including all markers as input in order to have a dimensionality-reduction visualization of the clusters.

Cytotoxicity Determined by Annexin V and 7-AAD Staining in Human PBMCs. Frozen PBMCs were resuspended in RPMI 1640 medium with 10% FBS, and then the concentration was adjusted to 20×10^6 cells/mL. Cells were plated in an ultralow-attachment 96-well plate at a density of 5×10^5 cells per well. Different concentrations of DMSO and compounds were added in the corresponding well and incubated at 37 °C for 4 h. Cells were then harvested and washed with PBS. After washing, cells were stained at 4 °C for 20 min with CD45 antibody (APC, HI30, Biolegend) diluted in staining buffer. After washing, cells were resuspended with 100 μ L of Annexin V binding buffer. Subsequently, 50 μ L of cell suspensions was further stained with Pacific Blue Annexin V apoptosis detection kit with 7-AAD (Biolegend) at RT for 15 min in the dark. Finally, Annexin V binding buffer was added to each

sample. Stained cells were measured by a BD CANTO II flow cytometer (BD Biosciences) with BD DIVA version 8.1 software. Data analysis was performed using FlowJo software version 10.1.

Table 12 The CyTOF antibody list.

target	isotope tag	clone	company
CD45	89Y	HI30	Fluidigm
HLA-DR	141Pr	L243	Biolegend
CXCR1	142Nd	8F1	Fluidigm
cPARP	143Nd	F21-852	Fluidigm
CD69	144Nd	FN50	Fluidigm
CD4	145Nd	RPA-T4	Fluidigm
CD64	146Nd	10.1	Fluidigm
CXCR2	147Sm	5.00E+08	Fluidigm
CD16	148Nd	3G8	Fluidigm
CD56	149Sm	NCAM16.2	Fluidigm
MIP-1 β (CCL4)	150Nd	D211351	Fluidigm
ICOS	151Eu	C398.4A	Fluidigm
CD66b	152Sm	80H3	Fluidigm
CD68	153Eu	Y1/82A	Biolegend
CD3	154Sm	UCHT1	Fluidigm
CD11c	155Gd	Bu15	Biolegend
IL-6	156Gd	MQ2-13AS	Fluidigm
CCR4	158Gd	L291H4	Biolegend
TIGIT	159Tb	MBSA43	Fluidigm
CD14	160Gd	RM052	Fluidigm
CTLA4	161Dy	14D3	Biolegend

Table 12 The CyTOF antibody list (Continued).

target	Isotope tag	clone	company
CD8	162Dy	RPA-T8	Fluidigm
CRTH2	163Dy	BM16	Fluidigm
CD28	164Dy	L293	Biolegend
IFN γ	165Ho	B27	Fluidigm
CD141	166Er	M80	Fluidigm
CCR7	167Er	G043H7	Biolegend
CCR9	168Er	L053E8	Biolegend
CD33	169Tm	WM53	Fluidigm
Tbet	170Er	4B10	Biolegend
CD161	171Yb	HP-3G10	Biolegend
OPN	172Yb	polyclonal	LSBio
CXCR4	173Yb	12G5	Fluidigm
IL-1 β	174Yb	CRM56	eBioscience
TNF	175Lu	Mab11	Fluidigm
CD127	176Yb	A019D5	Fluidigm
CD47	209Bi	CC2C6	Fluidigm

Calcium Influx Measurement in Human PBMCs. PBMCs were cultured in RPMI 1640 medium with 10% FBS. Cells were seeded in an ultralow-attachment 96-well plate with or without 1 μ M CM4620 (Letizia et al., 2022) or active compounds from *D. crumenatum* or DMSO and were then incubated at 37 °C for 4 h. After incubation, cells were stained with calcium indicator Fluo-4 AM on ice for 30 min in the dark. Subsequently, cells were washed with PBS in 5% BSA and were then incubated with anti-human antibodies including CD3 (PE/Cy7, UCHT1, Biolegend), CD4 (APC, OKT4, eBioscience), and CD8 (APC/Cy7, SK1, Biolegend) for 15 min on ice protected from the light. CM4620 and active compounds from *D. crumenatum* were

added in stained cells before flow cytometric measurement. All samples were analyzed using flow cytometry following a previous standard protocol (Böttcher, Fernández-Zapata, et al., 2019).

PMA/Ionomycin-Treated Multiple Sclerosis PBMCs Using Flow Cytometry.

For PMA/ionomycin-treated MS PBMC sample measurement, cells were stimulated with a final concentration of 20 ng/mL of PMA and 100 µg/mL of ionomycin for 2 h. Then, 10 µg/mL of brefeldin A was added into the cultured cells and incubated for 2 h. After incubation, cells were harvested and washed with PBS. Finally, cells were incubated with 10% BSA and SMART TUBE INC Proteomic Stabilizer at RT for 12 min and were then stored at –80 °C before staining. PMA/ionomycin-treated MS PBMCs were stained and measured with the same protocol as previously described (Böttcher, Fernández-Zapata, et al., 2019).

PMA/Ionomycin-Treated Multiple Sclerosis PBMCs Analyzed by CyTOF.

PMA/ionomycin-treated MS PBMCs were stained and analyzed using the same protocol as previously described (Böttcher, Fernández-Zapata, et al., 2019).

Statistical Analysis. GraphPad Prism v.9.0 software (San Diego, CA, USA) was used for statistical analysis in this study. Data were expressed as the mean ± standard deviation (SD). Group analysis was analyzed using one-way ANOVA followed by Tukey's test. The *p* values that were less than 0.05 were interpreted as statistical significance.

ASSOCIATED CONTENT

Supporting Information

The Supporting Information is available free of charge at <https://pubs.acs.org/doi/10.1021/acs.jnatprod.3c00107>.

Table of CyTOF antibodies, scheme of extraction and purification of active compounds from *Dendrobium crumenatum*, UV, IR, HR-ESI-MS, and NMR (1D and 2D) spectra of the four new compounds (**1–4**) (PDF).

AUTHOR INFORMATION

Corresponding Authors

Chotima Böttcher – Experimental and Clinical Research Center, a cooperation between the Max Delbrück Center for Molecular Medicine in the Helmholtz Association and Charité–Universitätsmedizin Berlin, Berlin 13125, Germany; Max Delbrück Center for Molecular Medicine in the Helmholtz Association (MDC), Berlin 13125, Germany;

Phone: +49 30 450 540 568; Email: chotima.boettcher@charite.de

Boonchoo Sritularak – Department of Pharmacognosy and Pharmaceutical Botany, Faculty of Pharmaceutical Sciences and Center of Excellence in Natural Products for Ageing and Chronic Diseases, Faculty of Pharmaceutical Sciences, Chulalongkorn University, Bangkok 10330, Thailand; orcid.org/0000-0001-8352-4122; Phone: +662 2188356; Email: boonchoo.sr@chula.ac.th

Authors

Virunh Kongkatitham – Pharmaceutical Sciences and Technology Program, Faculty of Pharmaceutical Sciences, Chulalongkorn University, Bangkok 10330, Thailand; Department of Pharmacognosy and Pharmaceutical Botany, Faculty of Pharmaceutical Sciences, Chulalongkorn University, Bangkok 10330, Thailand; orcid.org/0000-0001-5983-8041

Adeline Dehlinger – Experimental and Clinical Research Center, a cooperation between the Max Delbrück Center for Molecular Medicine in the Helmholtz Association and Charité–Universitätsmedizin Berlin, Berlin 13125, Germany; Max Delbrück Center for Molecular Medicine in the Helmholtz Association (MDC), Berlin 13125, Germany

Meng Wang – Experimental and Clinical Research Center, a cooperation between the Max Delbrück Center for Molecular Medicine in the Helmholtz Association and Charité–Universitätsmedizin Berlin, Berlin 13125, Germany; Max Delbrück Center for Molecular Medicine in the Helmholtz Association (MDC), Berlin 13125, Germany

Preeyaporn Poldorn – Center of Excellence in Biocatalyst and Sustainable Biotechnology, Department of Biochemistry, Faculty of Science, Chulalongkorn University, Bangkok 10330, Thailand

Carl Weidinger – Department of Gastroenterology, Infectious Diseases and Rheumatology, Charité–Universitätsmedizin Berlin, Corporate Member of Freie Universität Berlin, Humboldt-Universität zu Berlin and Berlin Institute of Health, Berlin 12203, Germany; Clinician Scientist Program, Berlin Institute of Health, Berlin 10117, Germany

Marilena Letizia – Department of Gastroenterology, Infectious Diseases and Rheumatology, Charité–Universitätsmedizin Berlin, Corporate Member of Freie Universität Berlin, Humboldt-Universität zu Berlin and Berlin Institute of Health, Berlin 12203, Germany

Chatchai Chaotham – Department of Biochemistry and Microbiology, Faculty of Pharmaceutical Sciences, Chulalongkorn University, Bangkok 10330, Thailand; orcid.org/0000-0002-3206-192X

Carolin Otto – Department of Neurology and Experimental Neurology, Charité–Universitätsmedizin Berlin, Berlin 10117, Germany

Klemens Ruprecht – Department of Neurology and Experimental Neurology, Charité–Universitätsmedizin Berlin, Berlin 10117, Germany

Friedemann Paul – Experimental and Clinical Research Center, a cooperation between the Max Delbrück Center for Molecular Medicine in the Helmholtz Association and Charité–Universitätsmedizin Berlin, Berlin 13125, Germany; Max Delbrück Center for Molecular Medicine in the Helmholtz Association (MDC), Berlin

13125, Germany; Department of Neurology and Experimental Neurology and NeuroCure Clinical Research Center, Charité–Universitätsmedizin Berlin, Berlin 10117, Germany

Thanyada Rungrotmongkol – Center of Excellence in Biocatalyst and Sustainable Biotechnology, Department of Biochemistry, Faculty of Science and Program in Bioinformatics and Computational Biology, Graduate School, Chulalongkorn University, Bangkok 10330, Thailand

Kittisak Likhitwitayawuid – Department of Pharmacognosy and Pharmaceutical Botany, Faculty of Pharmaceutical Sciences, Chulalongkorn University, Bangkok 10330, Thailand

Complete contact information is available at:

<https://pubs.acs.org/10.1021/acs.jnatprod.3c00107>

Author Contributions

V.K. and A.D. equally contributed to the paper. B.S. and C.B. conceived and designed the project. V.K. and A.D. performed all in vitro experiments and analysis of flow cytometry data. C.B. designed the antibody panels for mass cytometry. C.W., M.L., V.K., and A.D. performed the Ca^{2+} influx experiment. A.D. performed the CyTOF measurement and data analysis. C.O., K.R., and F.P. recruited MS patients and provided access to biomaterials. P.P. and T.R. performed and analyzed absolute configurations using ECD calculations. C.C. and K.L. performed data curation. V.K., A.D., C.B., and B.S. wrote the manuscript.

Notes

The authors declare no competing financial interest.

ACKNOWLEDGMENTS

This research project is supported by Second Century Fund (C2F), Chulalongkorn University, to V.K., P.P., and B.S. and funded by Thailand Science Research and Innovation Fund Chulalongkorn University (CU_FRB65_heal (57) 066_33_10). V.K. is grateful to C2F for a conducting research abroad scholarship, Chulalongkorn University for a Ph.D. research abroad. We would also like to acknowledge the assistance of the BIH Cytometry Core Facility (Charité-Universitätsmedizin Berlin, Germany).



3.2 Diverse modulatory effects of bibenzyls from *Dendrobium* species on human immune cell responses under inflammatory conditions

Virunh Kongkatitham^{1,2,¶}, Adeline Dehlinger^{2,¶}, Chatchai Chaotham³, Kittisak Likhitwitayawuid², Chotima Böttcher^{4,*}, Boonchoo Sritularak^{2,5,*}

1 Pharmaceutical Sciences and Technology Program, Faculty of Pharmaceutical Sciences, Chulalongkorn University, Bangkok 10330, Thailand,

2 Department of Pharmacognosy and Pharmaceutical Botany, Faculty of Pharmaceutical Sciences, Chulalongkorn University, Bangkok 10330, Thailand,

3 Experimental and Clinical Research Center, a cooperation between the Max Delbrück Center for Molecular Medicine in the Helmholtz Association and Charité – Universitätsmedizin Berlin, 13125 Berlin, Germany,

4 Department of Biochemistry and Microbiology, Faculty of Pharmaceutical Sciences, Chulalongkorn University, Bangkok 10330, Thailand,

5 Center of Excellence in Natural Products for Ageing and Chronic Diseases, Faculty of Pharmaceutical Sciences, Chulalongkorn University, Bangkok, 10330, Thailand,

¶ These authors contributed equally to this work.

* Corresponding author

Chotima Böttcher, Experimental and Clinical Research Center, Lindenberger Weg 80, 13125 Berlin, Germany.

Tel.: +49 30 450 540 568

E-mail address: chotima.boettcher@charite.de

Boonchoo Sritularak, 254 Phaya Thai Road, Pathum Wan, Department of Pharmacognosy and Pharmaceutical Botany, Faculty of Pharmaceutical Sciences, Chulalongkorn University, Bangkok, Thailand

Tel.: +662 2188356

E-mail address: boonchoo.sr@chula.ac.th

Abstract

Dendrobium plants are widely used in traditional medicine. Their secondary metabolites such as bibenzyls and phenanthrenes show various pharmacological benefits such as immunomodulating effects and inhibitory effects on cancer cell growth. However, our previous study also showed that some of these promising compounds (i.e., gigantol and cypripedin) also induced expression of inflammatory cytokines including TNF in monocytes obtained from human donors. Our findings have raised caution about the use of these compounds in clinical application. Furthermore, the effects of these therapeutic compounds on multiple immune cell types apart from monocytes remain to be evaluated. In this study, we aim to analyze the immunomodulatory effects of seven known bibenzyl compounds purified from *Dendrobium* species in human peripheral blood mononuclear cells (PBMCs). In this study, the immunomodulatory effects of seven known bibenzyls from *Dendrobium* orchids were screened by flow cytometry in LPS-stimulated PBMCs (three biological replications). Annexin V Apoptosis Detection Kit with 7-AAD was used to determine cytotoxicity of the defined active bibenzyls. We use high-dimensional single-cell mass cytometry (CyTOF) to assess immunomodulatory effects and the phosphorylation state of multiple phosphor-proteins of the active compounds on multiple immune cell types. The LPS stimulation exhibited significant increase of TNF expression only in CD14⁺ cells. Two bibenzyls (i.e., moscatilin (**3**) and crepidatin (**4**)) showed significant inhibitory effects in a dose-dependent manner of TNF expression in LPS-stimulated PBMCs. For cytotoxicity staining with Annexin V and 7-AAD, only compound **4** at 20 μ M revealed significant increase in cell death in late apoptosis state. Treatment of LPS-stimulated PBMCs with moscatilin and crepidatin (both at the concentration of 10 μ M) revealed a reduction of NK cells with effector functions, as well as pSTAT5⁺ non-classical monocytes and monocytes expressing co-stimulatory molecule CD86. Our study demonstrated broad immunomodulatory effects of *Dendrobium* compounds on multiple immune cell types, apart from CD14⁺ monocytes. Our findings suggest a broad spectrum of activity on immune responses

of *Dendrobium* compounds, which may lead to effectively therapeutic potential of these compounds in complex disease conditions including inflammation. However, these results could also imply possible adverse effects in diverse immune cell types, and thus a good monitoring is required. To evaluate therapeutic effects as well as adverse effects of such active compounds on multiple human immune cell populations, multi-parameter immune profiling method is required.

Introduction

Orchidaceae is one of the most prominent families of flowering plants with approximately 25,000 species known worldwide (S. Zhang et al., 2018). *Dendrobium* is one of the largest genera in the orchid family with more than 1,500 species and distributed in a wide area including tropical and subtropical Asia and Oceania region (Hou et al., 2017; Zheng et al., 2018). In China, some of the native species of *Dendrobium* have been used in the tradition Chinese medicine and have become a big plant industry (Cheng et al., 2019). In China, *Dendrobium*, known as "Shihu", is also used as functional food in many dietary supplements such as Shihu wine and Fengdou Shihu (Liu et al., 2015). Secondary metabolites from *Dendrobium* such as flavonoids, bibenzyls, phenanthrenes, alkaloids and sesquiterpenoids have been reported to provide various pharmacological activities, for instance, anti-inflammatory, antioxidant, antiangiogenic, anticancer, antimicrobial, neuroprotective and immunomodulatory activities (Busaranon et al., 2016; Chanvorachote et al., 2013; He et al., 2020; Khoonrit et al., 2020; Lam et al., 2015; Teixeira da Silva & Ng, 2017; Treesuwan et al., 2018; Unahabhokha et al., 2016; Wang, 2021b). However, these studies were mostly performed in cell lines or animal models. Very few were performed using primary human cell culture, for example, a study of immunomodulatory effects of a bibenzyl compound (i.e., 4,5-dihydroxy-3,3',4'-trimethoxybibenzyl) isolated from *D. lindleyi* Steud. in CD14⁺ monocytes under inflammatory conditions (Khoonrit et al., 2020). Furthermore, we have previously shown that gigantol and cypripedin could also induce the expression of inflammatory

cytokines TNF and IL-6 in monocytes, suggesting also adverse effects of these compounds on primary human immune cells. Therefore, the evaluation of both therapeutic potential and mechanism of action as well as potential adverse effects of natural active compounds in human system is required before an application in clinical settings.

Inflammation is a defense mechanism against various stimuli such as pathogens, toxic substances or damaged cells (Medzhitov, 2010). During the inflammatory response, innate immune cells including dendritic cells (DCs), neutrophils, monocytes and macrophages interact with exogenous or endogenous molecules to mediate inflammation (Nowarski et al., 2013). These cells express receptors such as Toll-like receptors 9 (TLR9) which recognize DNA from damaged tissues, known as danger-associated molecular patterns (DAMPs), or TLR4 for pathogen-associated molecular patterns (PAMPs) such as lipopolysaccharide (LPS) (Chen et al., 2018; Mogensen, 2009; Roh & Sohn, 2018). LPS, an outer membrane substance of gram-negative bacteria, is widely used as a model for inflammatory conditions (Ngkelo et al., 2012). LPS is bound to CD14, a glycosylphosphatidylinositol (GPI)-linked surface protein which is mostly expressed on myeloid cells and transferred to TLR4 complex. This interaction activates various intracellular signaling responses resulting in the promotion of expression of inflammatory cytokines such as tumor necrosis factor (TNF), interleukin-2 (IL-2) and interferon- γ (IFN- γ) (Ciesielska et al., 2021; Płóciennikowska et al., 2015; Ramírez-Pérez et al., 2020). LPS stimulation induces the production of inflammatory mediators via intracellular phosphor-molecules such as phosphorylated extracellular signal-regulated kinase 1/2 (pERK1/2), phosphorylated signal transducer and activator of transcription 1 and 5 (pSTAT1 and pSTAT5) (Phongpreecha et al., 2020).

In this study, we screened the potential immunomodulatory and anti-inflammatory effects of seven known bibenzyls from *Dendrobium* plants on multiple human immune cells. We demonstrated herein decreased inflammatory responses of LPS-treated CD14⁺ monocytes, demonstrated by the reduction of inflammatory

cytokine TNF. Further deep immune profiling showed that the natural active compounds also modulated (apart from CD14⁺ monocytes) the LPS-induced responses of non-classical monocytes and nature killer cells. Finally, we also reported here potential modulation of the active compounds on the human immune cells in non-inflammatory conditions.

Materials and methods

Plant materials

The whole plants of *Dendrobium scabrilingue* Lindl., *Dendrobium capillipes* Rchb.f., *Dendrobium secundum* (Blume) Lindl. and *Dendrobium signatum* Rchb. f. were purchased from Jatuchak market, Bangkok (Mittraphab et al., 2016; Phechrmeekha et al., 2012; Sarakulwattana et al., 2020). *D. scabrilingue* was identified by one of authors (B.S.) (Sarakulwattana et al., 2020). *D. secundum* and *D. capillipes* were identified by comparison with the authentic samples (BKF Nos 110498 and 114946 for *D. secundum* and *D. capillipes*, respectively) (Phechrmeekha et al., 2012) and *D. signatum* was authenticated by a comparison with herbarium specimens at the Department of National Park, Wildlife and Plant Conservation, Ministry of National Resources and Environment (Mittraphab et al., 2016). The voucher specimens of *D. scabrilingue* (BS-DScab-12255), *D. secundum* (DS/BS-092552), *D. capillipes* (DC-082553) and *D. signatum* (BS-DS-102555) have been deposited at the Department of Pharmacognosy and Pharmaceutical Botany, Faculty of Pharmaceutical Sciences, Chulalongkorn University (Mittraphab et al., 2016; Phechrmeekha et al., 2012; Sarakulwattana et al., 2020).

Compounds and reagents

Seven bibenzyls [Figure 19] were isolated from *Dendrobium* plants. The ethyl acetate (EtOAc) extract from *Dendrobium scabrilingue* Lindl. was subjected to vacuum-liquid chromatography (VLC) over silica gel using EtOAc-hexane, gradient to give 8 fractions (A-H). Fraction D was fractionated by column chromatography (CC) on silica gel (EtOAc-hexane, gradient) to obtain 14 fractions (DI-DXIV). Fraction DIX was

purified by Sephadex LH-20 (MeOH) and then separated by CC (silica gel, EtOAc-CH₂Cl₂, gradient) to give batatasin III (**1**). Aloifol I (**7**) was obtained from fraction DX after purification on Sephadex LH-20 (MeOH) and CC (silica gel, CH₂Cl₂) (Sarakulwattana et al., 2020). The methanol (MeOH) extract from *Dendrobium secundum* was separated by VLC over silica gel (EtOAc-hexane and MeOH-CH₂Cl₂, gradient) to give 8 fractions (A-H) Fraction G was fractionated by VLC on silica gel (MeOH-CH₂Cl₂, gradient) to obtain six fractions (G1-G6). Fraction G4 was further separated by CC (silica gel, acetone-CH₂Cl₂, gradient) and purified by CC (EtOAc-hexane, gradient) to yield 4,5,4'-trihydroxy-3,3'-dimethoxybibenzyl (**2**) (Phechrmeekha et al., 2012). The MeOH extract from *Dendrobium capillipes* was subjected to VLC on silica gel (MeOH-EtOAc-CH₂Cl₂, gradient) to give 7 fractions (I-VII). Fraction IV was fractionated by VLC over silica gel (EtOAc-hexane, gradient) to obtain 13 fractions (IV-A to IV-J). Fraction IV-J was separated by CC (silica gel, acetone-petroleum ether, gradient) and further purified on Sephadex LH-20 (MeOH-CH₂Cl₂, 1:1) to yield crepidatin (**4**). Moscatilin (**3**) and chrysotoxine (**5**) were obtained from fraction V after separation by VLC over silica gel using gradient elution of MeOH-EtOAc-CH₂Cl₂-hexane, further separation by CC (silica gel, acetone-CH₂Cl₂, gradient) and purification on Sephadex LH-20 (acetone) (Phechrmeekha et al., 2012). The EtOAc extract from *Dendrobium signatum* Rchb. f. was subjected to VLC on silica gel (acetone-hexane, gradient) to give 8 fractions (A-H). 3,4-Dihydroxy-5,4'-dimethoxybibenzyl (**6**) was yielded from fraction E after fractionation by CC (silica gel, acetone-hexane, gradient) and purification on Sephadex LH-20 (acetone) (Mitrphab et al., 2016). Dimethyl sulfoxide (DMSO), LPS and brefeldin A were purchased from Sigma Aldrich (St. Louis, MO, USA). Roswell Park Memorial Institute (RPMI) 1640, fetal bovine serum (FBS), phosphate buffered saline (PBS), SMART TUBE INC Proteomic Stabilizer and 16% w/v formaldehyde (FA) were purchased from Thermo Fisher Scientific Inc. (Rockford, IL, USA). Anti-human antibodies were purchased pre-conjugated to metal isotopes (Fluidigm) or conjugated in house following the manufacturer's protocol by using the MaxPar X8 kit (Fluidigm).

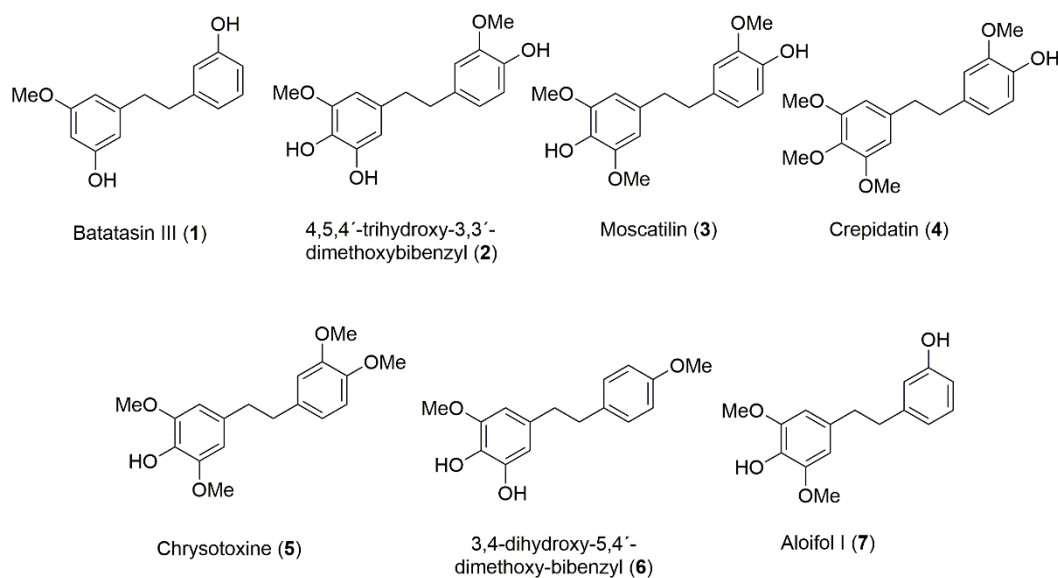


Figure 19 Chemical structures of seven known bibenzyls from *Dendrobium* plants.

Ethics and cells

This study was approved by the Ethics Committee of Charité – Universitätsmedizin Berlin. Buffy coats from three healthy blood donors were obtained from the German Red Cross (GRC) for research use. Human PBMCs were isolated, aliquoted at 20×10^6 cells/mL and were cryopreserved in liquid nitrogen tank, as described in the previous study (Khoonrit et al., 2020).

LPS stimulation in human PBMCs

Frozen PBMCs were resuspended in RPMI 1640 medium with 10% FBS and cell concentration was adjusted to 20×10^6 cells/mL. Cells were plated in an ultralow-attachment 96-well plate (Corning, New York, USA) at a density of 5×10^5 cells per well. Four different concentrations of compounds were then added to the corresponding well. For cell stimulation, a final concentration of 100 ng/mL of LPS was added into the cultured cells. After a 2 h incubation, a total concentration of 10 μ g/mL of brefeldin A was added into the wells and further incubated for another 2 h. Cells were then harvested into 1.5 mL microtubes and washed with PBS. Finally,

cells were resuspended in 10% BSA and incubated with SMART TUBE INC Proteomic Stabilizer for 12 min at RT. Stabilized cells were stored at -80 °C before staining.

Flow cytometry

Cells were thawed, washed twice and transferred into 1.5 mL microtubes. Cells were incubated in FcR-blocking buffer (1:100; Miltenyi Biotec, Bergisch Gladbach, Germany) at 4 °C for 10 min to block unspecific antibodies binding to Fc receptors. Cells were incubated for 20 min at 4 °C with fluorochrome-conjugated extracellular antibodies for CD3 (APC, HIT3a, Biolegend), CD14 (FITC, RMO52, Beckman Coulter), CD19 (PE, HIB19, Biolegend) and HLA-DR (APC/Cy7, L243, Biolegend) diluted in staining buffer (0.5% BSA in PBS containing 2 mM EDTA). Cells were washed with staining buffer and were then fixed with 2% methanol-free FA at 4 °C for 30 min. After washing with staining buffer, cells were incubated for 30 min at 4 °C with fluorochrome-conjugated antibodies for intracellular proteins including TNF (brilliant violet, MAb11, Biolegend), IL-2 (PerCP/Cy5.5, MQ1-17H12, Biolegend) and IFN- γ (PE/Cy7, 4S.B3, Biolegend) diluted in permeabilization buffer (eBioscience, California, USA). Furthermore, cells were washed with staining buffer and were fixed with 4% methanol-free FA at 4 °C for 10 min, then washed with staining buffer and centrifugated at 600 x g at 12 °C for 5 min. Subsequently, pellets were resuspended in staining buffer and were acquired on BD CANTO II flow cytometer (BD Biosciences, New Jersey, USA) with software BD DIVA version 8.1. Data analysis was performed using FlowJo software version 10.1 (Ashland, OR, USA).

CyTOF measurement

For phosphoproteins measurement, cells were incubated with 100 ng/mL of LPS for 15 min. Cells were incubated with Cisplatin-¹⁹⁵Pt (1:3000) for 1 min at RT and then fixed with 16% methanol-free FA. Cells were harvested into 1.5 mL microtubes and washed with PBS. Finally, cells were resuspended in 10% BSA and incubated with SMART TUBE INC Proteomic Stabilizer for 12 min at RT. Stabilized cells were

stored at -80°C before staining. Cells were stained and analysed according to our standard protocol (Linsley & Ledbetter, 1993).

Intracellular Barcoding

After fixation and storage at -80°C , cells were thawed and subsequently stained with premade combinations of the palladium isotopes ^{102}Pd , ^{104}Pd , ^{105}Pd , ^{106}Pd , ^{108}Pd and ^{110}Pd (Cell-ID 20-plex Pd Barcoding Kit, Fluidigm). Each sample received a unique combination of three different palladium isotopes. Therefore, it was possible to generate up to twenty different unique barcodes. One sample did not receive a barcode allowing to increase the sample size to 21 samples. Cells were stained with the barcodes for 30 min at RT and then washed twice with cell staining buffer. The 21 samples were pooled together, washed and further stained with antibodies.

Antibody staining

Samples were pooled, then resuspended in 50 μL of antibody cocktail against surface markers and incubated for 30 min at 4°C . Cells were washed twice with staining buffer and subsequently fixed overnight with 2% methanol-free FA solution. Fixed cells were washed with staining buffer, then permeabilized with 100 μL ice-cold methanol for 10 min at 4°C . Cells were washed twice in staining buffer and resuspended with 100 μL of antibody cocktail against phosphor-protein markers. After 30 min of incubation at RT, samples were washed twice with staining buffer and resuspended in 1 mL of iridium mix (1:1000 Iridium in PBS containing 2% FA) for 30 min at RT. Cells were washed twice with staining buffer and kept at 4°C until CyTOF measurement. All antibodies used are listed in **Table 13**.

Mass cytometry data processing and analysis

Initial manual gating of $\text{CD}45^+\text{DNA}^+$ and gating out of $\text{CD}3^+\text{CD}19^+$ cells and debarcoding according to the barcode combination were performed on FlowJo. De-

barcoded samples were exported as individual FCS files for further analysis. Using the R package CATALYST, each file was compensated for signal spillover. Using FlowJo, dead cells, which are Cisplatin⁺, were gated out and FCS files were exported. For further analysis, we used previously described scripts and workflows. We created multi-dimensional scaling (MDS) plots on median marker expression from all markers for first evaluation of the overall similarities between samples and conditions. In order to perform unsupervised clustering, we used the FlowSOM/ConsensusClustserPlus algorithms of the CATALYST package. We opted for a total number of 20 meta clusters based on the phenotypic heatmaps and the delta area plot. We generated UMAP representations including all markers as input in order to have a dimensionality reduction visualization of the clusters.

Cytotoxicity determined by Annexin V and 7-AAD staining in human PBMCs

Frozen PBMCs were resuspended in RPMI 1640 medium with 10% FBS and cell concentration was adjusted to 20×10^6 cells/mL. Cells were seeded at a density of 5×10^5 cells/10 μ L in each well of an ultra-low attachment 96-well plate. Different concentrations of compounds were then added to the corresponding wells and incubated for 4 h. Cells were harvested, washed and transferred into 1.5 mL microtubes. Cells were subsequently incubated in CD45 antibody (APC, HI30, Biolegend) diluted in staining buffer at 4 °C for 20 min. After washing, cells were resuspended with 100 μ L of Annexin V binding buffer. Cell suspensions were then transferred into new microtubes, and further incubated with Pacific Blue™ Annexin V Apoptosis Detection Kit with 7-AAD (Biolegend) at RT for 15 min in the dark. Annexin V binding buffer was added to each cell suspension. Stained cells were acquired on BD CANTO II flow cytometer (BD Biosciences, New Jersey, USA) with software BD DIVA version 8.1. The obtained data were analysed using FlowJo software version 10.1 (Ashland, OR, USA).

Statistical analysis

Data expressed as the mean \pm standard deviation (SD) were analyzed for statistical significance ($p < 0.05$) using one-way ANOVA with Tukey's test in GraphPad Prism v.9.0 software (San Diego, CA, USA).

Results

Immune modulatory effects of bibenzyls from *Dendrobium* species on primary human immune cells

To evaluate immunomodulatory effects, we first induced inflammatory conditions in human PBMCs using LPS, as previously described (Khoonrit et al., 2020). LPS-stimulated PBMCs were treated with seven known bibenzyl compounds isolated from *Dendrobium* plants including batatacin III (1), 4,5,4'-trihydroxy-3,3'-dimethoxybibenzyl (2), moscatilin (3), crepidatin (4), chrysotoxine (5), 3,4-dihydroxy-5,4'-dimethoxy-bibenzyl (6) and aloifol I (7) were diluted in DMSO. Four known concentrations (1, 5, 10 and 20 μ M) that have been previously investigated were used (Khoonrit et al., 2020; Unahabhokha et al., 2016). In addition, DMSO with the same concentration as the compounds was used as control. After 4 h of LPS stimulation, we determined the specifically increased frequency of TNF-expressing CD14⁺ monocyte population, whereas IL-2 and IFN- γ were detected unchanged, showing specific responses of monocytes to LPS in TNF expression [Figure 20]. We detected significantly decreased frequencies of LPS-induced TNF expression in CD14⁺ monocytes treated with all bibenzyl compounds, except batatacin III (1) [Figure 21]. This effect was not found in other immune cell populations, as well as in DMSO-treated condition. No changes in LPS-induced IL-2 and IFN- γ expression were detected in either monocytes or other immune subsets and DMSO-treated PBMCs. Nevertheless, only two compounds (i.e., moscatilin (3) and crepidatin (4)) exhibited inhibitory effects in a dose-dependent manner and decreased LPS-induced TNF expression significantly at the concentration of 5, 10 and 20 μ M [Figure 21]. Therefore, we selected both compounds 3 and 4 for further investigations.

Table 13 The CyTOF antibody list.

Target	Isotope tag	Clone	Company
CD45	⁸⁶ Y	HI30	Fluidigm
HLADR	¹⁴¹ Pr	L243	BioLegend
CD19	¹⁴² Nd	HIB19	Fluidigm
p53	¹⁴³ Nd	7F5	Fluidigm
CD69	¹⁴⁴ Nd	FN50	Fluidigm
CD4	¹⁴⁵ Nd	RPA-T4	Fluidigm
CD64	¹⁴⁶ Nd	10.1	Fluidigm
pH2AX	¹⁴⁷ Sm	JBW301	Fluidigm
CD16	¹⁴⁸ Nd	3G8	Fluidigm
CD56	¹⁴⁹ Sm	NCAM16.2	BD Biosciences
pSTAT5	¹⁵⁰ Nd	47	Fluidigm
ICOS	¹⁵¹ Eu	C398.4A	Fluidigm
pAKT	¹⁵² Sm	D9E	DVS Science
pSTAT1	¹⁵³ Eu	58D6	Fluidigm
CD3	¹⁵⁴ Sm	UCHT1	Fluidigm
CD11c	¹⁵⁵ Gd	Bu15	BioLegend
CD86	¹⁵⁶ Gd	IT2.2	Fluidigm
pSTAT3	¹⁵⁸ Gd	4/P-Stat3	Fluidigm
CD1c	¹⁵⁹ Tb	L161	BioLegend
CD14	¹⁶⁰ Gd	RM052	Fluidigm
CTLA4	¹⁶¹ Dy	14D3	Fluidigm
CD8	¹⁶² Dy	RPA-T8	Fluidigm
CRTH2	¹⁶³ Dy	BM16	Fluidigm
Ikba	¹⁶⁴ Dy	L35A5	Fluidigm
pCREB	¹⁶⁵ Ho	87G3	DVS Science
pnFkBp65	¹⁶⁶ Er	K10895.12.50	Fluidigm
CCR7	¹⁶⁷ Er	G043H7	Fluidigm
CCR9	¹⁶⁸ Er	L053E8	Fluidigm
CD33	¹⁶⁹ Tm	WM53	Fluidigm
Tbet	¹⁷⁰ Er	4B10	BioLegend
pERK1/2	¹⁷¹ Yb	D13.14.4E	Fluidigm
CX3CR1	¹⁷² Yb	2A9-1	BioLegend
CXCR4	¹⁷³ Yb	12G5	Fluidigm
PD1	¹⁷⁴ Yb	EH12.2H7	Fluidigm
pS6	¹⁷⁵ Lu	N7-548	Fluidigm
CD11b	²⁰⁹ Bi	ICRF44	Fluidigm

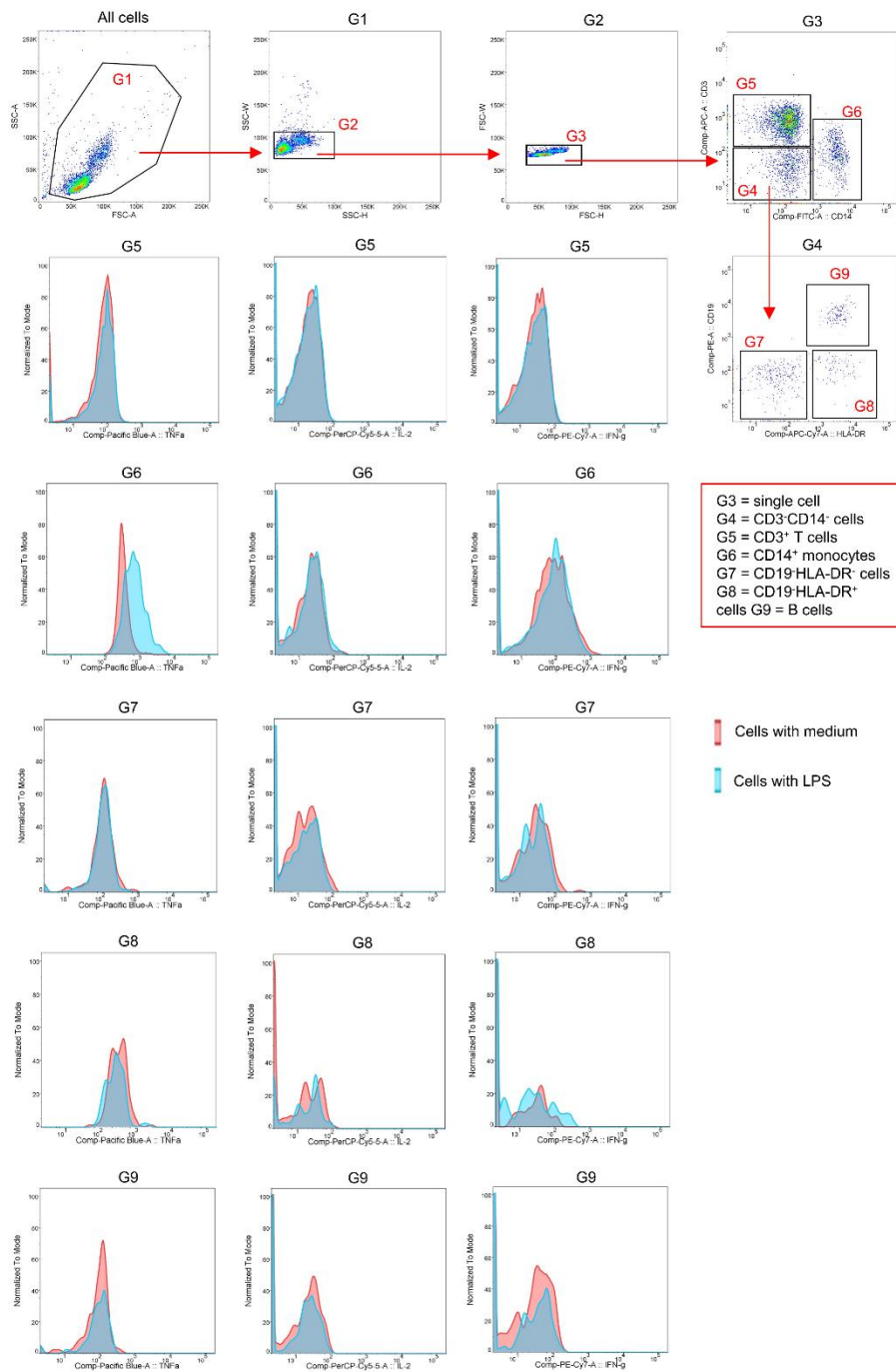


Figure 20 Flow cytometry analysis. Dot plots exhibit gating strategy of human primary T cells (G5), monocytes (G6), CD19⁻HLA-DR⁻ (G7), CD19⁺HLA-DR⁺ (G8) and B cells (G9). The histograms plots show LPS-induced expression of inflammatory cytokines (i.e., TNF- α , IL-2 and IFN- γ) in G5, G6 and G9.

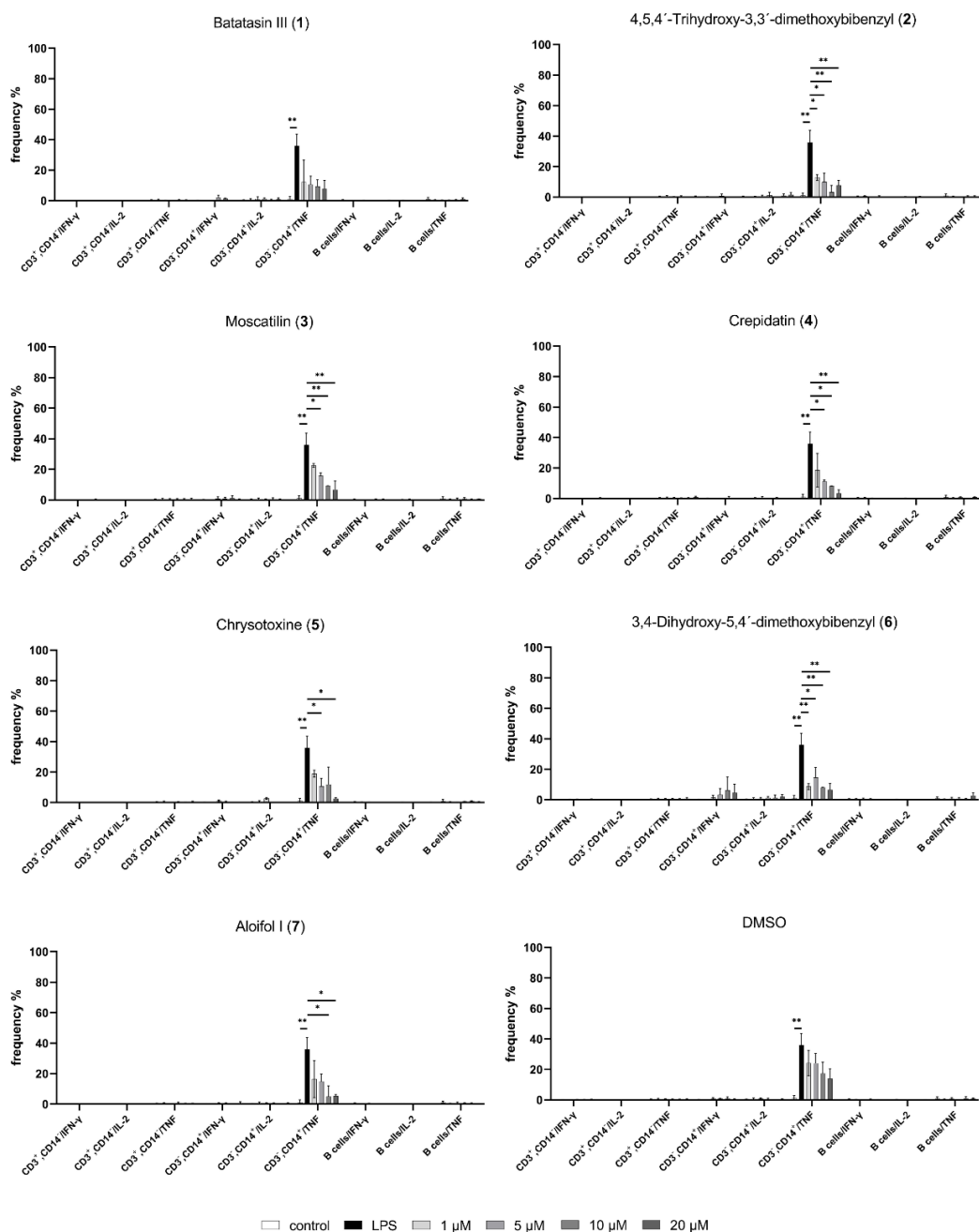


Figure 21 Bar graphs show the mean frequency (%) of inflammatory cytokines (TNF- α , IL-2 and IFN- γ) expression in T cells, monocytes and B cells after 4 h incubation with 1, 5, 10 or 20 μ M seven known bibenzyls with or without LPS stimulation. One-way ANOVA, corrected for multiple comparisons by Tukey Test, *p < 0.05, **p < 0.01.

Investigation of potential cytotoxicity of moscatilin and crepidatin

We next proved whether the immune modulatory effects through inhibition of TNF expression from moscatilin (3) and crepidatin (4) were not caused by cytotoxicity of the compounds resulted in decreased cell number or cell death. To do so, we determine apoptotic states of human PMBCs using the same tested concentrations of DMSO, moscatilin (3) and crepidatin (4) after 4 h co-incubation. No significant increase in cell death in either early or late apoptotic state after treatment with DMSO and moscatilin (3) [Figure 22]. However, we detected significant increase in cell death at late apoptotic state after treatment with 20 μ M of crepidatin (4) [Figure 22]. For further deep immune profiling using mass cytometry, we therefore decided to use the concentration of 10 μ M for both moscatilin and crepidatin.

Deep immune profiling revealed a broad spectrum of immunomodulatory effects of moscatilin and crepidatin

To further characterize the modulatory effects of moscatilin and crepidatin on a wide spectrum of immune cell types, we applied our previously validated immune profiling workflow using CyTOF (Böttcher, Fernández-Zapata, et al., 2019). PMBCs from three healthy donors were incubated with either LPS, an active compound (i.e., moscatilin or crepidatin) or LPS together with an active compound. After 4 hours incubation, we stained the samples with an antibody panel of 37 antibodies including ten phospho-molecule antibodies (i.e., pNFkBp65, pSTAT1, pSTAT3, pSTAT5, CREB, pS6, p53, pH2AX, pAKT, pERK). The antibody panel also allows to determine the major circulating immune cell subsets such as T and B cells, myeloid cells (i.e., monocytes and dendritic cells) and natural killer (NK) cells. As previously described, the acquired CyTOF data were preprocessed (i.e., de-barcoding, compensation and quality control), then clustering analysis was performed using our previously established data analysis workflow [Figure 23A] (Böttcher, Fernández-Zapata, et al., 2019). A total of twenty clusters were identified [Figure 23B and 23C]. The highest cell frequency was detected in cluster 1 and 9 [Figure 23C, lower panel]. Decreased

abundance of CD56⁺CD16⁺Tbet⁺ effector NK cells [cluster 4, **Figure 23D**], CD14⁺CD16⁺CD11c⁺CXCR4⁺ non-classical monocytes [cluster 7, **Figure 23E**] and CD14⁺CD16^{low} monocytes expressing co-stimulatory molecule CD86 [cluster 19, **Figure 23F**] have been detected in LPS-treated PBMCs after the treatment with crepidatin (**4**), compared to LPS-treated PBMCs. Interestingly, non-classical monocytes (cluster 7) were positive for pSTAT5 [**Figure 23G**], thus could be identified as inflammatory monocytes. On the contrary, we couldn't observe these positive effects in moscatilin-treated samples.

Of note, we have observed that the abundance of these three activated clusters were also increased in PBMCs after an incubation with both moscatilin and crepidatin. Nevertheless, one of the three donors showed high abundance of all three activated immune cell types at the baseline (i.e., at “no stimulation” condition), and no changes in immune phenotypes were observed in this donor across conditions. This result suggests possible high variation of immune responses between individuals, which most likely will occur in the real clinical application. Hence, an application of these active compounds or other natural products from *Dendrobium* plants with immunomodulatory effects requires a well monitoring of changes in immune phenotypes.

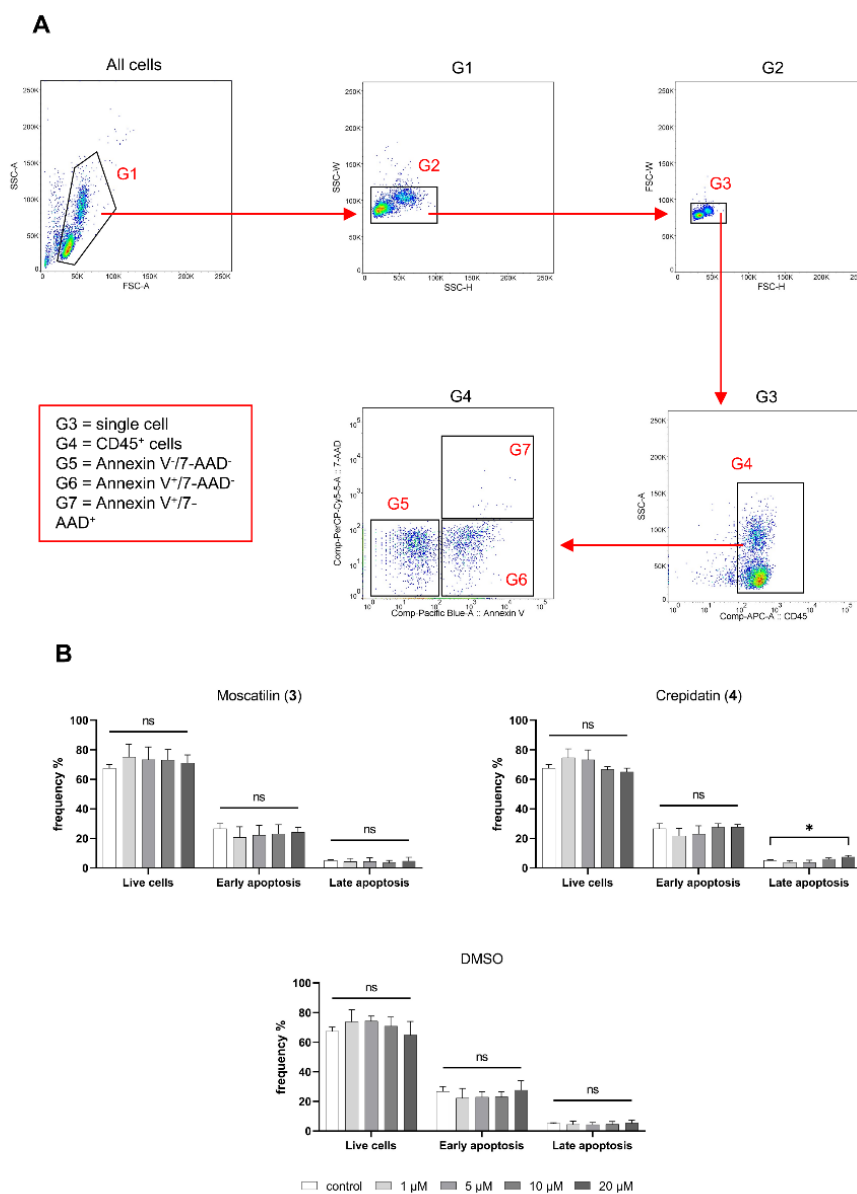


Figure 22 (A) Dot plots demonstrate gating strategy from flow cytometry in cytotoxicity staining with Annexin V and 7-AAD in human PBMCs used to obtain CD45 cells (G4) and determine the apoptosis state including live cells (G5), early (G6) and late apoptosis (G7). (B) Bar graphs show the mean frequency (%) changes of live cells and apoptosis state in human PBMCs treated with bibenzyl compounds **3**, **4** and DMSO, compared with only cells with medium. One-way ANOVA, corrected for multiple comparisons by Tukey Test, * $p < 0.05$.

Discussion

In this study we used LPS-induced PBMCs as a model for studying immunomodulatory activity of isolated known *Dendrobium* bibenzyl compounds. We showed here immunomodulatory effects of moscatilin (**3**) and crepidatin (**4**), indicated by the reduction of TNF expression of CD14⁺ monocytes in dose-dependent manner, suggesting potentially immune modulatory effects of these compounds. The others known bibenzyls including batatasin III (**1**), 4,5,4'-trihydroxy-3,3'-dimethoxybibenzyl (**2**), chrysotoxine (**5**), 3,4-dihydroxy-5,4'-dimethoxy-bibenzyl (**6**) and aloifol I (**7**) were tested in the same condition. However, they showed less dose-dependent inhibitory effects to LPS-induced TNF expression in CD14⁺ monocytes, compared to the compound **3** and **4**. Deep immune profiling using mass cytometry revealed immunomodulatory effects under LPS-induced inflammatory conditions of both moscatilin and crepidatin in multiple immune cell subsets, including effector NK cells, CD86-expressing non-classical monocytes and pSTAT5⁺ monocytes.

In line with our previous study (Khoonrit et al., 2020), these findings confirm a common immunomodulatory effects of *Dendrobium* compounds and further suggest a possible mechanism of action, an inhibition of an activation of phospho-molecule such as STAT5. In the immune modulatory effects test, compound **3** and **4** showed immune modulatory effects which could be related to their structure-activity relationships (SAR). They contain the similar core structure including one hydroxy group at C-4' and three methoxy groups at C-3, C-5 and C-3', suggesting this core structure may be specific as a pharmacophore for inhibition of LPS-induced TNF expression possibly via an activation of STAT5 in monocytes. In addition to reduction of pSTAT5⁺ monocytes, we also detected decreased abundance of Tbet⁺ NK cells in LPS-stimulated cells treated with active compounds. It has been shown that Tbet is an important transcription factor, which is essential for NK cell effector functions including sustained IFN- γ production as well as rapid production of perforin and granzymes for cytolytic activity (Huang & Bi, 2021). Furthermore, CD86-expressing

CD14⁺ monocytes were also found reduced in the presence of active compounds under LPS stimulation. The co-stimulatory molecule CD86 expressed on monocytes is required for activating lymphocytes (Linsley et al., 1994; Linsley & Ledbetter, 1993). CD86 can bind two main receptors present on the surface of T lymphocytes, CD28 and cytotoxic T lymphocyte associated protein 4 (CTLA-4). Binding to CD28 results in T cell activation and can consequently enhance the immune response, whereas binding to CTLA-4 can lead to inhibition of T cell activation, thereby downregulating immunity (Hathcock et al., 1994; Zheng et al., 2004). It remains unclear how moscatilin (3) and crepidatin (4) can regulate T cell function via this CD86-expressing monocyte.

Conclusions

In summary, we have demonstrated herein immunomodulatory effects of bibenzyl compounds from *Dendrobium* species, especially moscatilin (3) and crepidatin (4), on multiple immune cell types, which can consequently result in either the resolution of inflammation or, in the case of imbalance of immune responses, enhancement of inflammation. Therefore, although bibenzyl compounds from *Dendrobium* plants have high therapeutic potentials in treatment of inflammatory diseases or cancer, a well monitoring of immune cell responses apart from therapeutic effects is essential to evaluate the balance between beneficial effects and immune responses.

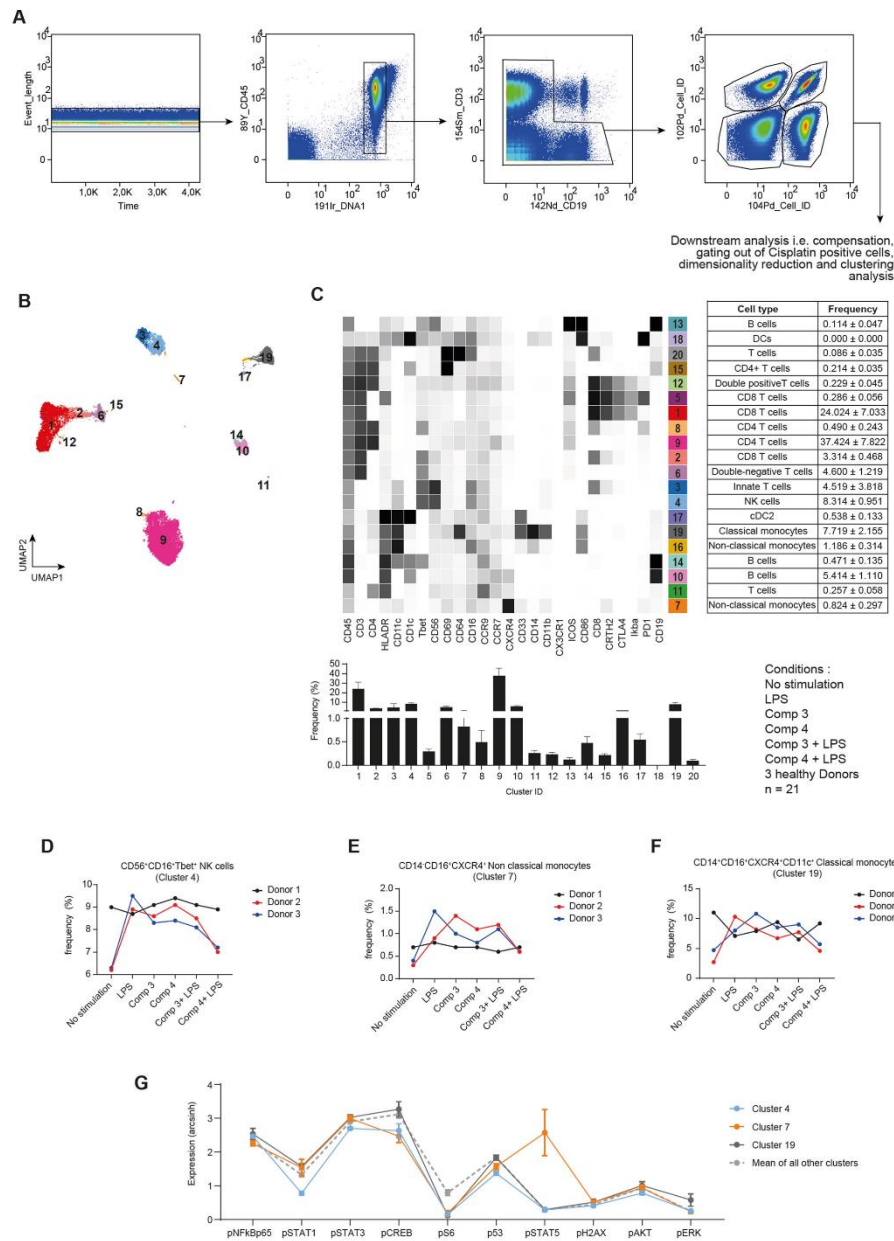


Figure 23 Deep immune profiling using CyTOF. (A) Gating strategy of the CyTOF data and downstream analysis such as selection of CD45⁺ singlets cells, de-barcoding based on Boolean gating of palladium barcodes, selection of cisplatin- cells and clustering. (B) UMAP projection from all samples with 20 individually colored clusters representing diverse immune cell phenotypes, priorly defined by the FlowSOM

algorithm (C) (top left) heatmap cluster illustrating the median expression levels of all markers analyzed with heat colors of expression levels scaled for each marker individually (to the 1st and 5th quintiles) (black: high expression, white: no expression); (top right) Cell type of each cluster and its respective frequency (mean \pm SD); (lower panel) frequency plot (mean \pm SD) of each cluster. (D-F) Frequency plots of differentially abundant clusters i.e., CD56⁺CD16⁺Tbet⁺CD45⁺ NK cells (D), CD14⁺CD16⁺CXCR4⁺ non-classical monocytes (E) and CD14⁺CD16^{low}CD86⁺ monocytes (F) between different PBMC-treated conditions from the three healthy donors. (G) Line graph of the arcsinh marker expression (mean \pm SD) of the phosphor specific markers in each cluster.

Acknowledgments

This research project is supported by Second Century Fund (C2F), Chulalongkorn University to V.K. and B.S. and funded by Thailand Science research and Innovation Fund Chulalongkorn University (CU_FRB65_heal (57)_066_33_10). V.K. is grateful to C2F for conducting research abroad scholarship, Chulalongkorn University for a Ph.D. research abroad. We would also like to acknowledge the assistance of the BIH Cytometry Core Facility (Charité – Universitätsmedizin Berlin, Germany).

Author Contributions

Conceptualization: Chotima Böttcher, Boonchoo Sritularak.

Data curation: Virunh Kongkatitham, Adeline Dehlinger, Chatchai Chaotham, Kittisak Likhitwitayawuid, Chotima Böttcher.

Investigation: Virunh Kongkatitham, Adeline Dehlinger, Chotima Böttcher, Boonchoo Sritularak.

Methodology: Virunh Kongkatitham, Adeline Dehlinger, Chotima Böttcher, Boonchoo Sritularak.

Visualization: Virunh Kongkatitham, Adeline Dehlinger, Chotima Böttcher, Boonchoo Sritularak.

Writing – original draft: Virunh Kongkatitham, Adeline Dehlinger, Chotima Böttcher, Boonchoo Sritularak.

Writing – review and editing: Virunh Kongkatitham, Adeline Dehlinger, Chotima Böttcher, Boonchoo Sritularak.



CHAPTER IV

DISCUSSION

In this dissertation, four new compounds and four known compounds isolated from *D. crumenatum* were demonstrated for anti-inflammation based on immune modulatory activity in human PBMCs. The new phenanthrene derivatives, dendrocruenenols B and D, exhibited the most promising anti-inflammatory effects indicated by inhibition of inflammatory cytokines in both monocytes and T cells of PMA/Iono-treated PBMCs when compared to the other compounds. The inflammatory condition in PBMCs was stimulated by PMA/Ionomycin. PMA stimulation is related to T cells receptor and co-stimulation signaling. It activates several intracellular molecules such as IKK and MAPK, whereas ionomycin activates intracellular Ca^{2+} , calmodulin and calcineurin (Macián et al., 2002). The activation from PMA and ionomycin affects the activation of intracellular inflammatory molecules such as AP-1, NF- κ B and NFAT resulting to promote the production of inflammatory cytokines (Brignall et al., 2017; Macián et al., 2002).

Furthermore, dendrocruenenols B and D showed the similar effects through inhibition of TNF, IL-2 and IFN- γ in only T cells of PMA/Iono-treated PBMCs of MS patients. MS is a chronic inflammatory autoimmune demyelinating and neurodegenerative disease in the human CNS (Dahmardeh & Amirifard, 2018; Huang et al., 2017). The immune cells such as monocytes and macrophages have been proposed to be associated in MS pathology. The pathologies of MS are initiated from infiltration of T helper (Th) 1 and Th17 with specificity for CNS antigens resulting to damage the myelin sheets (Dendrou et al., 2015). From this effect, microglia and infiltrating myeloid cells respond to local inflammatory signals and T cell-derived cytokines, whereas disease emergence and progression are considered to be an outcome of systemic immune deviation, and not intrinsic dysregulation of the CNS. From the previous study, the immune profiling of PBMCs from early MS patient using CyTOF

revealed the imbalanced interactions between T cells, myeloid cells, B cells and their effector and regulatory subpopulations which could affect the disease state and response to treatment of MS (Böttcher, Fernández-Zapata, et al., 2019).

Nevertheless, PMA/Ionomycin induced the inflammation through the activation of intracellular Ca^{2+} level via SOCE pathway. For instance, natural compound, ellagic acid, has been shown to exhibit the reduction of cytokine production via inhibiting SOCE mediated Ca^{2+} influx (Murphy et al., 2020). To prove this SOCE pathway involving the inflammation, thapsigargin was used to permeate the entry of extracellular Ca^{2+} to the cells regulated by ORAI1, STIMs 1 and 2 which associated with the complexation of CRAC channel (Avila-Medina et al., 2018). The changed level of intracellular Ca^{2+} also activates calcineurin to dephosphorylate NFAT which translocate to nucleus resulting to promote the expression of inflammatory cytokines (Hann et al., 2020). The CRAC channel inhibitor, CM4620, from previous study was used as a positive control to block this SOCE pathway (Letizia et al., 2022). The result showed that CM4620 significantly inhibited the Ca^{2+} influx rate in both CD4^+ and CD8^+ T cells, whereas dendrocruenenols B and D showed no different inhibition of Ca^{2+} influx rate in T cells. Therefore, the immune modulatory effects from dendrocruenenols B and D were independent of SOCE pathway. The deep immune profiling of dendrocruenenol D was determine using single-cell CyTOF. The result from CyTOF revealed that the PMA/Ion stimulation increased the frequency of subpopulation of CD161^+ T cells in healthy PBMCs and $\text{CTLA4}^+\text{CRTH2}^+\text{CD8}^+$ T cells in PBMCs from MS patients. In addition, dendrocruenenol D treated with PMA/Iono increased the proportion of $\text{CTLA4}^+\text{CRTH2}^+\text{CD8}^+$ T cells, however it also decreased the frequency of $\text{ICOS}^+\text{CCR7}^+\text{CD4}^+$ T cells in PBMCs from MS patients. This result confirmed the immune modulatory effects of dendrocruenenol D through the reduction of activated T cells population.

Next, the seven known bibenzyl compounds from *Dendrobium* plants were investigated for anti-inflammation based on immune modulatory effects in human PBMCs. LPS was used to stimulate the inflammatory condition in PBMCs. LPS

stimulates the inflammatory response through the activation of TLR4 associated with CD14 monocytes (Ciesielska et al., 2021). The interaction between TLR4 and LPS affects to activate intracellular inflammatory pathways such as MAPK and NF- κ B pathways resulting to promote the expression of inflammatory cytokines (Yesudhas et al., 2014). From this study, two bibenzyls, moscatilin and crepidatin, exhibited the most promising immune modulatory effects through inhibition of TNF-expressed CD14 monocytes in dose-dependent manner in LPS-treated PBMCs. The others bibenzyls also showed these effects but less dose-dependent inhibitory activity. This result also confirmed by the immunomodulatory effects of bibenzyl named 4,5-dihydroxy-3,3',4'-trimethoxybibenzyl from *D. lindleyi* which showed the potent immunomodulatory effects of this bibenzyl from *Dendrobium* species in LPS-treated PBMCs (Khoonrit et al., 2020). In addition, this immunomodulatory effects of bibenzyls could be related to their structure-activity relationships (SAR). The pharmacophore of these two bibenzyls should be one hydroxy group at C-4' and three methoxy groups at C-3, C-5 and C-3' which are the same substitute positions of moscatilin and crepidatin. Furthermore, moscatilin and crepidatin were determined the deep immune profiling using CyTOF. The result from CyTOF showed the decreasing of the frequency of CD56⁺CD16⁺Tbet⁺ NK cells, CD14⁺CD16⁺CD11c⁺CXCR4⁺ non-classical monocytes with effector pSTAT5⁺ and CD14⁺CD16^{low} monocytes expressing co-stimulatory molecule CD86 from the treatment of crepidatin in LPS-treated PBMCs. On the other hand, the treatment of moscatilin in LPS-treated PBMCs did not show this effect. This result confirmed the immune modulatory effects of crepidatin through the reduction of the frequency of NK cells and monocytes.

CHAPTER V

CONCLUSION

In these two studies, first, the EtOAc extract of *Dendrobium crumenatum* Sw. was isolated by chromatographic methods to obtain four new compounds (dendrocruenols A-D) and four known compounds including gigantol [16], 3,7-dihydroxy-2,4,8-trimethoxyphenanthrene, densiflorol B [105], and cypripedin [104]. The isolated compounds from *D. crumenatum* were evaluated for their immunomodulatory effects in human healthy and MS patient's PBMCs. The new compounds dendrocruenols B and D exhibited the most promising anti-inflammatory effects through reduction of TNF and IL-2 production in monocytes and T cells which were treated with PMA/Iono. Moreover, the deep immune profiling of dendrocruenol D using CyTOF revealed the reduction of the population of activated T cells in PMA/Iono-treated PBMCs when compared with untreated control. In the second study, the seven known bibenzyls from *Dendrobium* plants were investigated for their immunomodulatory activity in LPS-treated human PBMCs. The two bibenzyl compounds including moscatilin [21] and crepidatin [8] showed the strongest inhibition of TNF-expressed monocytes in LPS-treated PBMCs when compared to other bibenzyls. Furthermore, the deep immune profiling of crepidatin by CyTOF established the decreasing of NK cells, pSTAT5⁺ non-classical monocytes and monocytes expressing co-stimulatory molecule CD86. Therefore, the phytochemical data from *D. crumenatum* would be the information for the chemotaxonomic study of *Dendrobium* plants. The data of anti-inflammation based on immunomodulatory effects of isolated *D. crumenatum*'s compounds and known bibenzyls from *Dendrobium* plants would be the information to develop the medicine from natural products using for treatment of inflammatory diseases.





Charité | 10117 Berlin

Frau
PD Dr. rer. nat. Chotima Böttcher
Klinik für Psychiatrie und Psychotherapie
CCM

Ethikkommission
Ethikausschuss am Campus Charité - Mitte

Vorsitzender: Prof. Dr. R. Morgenstern

Geschäftsführung: Dr. med. Katja Orzechowski
ethikkommission@charite.de

Korrespondenzadresse: Charitéplatz 1, 10117 Berlin
Tel.: 030 450-517222
Fax: 030 450-517952

<http://ethikkommission.charite.de>

Datum: 21.01.2021

Einzelzell-Atlas des Nervenwassers (Liquor) und des peripheren Bluts
Antragsnummer: EA1/386/20

Sehr geehrter Frau Dr. Böttcher,

der von Ihnen eingereichte Antrag wurde durch den Ethikausschuss CCM der Ethikkommission in der Sitzung am 14.01.2021 beraten.

Die Ethikkommission stimmt dem o.g. Vorhaben zu.

Hinweis: die vorgelegten Dokumente zu Studieninformation und Einwilligung zur Sammlung der Daten und Proben in der Biobank unter dem Ethikvotum EA4/01B/17 entsprechen nicht den aktuellsten Versionen und waren nicht Gegenstand der Beratung.

Die nachfolgend aufgeführte Unterlage war Gegenstand der Beratung:

- Ethikantrag, 25.11.2020

Datenschutzrechtliche Aspekte von Forschungsvorhaben werden durch die Ethikkommission grundsätzlich nur cursorisch geprüft. Dieses Votum ersetzt mithin nicht die Konsultation des zuständigen Datenschutzbeauftragten.

Die Ethikkommission weist darauf hin, dass die ethische und rechtliche Verantwortung für die Durchführung des Forschungsprojektes -vom Beratungsergebnis der Ethikkommission unabhängig- beim Leiter des Forschungsvorhabens und seinen Mitarbeitern verbleibt.

Mit freundlichen Grüßen

Prof. Dr. med. R. Morgenstern
-Vorsitzender-

CHARITÉ - UNIVERSITÄTSMEDIZIN BERLIN
Schumannstr. 20/21 | 10098 Berlin | Telefon +49 30 450-0 | www.charite.de
Bankinstitut | BLZ Bankleitzahl | Konto Kontonummer

Figure 24 Ethical number for studying in human cells.



CCC
RightsLink


Home


Help ▾


Live Chat


Sign in


Create Account



ACS Publications
Most Trusted. Most Cited. Most Read.

Immunomodulatory Effects of New Phenanthrene Derivatives from *Dendrobium crumenatum*

Author: Virunh Kongkatitham, Adeline Dehlinger, Meng Wang, et al

Publication: Journal of Natural Products

Publisher: American Chemical Society

Date: May 1, 2023

Copyright © 2023, American Chemical Society

PERMISSION/LICENSE IS GRANTED FOR YOUR ORDER AT NO CHARGE

This type of permission/license, instead of the standard Terms and Conditions, is sent to you because no fee is being charged for your order. Please note the following:

- Permission is granted for your request in both print and electronic formats, and translations.
- If figures and/or tables were requested, they may be adapted or used in part.
- Please print this page for your records and send a copy of it to your publisher/graduate school.
- Appropriate credit for the requested material should be given as follows: "Reprinted (adapted) with permission from {COMPLETE REFERENCE CITATION}. Copyright {YEAR} American Chemical Society." Insert appropriate information in place of the capitalized words.
- One-time permission is granted only for the use specified in your RightsLink request. No additional uses are granted (such as derivative works or other editions). For any uses, please submit a new request.

If credit is given to another source for the material you requested from RightsLink, permission must be obtained from that source.

BACK
CLOSE WINDOW

Figure 25 Permission for reusing the research article in this dissertation.

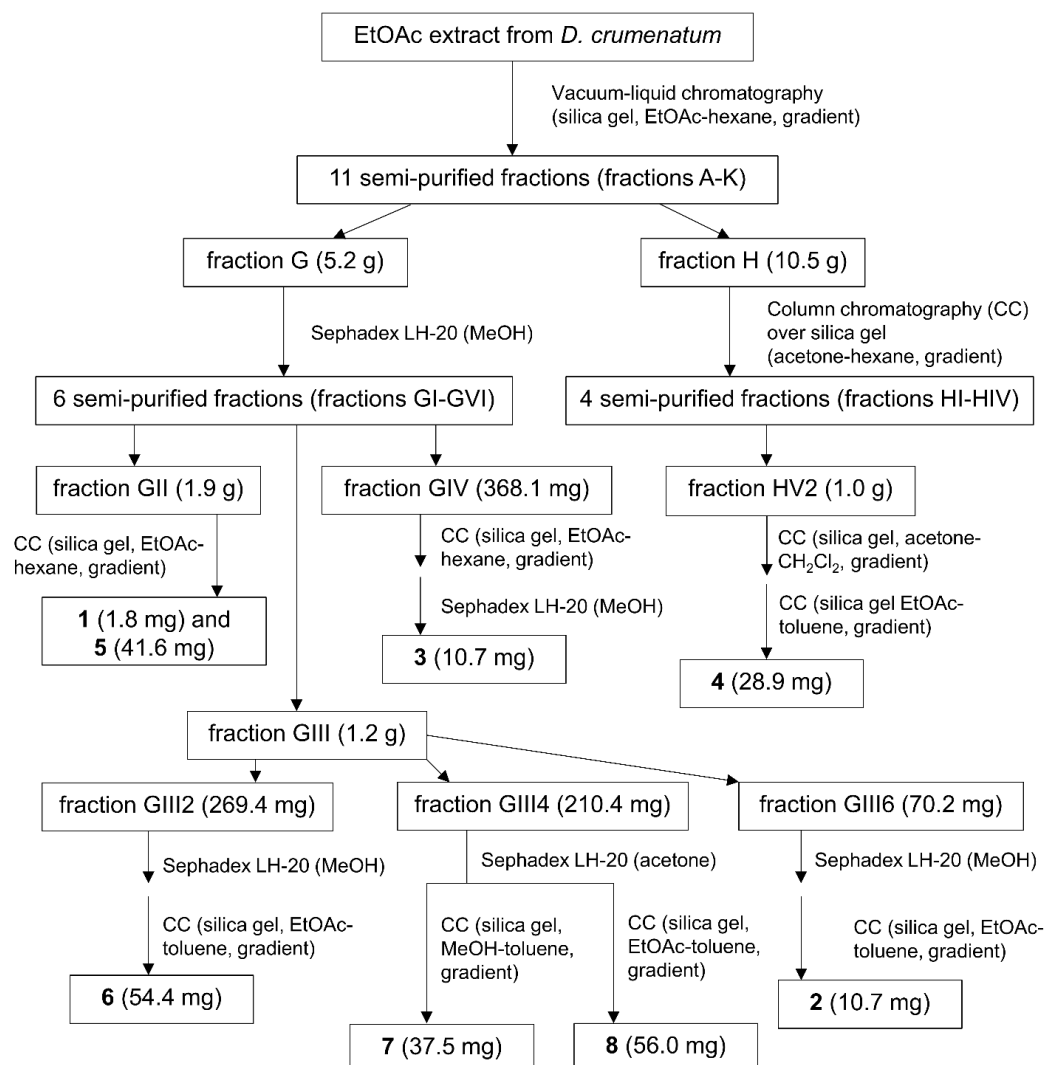


Figure 26 The Flow chart of the extraction steps from *D. crumenatum*.

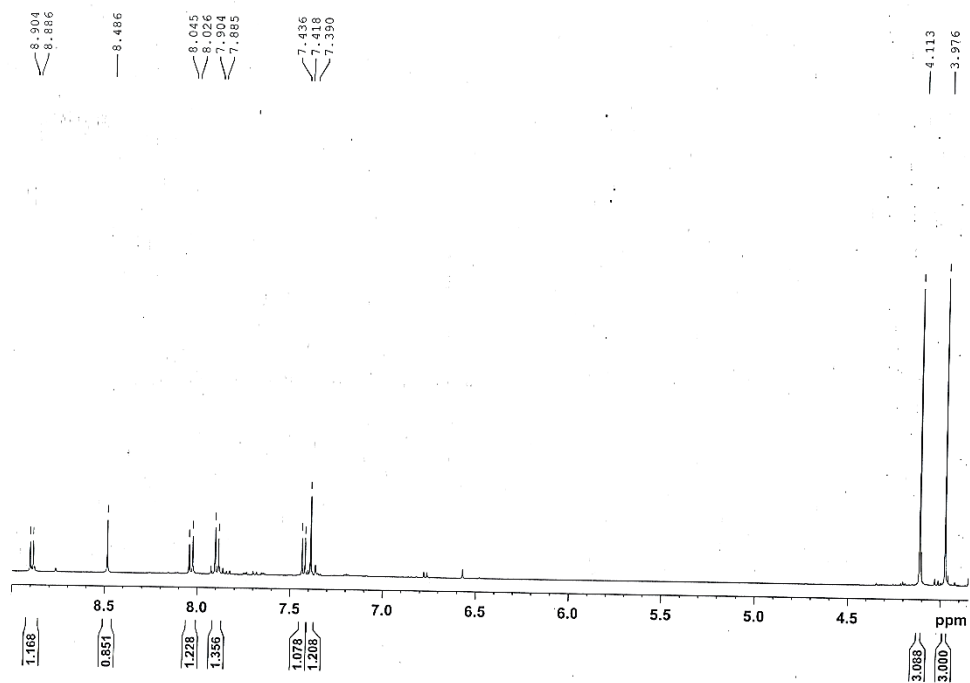


Figure 27 ^1H NMR spectrum of dendrocumenol A (**1**) (500 MHz) in acetone- d_6 .

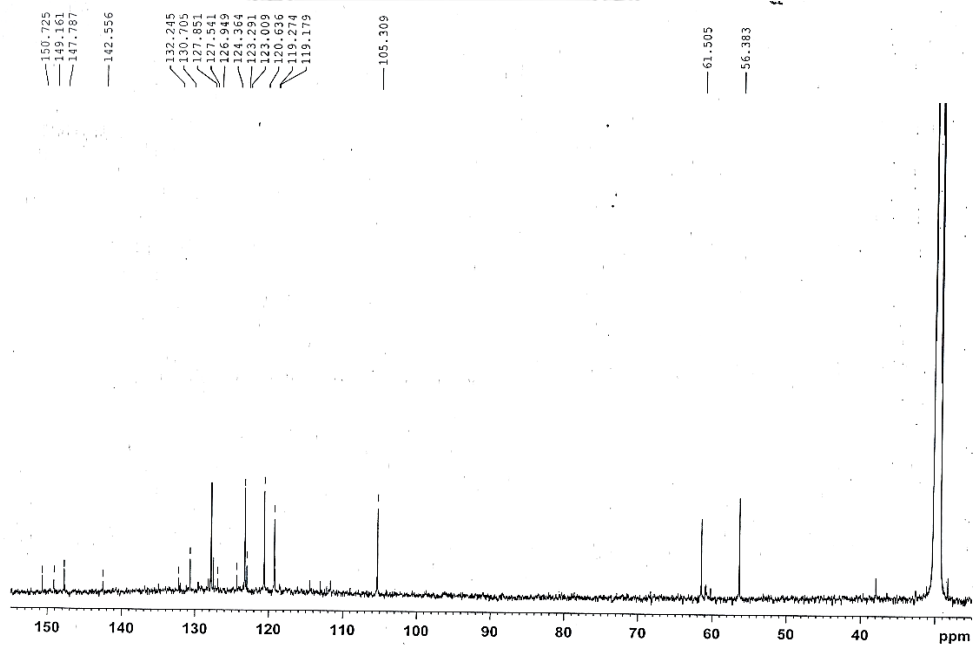


Figure 28 ^{13}C NMR spectrum of dendrocumenol A (**1**) (125 MHz) in acetone- d_6 .

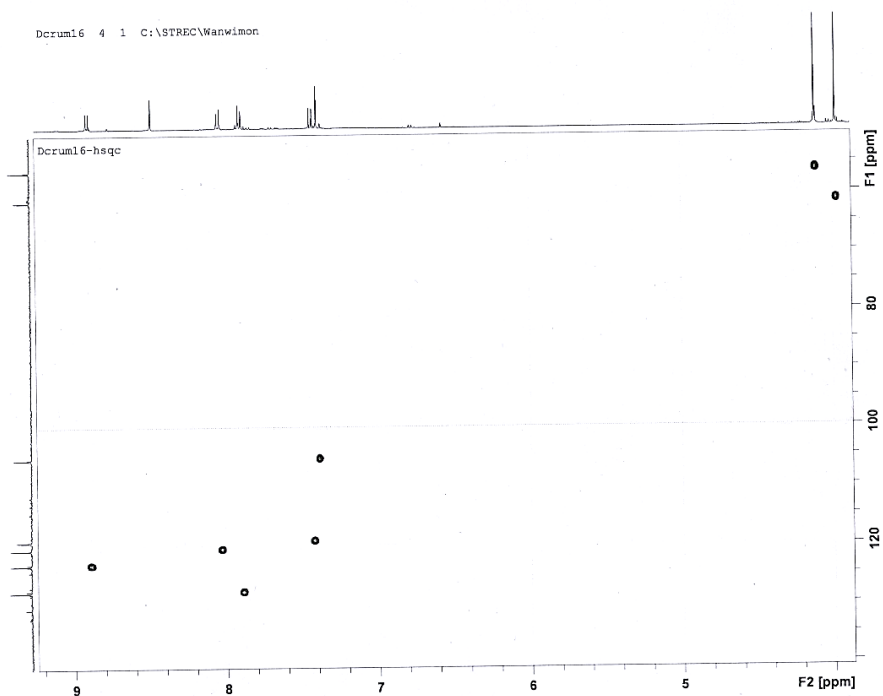


Figure 29 HSQC spectrum of dendrocumenol A (1) in acetone- d_6 .

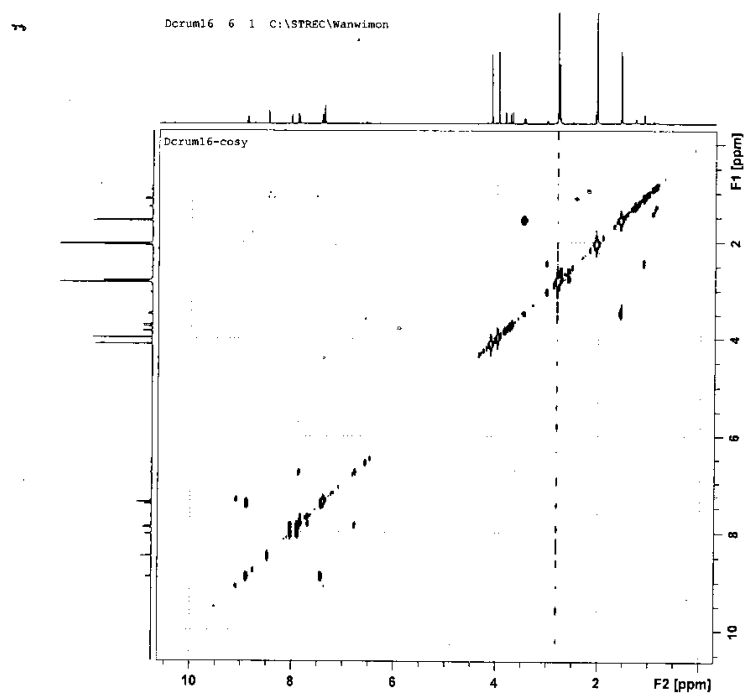


Figure 30 COSY spectrum of dendrocumenol A (1) in acetone- d_6 .

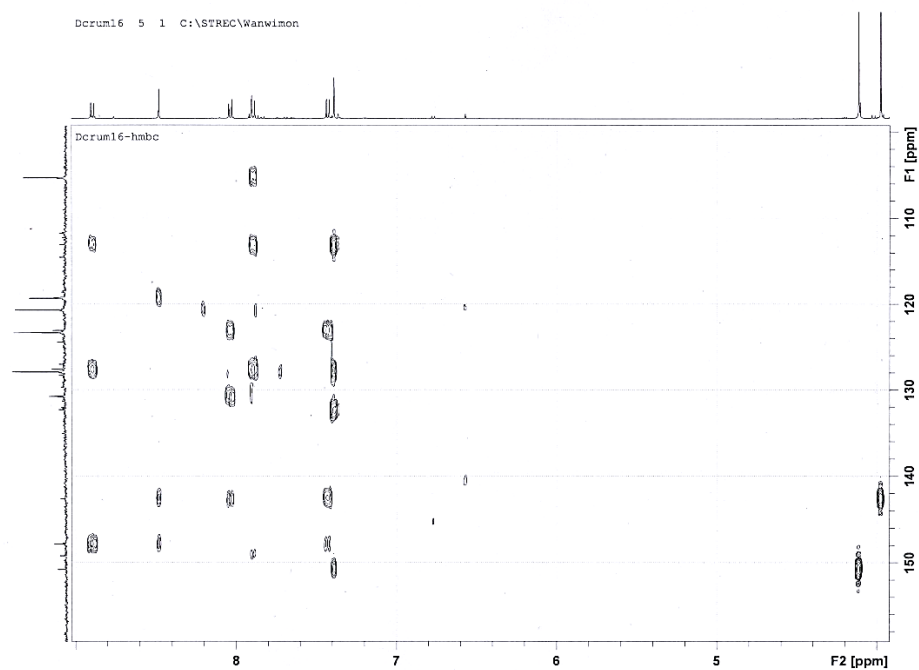


Figure 31 HMBC spectrum of dendrocruenol A (1) in acetone- d_6 .

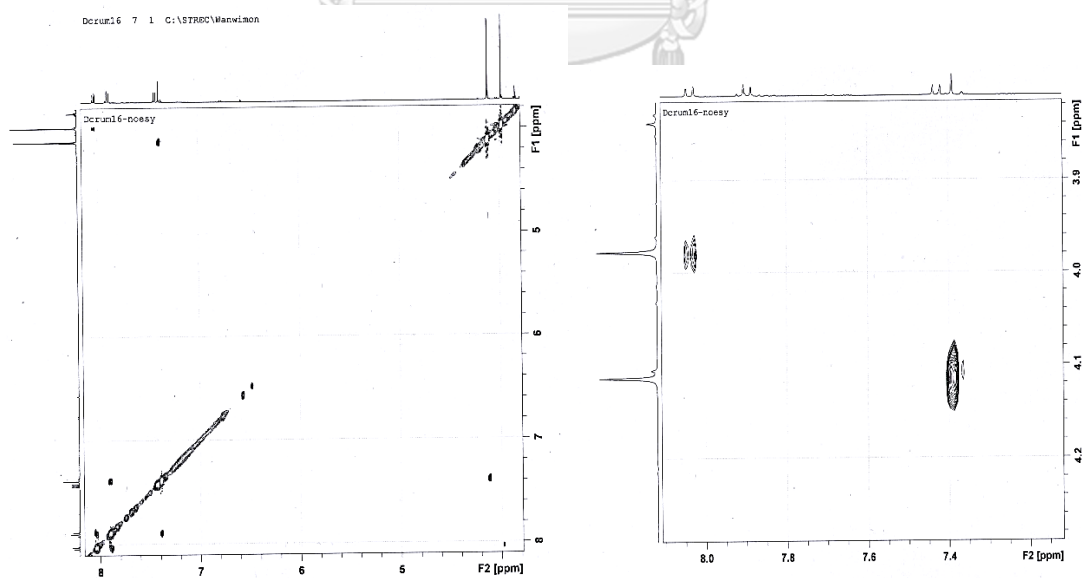


Figure 32 NOESY spectrum of dendrocruenol A (1) in acetone- d_6 .

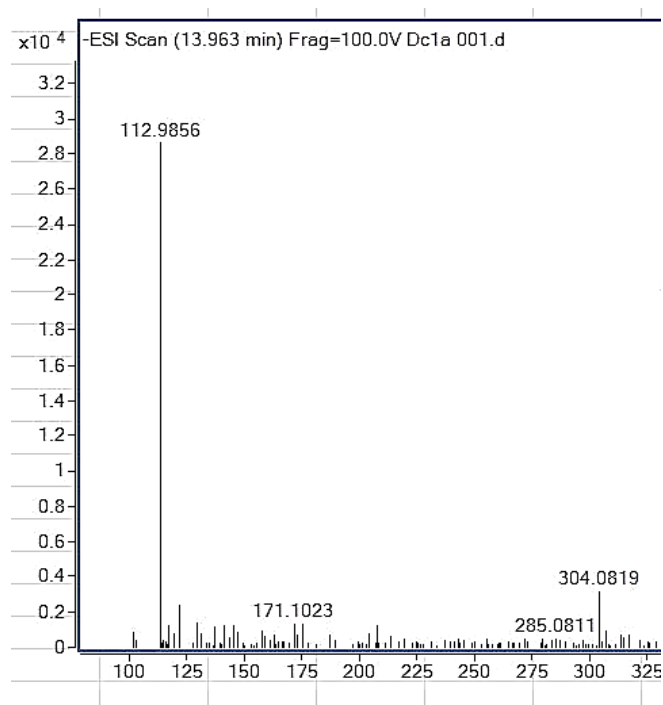


Figure 33 HR-ESI-MS spectrum of dendrocumenol A (1).

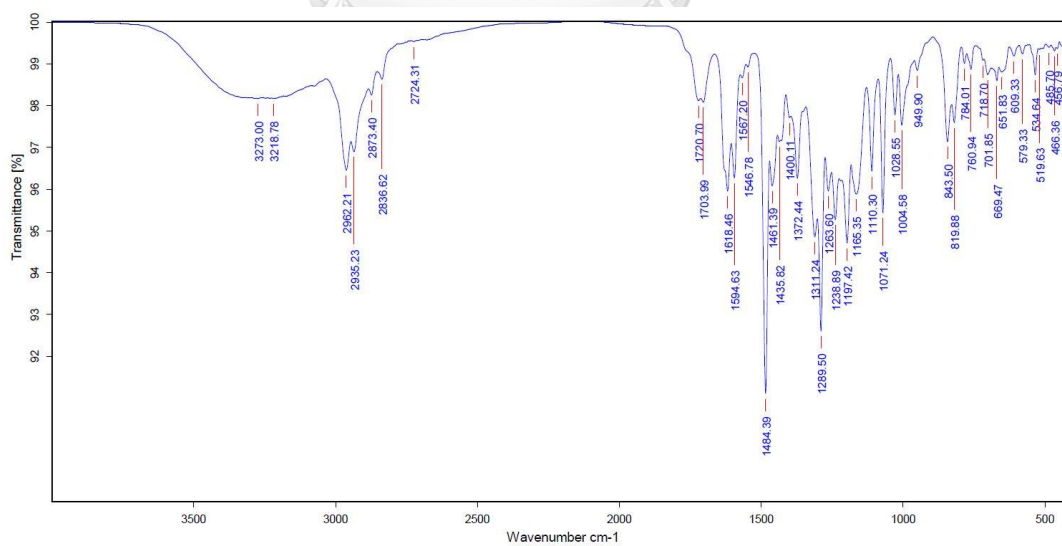


Figure 34 IR spectrum of dendrocumenol A (1).

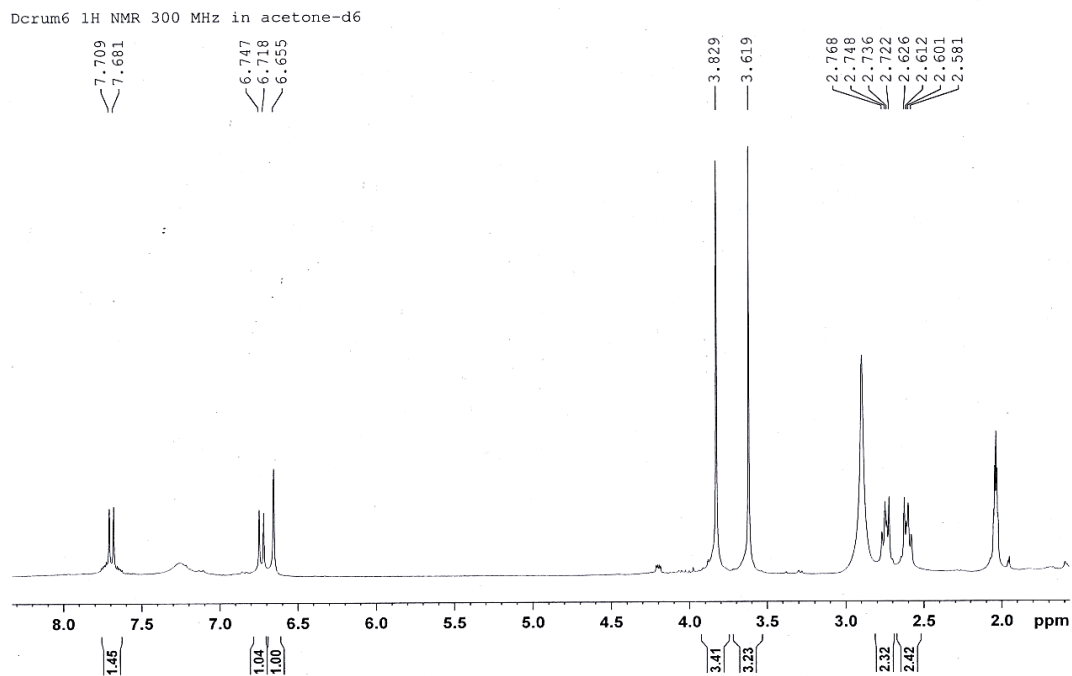


Figure 35 ^1H NMR spectrum of dendrocumenol B (2) (300 MHz) in acetone- d_6 .

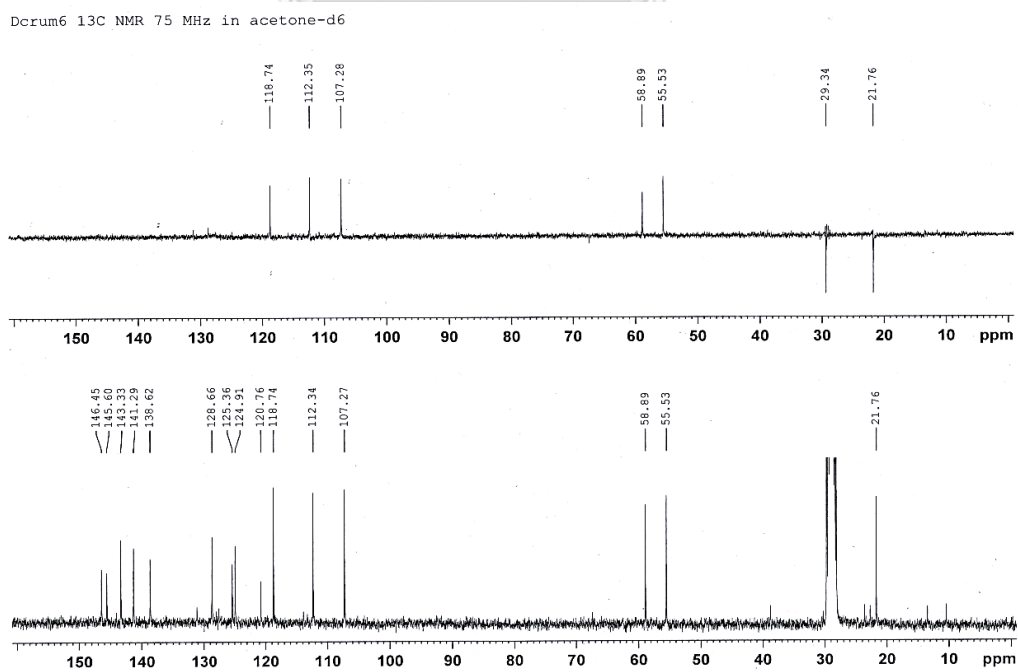


Figure 36 ^{13}C NMR spectrum of dendrocumenol B (2) (75 MHz) in acetone- d_6 .

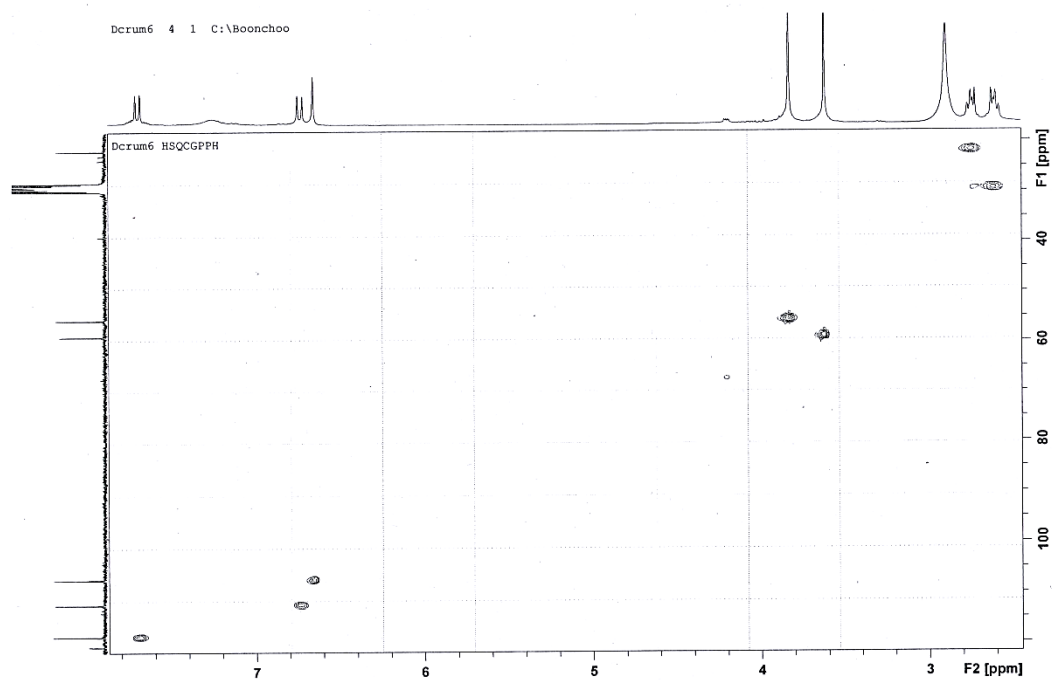


Figure 37 HSQC spectrum of dendrocruenol B (2) in acetone- d_6 .

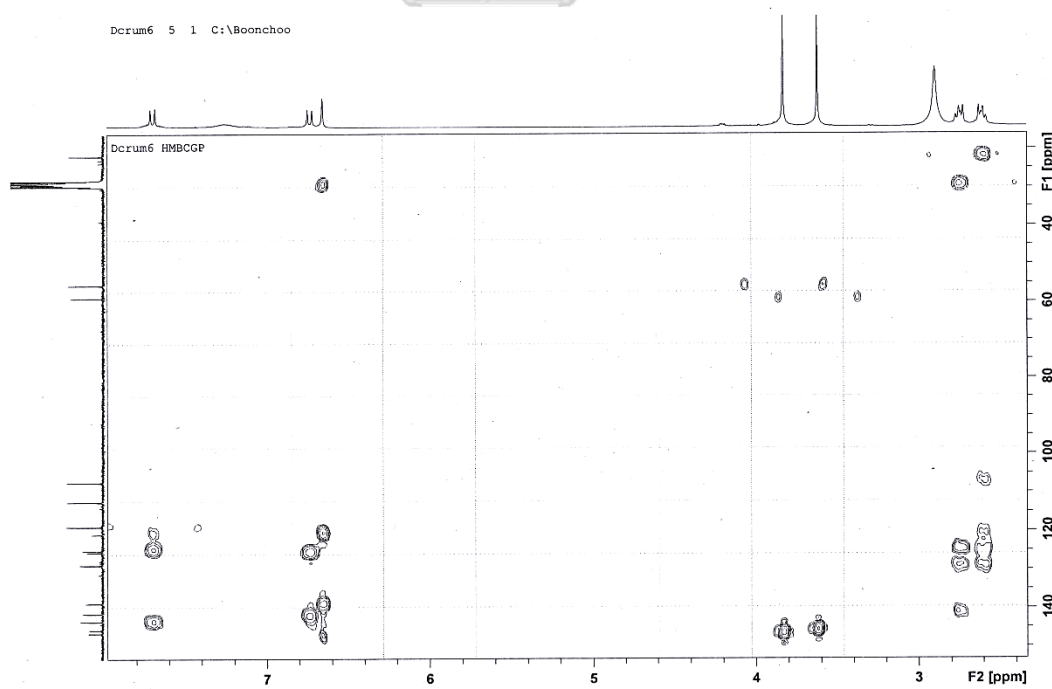


Figure 38 HMBC spectrum of dendrocruenol B (2) in acetone- d_6 .

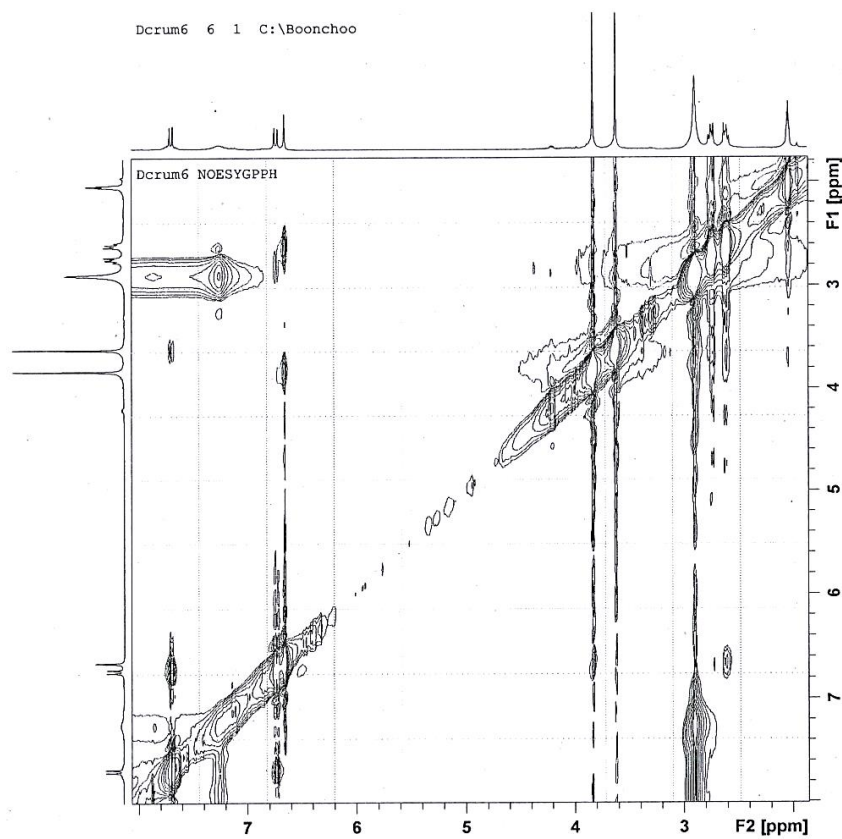


Figure 39 NOESY spectrum of dendrocumenol B (2) in acetone- d_6

Mass Spectrum List Report

Analysis Info

Analysis Name	OSCUHTS06082019003.d	Acquisition Date	8/6/2019 2:39:20 PM
Method	Tune_low_120_04092017.m	Operator	Administrator
Sample Name	Dcrum 6	Instrument	microTOF 72
	06082019		

Acquisition Parameter

Source Type	ESI	Ion Polarity	Positive	Set Corrector Fill	50 V
Scan Range	n/a	Capillary Exit	120.0 V	Set Pulsar Pull	337 V
Scan Begin	50 m/z	Hexapole RF	120.0 V	Set Pulsar Push	337 V
Scan End	3000 m/z	Skimmer 1	60.0 V	Set Reflector	1300 V
		Hexapole 1	23.0 V	Set Flight Tube	9000 V
				Set Detector TOF	2295 V

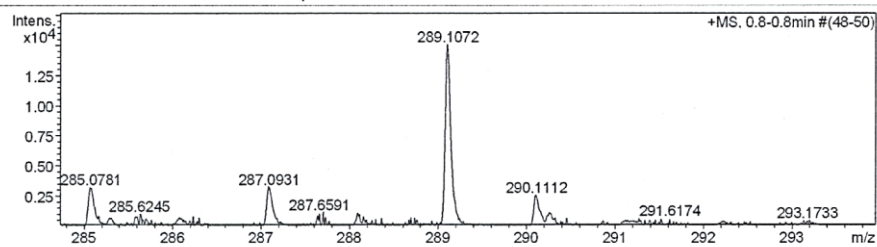


Figure 40 HR-ESI-MS spectrum of dendrocumenol B (2).

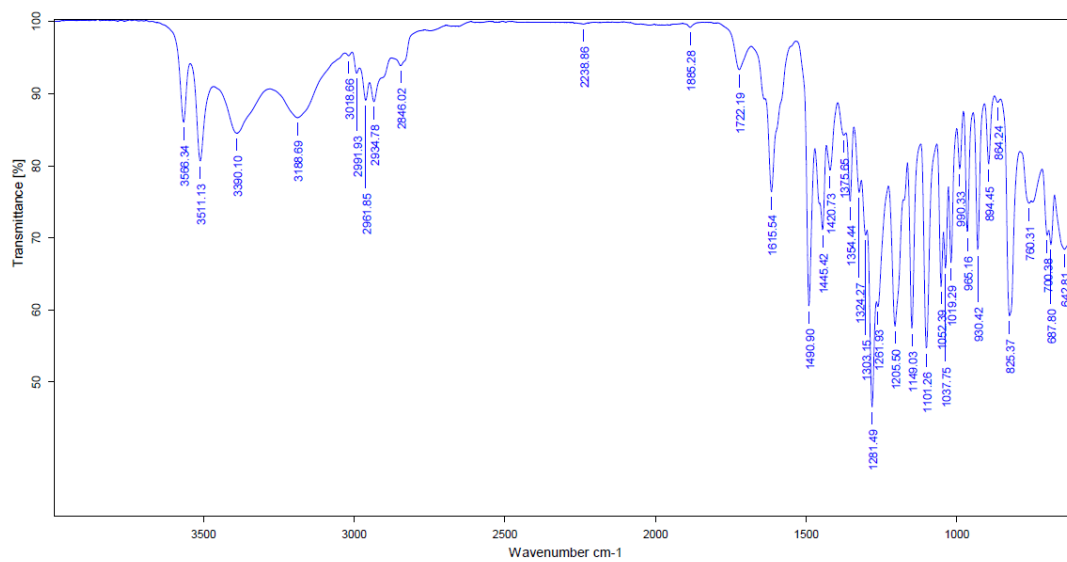


Figure 41 IR spectrum of dendrocumenol B (2).

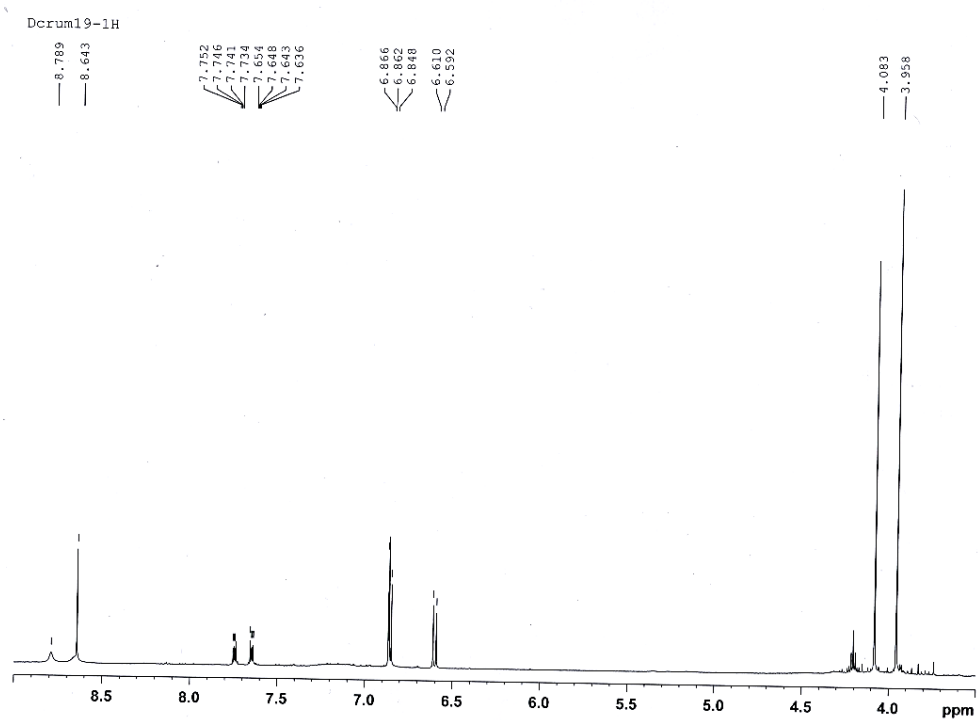


Figure 42 ¹H NMR spectrum of dendrocumenol C (3) (500 MHz) in acetone-*d*₆.

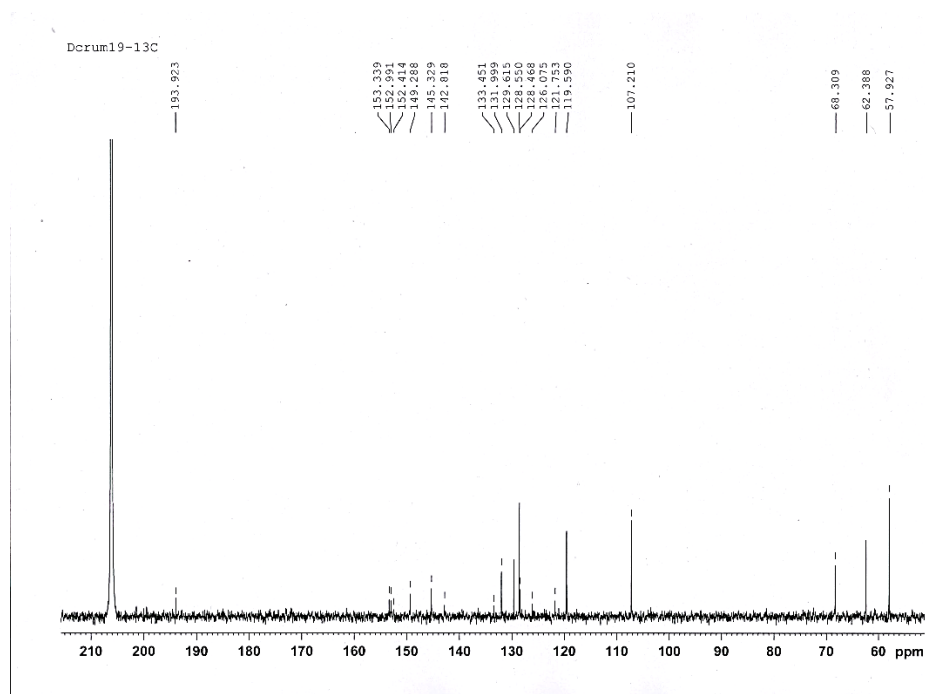


Figure 43 ^{13}C NMR spectrum of dendrocruemol C (**3**) (125 MHz) in acetone- d_6 .

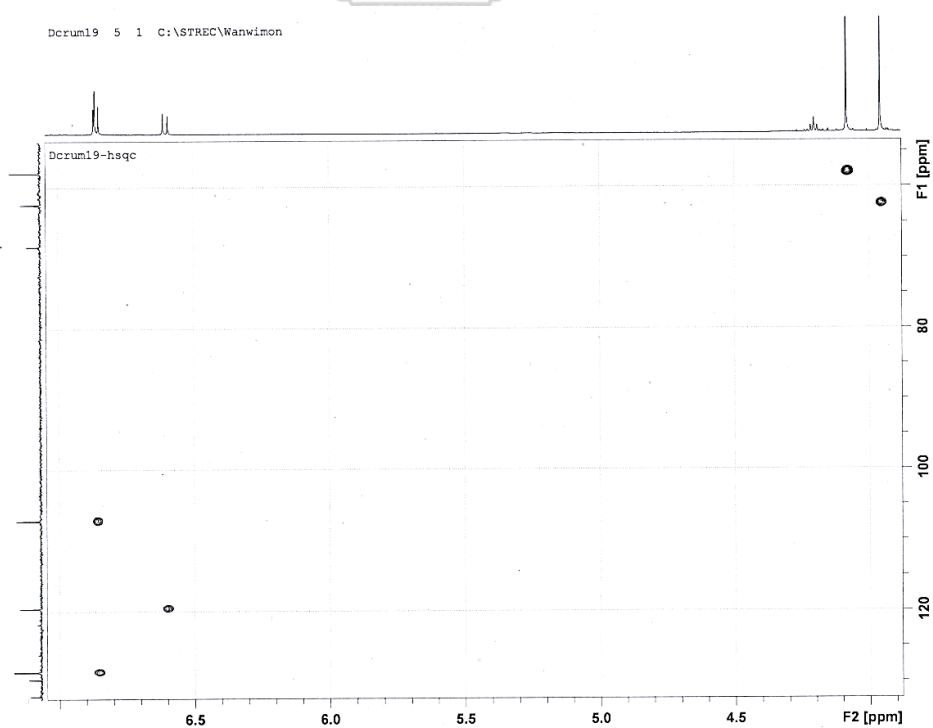


Figure 44 HSQC spectrum of dendrocruemol C (**3**) in acetone- d_6 .

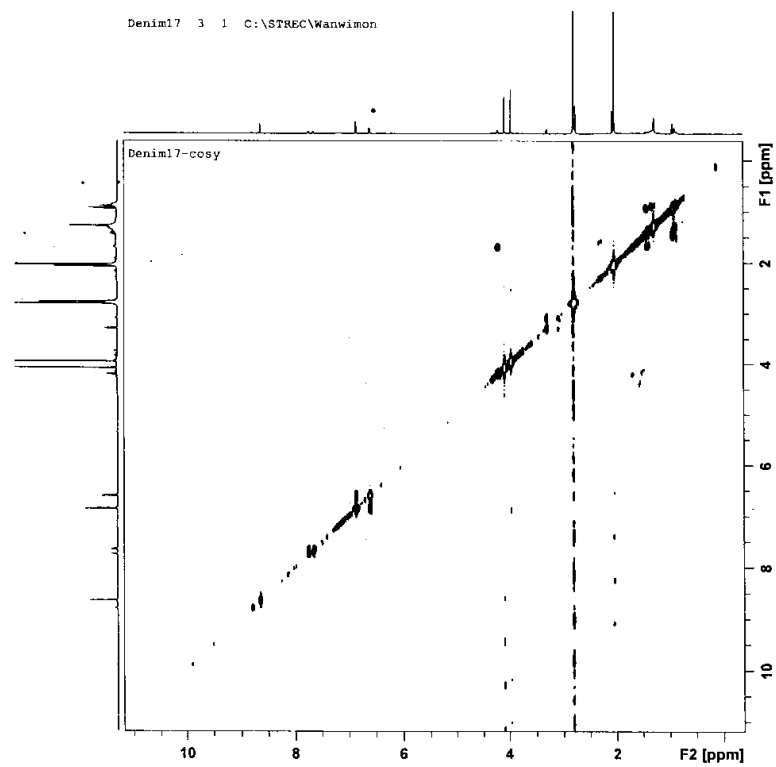


Figure 45 COSY spectrum of dendrocrumenol C (**3**) in acetone- d_6 .

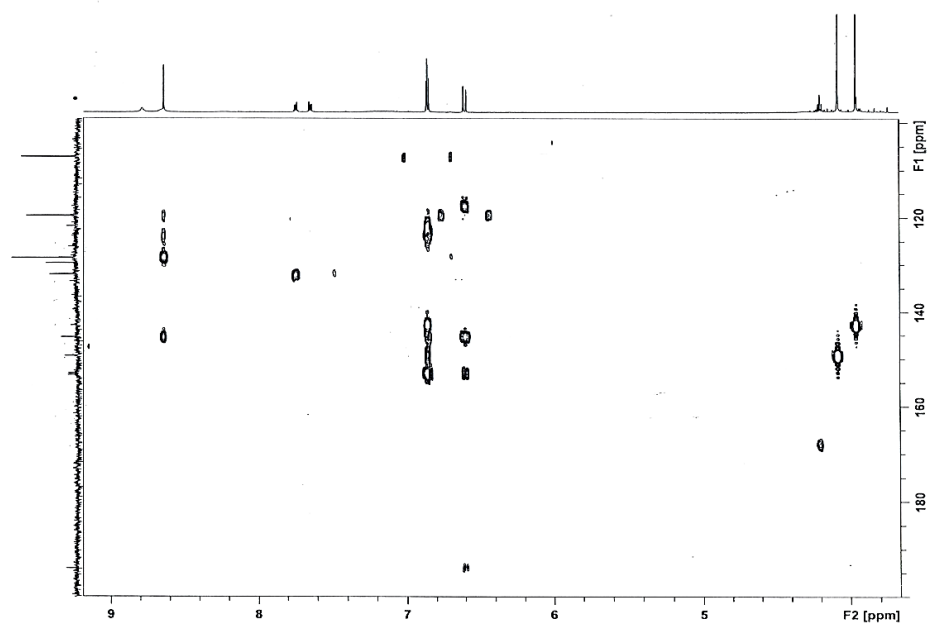


Figure 46 HMBC spectrum of dendrocrumenol C (**3**) in acetone- d_6 .

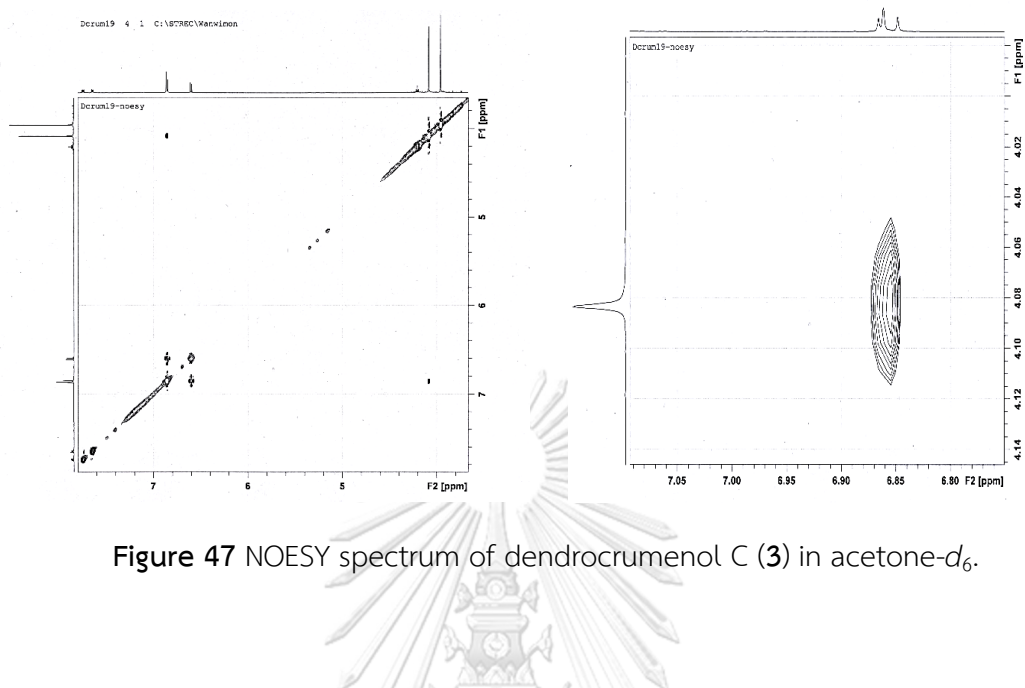


Figure 47 NOESY spectrum of dendrocumenol C (3) in acetone- d_6 .

Mass Spectrum List Report

Analysis Info

Analysis Name 01122021_OSCUCP_Dc19_1.d
 Method Tune_low_Neg_90-250_NATTHAPAT.m
 Sample Name Dc19
 01122021

Acquisition Date 12/2/2021 3:08:48 PM
 Operator Administrator
 Instrument micrOTOF 72

Acquisition Parameter

Source Type ESI
 Scan Range n/a
 Scan Begin 50 m/z
 Scan End 3000 m/z

Ion Polarity Negative
 Capillary Exit -130.0 V
 Hexapole RF 120.0 V
 Skimmer 1 -50.0 V
 Hexapole 1 -25.0 V

Set Corrector Fill 75 V
 Set Pulsar Pull 372 V
 Set Pulsar Push 372 V
 Set Reflector 1300 V
 Set Flight Tube 9000 V
 Set Detector TOF 2295 V

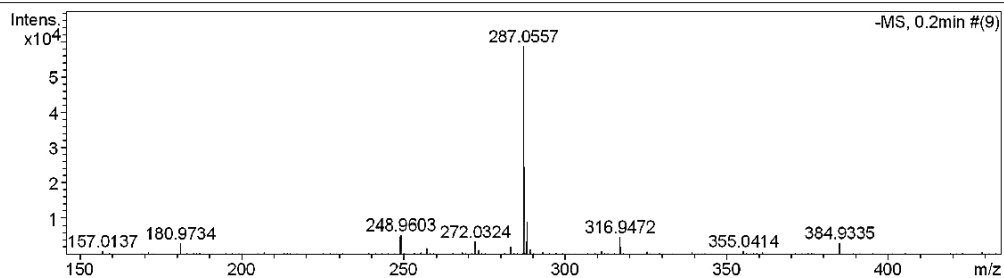


Figure 48 HR-ESI-MS spectrum of dendrocumenol C (3).

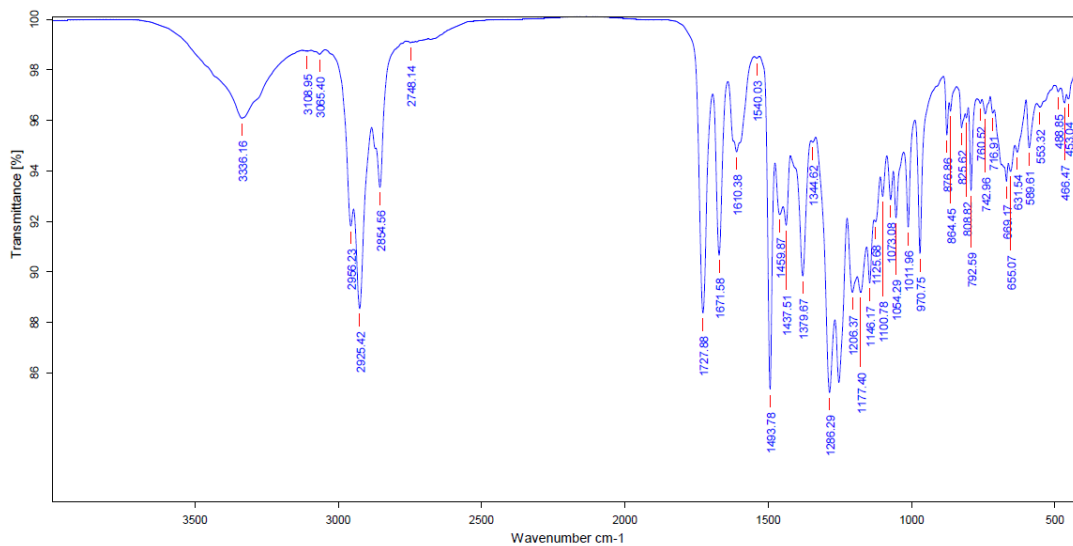


Figure 49 IR spectrum of dendrocromenol C (3).

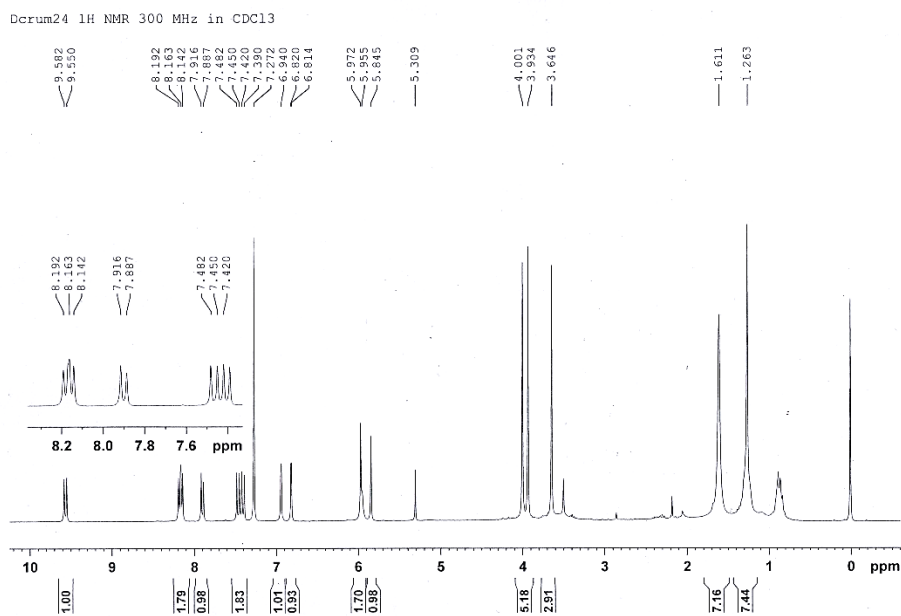


Figure 50 ¹H NMR spectrum of dendrocromenol D (4) (300 MHz) in CDCl₃.

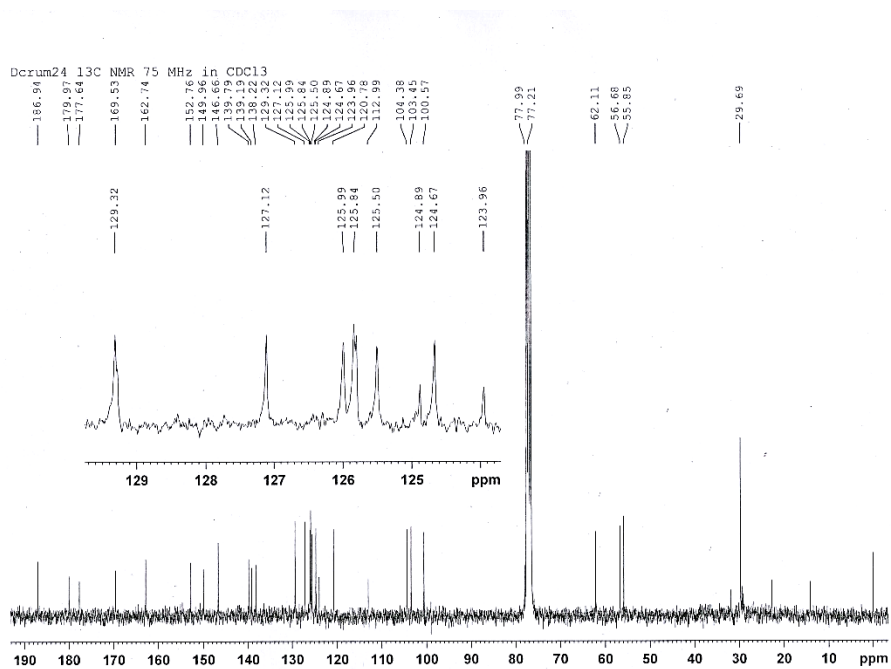


Figure 51 ^{13}C NMR spectrum of dendrocruenol D (4) (75 MHz) in CDCl_3 .

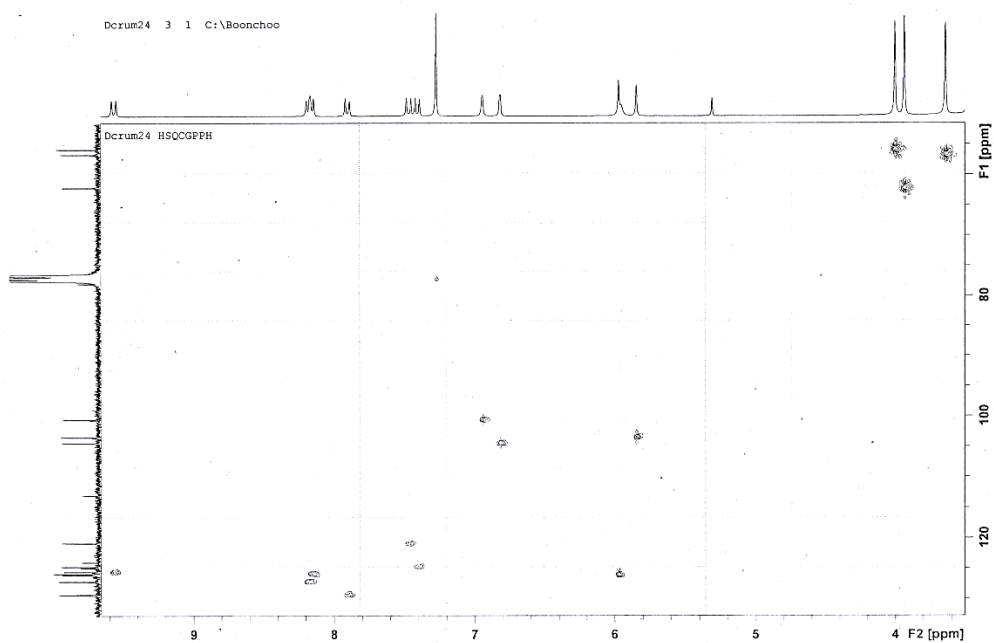


Figure 52 HSQC spectrum of dendrocruenol D (4) in CDCl_3 .

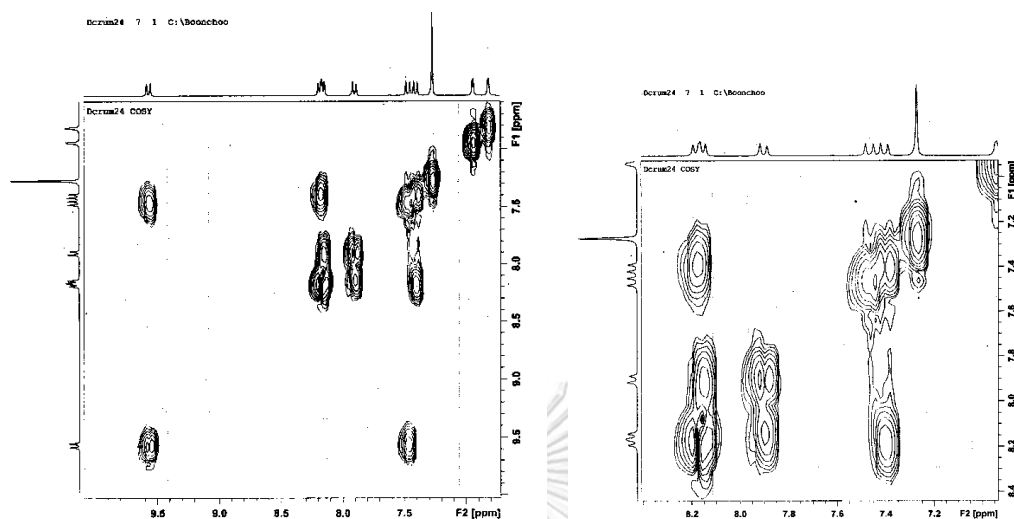


Figure 53 COSY spectrum of dendrocumenol D (4) in CDCl_3 .

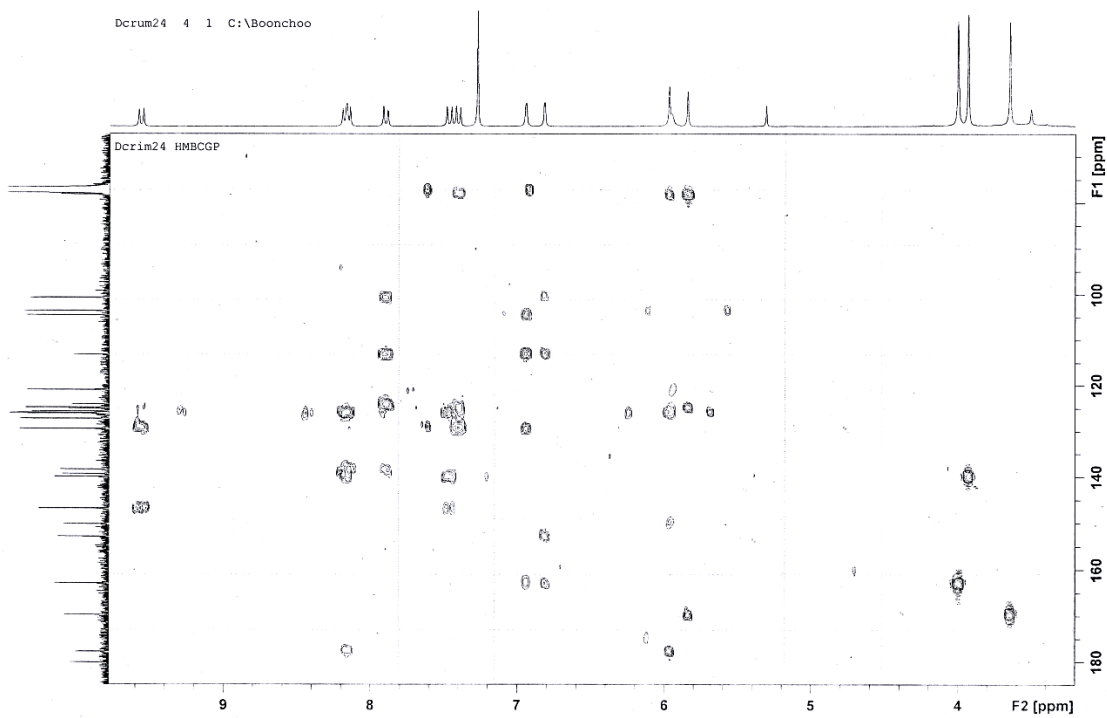


Figure 54 HMBC spectrum of dendrocumenol D (4) in CDCl_3 .

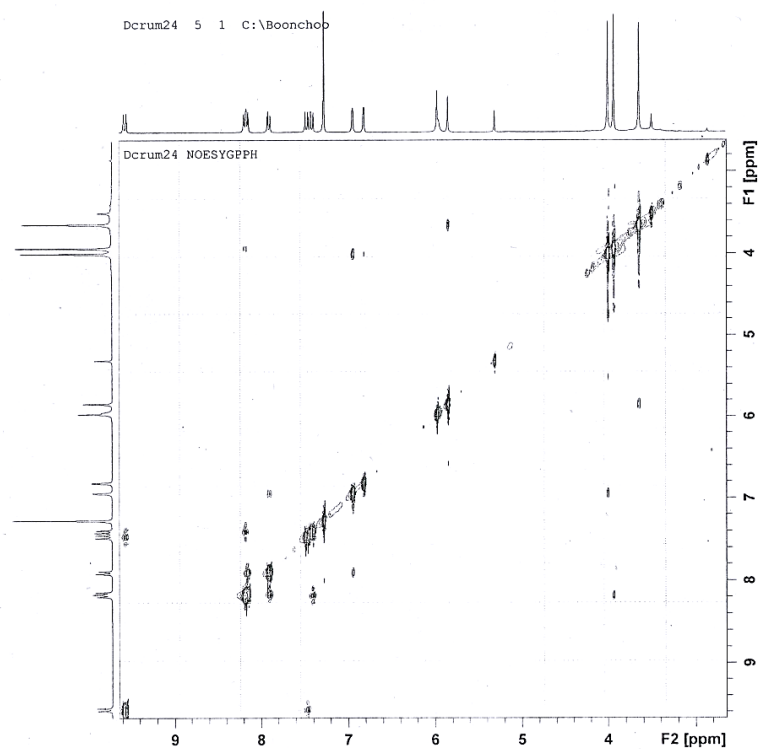


Figure 55 NOESY spectrum of dendrocumenol D (**4**) in CDCl_3 .

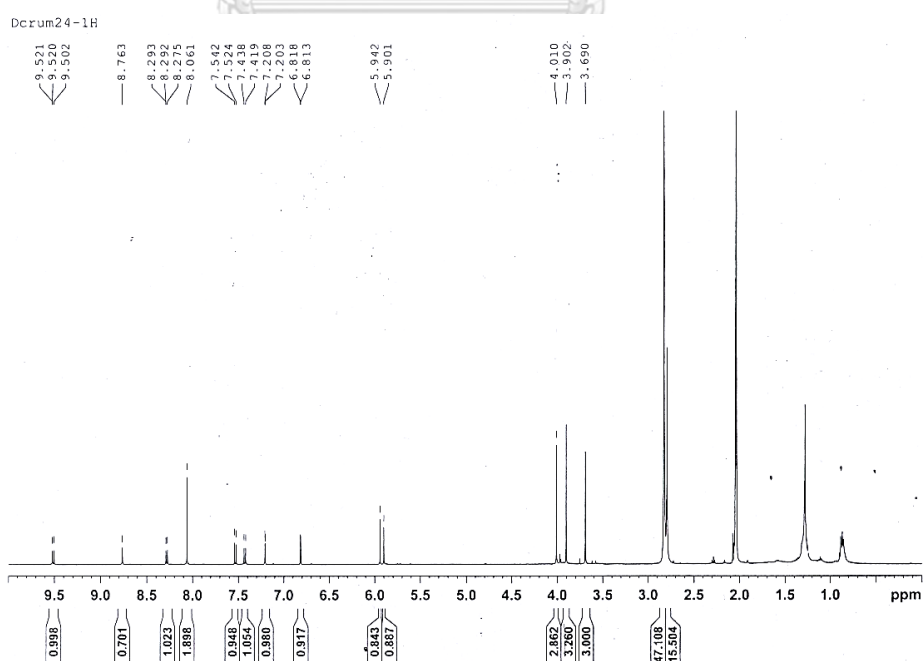


Figure 56 ^1H NMR spectrum of dendrocumenol D (**4**) (500 MHz) in acetone- d_6 .

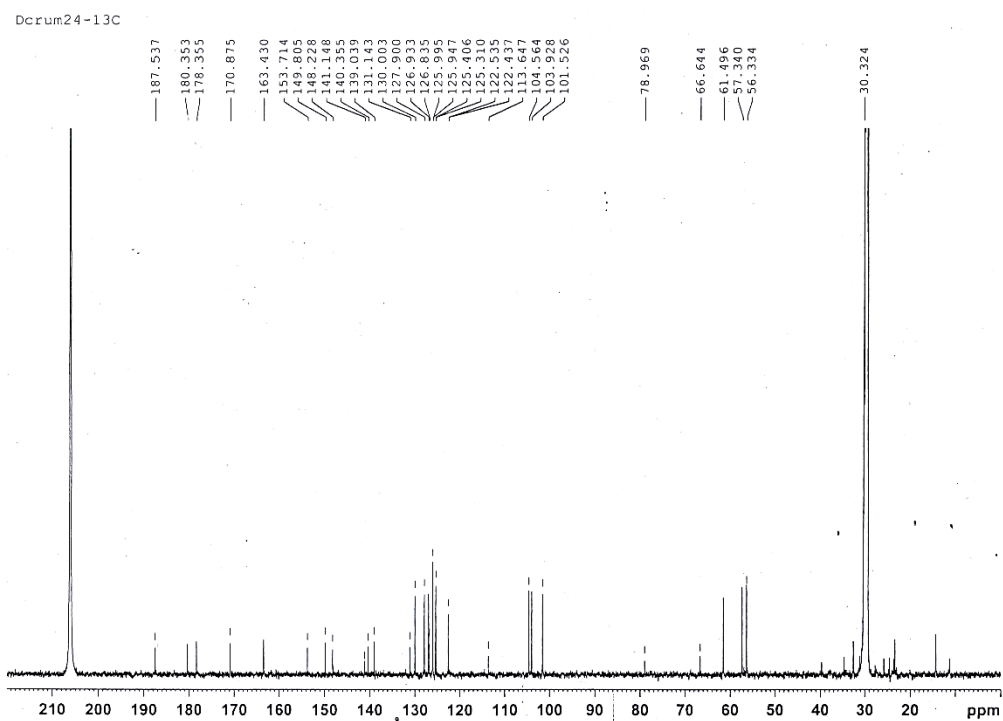


Figure 57 ^{13}C NMR spectrum of dendrocruenol D (**4**) (125 MHz) in acetone- d_6 .

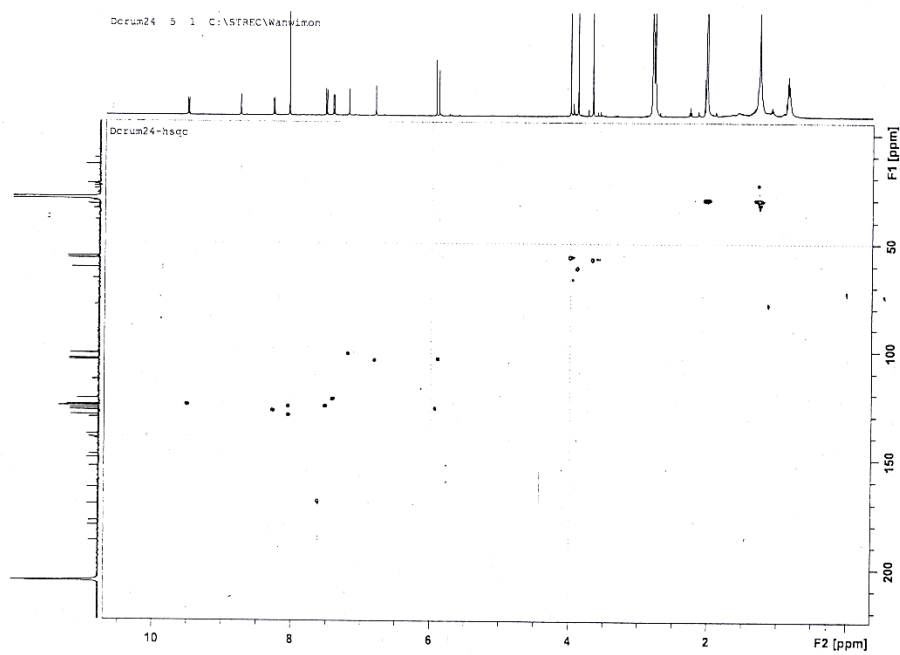


Figure 58 HSQC spectrum of dendrocruenol D (**4**) in acetone- d_6 .

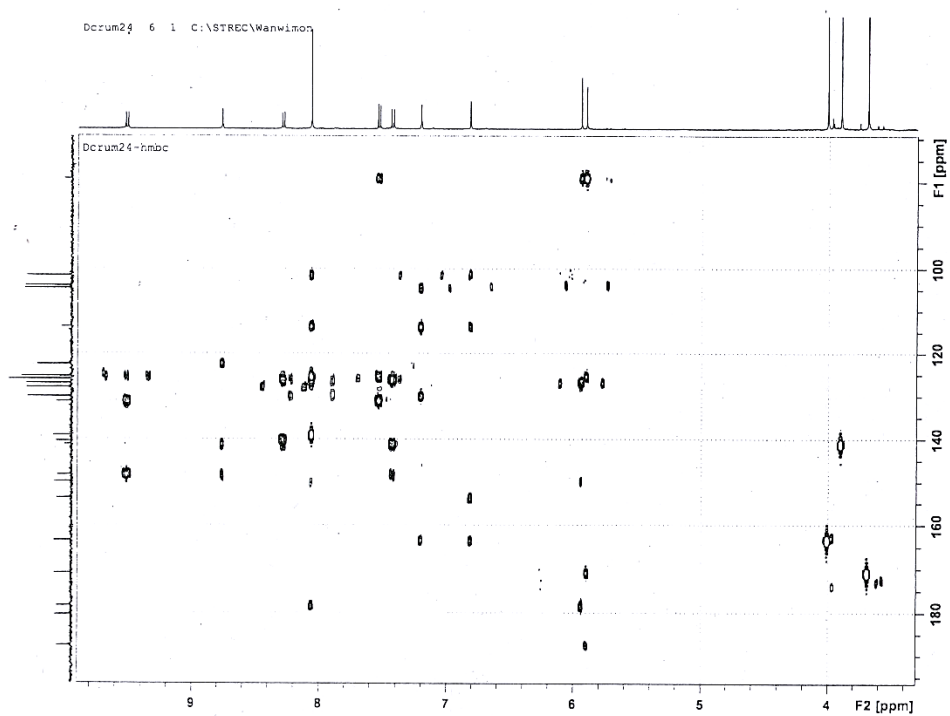


Figure 59 HMBC spectrum of dendrocruenol D (4) in acetone-*d*₆.

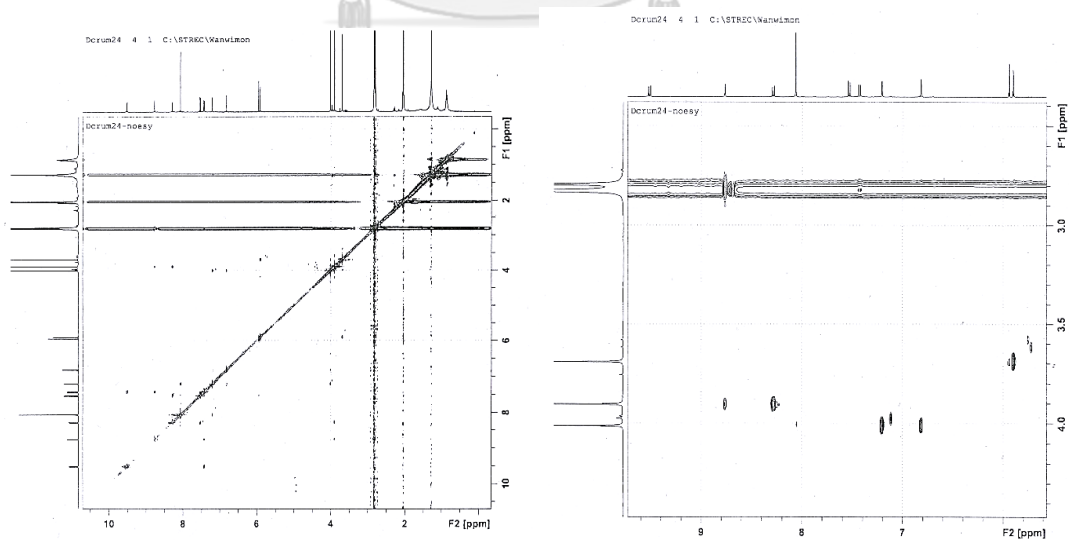


Figure 60 NOESY spectrum of dendrocruenol D (4) in acetone-*d*₆.

Mass Spectrum List Report

Analysis Info

Analysis Name	17122020_CU_Dcrum 24.d	Acquisition Date	12/17/2020 12:14:49 PM
Method	Tune_low_300_400_022020_NATTHAPAT.m	Operator	Administrator
Sample Name	Dcrum 24	Instrument	micrOTOF 72
	17122020		

Acquisition Parameter

Source Type	ESI	Ion Polarity	Positive	Set Corrector Fill	50 V
Scan Range	n/a	Capillary Exit	180.0 V	Set Pulsar Pull	337 V
Scan Begin	50 m/z	Hexapole RF	300.0 V	Set Pulsar Push	337 V
Scan End	3000 m/z	Skimmer 1	70.0 V	Set Reflector	1300 V
		Hexapole 1	23.0 V	Set Flight Tube	9000 V
				Set Detector TOF	2295 V

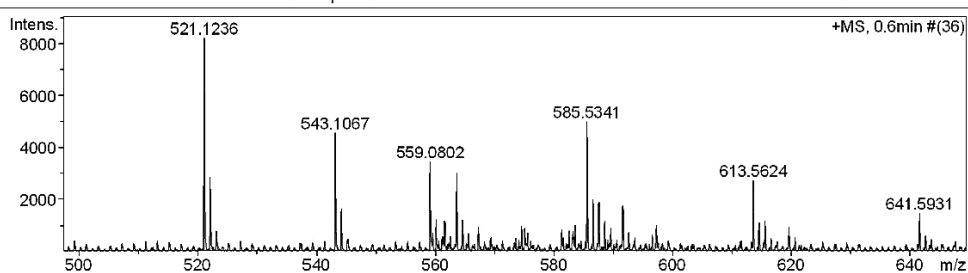


Figure 61 HR-ESI-MS spectrum of dendrocruenol D (4).

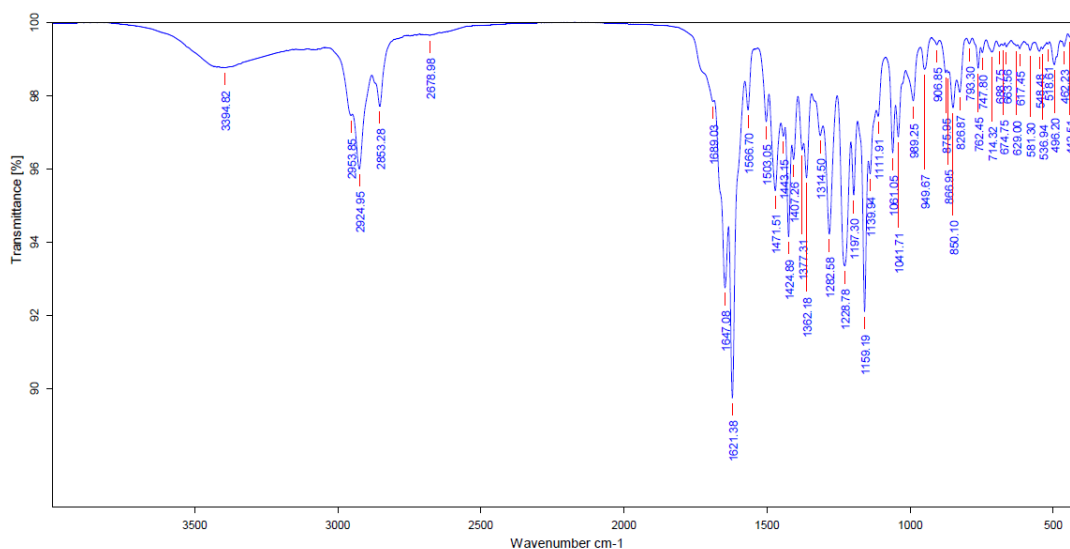


Figure 62 IR spectrum of dendrocruenol D (4).

REFERENCES

- Akira, S., Uematsu, S., & Takeuchi, O. (2006). Pathogen recognition and innate immunity. *Cell*, 124(4), 783-801.
- Amarante-Mendes, G. P., Adjemian, S., Branco, L. M., Zanetti, L. C., Weinlich, R., & Bortoluci, K. R. (2018). Pattern recognition receptors and the host cell death molecular machinery. *Frontiers in immunology*, 9, 2379.
- Avila-Medina, J., Mayoral-Gonzalez, I., Dominguez-Rodriguez, A., Gallardo-Castillo, I., Ribas, J., Ordoñez, A., Rosado, J. A., & Smani, T. (2018). The complex role of store operated calcium entry pathways and related proteins in the function of cardiac, skeletal and vascular smooth muscle cells. *Frontiers in physiology*, 9, 257.
- Bar-Or, A., & Li, R. (2021). Cellular immunology of relapsing multiple sclerosis: interactions, checks, and balances. *The Lancet Neurology*, 20(6), 470-483.
- Bi, Z.-M., Wang, Z.-T., & Xu, L.-S. (2004). Chemical constituents of *Dendrobium moniliforme*. *ACTA BOTANICA SINICA-ENGLISH EDITION*, 46(1), 124-126.
- Bing, X., Xuelei, L., Wanwei, D., Linlang, L., & Keyan, C. (2017). EGCG maintains Th1/Th2 balance and mitigates ulcerative colitis induced by dextran sulfate sodium through TLR4/MyD88/NF- κ B signaling pathway in rats. *Canadian Journal of Gastroenterology and Hepatology*, 2017.
- Böttcher, C., Fernández-Zapata, C., Schlickeiser, S., Kunkel, D., Schulz, A. R., Mei, H. E., Weidinger, C., Gieß, R. M., Asseyer, S., & Siegmund, B. (2019). Multi-parameter immune profiling of peripheral blood mononuclear cells by multiplexed single-cell mass cytometry in patients with early multiple sclerosis. *Scientific Reports*, 9(1), 1-14.
- Böttcher, C., Schlickeiser, S., Sneeboer, M. A., Kunkel, D., Knop, A., Paza, E., Fidzinski, P., Kraus, L., Snijders, G. J., & Kahn, R. S. (2019). Human microglia regional heterogeneity and phenotypes determined by multiplexed single-cell mass cytometry. *Nature neuroscience*, 22(1), 78-90.
- Brignall, R., Cauchy, P., Bevington, S. L., Gorman, B., Pisco, A. O., Bagnall, J., Boddington,

- C., Rowe, W., England, H., & Rich, K. (2017). Integration of kinase and calcium signaling at the level of chromatin underlies inducible gene activation in T cells. *The Journal of Immunology*, 199(8), 2652-2667.
- Bruhn, T., Schaumlöffel, A., Hemberger, Y., & Bringmann, G. (2013). SpecDis: Quantifying the comparison of calculated and experimental electronic circular dichroism spectra. *Chirality*, 25(4), 243-249.
- Busaranon, K., Plaimee, P., Sritularak, B., & Chanvorachote, P. (2016). Moscatilin inhibits epithelial-to-mesenchymal transition and sensitizes anoikis in human lung cancer H460 cells. *Journal of natural medicines*, 70, 18-27.
- Byun, J.-K., Yoon, B.-Y., Jhun, J.-Y., Oh, H.-J., Kim, E.-k., Min, J.-K., & Cho, M.-L. (2014). Epigallocatechin-3-gallate ameliorates both obesity and autoinflammatory arthritis aggravated by obesity by altering the balance among CD4+ T-cell subsets. *Immunology Letters*, 157(1-2), 51-59.
- Cacciapaglia, F., Perniola, S., Urso, L., Fornaro, M., & Iannone, F. (2020). Phosphorylated signal transducer and activator of transcription 3 (pSTAT3) is highly expressed in CD14+ circulating cells of scleroderma patients. *Rheumatology*, 59(6), 1442-1444.
- Cakova, V., Bonte, F., & Lobstein, A. (2017). *Dendrobium*: sources of active ingredients to treat age-related pathologies. *Aging and disease*, 8(6), 827.
- Chan, D. V., Gibson, H. M., Aufiero, B. M., Wilson, A. J., Hafner, M. S., Mi, Q.-S., & Wong, H. K. (2014). Differential CTLA-4 expression in human CD4+ versus CD8+ T cells is associated with increased NFAT1 and inhibition of CD4+ proliferation. *Genes & Immunity*, 15(1), 25-32.
- Chan, M. A., Kohlmeier, J. E., Branden, M., Jung, M., & Benedict, S. H. (1999). Triptolide is more effective in preventing T cell proliferation and interferon-gamma production than is FK506. *Phytotherapy Research: An International Journal Devoted to Pharmacological and Toxicological Evaluation of Natural Product Derivatives*, 13(6), 464-467.
- Chang, C.-C., Ku, A. F., Tseng, Y.-Y., Yang, W.-B., Fang, J.-M., & Wong, C.-H. (2010). 6, 8-Di-C-glycosyl flavonoids from *Dendrobium huoshanense*. *Journal of natural*

products, 73(2), 229-232.

- Chang, S.-J., Lin, T.-H., & Chen, C.-C. (2001). Constituents from the stems of *Dendrobium clavatum* var. *aurantiacum*. *Chinese Medical Journal*, 12(3), 211-218.
- Chang, S. N., Dey, D. K., Oh, S. T., Kong, W. H., Cho, K. H., Al-Olayan, E. M., Hwang, B. S., Kang, S. C., & Park, J. G. (2020). Phorbol 12-myristate 13-acetate induced toxicity study and the role of tangeretin in abrogating hif-1 α -nf- κ b crosstalk in vitro and in vivo. *International Journal of Molecular Sciences*, 21(23), 9261.
- Chanvorachote, P., Kowitdamrong, A., Ruanghirun, T., Sritularak, B., Mungmee, C., & Likhitwitayawuid, K. (2013). Anti-metastatic activities of bibenzyls from *Dendrobium pulchellum*. *Natural Product Communications*, 8(1), 1934578X1300800127.
- Chen, C.-C., Wu, L.-G., Ko, F.-N., & Teng, C.-M. (1994). Antiplatelet aggregation principles of *Dendrobium loddigesii*. *Journal of natural products*, 57(9), 1271-1274.
- Chen, D.-N., Wang, Y.-Y., Liu, W.-J., Chen, Y.-J., Wu, Y.-P., Wang, J.-X., He, F., & Jiang, L. (2020). Stilbenoids from aerial parts of *Dendrobium plicatile*. *Natural Product Research*, 34(3), 323-328.
- Chen, L., Deng, H., Cui, H., Fang, J., Zuo, Z., Deng, J., Li, Y., Wang, X., & Zhao, L. (2018). Inflammatory responses and inflammation-associated diseases in organs. *Oncotarget*, 9(6), 7204.
- Chen, X.-J., Mei, W.-L., Cai, C.-H., Guo, Z.-K., Song, X.-Q., & Dai, H.-F. (2014). Four new bibenzyl derivatives from *Dendrobium sinense*. *Phytochemistry Letters*, 9, 107-112.
- Chen, Y., Li, J., Wang, L., & Liu, Y. (2008). Aromatic compounds from *Dendrobium aphyllum*. *Biochemical Systematics and Ecology*, 5(36), 458-460.
- Chen, Y., Liu, Y., Jiang, J., Zhang, Y., & Yin, B. (2008). Dendronone, a new phenanthrenequinone from *Dendrobium cariniferum*. *Food Chemistry*, 111(1), 11-12.
- Chen, Z. J. (2012). Ubiquitination in signaling to and activation of IKK. *Immunological reviews*, 246(1), 95-106.
- Cheng, J., Dang, P.-P., Zhao, Z., Yuan, L.-C., Zhou, Z.-H., Wolf, D., & Luo, Y.-B. (2019). An assessment of the Chinese medicinal *Dendrobium* industry: Supply, demand

- and sustainability. *Journal of Ethnopharmacology*, 229, 81-88.
- Cheng, L., Fang, Y.-K., Zhang, M.-S., Wang, G., Dong, M.-J., Sun, C.-X., & Xiao, S.-J. (2022). Dihydrophenanthrenes and phenanthrenes from *Dendrobium terminale*. *Natural Product Research*, 1-8.
- Cheng, L., Guo, D.-L., Zhang, M.-S., Linghu, L., Fu, S.-B., Deng, Y., He, Y.-Q., & Xiao, S.-J. (2020). Dihydrophenanthrofurans and bisbibenzyl derivatives from the stems of *Dendrobium nobile*. *Fitoterapia*, 143, 104586.
- Chevrier, M. R., Ryan, A. E., Lee, D. Y.-W., Zhongze, M., Wu-Yan, Z., & Via, C. S. (2005). *Boswellia carterii* extract inhibits TH1 cytokines and promotes TH2 cytokines in vitro. *Clinical and Vaccine Immunology*, 12(5), 575-580.
- Chugtai, A., Hasan, W., Mahdi, A. A., & Islam, N. (2018). Effect of resveratrol on the biomarkers of oxidative stress and inflammation in monocyte cultures from pbmc's of patients with myocardial infarction. *Indian Journal of Biochemistry and Biophysics*, 55, 328-333.
- Ciesielska, A., Matyjek, M., & Kwiatkowska, K. (2021). TLR4 and CD14 trafficking and its influence on LPS-induced pro-inflammatory signaling. *Cellular and molecular life sciences*, 78, 1233-1261.
- Clifford, P., & Kobayashi, K. (2012). Naturalizing orchids and the Hawaii Pacific weed risk assessment system. *Ornamentals and Flowers*, 51, 1-5.
- Dahmardeh, H., & Amirifard, H. (2018). Evaluating the impact of self-care program based on Orem model on self-efficacy of patients suffering from multiple sclerosis. *International Journal of Pharmaceutical and Phytopharmacological Research*, 8(5), 88-93.
- Dahmén, J., & Leander, K. (1978). Amotin and amoenin, two sesquiterpenes of the picrotoxane group from *Dendrobium amoenum*. *Phytochemistry*, 17(11), 1949-1952.
- Dan, Y., Cheng, Z.-Q., Cheng-Ting, Z., Liu, Y., Fa-Wu, D., Jiang-Miao, H., & Jun, Z. (2019). Four new sesquiterpene derivatives from *Dendrobium findlayanum*. *Chinese journal of natural medicines*, 17(12), 900-905.
- Dendrou, C. A., Fugger, L., & Friese, M. A. (2015). Immunopathology of multiple sclerosis. *Nature Reviews Immunology*, 15(9), 545-558.

- Ding, X.-Q., Zou, Y.-Q., Liu, J., Wang, X.-C., Hu, Y., Liu, X., & Zhang, C.-F. (2021). Dendrocrepidamine, a novel octahydroindolizine alkaloid from the roots of *Dendrobium crepidatum*. *Journal of Asian natural products research*, 23(11), 1085-1092.
- Fahey, A. J., Adrian Robins, R., & Constantinescu, C. S. (2007). Curcumin modulation of IFN- β and IL-12 signalling and cytokine induction in human T cells. *Journal of cellular and molecular medicine*, 11(5), 1129-1137.
- Fan, C., Wang, W., Wang, Y., Qin, G., & Zhao, W. (2001). Chemical constituents from *Dendrobium densiflorum*. *Phytochemistry*, 57(8), 1255-1258.
- Fan, D., He, X., Bian, Y., Guo, Q., Zheng, K., Zhao, Y., Lu, C., Liu, B., Xu, X., & Zhang, G. (2016). Triptolide modulates TREM-1 signal pathway to inhibit the inflammatory response in rheumatoid arthritis. *International Journal of Molecular Sciences*, 17(4), 498.
- Fan, W.-W., Xu, F.-Q., Dong, F.-W., Li, X.-N., Li, Y., Liu, Y.-Q., Zhou, J., & Hu, J.-M. (2013). Dendrowardol C, a novel sesquiterpenoid from *Dendrobium wardianum* Warner. *Natural Products and Bioprospecting*, 3, 89-92.
- Fernández Zapata, C., Giacomello, G., Spruth, E. J., Middeldorp, J., Gallaccio, G., Dehlinger, A., Dames, C., Leman, J. K., van Dijk, R. E., & Meisel, A. (2022). Differential compartmentalization of myeloid cell phenotypes and responses towards the CNS in Alzheimer's disease. *Nature Communications*, 13(1), 7210.
- Feske, S., Wulff, H., & Skolnik, E. Y. (2015). Ion channels in innate and adaptive immunity. *Annual review of immunology*, 33, 291-353.
- Fitzgerald, K. A., Rowe, D. C., Barnes, B. J., Caffrey, D. R., Visintin, A., Latz, E., Monks, B., Pitha, P. M., & Golenbock, D. T. (2003). LPS-TLR4 signaling to IRF-3/7 and NF- κ B involves the toll adapters TRAM and TRIF. *The Journal of experimental medicine*, 198(7), 1043-1055.
- Foster, E., Ackerman, J. D., & Falcón L, W. (2019). Identifying Refugia and Barriers to the Spread of *A. graminifolia* and *D. crumenatum* in Puerto Rico. *bioRxiv*, 828517.
- Frisch, M., Trucks, G., Schlegel, H., Scuseria, G., Robb, M., Cheeseman, J., Scalmani, G., Barone, V., Petersson, G., & Nakatsuji, H. (2016). Gaussian 16, Revision A. 03, Gaussian. Inc., Wallingford CT, 3.

- Gay, N. J., Symmons, M. F., Gangloff, M., & Bryant, C. E. (2014). Assembly and localization of Toll-like receptor signalling complexes. *Nature Reviews Immunology*, 14(8), 546-558.
- Geremia, A., Biancheri, P., Allan, P., Corazza, G. R., & Di Sabatino, A. (2014). Innate and adaptive immunity in inflammatory bowel disease. *Autoimmunity reviews*, 13(1), 3-10.
- Haddad, P. S., Azar, G. A., Groom, S., & Boivin, M. (2005). Natural health products, modulation of immune function and prevention of chronic diseases. *Evidence-Based Complementary and Alternative Medicine*, 2(4), 513-520.
- Hann, J., Bueb, J. L., Tolle, F., & Brécard, S. (2020). Calcium signaling and regulation of neutrophil functions: Still a long way to go. *Journal of leukocyte biology*, 107(2), 285-297.
- Hari, A., Flach, T. L., Shi, Y., & Mydlarski, P. R. (2010). Toll-like receptors: role in dermatological disease. *Mediators of inflammation*, 2010.
- Hathcock, K. S., Laszlo, G., Pucillo, C., Linsley, P., & Hodes, R. J. (1994). Comparative analysis of B7-1 and B7-2 costimulatory ligands: expression and function. *The Journal of experimental medicine*, 180(2), 631-640.
- Haverstick, D. M., Dicus, M., Resnick, M. S., Sando, J. J., & Gray, L. S. (1997). A role for protein kinase C β in the regulation of Ca $^{2+}$ entry in Jurkat T cells. *Journal of Biological Chemistry*, 272(24), 15426-15433.
- He, L., Su, Q., Bai, L., Li, M., Liu, J., Liu, X., Zhang, C., Jiang, Z., He, J., & Shi, J. (2020). Recent research progress on natural small molecule bibenzyls and its derivatives in *Dendrobium* species. *European Journal of Medicinal Chemistry*, 204, 112530.
- Herbarium, B. F. (2014). Thai Plant Names Tem Smitinand Revised. *Forest and Plant Conservation Research Office, Department of National Parks, Wildlife and Plant Conservation, Ministry of Natural Resources and Environment, Bangkok.(in Thai)*.
- Honda, C., & Yamaki, M. (2000). Phenanthrenes from *Dendrobium plicatile*. *Phytochemistry*, 53(8), 987-990.
- Hou, B., Luo, J., Zhang, Y., Niu, Z., Xue, Q., & Ding, X. (2017). Iteration expansion and regional evolution: phylogeography of *Dendrobium officinale* and four related

- taxa in southern China. *Scientific Reports*, 7(1), 43525.
- Hu, J.-M., Chen, J.-J., Yu, H., Zhao, Y.-X., & Zhou, J. (2008a). Five new compounds from *Dendrobium longicornu*. *Planta medica*, 74(05), 535-539.
- Hu, J.-M., Chen, J.-J., Yu, H., Zhao, Y.-X., & Zhou, J. (2008b). Two novel bibenzyls from *Dendrobium trigonopus*. *Journal of Asian natural products research*, 10(7), 647-651.
- Hu, J.-M., Zhao, Y.-X., Miao, Z.-H., & Zhou, J. (2009). Chemical components of *Dendrobium polyanthum*. *Bulletin of the Korean Chemical Society*, 30(9), 2098-2100.
- Hu, J., Fan, W., Dong, F., Miao, Z., & Zhou, J. (2012). Chemical components of *Dendrobium chrysotoxum*. *Chinese Journal of Chemistry*, 30(6), 1327-1330.
- Huang, C., & Bi, J. (2021). Expression regulation and function of T-Bet in NK cells. *Frontiers in immunology*, 12, 761920.
- Huang, W. J., Chen, W. W., & Zhang, X. (2017). Multiple sclerosis: Pathology, diagnosis and treatments. *Experimental and Therapeutic Medicine*, 13(6), 3163-3166.
- Hwang, J. S., Lee, S. A., Hong, S. S., Han, X. H., Lee, C., Kang, S. J., Lee, D., Kim, Y., Hong, J. T., & Lee, M. K. (2010). Phenanthrenes from *Dendrobium nobile* and their inhibition of the LPS-induced production of nitric oxide in macrophage RAW 264.7 cells. *Bioorganic & Medicinal Chemistry Letters*, 20(12), 3785-3787.
- Inthongkaew, P., Chatsumpun, N., Supasuteekul, C., Kitisripanya, T., Putalun, W., Likhitwitayawuid, K., & Sritularak, B. (2017). α -Glucosidase and pancreatic lipase inhibitory activities and glucose uptake stimulatory effect of phenolic compounds from *Dendrobium formosum*. *Revista brasileira de farmacognosia*, 27, 480-487.
- Ito, M., Matsuzaki, K., Wang, J., Daikonya, A., Wang, N. L., Yao, X. S., & Kitanaka, S. (2010). New phenanthrenes and stilbenes from *Dendrobium loddigesii*. *Chemical and Pharmaceutical Bulletin*, 58(5), 628-633.
- Joosten, L. A., Abdollahi-Roodsaz, S., Dinarello, C. A., O'Neill, L., & Netea, M. G. (2016). Toll-like receptors and chronic inflammation in rheumatic diseases: new developments. *Nature Reviews Rheumatology*, 12(6), 344-357.
- Khoonrit, P., Mirdogan, A., Dehlinger, A., Mekboonsonglarp, W., Likhitwitayawuid, K.,

- Priller, J., Böttcher, C., & Sritularak, B. (2020). Immune modulatory effect of a novel 4, 5-dihydroxy-3, 3, 4-trimethoxybibenzyl from *Dendrobium lindleyi*. *Plos one*, 15(9), e0238509.
- Khumploy, P., Raksat, A., Choodej, S., Aree, T., Ngamrojanavanich, N., & Pudhom, K. (2021). Picrotoxane sesquiterpene and α -pyrone derivative from *Dendrobium signatum* and their free radical scavenging potency. *Journal of natural medicines*, 75, 967-974.
- Kim, J. H., Oh, S.-Y., Han, S.-B., Uddin, G. M., Kim, C. Y., & Lee, J. K. (2015). Anti-inflammatory effects of *Dendrobium nobile* derived phenanthrenes in LPS-stimulated murine macrophages. *Archives of pharmacal research*, 38, 1117-1126.
- Klinder, A., Seyfarth, A., Hansmann, D., Bader, R., & Jonitz-Heincke, A. (2018). Inflammatory response of human peripheral blood mononuclear cells and osteoblasts incubated with metallic and ceramic submicron particles. *Frontiers in immunology*, 9, 831.
- Klongkumnuankarn, P., Busaranon, K., Chanvorachote, P., Sritularak, B., Jongbunprasert, V., & Likhitwitayawuid, K. (2015). Cytotoxic and antimigratory activities of phenolic compounds from *Dendrobium brymerianum*. *Evidence-Based Complementary and Alternative Medicine*, 2015.
- Kongkatitham, V., Muangnoi, C., Kyokong, N., Thaweesest, W., Likhitwitayawuid, K., Rojsitthisak, P., & Sritularak, B. (2018). Anti-oxidant and anti-inflammatory effects of new bibenzyl derivatives from *Dendrobium parishii* in hydrogen peroxide and lipopolysaccharide treated RAW264. 7 cells. *Phytochemistry Letters*, 24, 31-38.
- Kyokong, N., Muangnoi, C., Thaweesest, W., Kongkatitham, V., Likhitwitayawuid, K., Rojsitthisak, P., & Sritularak, B. (2019). A new phenanthrene dimer from *Dendrobium palpebrae*. *Journal of Asian natural products research*, 21(4), 391-397.
- Lam, Y., Ng, T. B., Yao, R. M., Shi, J., Xu, K., Sze, S. C. W., & Zhang, K. Y. (2015). Evaluation of chemical constituents and important mechanism of pharmacological biology in *Dendrobium* plants. *Evidence-Based Complementary and Alternative Medicine*, 841752, 1-25.

- Leelawat, S., & Leelawat, K. (2018). Cytokine secretion of peripheral blood mononuclear cells by hydnocarpus anthelminthicus seeds. *Journal of Tropical Medicine*, 6854835, 1-8.
- Letizia, M., Wang, Y. H., Kaufmann, U., Gerbeth, L., Sand, A., Brunkhorst, M., Weidner, P., Ziegler, J. F., Böttcher, C., & Schlickeiser, S. (2022). Store-operated calcium entry controls innate and adaptive immune cell function in inflammatory bowel disease. *EMBO Molecular Medicine*, 14(9), e15687.
- Li, C.-B., Wang, C., Fan, W.-W., Dong, F.-W., Xu, F.-Q., Wan, Q.-L., Luo, H.-R., Liu, Y.-Q., Hu, J.-M., & Zhou, J. (2013). Chemical components of *Dendrobium crepidatum* and their neurite outgrowth enhancing activities. *Natural Products and Bioprospecting*, 3, 70-73.
- Li, J.-T., Yin, B.-L., Liu, Y., Wang, L.-Q., & Chen, Y.-G. (2009). Mono-aromatic constituents of *Dendrobium longicornu*. *Chemistry of natural compounds*, 45, 234-236.
- Li, X.-h., Guo, L., Yang, L., Peng, C., He, C.-j., Zhou, Q.-m., Xiong, L., Liu, J., & Zhang, T.-m. (2014). Three new neolignan glucosides from the stems of *Dendrobium aurantiacum* var. *denneanum*. *Phytochemistry Letters*, 9, 37-40.
- Li, Y.-P., Qing, C., Fang, T.-T., Liu, Y., & Chen, Y.-G. (2009). Chemical constituents of *Dendrobium chrysotoxum*. *Chemistry of natural compounds*, 45, 414-416.
- Li, Y., Wang, C.-L., Guo, S.-X., Yang, J.-S., & Xiao, P.-G. (2008). Two new compounds from *Dendrobium candidum*. *Chemical and Pharmaceutical Bulletin*, 56(10), 1477-1479.
- Limpanit, R., Chuanasa, T., Likhitwitayawuid, K., Jongbunprasert, V., & Sritularak, B. (2016). α -Glucosidase inhibitors from *Dendrobium tortile*. *Records of Natural Products*, 10(5), 609.
- Lin, S.-C., Lo, Y.-C., & Wu, H. (2010). Helical assembly in the MyD88–IRAK4–IRAK2 complex in TLR/IL-1R signalling. *Nature*, 465(7300), 885-890.
- Lin, T.-H., Chang, S.-J., Chen, C.-C., Wang, J.-P., & Tsao, L.-T. (2001). Two Phenanthraquinones from *Dendrobium moniliforme*. *Journal of natural products*, 64(8), 1084-1086.
- Lin, X., Shi, H., Cui, Y., Wang, X., Zhang, J., Yu, W., & Wei, M. (2018). *Dendrobium* mixture regulates hepatic gluconeogenesis in diabetic rats via the phosphoinositide-3-

- kinase/protein kinase B signaling pathway. *Experimental and Therapeutic Medicine*, 16(1), 204-212.
- Linsley, P. S., Greene, J. L., Brady, W., Bajorath, J., Ledbetter, J. A., & Peach, R. (1994). Human B7-1 (CD80) and B7-2 (CD86) bind with similar avidities but distinct kinetics to CD28 and CTLA-4 receptors. *Immunity*, 1(9), 793-801.
- Linsley, P. S., & Ledbetter, J. A. (1993). The role of the CD28 receptor during T cell responses to antigen. *Annual review of immunology*, 11(1), 191-212.
- Liu, Y., Jiang, J.-H., Zhang, Y., & Chen, Y.-G. (2009). Chemical constituents of *Dendrobium aurantiacum* var. *denneanum*. *Chemistry of natural compounds*, 45(4), 525-527.
- Liu, Y., Wang, Z., & Zhang, J. (2015). Dietary Chinese Herbs. *Springer, Vienna*, 425-430.
- Lu, Y., Kuang, M., Hu, G.-P., Wu, R.-B., Wang, J., Liu, L., & Lin, Y.-C. (2014). Loddigesiinols G–J: α -glucosidase inhibitors from *Dendrobium loddigesii*. *Molecules*, 19(6), 8544-8555.
- Ma, G.-X., Wang, T.-S., Yin, L., Pan, Y., Xu, G.-J., & Xu, L.-S. (1998). Studies on Chemical Constituents of *Dendrobium chryseum*. *Journal of Chinese Pharmaceutical Sciences*, 7, 52-54.
- Ma, G.-X., Wang, Z.-T., Xu, L.-S., & Xu, G.-J. (1998). A new fluorenone derivative from *Dendrobium chrysotoxum*. *Journal of Chinese Pharmaceutical Sciences*, 7, 59-61.
- Machura, E., Mazur, B., Kwiecień, J., & Karczewska, K. (2007). Intracellular production of IL-2, IL-4, IFN- γ , and TNF- α by peripheral blood CD3⁺ and CD4⁺ T cells in children with atopic dermatitis. *European journal of pediatrics*, 166, 789-795.
- Macián, F., García-Cózar, F., Im, S.-H., Horton, H. F., Byrne, M. C., & Rao, A. (2002). Transcriptional mechanisms underlying lymphocyte tolerance. *Cell*, 109(6), 719-731.
- Maitreesophon, P., Khine, H. E. E., Nealiga, J. Q. L., Kongkatitham, V., Panuthai, P., Chaotham, C., Likhitwitayawuid, K., & Sritularak, B. (2022). α -Glucosidase and pancreatic lipase inhibitory effects and anti-adipogenic activity of dendrofalconerol B, a bisbibenzyl from *Dendrobium harveyanum*. *South African Journal of Botany*, 146, 187-195.
- Majumder, P., & Chatterjee, S. (1989). Crepidatin, a bibenzyl derivative from the orchid

- Dendrobium crepidatum*. *Phytochemistry*, 28(7), 1986-1988.
- Majumder, P., Guha, S., & Sen, S. (1999). Bibenzyl derivatives from the orchid *Dendrobium amoenum*. *Phytochemistry*, 52(7), 1365-1369.
- Majumder, P., & Pal, S. (1992). Rotundatin, a new 9, 10-didydrophenanthrene derivative from *Dendrobium rotundatum*. *Phytochemistry*, 31(9), 3225-3228.
- Majumder, P., & Pal, S. (1993). Cumulatin and tristin, two bibenzyl derivatives from the orchids *Dendrobium cumulatum* and *Bulbophyllum triste*. *Phytochemistry*, 32(6), 1561-1565.
- Majumder, P., Roychowdhury, M., & Chakraborty, S. (1998). Thunalbene, a stilbene derivative from the orchid *Thunia alba*. *Phytochemistry*, 49(8), 2375-2378.
- Majumder, P., & Sen, R. (1987). Moscatilin, a bibenzyl derivative from the orchid *Dendrobium moscatum*. *Phytochemistry*, 26(7), 2121-2124.
- Malaguarnera, L. (2019). Influence of resveratrol on the immune response. *Nutrients*, 11(5), 946.
- Mazgaeen, L., & Gurung, P. (2020). Recent advances in lipopolysaccharide recognition systems. *International Journal of Molecular Sciences*, 21(2), 379.
- Medzhitov, R. (2008). Origin and physiological roles of inflammation. *Nature*, 454(7203), 428-435.
- Medzhitov, R. (2010). Inflammation 2010: new adventures of an old flame. *Cell*, 140(6), 771-776.
- Meesawat, U., & Kanchanapoom, K. (2007). Understanding the flowering behavior of pigeon orchid (*Dendrobium crumenatum* Swartz). *Orchid Science and Biotechnology*, 1, 6-14.
- Meesawat, U., Srisawat, T., Eksomtramage, L., & Kanchanapoom, K. (2008). Nuclear DNA content of the pigeon orchid (*Dendrobium crumenatum* Sw.) with the analysis of flow cytometry. *Songklanakarin Journal of Science & Technology*, 30(3), 277-280.
- Mittraphab, A., Muangnoi, C., Likhitwitayawuid, K., Rojsitthisak, P., & Sritularak, B. (2016). A new bibenzyl-phenanthrene derivative from *Dendrobium signatum* and its cytotoxic activity. *Natural Product Communications*, 11(5), 1934578X1601100526.

- Miyazawa, M., Shimamura, H., Nakamura, S.-i., Sugiura, W., Kosaka, H., & Kameoka, H. (1999). Moscatilin from *Dendrobium nobile*, a naturally occurring bibenzyl compound with potential antimutagenic activity. *Journal of agricultural and food chemistry*, 47(5), 2163-2167.
- Mogensen, T. H. (2009). Pathogen recognition and inflammatory signaling in innate immune defenses. *Clinical microbiology reviews*, 22(2), 240-273.
- Mou, Z., Zhao, Y., Ye, F., Shi, Y., Kennelly, E. J., Chen, S., & Zhao, D. (2021). Identification, biological activities and biosynthetic pathway of *Dendrobium* alkaloids. *Frontiers in Pharmacology*, 12, 605994.
- Moudgil, K. D., & Venkatesha, S. H. (2022). The Anti-Inflammatory and Immunomodulatory Activities of Natural Products to Control Autoimmune Inflammation. *International Journal of Molecular Sciences*, 24(1), 95.
- Murphy, M. T., Qin, X., Kaul, S., Barrientos, G., Zou, Z., Mathias, C. B., Thomas, D., & Bose, D. D. (2020). The polyphenol ellagic acid exerts anti-inflammatory actions via disruption of store-operated calcium entry (SOCE) pathway activators and coupling mediators. *European Journal of Pharmacology*, 875, 173036.
- Muszynski, J. A., Thakkar, R., & Hall, M. W. (2016). Inflammation and innate immune function in critical illness. *Current opinion in pediatrics*, 28(3), 267-273.
- Na Ranong, S., Likhitwitayawuid, K., Mekboonsonglarp, W., & Sritularak, B. (2019). New dihydrophenanthrenes from *Dendrobium infundibulum*. *Natural Product Research*, 33(3), 420-426.
- Natarajan, C., & Bright, J. J. (2002). Curcumin inhibits experimental allergic encephalomyelitis by blocking IL-12 signaling through Janus kinase-STAT pathway in T lymphocytes. *The Journal of Immunology*, 168(12), 6506-6513.
- Ng, T. B., Liu, J., Wong, J. H., Ye, X., Wing Sze, S. C., Tong, Y., & Zhang, K. Y. (2012). Review of research on *Dendrobium*, a prized folk medicine. *Applied Microbiology and Biotechnology*, 93, 1795-1803.
- Ngkelo, A., Meja, K., Yeadon, M., Adcock, I., & Kirkham, P. A. (2012). LPS induced inflammatory responses in human peripheral blood mononuclear cells is mediated through NOX4 and Gi α dependent PI-3kinase signalling. *Journal of inflammation*, 9(1), 1-7.

- Nowarski, R., Gagliani, N., Huber, S., & Flavell, R. A. (2013). Innate immune cells in inflammation and cancer. *Cancer immunology research*, 1(2), 77-84.
- O'Neill, L. A., & Bowie, A. G. (2007). The family of five: TIR-domain-containing adaptors in Toll-like receptor signalling. *Nature Reviews Immunology*, 7(5), 353-364.
- O'Neill, L. A., Fitzgerald, K. A., & Bowie, A. G. (2003). The Toll-IL-1 receptor adaptor family grows to five members. *Trends in immunology*, 24(6), 286-289.
- Obasanmi, G., Lois, N., Armstrong, D., Hombrebueno, J. M. R., Lynch, A., Chen, M., & Xu, H. (2023). Peripheral Blood Mononuclear Cells from Patients with Type 1 Diabetes and Diabetic Retinopathy Produce Higher Levels of IL-17A, IL-10 and IL-6 and Lower Levels of IFN- γ —A Pilot Study. *Cells*, 12(3), 467.
- Oz, H. S., Chen, T., & de Villiers, W. J. (2013). Green tea polyphenols and sulfasalazine have parallel anti-inflammatory properties in colitis models. *Frontiers in immunology*, 4, 132.
- Pan, H., Chen, B., Li, F., & Wang, M. (2012). Chemical constituents of *Dendrobium denneanum*. *Chin J Appl Environ Biol*, 18(3), 378-380.
- Pann Phyu, M., Kongkatitham, V., Mekboonsonglarp, W., Likhitwitayawuid, K., & Sritularak, B. (2022). Phenanthrenes from *Dendrobium senile* and their pancreatic lipase inhibitory activity. *Journal of Asian natural products research*, 24(7), 697-702.
- Phechrmeekha, T., Sritularak, B., & Likhitwitayawuid, K. (2012). New phenolic compounds from *Dendrobium capillipes* and *Dendrobium secundum*. *Journal of Asian natural products research*, 14(8), 748-754.
- Phongpreecha, T., Fernandez, R., Mrdjen, D., Culos, A., Gajera, C. R., Wawro, A. M., Stanley, N., Gaudilliere, B., Poston, K. L., & Aghaeepour, N. (2020). Single-cell peripheral immunoprofiling of Alzheimer's and Parkinson's diseases. *Science advances*, 6(48), eabd5575.
- Phueakklai, O., Suddee, S., Hodgkinson, T. R., Srisom, P., & Sungkaew, S. (2018). *Dendrobium chrysocrepis* (Orchidaceae), a new record for Thailand. *Thai Forest Bulletin (Botany)*, 46(2), 134-137.
- Płóciennikowska, A., Hromada-Judycka, A., Borzęcka, K., & Kwiatkowska, K. (2015). Cooperation of TLR4 and raft proteins in LPS-induced pro-inflammatory signaling.

Cellular and molecular life sciences, 72, 557-581.

- Prakriya, M., & Lewis, R. S. (2015). Store-operated calcium channels. *Physiological reviews*, 95, 1383-1436.
- Pridgeon, A. M., Cribb, P. J., Chase, M. W., & Rasmussen, F. N. (2014). *Genera Orchidacearum Volume 6: Epidendroideae (Part 3)*. OUP Oxford.
- Puleo, A., Carroll, C., Maecker, H. T., & Gupta, R. (2017). Isolation of Peripheral Blood Mononuclear Cells Using Vacutainer (R) Cellular Preparation Tubes (CPT (TM)). *BIO-PROTOCOL*, 7(2).
- Qiang, Z., Ko, C.-H., Siu, W.-S., Kai-Kai, L., Wong, C.-W., Xiao-Qiang, H., Liu, Y., Bik-San Lau, C., Jiang-Miao, H., & Leung, P.-C. (2018). Inhibitory effect of different *Dendrobium* species on LPS-induced inflammation in macrophages via suppression of MAPK pathways. *Chinese journal of natural medicines*, 16(7), 481-489.
- Qin, X.-D., Qu, Y., Ning, L., Liu, J.-K., & Fan, S.-K. (2011). A new picrotoxane-type sesquiterpene from *Dendrobium findlayanum*. *Journal of Asian natural products research*, 13(11), 1047-1050.
- Qiu, H., Song, L.-X., Yang, Y.-B., Zhang, S.-Y., Han, Z.-Z., Wang, Z.-T., & Yang, L. (2023). Two new stilbenoid diglycosides from the stems of *Dendrobium 'Sonia'*. *Journal of Asian natural products research*, 25(3), 245-251.
- Ram, A. T., Shamina, M., & Pradeep, A. (2015). *Dendrobium crumenatum* (Orchidaceae): A new record for mainland India. *Rheedea*, 25(1), 69-71.
- Ramírez-Pérez, S., Hernández-Palma, L. A., Oregon-Romero, E., Anaya-Macías, B. U., García-Arellano, S., González-Estevez, G., & Muñoz-Valle, J. F. (2020). Downregulation of inflammatory cytokine release from IL-1 β and Lps-stimulated PbmC orchestrated by St2825, a Myd88 dimerisation inhibitor. *Molecules*, 25(18), 4322.
- Roe, K. (2021). An inflammation classification system using cytokine parameters. *Scandinavian Journal of Immunology*, 93(2), e12970.
- Roh, J. S., & Sohn, D. H. (2018). Damage-associated molecular patterns in inflammatory diseases. *Immune network*, 18(4), e27, 1-14.
- Rujichaipimon, W., Phueakhlai, O., Suddee, S., Sungkaew, S., & Traiperm, P. (2019). On scientific requirements for presentation of "new records": the case of

- Dendrobium ruckeri* (Orchidaceae). *Thai Forest Bulletin (Botany)*, 47(2), 152-158.
- Rungwichaniwat, P., Sritularak, B., & Likhitwitayawuid, K. (2014). Chemical Constituents of *Dendrobium williamsonii*. *Pharmacognosy journal*, 6(3), 36-41.
- Sandrasagaran, U. M., Subramaniam, S., & Murugaiyah, V. (2014). New perspective of *Dendrobium crumenatum* orchid for antimicrobial activity against selected pathogenic bacteria. *Pakistan Journal of Botany*, 46(2), 719-724.
- Sarakulwattana, C., Mekboonsonglarp, W., Likhitwitayawuid, K., Rojsitthisak, P., & Sritularak, B. (2020). New bisbibenzyl and phenanthrene derivatives from *Dendrobium scabrilingue* and their α -glucosidase inhibitory activity. *Natural Product Research*, 34(12), 1694-1701.
- Sato, S., Sugiyama, M., Yamamoto, M., Watanabe, Y., Kawai, T., Takeda, K., & Akira, S. (2003). Toll/IL-1 receptor domain-containing adaptor inducing IFN- β (TRIF) associates with TNF receptor-associated factor 6 and TANK-binding kinase 1, and activates two distinct transcription factors, NF- κ B and IFN-regulatory factor-3, in the Toll-like receptor signaling. *The Journal of Immunology*, 171(8), 4304-4310.
- Serhan, C. N. (2017). Treating inflammation and infection in the 21st century: new hints from decoding resolution mediators and mechanisms. *The FASEB Journal*, 31(4), 1273.
- Shah, V. O., Ferguson, J. E., Hunsaker, L. A., Deck, L. M., & Vander Jagt, D. L. (2010). Natural products inhibit LPS-induced activation of pro-inflammatory cytokines in peripheral blood mononuclear cells. *Natural Product Research*, 24(12), 1177-1188.
- Shaw, P. J., & Feske, S. (2012). Physiological and pathophysiological functions of SOCE in the immune system. *Frontiers in Bioscience-Elite*, 4(6), 2253-2268.
- Shukla, N. M., Lotze, T. E., & Muscal, E. (2021). Inflammatory diseases of the central nervous system. *Neurologic Clinics*, 39(3), 811-828.
- Singh, U. P., Singh, N. P., Singh, B., Hofseth, L. J., Price, R. L., Nagarkatti, M., & Nagarkatti, P. S. (2010). Resveratrol (trans-3, 5, 4'-trihydroxystilbene) induces silent mating type information regulation-1 and down-regulates nuclear transcription factor- κ B activation to abrogate dextran sulfate sodium-induced colitis. *Journal of Pharmacology and experimental therapeutics*, 332(3), 829-839.

- Sorriento, D., & Iaccarino, G. (2019). Inflammation and cardiovascular diseases: the most recent findings. *International Journal of Molecular Sciences*, 20(16), 3879.
- Sritularak, B., Anuwat, M., & Likhitwitayawuid, K. (2011). A new phenanthrenequinone from *Dendrobium draconis*. *Journal of Asian natural products research*, 13(03), 251-255.
- Sritularak, B., Duangrak, N., & Likhitwitayawuid, K. (2011). A new bibenzyl from *Dendrobium secundum*. *Zeitschrift für Naturforschung C*, 66(5-6), 205-208.
- Sritularak, B., & Likhitwitayawuid, K. (2009). New bisbibenzyls from *Dendrobium falconeri*. *Helvetica chimica acta*, 92(4), 740-744.
- Sukphan, P., Sritularak, B., Mekboonsonglarp, W., Lipipun, V., & Likhitwitayawuid, K. (2014). Chemical constituents of *Dendrobium venustum* and their antimalarial and anti-herpetic properties. *Natural Product Communications*, 9(6), 1934578X1400900625.
- Sun, C., Zhang, N., Xu, G., Jiang, P., Huang, S., Zhao, Q., & He, Y. (2022). Anti-tumor and immunomodulation activity of polysaccharides from *Dendrobium officinale* in S180 tumor-bearing mice. *Journal of Functional Foods*, 94, 105105.
- Sun, J., Liu, J., Liu, Y., Chen, R., Li, Y., Cen, S., Chen, X., Guo, S., & Dai, J. (2021). Dengratiols A–D, four new bibenzyl derivatives from *Dendrobium gratiosissimum*. *Fitoterapia*, 152, 104926.
- Sun, J., Zhang, F., Yang, M., Zhang, J., Chen, L., Zhan, R., Li, L., & Chen, Y. (2014). Isolation of α -glucosidase inhibitors including a new flavonol glycoside from *Dendrobium devonianum*. *Natural Product Research*, 28(21), 1900-1905.
- Sun, Q., Zheng, Y., Zhang, X., Hu, X., Wang, Y., Zhang, S., Zhang, D., & Nie, H. (2013). Novel immunoregulatory properties of EGCG on reducing inflammation in EAE. *Frontiers in Bioscience-Landmark*, 18(1), 332-342.
- Takeuchi, O., & Akira, S. (2010). Pattern recognition receptors and inflammation. *Cell*, 140(6), 805-820.
- Talapatra, B., Das, A. K., & Talapatra, S. K. (1989). Defuscin, a new phenolic ester from *Dendrobium fuscescens*: Conformation of shikimic acid. *Phytochemistry*, 28(1), 290-292.
- Tanagornmeatar, K., Chaotham, C., Sritularak, B., Likhitwitayawuid, K., & Chanvorachote,

- P. (2014). Cytotoxic and anti-metastatic activities of phenolic compounds from *Dendrobium ellipsophyllum*. *Anticancer Research*, 34(11), 6573-6579.
- Tang, D., Kang, R., Coyne, C. B., Zeh, H. J., & Lotze, M. T. (2012). PAMPs and DAMPs: signals that spur autophagy and immunity. *Immunological reviews*, 249(1), 158-175.
- Tatematsu, M., Ishii, A., Oshiumi, H., Horiuchi, M., Inagaki, F., Seya, T., & Matsumoto, M. (2010). A molecular mechanism for Toll-IL-1 receptor domain-containing adaptor molecule-1-mediated IRF-3 activation. *Journal of Biological Chemistry*, 285(26), 20128-20136.
- Teixeira da Silva, J. A., & Ng, T. B. (2017). The medicinal and pharmaceutical importance of *Dendrobium* species. *Applied Microbiology and Biotechnology*, 101, 2227-2239.
- Tenoever, B. R., Ng, S.-L., Chua, M. A., McWhirter, S. M., García-Sastre, A., & Maniatis, T. (2007). Multiple functions of the IKK-related kinase IKK ϵ in interferon-mediated antiviral immunity. *Science*, 315(5816), 1274-1278.
- Terrell, A. M., Crisostomo, P. R., Wairiuko, G. M., Wang, M., Morrell, E. D., & Meldrum, D. R. (2006). Jak/STAT/SOCS signaling circuits and associated cytokine-mediated inflammation and hypertrophy in the heart. *Shock*, 26(3), 226-234.
- Thant, M. T., Chatsumpun, N., Mekboonsonglarp, W., Sritularak, B., & Likhitwitayawuid, K. (2020). New fluorene derivatives from *Dendrobium gibsonii* and their α -glucosidase inhibitory activity. *Molecules*, 25(21), 4931.
- Treesuwan, S., Sritularak, B., Chanvorachote, P., & Pongrakhananon, V. (2018). Cyripedin diminishes an epithelial-to-mesenchymal transition in non-small cell lung cancer cells through suppression of Akt/GSK-3 β signalling. *Scientific Reports*, 8(1), 8009.
- Tsuda, H., Michimata, T., Sakai, M., Nagata, K., Nakamura, M., & Saito, S. (2001). A novel surface molecule of Th2-and Tc2-type cells, CRTH2 expression on human peripheral and decidual CD4+ and CD8+ T cells during the early stage of pregnancy. *Clinical & Experimental Immunology*, 123(1), 105-111.
- Unahabhokha, T., Chanvorachote, P., Sritularak, B., Kitsongsermthon, J., & Pongrakhananon, V. (2016). Gigantol inhibits epithelial to mesenchymal process

- in human lung cancer cells. *Evidence-Based Complementary and Alternative Medicine*, 4561674, 1-10.
- Vaddhanaphuti, N. (2005). *A field guide to the wild orchids of Thailand*. Silkworm Books.
- Vaeth, M., Kahlfuss, S., & Feske, S. (2020). CRAC channels and calcium signaling in T cell-mediated immunity. *Trends in immunology*, 41(10), 878-901.
- Vallejo, J. G. (2011). Role of toll-like receptors in cardiovascular diseases. *Clinical science*, 121(1), 1-10.
- Veerraju, P., Rao, N. P., Rao, L. J., Rao, K. J., & Rao, P. M. (1989). Amoenumin, a 9, 10-dihydro-5H-phenanthro-(4, 5-b, c, d)-pyran from *Dendrobium amoenum*. *Phytochemistry*, 28(3), 950-951.
- Wang, C., Deng, L., Hong, M., Akkaraju, G. R., Inoue, J.-i., & Chen, Z. J. (2001). TAK1 is a ubiquitin-dependent kinase of MKK and IKK. *Nature*, 412(6844), 346-351.
- Wang, H., Zhao, T., & Che, C.-T. (1985). Dendrobine and 3-hydroxy-2-oxodendrobine from *Dendrobium nobile*. *Journal of natural products*, 48(5), 796-801.
- Wang, L., Zhang, C.-F., Wang, Z.-T., Zhang, M., & Xu, L.-S. (2009). Five new compounds from *Dendrobium crystallinum*. *Journal of Asian natural products research*, 11(11), 903-911.
- Wang, P., Chen, X., Cai, C.-H., Kong, F.-D., Huang, S.-Z., Yuan, J.-Z., Xu, X.-L., Mei, W.-L., & Dai, H.-F. (2022). A new picrotoxane-type sesquiterpene from *Dendrobium nobile* Lindl. *Natural Product Research*, 36(8), 2112-2117.
- Wang, P., Chen, X., Wang, H., Huang, S., Cai, C., Yuan, J., Zhu, G., Xu, X., Mei, W., & Dai, H. (2019). Four new picrotoxane-type sesquiterpenes from *Dendrobium nobile* Lindl. *Frontiers in Chemistry*, 7, 812.
- Wang, Y.-H. (2021a). Traditional uses and pharmacologically active constituents of *Dendrobium* plants for dermatological disorders: a review. *Natural Products and Bioprospecting*, 11, 465-487.
- Wang, Y.-H. (2021b). Traditional uses, chemical constituents, pharmacological activities, and toxicological effects of *Dendrobium* leaves: A review. *Journal of Ethnopharmacology*, 270, 113851.
- Wang, Y., Mei, Y., Feng, D., & Xu, L. (2008). Triptolide modulates T-cell inflammatory

- responses and ameliorates experimental autoimmune encephalomyelitis. *Journal of neuroscience research*, 86(11), 2441-2449.
- Wang, Y., Zuo, Z.-T., Huang, H.-Y., & Wang, Y.-Z. (2019). Original plant traceability of *Dendrobium* species using multi-spectroscopy fusion and mathematical models. *Royal Society Open Science*, 6(5), 190399.
- Wang, Z., Zhao, M., Cui, H., Li, J., & Wang, M. (2020). Transcriptomic landscape of medicinal *Dendrobium* reveals genes associated with the biosynthesis of bioactive components. *Frontiers in Plant Science*, 11, 391.
- Warinhomhoun, S., Muangnoi, C., Buranasudja, V., Mekboonsonglarp, W., Rojsitthisak, P., Likhitwitayawuid, K., & Sritularak, B. (2021). Antioxidant activities and protective effects of dendropachol, a new bisbibenzyl compound from *Dendrobium pachyglossum*, on hydrogen peroxide-induced oxidative stress in HaCaT keratinocytes. *Antioxidants*, 10(2), 252.
- Wattanathamsan, O., Treesuwan, S., Sritularak, B., & Pongrakhananon, V. (2018). Cypripedin, a phenanthrenequinone from *Dendrobium densiflorum*, sensitizes non-small cell lung cancer H460 cells to cisplatin-mediated apoptosis. *Journal of natural medicines*, 72, 503-513.
- Wei, X., Sun, W., Zhu, P., Ou, G., Zhang, S., Li, Y., Hu, J., Qu, X., Zhong, Y., & Yu, W. (2022). Refined polysaccharide from *Dendrobium devonianum* resists H1N1 influenza viral infection in mice by activating immunity through the TLR4/MyD88/NF- κ B pathway. *Frontiers in immunology*, 13, 999945.
- Wiat, C. (2012). *Medicinal plants of China, Korea, and Japan: bioresources for tomorrow's drugs and cosmetics*. CRC press.
- Wu, L., Lu, Y., Ding, Y., Zhao, J., Xu, H., & Chou, G. (2019). Four new compounds from *Dendrobium devonianum*. *Natural Product Research*, 33(15), 2160-2168.
- Xie, H., Fang, J., Farag, M. A., Li, Z., Sun, P., & Shao, P. (2022). *Dendrobium officinale* leaf polysaccharides regulation of immune response and gut microbiota composition in cyclophosphamide-treated mice. *Food Chemistry: X*, 13, 100235.
- Xiong, L., Cao, Z.-X., Peng, C., Li, X.-H., Xie, X.-F., Zhang, T.-M., Zhou, Q.-M., Yang, L., & Guo, L. (2013). Phenolic glucosides from *Dendrobium aurantiacum* var. *denneanum* and their bioactivities. *Molecules*, 18(6), 6153-6160.

- Xu, F.-Q., Xu, F.-C., Hou, B., Fan, W.-W., Zi, C.-T., Li, Y., Dong, F.-W., Liu, Y.-Q., Sheng, J., & Zuo, Z.-L. (2014). Cytotoxic bibenzyl dimers from the stems of *Dendrobium fimbriatum* Hook. *Bioorganic & Medicinal Chemistry Letters*, 24(22), 5268-5273.
- Xu, X., Chen, X., Yang, R., Li, Z., Zhou, H., Bai, Y., Yu, M., Li, B., & Ding, G. (2020). Crepidtuminines A and B, two novel indolizidine alkaloids from *Dendrobium crepidatum*. *Scientific Reports*, 10(1), 1-8.
- Xu, X., Li, Z., Yang, R., Zhou, H., Bai, Y., Yu, M., Ding, G., & Li, B. (2019). Crepidatumines C and D, Two New Indolizidine Alkaloids from *Dendrobium crepidatum* Lindl. ex Paxt. *Molecules*, 24(17), 3071.
- Xu, Z., Wei, C., Zhang, R., Yao, J., Zhang, D., & Wang, L. (2015). Epigallocatechin-3-gallate-induced inhibition of interleukin-6 release and adjustment of the regulatory T/T helper 17 cell balance in the treatment of colitis in mice. *Experimental and Therapeutic Medicine*, 10(6), 2231-2238.
- Yamaki, M., & Honda, C. (1996). The stilbenoids from *Dendrobium plicatile*. *Phytochemistry*, 43(1), 207-208.
- Yang, D., Cheng, Z.-Q., Yang, L., Hou, B., Yang, J., Li, X.-N., Zi, C.-T., Dong, F.-W., Liu, Z.-H., & Zhou, J. (2018). Seco-dendrobine-type alkaloids and bioactive phenolics from *Dendrobium findlayanum*. *Journal of natural products*, 81(2), 227-235.
- Yang, D., Liu, L.-Y., Cheng, Z.-Q., Xu, F.-Q., Fan, W.-W., Zi, C.-T., Dong, F.-W., Zhou, J., Ding, Z.-T., & Hu, J.-M. (2015). Five new phenolic compounds from *Dendrobium aphyllum*. *Fitoterapia*, 100, 11-18.
- Yang, H., Chou, G. X., Wang, Z. T., Guo, Y. W., Hu, Z. B., & Xu, L. S. (2004). Two new compounds from *Dendrobium chrysotoxum*. *Helvetica chimica acta*, 87(2), 394-399.
- Yang, H., Sung, S. H., & Kim, Y. C. (2007). Antifibrotic phenanthrenes of *Dendrobium nobile* stems. *Journal of natural products*, 70(12), 1925-1929.
- Yang, L., Qin, L.-H., Bligh, S. A., Bashall, A., Zhang, C.-F., Zhang, M., Wang, Z.-T., & Xu, L.-S. (2006). A new phenanthrene with a spiro lactone from *Dendrobium chrysanthum* and its anti-inflammatory activities. *Bioorganic & medicinal chemistry*, 14(10), 3496-3501.
- Yang, L., Wang, Z., & Xu, L. (2006a). Phenols and a triterpene from *Dendrobium*

- aurantiacum* var. *denneanum* (Orchidaceae). *Biochemical Systematics and Ecology*, 8(34), 658-660.
- Yang, L., Wang, Z., & Xu, L. (2006b). Simultaneous determination of phenols (bibenzyl, phenanthrene, and fluorenone) in *Dendrobium* species by high-performance liquid chromatography with diode array detection. *Journal of Chromatography A*, 1104(1-2), 230-237.
- Yang, M., Chen, L.-J., Zhang, Y., & Chen, Y.-G. (2019). Two new picrotoxane-type sesquiterpenoid lactones from *Dendrobium williamsonii*. *Journal of Asian natural products research*, 21(2), 129-133.
- Yang, M., Zhang, Y., Chen, L., & Chen, Y. (2018). A new (propylphenyl) bibenzyl derivative from *Dendrobium williamsonii*. *Natural Product Research*, 32(14), 1699-1705.
- Yang, Y., Lv, J., Jiang, S., Ma, Z., Wang, D., Hu, W., Deng, C., Fan, C., Di, S., & Sun, Y. (2016). The emerging role of Toll-like receptor 4 in myocardial inflammation. *Cell death & disease*, 7(5), e2234-e2234.
- Ye, Q., Mei, Y., Yang, P., Cheng, L., & Kong, D. (2016). A new 9, 10-dihydrophenanthrene glycoside from *Dendrobium primulinum*. *Chemistry of natural compounds*, 52, 381-383.
- Ye, Q., & Zhao, W. (2002). New alloaromadendrane, cadinene and cyclocopacamphane type sesquiterpene derivatives and bibenzyls from *Dendrobium nobile*. *Planta medica*, 68(08), 723-729.
- Ye, Y., Zhang, Y., Lu, X., Huang, X., Zeng, X., Lai, X., & Zeng, Y. (2011). The anti-inflammatory effect of the SOCC blocker SK&F 96365 on mouse lymphocytes after stimulation by Con A or PMA/ionomycin. *Immunobiology*, 216(9), 1044-1053.
- Yesudhas, D., Gosu, V., Anwar, M. A., & Choi, S. (2014). Multiple roles of toll-like receptor 4 in colorectal cancer. *Frontiers in immunology*, 5, 334.
- Zhang, C. C., Kong, Y. L., Zhang, M. S., Wu, Q., & Shi, J. S. (2023). Two new alkaloids from *Dendrobium nobile* Lindl. exhibited neuroprotective activity, and dendrobine alleviated A β ₁₋₄₂-induced apoptosis by inhibiting CDK5 activation in PC12 cells. *Drug Development Research*, 84(2), 262-274.

- Zhang, G.-N., Zhong, L.-Y., Bligh, S. A., Guo, Y.-L., Zhang, C.-F., Zhang, M., Wang, Z.-T., & Xu, L.-S. (2005). Bi-bicyclic and bi-tricyclic compounds from *Dendrobium thysiflorum*. *Phytochemistry*, 66(10), 1113-1120.
- Zhang, M.-S., Linghu, L., Wang, G., He, Y.-Q., Sun, C.-X., & Xiao, S.-J. (2022). Dendrobine-type alkaloids from *Dendrobium nobile*. *Natural Product Research*, 36(21), 5393-5399.
- Zhang, M., Wu, J., Han, J., Shu, H., & Liu, K. (2018). Isolation of polysaccharides from *Dendrobium officinale* leaves and anti-inflammatory activity in LPS-stimulated THP-1 cells. *Chemistry Central journal*, 12, 1-9.
- Zhang, S., Yang, Y., Li, J., Qin, J., Zhang, W., Huang, W., & Hu, H. (2018). Physiological diversity of orchids. *Plant diversity*, 40(4), 196-208.
- Zhang, X., Gao, H., Wang, N.-L., & Yao, X.-S. (2006). Three new bibenzyl derivatives from *Dendrobium nobile*. *Journal of Asian natural products research*, 8(1-2), 113-118.
- Zhang, X., Xu, J.-K., Wang, J., Wang, N.-L., Kurihara, H., Kitanaka, S., & Yao, X.-S. (2007). Bioactive bibenzyl derivatives and fluorenones from *Dendrobium nobile*. *Journal of natural products*, 70(1), 24-28.
- Zhang, X., Xu, J.-K., Wang, N.-L., Kurihara, H., & Yao, X. (2008). Antioxidant phenanthrenes and lignans from *Dendrobium nobile*. *Journal of Chinese Pharmaceutical Sciences*, 17(4), 314-318.
- Zhang, Y.-Y., Wang, P., Song, X.-Q., Zuo, W.-J., Wang, H., Chen, L.-L., Mei, W.-L., & Dai, H.-F. (2019). Chemical constituents from *Dendrobium hainanense*. *Journal of Asian natural products research*, 21(9), 873-880.
- Zhao, C., Liu, Q., Halaweish, F., Shao, B., Ye, Y., & Zhao, W. (2003). Copacamphane, Picrotoxane, and Alloaromadendrane Sesquiterpene Glycosides and Phenolic Glycosides from *Dendrobium moniliforme*. *Journal of natural products*, 66(8), 1140-1143.
- Zhao, G.-Y., Deng, B.-W., Zhang, C.-Y., Cui, Y.-D., Bi, J.-Y., & Zhang, G.-G. (2018). New phenanthrene and 9, 10-dihydrophenanthrene derivatives from the stems of *Dendrobium officinale* with their cytotoxic activities. *Journal of natural medicines*, 72, 246-251.
- Zhao, G., Liu, Y., Yi, X., Wang, Y., Qiao, S., Li, Z., Ni, J., & Song, Z. (2017). Curcumin

- inhibiting Th17 cell differentiation by regulating the metabotropic glutamate receptor-4 expression on dendritic cells. *International immunopharmacology*, 46, 80-86.
- Zhao, W., Ye, Q., Tan, X., Jiang, H., Li, X., Chen, K., & Kinghorn, A. D. (2001). Three New Sesquiterpene Glycosides from *Dendrobium nobile* with Immunomodulatory Activity. *Journal of natural products*, 64(9), 1196-1200.
- Zheng, S.-g., Hu, Y.-d., Zhao, R.-x., Yan, S., Zhang, X.-q., Zhao, T.-m., & Chun, Z. (2018). Genome-wide researches and applications on *Dendrobium*. *Planta*, 248, 769-784.
- Zheng, Y., Manzotti, C. N., Liu, M., Burke, F., Mead, K. I., & Sansom, D. M. (2004). CD86 and CD80 differentially modulate the suppressive function of human regulatory T cells. *The Journal of Immunology*, 172(5), 2778-2784.
- Zhong, Y.-B., Kang, Z.-P., Zhou, B.-G., Wang, H.-Y., Long, J., Zhou, W., Zhao, H.-M., & Liu, D.-Y. (2021). Curcumin regulated the homeostasis of memory T cell and ameliorated dextran sulfate sodium-induced experimental colitis. *Frontiers in Pharmacology*, 11, 630244.
- Zhong, Z., Vong, C. T., Chen, F., Tan, H., Zhang, C., Wang, N., Cui, L., Wang, Y., & Feng, Y. (2022). Immunomodulatory potential of natural products from herbal medicines as immune checkpoints inhibitors: Helping to fight against cancer via multiple targets. *Medicinal Research Reviews*, 42(3), 1246-1279.
- Zhou, X.-M., Zheng, C.-J., Wu, J.-T., Chen, G.-Y., Chen, J., & Sun, C.-G. (2016). Five new lactone derivatives from the stems of *Dendrobium nobile*. *Fitoterapia*, 115, 96-100.
- Zhou, X.-M., Zheng, C.-J., Wu, J.-T., Chen, G.-Y., Zhang, B., & Sun, C.-G. (2017). A new phenolic glycoside from the stem of *Dendrobium nobile*. *Natural Product Research*, 31(9), 1042-1046.
- Zhu, L.-J., Wang, M.-Q., Qin, Y., Wang, M.-N., Zhang, G.-Q., Niu, L.-T., Chen, J.-B., Zhang, X., & Yao, X.-S. (2021). Two new dibenzyl derivatives from the stems of *Dendrobium catenatum*. *Journal of Asian natural products research*, 23(10), 955-960.



จุฬาลงกรณ์มหาวิทยาลัย
CHULALONGKORN UNIVERSITY



จุฬาลงกรณ์มหาวิทยาลัย
CHULALONGKORN UNIVERSITY

VITA

NAME Virunh Kongkatitham

DATE OF BIRTH 24 September 1992

PLACE OF BIRTH Bangkok

HOME ADDRESS 22/129 Moo 6 Salaya Phutthamonthon Nakhon Pathom
73170

PUBLICATION

1. Kongkatitham, V., Dehlinger, A., Wang, M., Poldorn, P., Weidinger, C., Letizia, M., Chaotham, C., Otto, C., Ruprecht, K., Paul, F., Rungrotmongkol, T., Likhitwitayawuid, K., Chotima Böttcher, C., Sritularak B. (2023). Immunomodulatory effects of new phenanthrene derivatives from *Dendrobium crumenatum*. *Journal of Natural Products*, 86, 1294-1306.
2. Panuthai, P., Phumsuay, R., Muangnoi, C., Maitreesophone, P., Kongkatitham, V., Mekboonsonglarp, W., Rojsitthisak, P., Likhitwitayawuid, K., Sritularak, B. (2023). Isolation and identification of dihydrophenanthrene derivatives from *Dendrobium virgineum* with protective effects against hydrogen-peroxide-induced oxidative stress of human retinal pigment epithelium ARPE-19 cells. *Antioxidants*, 12(3):624.
3. Maitreesophone, P., Khine, H.E.E., Nealiga, J.Q.L., Kongkatitham, V., Panuthai. P., Chaotham, C., Likhitwitayawuid, K., Sritularak, B. (2022). α -Glucosidase and pancreatic lipase inhibitory effects and anti-adipogenic activity of dendrofalconerol B, a bisbibenzyl from *Dendrobium harveyanum*. *South African Journal of Botany*, 146, 187-195.

4. Phyu. M.P., Kongkatitham. V., Mekboonsonglarp, W., Likhitwitayawuid, K., Sritularak, B. (2022). Phenanthrenes from *Dendrobium senile* and their pancreatic lipase inhibitory activity. *Journal of Asian Natural Products Research*, 24, 697-702.
5. Kyokong, N., Muangnoi, C., Thaweesest, W., Kongkatitham, V., Likhitwitayawuid, K., Rojsitthisak, P., Sritularak, B. (2019). A new phenanthrene dimer from *Dendrobium palpebrae*. *Journal of Asian Natural Products Research*, 21, 391-397.
6. Kongkatitham, V., Muangnoi, C., Kyokong, N., Thaweesest, W., Likhitwitayawuid, K., Rojsitthisak, P., Sritularak, B. (2018). Anti-oxidant and anti-inflammatory effects of new bibenzyl derivatives from *Dendrobium parishii* in hydrogen peroxide and lipopolysaccharide treated RAW264.7 cells. *Phytochemistry Letters*, 24, 31-38.
7. Nuntawong, P., Kongkatitham, V., Likhitwitayawuid, K., Mekboonsonglarp, W., Sukrong, S., Tanasupawat, S., Sritularak, B. New 2-arylbenzofurans from the root bark of *Artocarpus gomezianus* and their α -glucosidase inhibitory activity. *Natural Product Research*, 33, 1436-1441.

AWARD RECEIVED

The Second Century Fund (C2F) Ph.D. Scholarship,
Chulalongkorn University